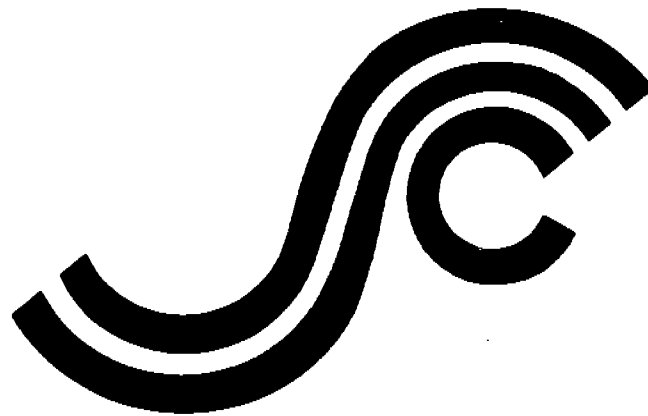


SSC-367

**FATIGUE TECHNOLOGY
ASSESSMENT AND STRATEGIES
FOR FATIGUE AVOIDANCE IN
MARINE STRUCTURES**



This document has been approved
for public release and sale; its
distribution is unlimited

SHIP STRUCTURE COMMITTEE

1993

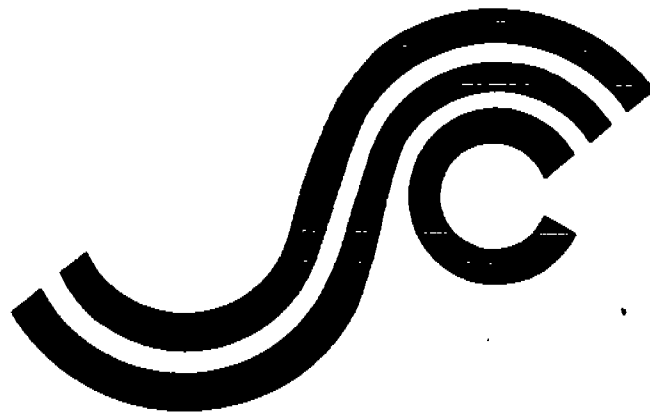
SSC-367 Fatigue Technology Assessment and Avoidance Strategies in Marine Structures – Ship Structure Committee 1993

SPNL 80107-657

1993

SSC-367

**FATIGUE TECHNOLOGY
ASSESSMENT AND STRATEGIES
FOR FATIGUE AVOIDANCE IN
MARINE STRUCTURES**



This document has been approved
for public release and sale; its
distribution is unlimited

SHIP STRUCTURE COMMITTEE

1993

SHIP STRUCTURE COMMITTEE

The SHIP STRUCTURE COMMITTEE is constituted to prosecute a research program to improve the hull structures of ships and other marine structures by an extension of knowledge pertaining to design, materials, and methods of construction.

	RADM A. E. Henn, USCG (Chairman) Chief, Office of Marine Safety, Security and Environmental Protection U. S. Coast Guard	
Mr. Thomas H. Peirce Marine Research and Development Coordinator Transportation Development Center Transport Canada	Mr. H. T. Haller Associate Administrator for Ship- building and Ship Operations Maritime Administration	Dr. Donald Liu Senior Vice President American Bureau of Shipping
Mr. Alexander Malakhoff Director, Structural Integrity Subgroup (SEA 05P) Naval Sea Systems Command	Mr. Thomas W. Allen Engineering Officer (N7) Military Sealift Command	CDR Stephen E. Sharpe, USCG Executive Director Ship Structure Committee U. S. Coast Guard

CONTRACTING OFFICER TECHNICAL REPRESENTATIVE

Mr. William J. Siekierka
SEA 05P4
Naval Sea Systems Command

SHIP STRUCTURE SUBCOMMITTEE

The SHIP STRUCTURE SUBCOMMITTEE acts for the Ship Structure Committee on technical matters by providing technical coordination for determining the goals and objectives of the program and by evaluating and interpreting the results in terms of structural design, construction, and operation.

AMERICAN BUREAU OF SHIPPING

Mr. Stephen G. Arntson (Chairman)
Mr. John F. Conlon
Dr. John S. Spencer
Mr. Glenn M. Ashe

NAVAL SEA SYSTEMS COMMAND

Dr. Robert A. Sielski
Mr. Charles L. Null
Mr. W. Thomas Packard
Mr. Allen H. Engle

TRANSPORT CANADA

Mr. John Grinstead
Mr. Ian Bayly
Mr. David L. Stocks
Mr. Peter Timonin

MILITARY SEALIFT COMMAND

Mr. Robert E. Van Jones
Mr. Rickard A. Anderson
Mr. Michael W. Touma
Mr. Jeffrey E. Beach

MARITIME ADMINISTRATION

Mr. Frederick Seibold
Mr. Norman O. Hammer
Mr. Chao H. Lin
Dr. Walter M. Maclean

U. S. COAST GUARD

CAPT T. E. Thompson
CAPT W. E. Colburn, Jr.
Mr. Rubin Scheinberg
Mr. H. Paul Cojeen

SHIP STRUCTURE SUBCOMMITTEE LIAISON MEMBERS

U. S. COAST GUARD ACADEMY

LCDR Bruce R. Mustain

U. S. MERCHANT MARINE ACADEMY

Dr. C. B. Kim

U. S. NAVAL ACADEMY

Dr. Ramswar Bhattacharyya

STATE UNIVERSITY OF NEW YORK
MARITIME COLLEGE

Dr. W. R. Porter

SOCIETY OF NAVAL ARCHITECTS AND
MARINE ENGINEERS

Dr. William Sandberg

OFFICE OF NAVAL RESEARCH

Dr. Yapa D. S. Rajapaske

NATIONAL ACADEMY OF SCIENCES -
MARINE BOARD

Mr. Alexander B. Stavovy

NATIONAL ACADEMY OF SCIENCES -
COMMITTEE ON MARINE STRUCTURES

Mr. Peter M. Palermo

WELDING RESEARCH COUNCIL

Dr. Martin Prager

AMERICAN IRON AND STEEL INSTITUTE

Mr. Alexander D. Wilson

DEPARTMENT OF NATIONAL DEFENCE - CANADA

Dr. Neil G. Pegg

C-2 80107-659

Member Agencies:

*United States Coast Guard
Naval Sea Systems Command
Maritime Administration
American Bureau of Shipping
Military Sealift Command
Transport Canada*



Address Correspondence to:

Executive Director
Ship Structure Committee
U. S. Coast Guard (G-M/R)
2100 Second Street, S.W.
Washington, D.C. 20593-0001
PH: (202) 267-0003
FAX: (202) 267-4677

An Interagency Advisory Committee

May 17, 1993

SSC-367

SR-1324

**FATIGUE TECHNOLOGY ASSESSMENT AND STRATEGIES FOR FATIGUE
AVOIDANCE IN MARINE STRUCTURES**

This report synthesizes the state-of-the-art in fatigue technology as it relates to the marine field. Over the years more sophisticated methods have been developed to anticipate the life cycle loads on structures and more accurately predict the failure modes. As new design methods have been developed and more intricate and less robust structures have been built it has become more critical than ever that the design tools used be the most effective for the task. This report categorizes fatigue failure parameters, identifies strengths and weaknesses of the available design methods, and recommends fatigue avoidance strategies based upon variables that contribute to the uncertainties of fatigue life. The report concludes with recommendations for further research in this field.

A. E. HENN
Rear Admiral, U.S. Coast Guard
Chairman, Ship Structure Committee

80107
650

1. Report No.		2. Government Accession No.		3. Recipient's Catalog No.	
4. Title and Subtitle FATIGUE DESIGN PROCEDURES				5. Report Date June 1992	
				6. Performing Organization Code	
7. Author(s) Cuneyt C. Capanoglu				8. Performing Organization Report No. SR-1324	
9. Performing Organization Name and Address EARL AND WRIGHT 180 Howard Street San Francisco, CA 94105				10. Work Unit No. (TRAIS)	
				11. Contract or Grant No. DTCG23-88-C-20029	
12. Sponsoring Agency Name and Address Ship Structure Committee U.S. Coast Guard (G-M) 2100 Second Street, SW Washington, DC 20593				13. Type of Report and Period Covered Final Report	
				14. Sponsoring Agency Code G-M	
15. Supplementary Notes Sponsored by the Ship Structure Committee and its members agencies.					
16. Abstract <u>ABSTRACT</u> This report provides an up-to-date assessment of fatigue technology, directed specifically toward the marine industry. A comprehensive overview of fatigue analysis and design, a global review of fatigue including rules and regulations and current practices, and a fatigue analysis and design criteria, are provided as a general guideline to fatigue assessment. A detailed discussion of all fatigue parameters is grouped under three analysis blocks: <ul style="list-style-type: none"> • Fatigue stress model, covering environmental forces, structure response and loading, stress response amplitude operations (RAOs) and hot-spot stresses • Fatigue stress history model covering long-term distribution of environmental loading • Fatigue resistance of structures and damage assessment methodologies <p>The analyses and design parameters that affect fatigue assessment are discussed together with uncertainties and research gaps, to provide a basis for developing strategies for fatigue avoidance. Additional in-depth discussions of wave environment, stress concentration factors, etc. are presented in the appendixes.</p>					
17. Key Words Assessment of fatigue technology, fatigue stress models, fatigue stress history models, fatigue resistance, fatigue parameters and fatigue avoidance strategies			18. Distribution Statement Available from: National Technical Information Serv. U. S. Department of Commerce Springfield, VA 22151		
19. Security Classif. (of this report) Unclassified		20. Security Classif. (of this page) Unclassified		21. No. of Pages 194 Excl. Appendixes	22. Price

METRIC CONVERSION FACTORS

Approximate Conversions to Metric Measures

Symbol	When You Know	Multiply by	To Find	Symbol
LENGTH				
in	inches	*2.5	centimeters	cm
ft	feet	30	centimeters	cm
yd	yards	0.9	meters	m
mi	miles	1.6	kilometers	km
AREA				
in ²	square inches	6.5	square centimeters	cm ²
ft ²	square feet	0.09	square meters	m ²
yd ²	square yards	0.8	square meters	m ²
mi ²	square miles	2.6	square kilometers	km ²
	acres	0.4	hectares	ha
MASS (weight)				
oz	ounces	28	grams	g
lb	pounds	0.45	kilograms	kg
	short tons (2000 lb)	0.9	tonnes	t
VOLUME				
tsp	teaspoons	5	milliliters	ml
Tbsp	tablespoons	15	milliliters	ml
fl oz	fluid ounces	30	milliliters	ml
c	cups	0.24	liters	l
pt	pints	0.47	liters	l
qt	quarts	0.95	liters	l
gal	gallons	3.8	liters	l
ft ³	cubic feet	0.03	cubic meters	m ³
yd ³	cubic yards	0.76	cubic meters	m ³
TEMPERATURE (exact)				
°F	Fahrenheit temperature	5/9 (after subtracting 32)	Celsius temperature	°C

*1 in = 2.54 (exactly). For other exact conversions and more detailed tables, see NBS Misc. Publ. 286, Units of Weights and Measures, Price \$2.25, SD Catalog No. C13.10:286.



Approximate Conversions from Metric Measures

Symbol	When You Know	Multiply by	To Find	Symbol
LENGTH				
mm	millimeters	0.04	inches	in
cm	centimeters	0.4	inches	in
m	meters	3.3	feet	ft
m	meters	1.1	yards	yd
km	kilometers	0.6	miles	mi
AREA				
cm ²	square centimeters	0.16	square inches	in ²
m ²	square meters	1.2	square yards	yd ²
km ²	square kilometers	0.4	square miles	mi ²
ha	hectares (10,000 m ²)	2.5	acres	
MASS (weight)				
g	grams	0.035	ounces	oz
kg	kilograms	2.2	pounds	lb
t	tonnes (1000 kg)	1.1	short tons	
VOLUME				
ml	milliliters	0.03	fluid ounces	fl oz
l	liters	2.1	pints	pt
l	liters	1.06	quarts	qt
l	liters	0.26	gallons	gal
m ³	cubic meters	35	cubic feet	ft ³
m ³	cubic meters	1.3	cubic yards	yd ³
TEMPERATURE (exact)				
°C	Celsius temperature	9/5 (then add 32)	Fahrenheit temperature	°F

**FATIGUE TECHNOLOGY ASSESSMENT AND DEVELOPMENT OF
STRATEGIES FOR FATIGUE AVOIDANCE IN MARINE STRUCTURES**

FINAL REPORT

CONTENTS

Abstract	i
Contents	ii
List of Figures	ix
Common Terms	xi
1. INTRODUCTION	
1.1 Background	1-1
1.2 Objectives	1-2
1.3 Scope	1-3
2. OVERVIEW OF FATIGUE	
2.1 Fatigue Phenomena	2-1
2.2 Fatigue Analysis	2-3
2.2.1 Analysis Sequence	
2.2.2 Analysis Methods	
2.3 Significance of Fatigue Failure	2-7
2.4 Fatigue Failure Avoidance	2-8
3. FATIGUE DESIGN AND ANALYSES PARAMETERS	
3.1 Review of Fatigue Design Parameters	3-1
3.1.1 Design Parameters	
3.1.2 Fabrication and Post Fabrication Parameters	
3.1.3 In-Service Parameters	
3.2 Review Of Fatigue Analysis Parameters	3-7
3.2.1 Fatigue Analysis Criteria	
3.2.2 Interacting Parameters	
3.2.3 Stress Model Parameters	
3.2.4 Stress History Model Parameters	
3.2.5 Fatigue Damage Computation Parameters	

4.	GLOBAL REVIEW OF FATIGUE	
4.1	Applicable Analysis Methods	4-1
4.1.1	Background	
4.1.2	Simplified Analysis and Design Methods	
4.1.3	Detailed Analyses and Design Methods	
4.1.4	Other Methods	
4.2	Fatigue Rules and Regulations	4-16
4.2.1	Applicable Methods	
4.2.2	SCFs, S-N Curves and Cumulative Damage	
4.2.3	Fatigue Analysis Based on Fracture Mechanics	
4.3	Current Industry Practices	4-23
4.3.1	Ordinary Designs	
4.3.2	Specialized Designs	
4.4	Sensitivity of Fatigue Parameters	4-25
4.5	Fatigue Design and Analysis Criteria	4-26
4.5.1	Basis for the Preparation of Criteria	
4.5.2	Applicable Software	
4.5.3	Fatigue Versus Other Design and Scheduling Requirements	
5.	FATIGUE STRESS MODELS	
5.1	Review of Applicable Modeling Strategies	5-1
5.1.1	Modeling Strategies	
5.1.2	Comparison of Structures	
5.2	Floating Marine Structures	5-4
5.2.1	Ship Structures	
5.2.2	Stationary Marine Structures	
5.2.3	Overview and Recommendations	
5.3	Bottom-Supported Marine Structures	5-16
5.3.1	Load or Hydrodynamics Model	
5.3.2	Mass Model	
5.3.3	Motions Model and Analyses Techniques	
5.3.4	Stiffness Model	
5.3.5	Overview and Recommendations	
5.4	Development of Hot Spot Stresses	5-25
5.4.1	Nominal Stresses and Stress RAOs	
5.4.2	Stress Concentration Factors and Hot Spot Stresses	
5.4.3	Empirical Equations	
5.4.4	Illustration of a T-Joint SCFs	
5.4.5	Overview and Recommendations	

6.	FATIGUE STRESS HISTORY MODELS	
6.1	Determination of Fatigue Environments	6-1
6.1.1	Data Sources	
6.1.2	Wave and Wind Spectra	
6.1.3	Scatter Diagram	
6.1.4	Directionality and Spreading	
6.2	Stress Spectrum	6-10
6.2.1	Stress RAOs	
6.2.2	Response Analysis	
6.2.3	Uncertainties and Gaps in Stress Spectrum Development	
6.2.4	Decompose into Stress Record	
6.3	Time-Domain Analyses	6-14
6.3.1	Stress Statistics	
6.3.2	70 Percentile Spectra	
6.4	Overview and Recommendations	6-15
7.	FATIGUE DAMAGE ASSESSMENT	
7.1	Basic Principles of Fatigue Damage Assessment	7-1
7.2	S-N Curves	7-2
7.2.1	Design Parameters	
7.2.2	Fabrication and Post-Fabrication Parameters	
7.2.3	Environmental Parameters	
7.3	Fatigue Damage Computation	7-11
7.3.1	Miner's Rule	
7.3.2	Alternative Rules	
7.4	Stress History and Upgraded Miner's Rule	7-14
7.4.1	Background	
7.4.2	Miner's Rule Incorporating Rainflow Correction	
7.4.3	Other Alternatives	
7.5	Overview and Recommendations	7-19
7.5.1	Application of S-N Curves	
7.5.2	Fatigue Damage Computation	

8.	FATIGUE DUE TO VORTEX SHEDDING	
8.1	Vortex Shedding Phenomenon	8-1
	8.1.1 Background	
	8.1.2 Vortex Induced Vibrations (VIV)	
8.2	Analyses and Design For Vortex Shedding	8-3
	8.2.1 Susceptibility to Vortex Shedding	
	8.2.2 VIV Response and Stresses	
8.3	Fatigue Damage Assessment	8-5
8.4	Methods of Minimizing Vortex Shedding Oscillations	8-6
8.5	Recommendations	8-6
9.	FATIGUE AVOIDANCE STRATEGY	
9.1	Review of Factors Contributing to Failure	9-1
9.2	Basic Fatigue Avoidance Strategies	9-2
	9.2.1 Basic Premises	
	9.2.2 Fatigue Avoidance Strategies	
9.3	Fatigue Strength Improvement Strategies	9-7
	9.3.1 Fabrication Effects	
	9.3.2 Post-Fabrication Strength Improvement	
	9.3.3 Comparison of Strength Improvement Strategies	
9.4	Fatigue Analysis Strategies	9-14
	9.4.1 Review of Uncertainties, Gaps and Research Needs	
	9.4.2 Recent Research Activities	
	9.4.3 Cost-Effective Analysis Strategies	
9.5	Recommendations	9-22
	9.5.1 Research Priorities	
	9.5.2 Rules and Regulations	
10.	REFERENCES	10-1

APPENDICIES

A. REVIEW OF OCEAN ENVIRONMENT

A.1	IRREGULAR WAVES	A-1
A.2	PROBABILITY CHARACTERISTICS OF WAVE SPECTRA	A-5
	A.2.1 Characteristic Frequencies and Periods	
	A.2.2 Characteristic Wave Heights	
A.3	WAVE SPECTRA FORMULAS	A-11
	A.3.1 Bretschneider and ISSC Spectrum	
	A.3.2 Pierson-Moskowitz Spectrum	
	A.3.3 JONSWAP and Related Spectra	
	A.3.4 Scott and Scott-Wiegel Spectra	
A.4	SELECTING A WAVE SPECTRUM	A-16
	A.4.1 Wave Hindcasting	
	A.4.2 Direct Wave Measurements	
A.5	WAVE SCATTER DIAGRAM	A-19
A.6	WAVE EXCEEDANCE CURVE	A-21
A.7	WAVE HISTOGRAM AND THE RAYLEIGH DISTRIBUTION	A-22
A.8	EXTREME VALUES AND THE WEIBULL DISTRIBUTION	A-22
A.9	WIND ENVIRONMENT	A-23
	A.9.1 Air Turbulence, Surface Roughness and Wind Profile	
	A.9.2 Applied, Mean and Cyclic Velocities	
	A.9.3 Gust Spectra	
A.10	REFERENCES	A-28

B.	REVIEW OF LINEAR SYSTEM RESPONSE TO RANDOM EXCITATION	
B.1	GENERAL	B-1
	B.1.1 Introduction	
	B.1.2 Abstract	
	B.1.3 Purpose	
B.2	RESPONSE TO RANDOM WAVES	B-2
	B.2.1 Spectrum Analysis Procedure	
	B.2.2 Transfer Function	
	B.2.3 Wave Spectra	
	B.2.4 Force Spectrum	
	B.2.5 White Noise Spectrum	
B.3	EXTREME RESPONSE	B-15
	B.3.1 Maximum Wave Height Method	
	B.3.2 Wave Spectrum Method	
B.4	OPERATIONAL RESPONSE	B-17
	B.4.1 Special Family Method	
	B.4.2 Wave Spectrum Method	
C.	STRESS CONCENTRATION FACTORS	
C.1	OVERVIEW	C-1
C.2	STRESS CONCENTRATION FACTOR EQUATIONS	C-4
	C.2.1 Kuang with Marshall Reduction	
	C.2.2 Smedley-Wordsworth	
C.3	PARAMETRIC STUDY RESULTS	C-6
	C.3.1 Figures	
	C.3.2 Tables	
C.4	FINITE ELEMENT ANALYSES RESULTS	C-15
	C.3.1 Column-Girder Connection	
C.5	REFERENCES	C-17

D. VORTEX SHEDDING AVOIDANCE AND FATIGUE DAMAGE COMPUTATION

	NOMENCLATURE	i
D.1	INTRODUCTION	D-1
D.2	VORTEX SHEDDING PARAMETERS	D-2
D.3	SUSCEPTIBILITY TO VORTEX SHEDDING	D-7
	D.3.1 In-Line Vortex Shedding	
	D.3.2 Cross-Flow Vortex Shedding	
	D.3.3 Critical Flow Velocities	
D.4	AMPLITUDES OF VIBRATION	D-9
	D.4.1 In-Line Vortex Shedding Amplitudes	
	D.4.2 Cross-Flow Vortex Shedding Amplitudes	
D.5	STRESSES DUE TO VORTEX SHEDDING	D-13
D.6	FATIGUE LIFE EVALUATION	D-14
D.7	EXAMPLE PROBLEMS	D-17
	D.7.1 Avoidance of Wind-Induced Cross-Flow Vortex Shedding	
	D.7.2 Analysis for Wind-Induced Cross-Flow Vortex Shedding	
D.8	METHODS OF MINIMIZING VORTEX SHEDDING OSCILLATIONS	D-23
	D.8.1 Control of Structural Design	
	D.8.2 Mass and Damping	
	D.8.3 Devices and Spoilers	
D.9	REFERENCES	D-27

LIST OF FIGURES

<u>FIGURE</u>	<u>TITLE</u>
2-1	Fatigue Phenomena Block Diagram Summary
2-2	Fatigue Analysis Block Diagram Summary
2-3	Mobile and Stationary Marine Structures
3-1	Fatigue Design and Analysis Parameters
3-2	Design Parameters
3-3	Fabrication and Post-Fabrication Parameters
3-4	In-Service Parameters
3-5	Strength Model Parameters
3-6	Time-History Model Parameters
3-7	Typical S-N Curves
4-1	Typical Fatigue Sensitive Ship Structure Details
4-2	Munse's Ship Details Design Procedure
4-3	A Typical Deterministic Fatigue Analysis Flow Chart
4-4	A Typical Spectral Fatigue Analysis Flow Chart
4-5	The DnV X- and The New T-Curves
4-6	API X- and X'-Curves and DnV T-Curve
4-7	Comparison of Recommendations: U.K. Guidance Notes, API RP 2A and DnV
5-1	Comparison of Heave Added Mass and Damping Coefficients Based on Different Methods
5-2	Comparison of Wave Loading Based on Conventional and Consistent Methods
5-3	Comparison of Mean C_d and C_m Values for Christchurch Bay Tower
5-4	Dynamic Wave Load Analysis Methodology
5-5	Comparison of Detailed Fatigue Analyses Techniques
5-6	Joint Geometry and Loading Types
5-7	Simple Joint Terminology
5-8	Common Joint Types
5-9	Joint Classification by Load Distribution
5-10	Sample Evaluation of a T-Joint
6-1	Typical Wave Scatter Diagram
6-2	Platform with Different Dynamic Response Characteristics in Two Orthogonal Axes
7-1	S-N Curve for a Transverse Butt Weld and Test Data
7-2	Theoretical Thickness Effect for a Cruciform Joint
7-3	Weld Profiles for API X and X' S-N Curves
7-4	DEn Guidance Notes Recommended Weld Profiling and Undercut
8-1	Regimes of Fluid Flow Across Circular Cylinders

LIST OF FIGURES
(cont.)

<u>FIGURE</u>	<u>TITLE</u>
9-1	Typical Methods to Improve Fatigue Strength
9-2	Typical Weld Toe Defects and Corrective Measures
9-3	Fatigue Life Improvement Due to Weld Toe Abrasive Water Jet Erosion
9-4	Comparison of Fatigue Strength Improvement Techniques
9-5	Summary of Relevant Research Activities

COMMON TERMS
USED
IN FATIGUE AND IN THIS REPORT

- BTM : Bottom turret mooring system for a tanker. Can be permanent or disconnectable.
- CAPEX : Capital expenditures incurred prior to structure commissioning and beginning operation.
- CATHODIC PROTECTION : An approach to reduce material corrosive action by making it the cathode of an electrolytic cell. This is done by utilizing sacrificial anodes (i.e. coupling with more electropositive metal) or impressed current.
- COMPLEX JOINT : An intersection of several members, having a subassemblage of component members. Applicable to a column-to-pontoon joint of a semisubmersible or a large leg joint of a platform containing stiffened bulkheads, diaphragms and other tubulars.
- CRUCIFORM JOINT : A transverse load carrying joint made up two plates welded on to either side of a perpendicular plate utilizing full penetration welds.
- DYNAMIC AMPLIFICATION FACTOR (DAF) : The maximum dynamic and static load ratios, such as the DAF applicable to base shear or overturning moment.
- HEAT AFFECTED ZONE (HAZ) : The area of parent plate material susceptible to material degradation due to welding process.

- HOT-SPOT STRESS** : The hot-spot stress is the peak stress in the immediate vicinity of a structural discontinuity, such as the stiffener edge or a cutout. On a tubular joint, the hot-spot stress usually occurs at the weld toe of the incoming tubular (brace) or the main tubular (chord).
- FATIGUE LIFE** : The number of stress cycles that occur before failure, typically corresponding to either first discernible surface cracking (N_1) or the first occurrence of through thickness cracking. (N_2)
- FATIGUE STRENGTH** : The stress range corresponding to a number of cycles at which failure occurs.
- FPSO** : Floating production, storage and offloading tanker.
- IRREGULARITY FACTOR** : The ratio of mean crossings with positive slopes to the number of peaks or valleys in the stress history.
- KEULEGAN-CARPENTER NUMBER, K_C** : A parameter used to define the flow properties around a cylinder. Equal to the product of the amplitude of velocity and oscillation period, divided by the cylinder diameter.
- MEAN ZERO-CROSSING PERIOD** : The mean zero-crossing period is the average time between successive wave crossings with a positive slope (up-crossing) of the zero axis in a time history.

- MODELING ERROR (X_{me}) : Typically defined as the ratio of actual behavior of the structure to the one predicted by the model. It is often used to assess the accuracy of excitational loads, motions, and stresses.
- MODELING UNCERTAINTY : The random component of the modeling error, X_{me} , and defined by its coefficient of variation, (C.O.V.) χ_{me} .
- NARROW-BAND LOADING : The stress cycles are readily identifiable, making the choice of counting method of stress cycles immaterial.
- NOMINAL STRESS : The nominal stress is the stress obtained by dividing the member generalized forces (forces and moments) by member section properties (cross-sectional area and section modulus).
- OPEX : Operating expenditures due to maintenance, inspection, repairs as well as cost of fuel, variables, personnel, etc. during the life of a structure.
- PLASMA DRESSING : Application of plasma arc welding technique to remelt the weld toe (similar to TIG dressing)
- POST WELD HEAT TREATMENT (PWHT) : A procedure of heating a welded joint to relieve residual fabrication stresses. Typically, the joint is heated to 1076 1150°F (580-620°C), held at that temperature for about an hour for each one inch (2.5 min/mm) thickness, and cooled in air.

- QA/QC : Quality Assurance/Quality Control
Quality assurance generally refers to the procedures and methods put into effect to ensure quality a priori, while quality control generally refers to reviews and checks after-the-fact to implement corrective measures, as necessary.
- RANDOM WAVES : The term random waves is used to characterize the irregular sea surface and associated water particle kinematics that occur in the ocean. Analytically random waves are represented as a summation of sinusoidal waves of different heights, periods, phases and directions.
- REGULAR WAVES : Regular waves are unidirectional and associated water particle kinematics and sea surface elevations are periodic.
- S-N CURVE : The S-N curves define the fatigue strength of a detail/joint by representing test data in an empirical form to establish a relationship between stress ranges and the number of cycles of stress range for fatigue failure.
- SEA STATE : An oceanographic environment with a wave height range characterized as a stationary random process for a specific duration.
- SIGNIFICANT WAVE HEIGHT : A statistic typically used to characterize the wave heights in a sea state. It is defined as the average height of the heighest one-third of all the individual waves present in a sea state.

- SIMPLE JOINT** : An intersection of two or more structural members. Also applicable to an intersection of unstiffened or ring-stiffened cylinders.
- STEADY STATE** : Generally refers to the periodic response of a dynamic system after initial starting transients have decayed to negligible amplitude.
- STRESS CONCENTRATION FACTOR (SCF)** : The ratio of hot-spot stress to the nominal stress (in neighborhood of hot-spot) and often maximized at geometric discontinuities.
- STRIP THEORY** : Applied to various strip methods to determine the hydrodynamic loadings on long slender bodies and can account for the effect of diffracted and radiated waves.
- TIG DRESSING** : Tungsten-inert-gas dressing is applied to remelt the weld toe material to reduce both the SCF by minimizing discontinuities and to remove defects such as slag inclusions.
- TRANSFER FUNCTION** : A transfer function defines the unitized structural response as a function of frequency (eg ratio of structural response to the wave amplitude applicable for each frequency).
- WELD TOE** : The point of intersection of the weld profile and parent plate.
- WIDE-BAND LOADING** : The smaller stress cycles are interspersed among larger stress cycles, making the definition of stress cycle more difficult. The use of different counting methods will result in different fatigue damage predictions.

1. INTRODUCTION

1.1 BACKGROUND

The detailed design of a structure focuses largely on sizing the structures component members and on developing the details to resist extreme functional and environmental loads. The analysis and design to resist extreme loading conditions is intended primarily to prevent material yield and buckling failures; the details are also chosen to help prevent fatigue failures due to cyclic loading.

The use of proven details and selection of steel with material properties resisting propagation of defects are longstanding design practices. Analysis and design to ensure that fatigue life is substantially in excess of the design life became generally accepted in the late 1960s. Initial simplistic analysis methods have gradually become more sophisticated. Oceanographic data collected over the last twenty years now allow better definition of wind and wave data over many parts of the world. Several test programs have allowed comparison of actual and analytically computed loads on marine structures. Laboratory test data and data from structures in service now allow better definition of defect (crack) propagation in an ocean environment.

Although engineers have progressed beyond simplified deterministic analyses, occasionally venturing into full probabilistic analysis, substantial uncertainties still are associated with fatigue analysis and design. Fatigue life may change dramatically with a small change in any of many variables, requiring that the fatigue analysis and design of a marine structure be conducted as a series of parametric studies. The results of these studies, used to upgrade fatigue-sensitive areas/details of the structure, allow development of a design that will provide a satisfactory level of confidence against fatigue failure.

Review of past fatigue failures shows that it is often difficult to determine whether a failure was due to poor design, material

imperfections, fabrication defects, improper inspection or maintenance, unpredicted loads or, more likely, a combination of these interacting variables. As the complexity of marine structures increases, better understanding of the variables contributing to the integrity of structure components and the global response of the structure becomes very important. Although several excellent documents on fatigue are available, most address fatigue design of either ship or offshore platform structures (References 1.1 through 1.8). Thus the engineer may have difficulty in assessing the significance of fatigue within the context of overall design of marine structures. It is also difficult to evaluate the sensitivity and interaction of variables affecting fatigue life or the relative uncertainties that are built in. The UEG Recommendations (Reference 1.8), although applicable to only tubular joints, provides a detailed discussion of various design requirements and code recommendations.

Fatigue analysis and design must be carried out while the structure is being designed and revised to satisfy numerous other pre-service and in-service loading conditions. Thus, to achieve an effective design the overall design strategy should incorporate fatigue as an integral part of design, with primary impact on design details, redundancy, material and fabrication specifications, operational performance, inspection program and cost. Because structures' susceptibility to fatigue and the severity of fatigue environment varies, the chosen fatigue design and analysis methodology, the sequence, and the extent of the fatigue design effort should be compatible with the overall design program and should be carefully planned and monitored to prevent construction delays or costly modifications during construction.

1.2

OBJECTIVES

This document was prepared to provide the engineer with an up-to-date assessment of fatigue analysis and design. It may be used either as a comprehensive guideline or a quick reference source. The first four sections of the report provide an overview and

general assessment of fatigue while the latter five sections provide in-depth discussion. The objectives of the document are:

- Review, assess and document all fatigue parameters that may be grouped into a set of parameters (i.e., strength models, stress history models, analysis methods, etc.)
- Review, assess and document strengths and weaknesses of current fatigue analysis and design procedures in conjunction with existing codes and standards.
- Document research gaps and recommend additional research based on numerous analytical and experimental work results published every year.
- Recommend a guideline on fatigue avoidance strategy based on numerous variables contributing to the uncertainty of fatigue life, on recent research results and on current practices.
- Assess and discuss the accuracy of fatigue life estimation and the complexity of computation based on the implication of uncertainties associated with the fatigue parameters and the time and effort necessary to carry out fatigue analysis and design to various levels of complexity.

1.3

SCOPE

The following tasks were key elements in preparation of this document.

- Review and assess global fatigue analysis, including fatigue as an integral part of design effort, current industry practices, codes and standards, and the implications of fatigue damage.
- Review and assess all parameters within the stress model umbrella for their relative accuracy as well as application,

including environmental conditions, structural response, generation of loads, development of stress response amplitude operators (RAOs) and hot-spot stresses.

- Review and assess all parameters within the stress history model umbrella, including scatter diagram, hindcasting, wave spectra and application ranges.
- Review fatigue damage assessment methodologies, including the effects of numerous analysis and design uncertainties, and prepare a guideline to both improve fatigue performance of marine structures and simplify fatigue analysis.
- Report the findings in a clear and concise document, including directly applicable unpublished and published data.

2. OVERVIEW OF FATIGUE

2.1 FATIGUE PHENOMENA

Metal structures subjected to variable or repeated loads can fail without ever reaching their static strength design loads. This type of failure, which consists of the formation and growth of a crack or cracks, has come to be known as "fatigue".

Failures observed due to the growth of defects subjected to cyclic loadings is due to a very complex phenomena, affected by many parameters. Any environment or condition that results in cyclic loading and reversal of component stresses may cause fatigue damage.

Cyclic stresses are typically caused by machinery vibrations, temperature changes and wind and wave actions. But although vibrations and temperature changes may be important to fatigue in a local component, these loadings are not a major concern in the global behavior of typical marine structures. Thus, the overview presented in this section addresses wave and wind environments, excitation forces on mobile and stationary structures and the response of these structures to excitation forces.

A defect subjected to a large number of cyclic stresses undergoes three phases of stable crack growth:

- Crack initiation, or development of a defect into a macroscopic crack.
- Crack propagation, or development of a crack into a critical size.
- Cracked weldment residual strength exceedence.

The relative durations of these three phases depend on many variables, including material properties, defect geometry, structure stiffness, stress cycle magnitudes, distribution and sequence, operating environment and maintenance. The objective is to prevent fatigue failure by designing to ensure that the time required to

complete the three-phase stable crack growth is always greater than the design fatigue life.

The basic characteristics of defects and the fatigue phenomena may be summarized as:

- Even the most thorough inspections at the fabrication facility will not reveal very small defects (less than 0.5 mm).
- These defects will grow when subjected to cyclic stresses due to environmental loads, structure dynamics (vortex shedding, machinery vibrations, etc.), temperature changes, etc.
- Repeated cyclic stresses and defect growth are additive, making the fatigue damage cumulative.
- In most cases, fatigue is insensitive to the presence of constant loads. Consequently, stress ranges (i.e., peak-to-peak values) are used to characterize fatigue stresses.
- Although a small number of extreme stress ranges may contribute to fatigue damage, most fatigue damage is due to the occurrence of a large number of small stress ranges.
- Poor structural design details will amplify peak stresses.
- Distortions and residual stresses introduced during original fabrication (as well as extensive repair efforts) often adversely affect material resistance to crack growth.
- Corrosion and ocean environment adversely affect material resistance to crack growth.

A simplified summary of fatigue phenomena is presented on Figure 2-1.

2.2 FATIGUE ANALYSIS

2.2.1 Analysis Sequence

The basic fatigue analysis sequence is shown as a block diagram on Figure 2-2 and further discussed in this overview and in Sections 3 through 7.

Fatigue Environment

Wave and wind environments are both site- and time-dependent. A brief observation of wind and the waves it generates shows that they are random phenomena, where wind speed, direction and duration and wave height, period and breadth continually change.

Although the real sea is random, the wave environment can be described by two methods. In the deterministic method, the sea is described as composed of identical, regular, individual waves. In the spectral method, the sea is described as a function of sea surface elevation due to regular waves combining to form an irregular sea.

The service life of a vessel/structure may be 20 to 40 years. During the service life more than 500 million waves are likely to be applied on the vessel/structure. The fatigue environment is often defined based on a series of 15 or 20 minutes records taken every 3 or 4 hours. The environment is summarized in a wave scatter diagram. The wave scatter diagram is a grid of boxes with rows of equal H_s (significant wave height) and columns for characteristic period, often T_z (zero up-crossing period) or T_s (significant period).

For example: Wave records taken by a weather buoy can be sampled every four hours. The sample records are reduced by Fast Fourier Transform (FFT) and integrated to derive the statistical parameters of H_s and T_z . The whole of the sample parameters are sorted by H_s and T_z . The number of samples of each H_s - T_z combination are placed in the corresponding box in the scatter diagram. Often the scatter

diagram boxes are normalized so that the sum of all of the numbers is 1000. The shapes of the reduced spectra can be compared and a representative spectrum formula can be fit to the typical shape. The JONSWAP spectrum is often used to fit sampled spectra shapes, because of the flexibility offered by the Gamma and Sigma parameters; see Appendix A, Section 3.3. Similar seastates are then combined into a scatter diagram.

The wind loading on a structure is composed of mean and cyclic components. To carry out a fatigue analysis of a structure subjected to cyclic wind loading the magnitude of loading and associated frequencies must be quantified. Individual component members of a structure subjected to continuous mean wind loading may be susceptible to vortex shedding vibrations. A comprehensive coverage of wind-induced fatigue phenomena is presented in Appendix D.

A comprehensive review of ocean environment, covering both waves and wind, is presented in Appendices A and B.

Fatigue Stress Model

The term fatigue stress model is often used to define a combination of analysis steps, covering:

- Generation of loads
- Structural analysis to determine nominal stresses
- Estimation of hot spot stresses

These analysis steps are identified as fatigue analysis blocks and combined into a single stress model block on Figure 2-2.

The analysis steps undertaken to determine the local hot spot stresses are sequential and an inaccuracy at any step contributes to compounding of the overall inaccuracy. Although many variables directly influence the accuracy of estimated hot spot stresses, some of the more important variables are listed below:

- Loads generated as affected by the definition of environment, selection of wave theories, response characteristics of the vessel/structure subjected to excitational environmental loads and computer modeling.
- Structural analysis as affected by the computer model, software package and engineering decision/selection of locations for determining of nominal stress.
- Hot spot stresses as affected by determination of stress concentration factors (SCFs determined from empirical formulas based on databases of numerical and experimental work) and the engineering decision on multiple recomputation of SCFs to account for variations in stress distribution (i.e., reclassification of detail/joint for each transfer function).

Another very important variable, fatigue analysis method, is briefly discussed in Section 2.2.2.

Fatigue Stress History Model

The stresses computed may be either stress states (defined by wave height and wave period and representing a single cycle of loading) or peak values associated with discrete waves. A generalized stress history model combines this data with long-term wind and wave distributions (scatter diagram, spectra, directionality, etc.) to develop a long-term distribution of stresses.

Material Resistance to Fatigue Failure (Strength Model)

The material resistance to fatigue failure will primarily depend on the characteristics of detail/joint geometry, material chemical composition and mechanical properties, and the service environment.

The material resistance is typically determined in a laboratory environment by the application of constant amplitude stress cycle on various detail/joint geometries until fatigue failure occurs. By

carrying out similar tests for different stress amplitudes a relationship between the stress amplitude (S) and the number of cycles (N) is established. The S-N curves developed for simple details (i.e., stiffener, cutout, etc., applicable for most ship details) account for the peak (hot spot) stresses and can be directly used with the member nominal stresses.

The tubular joint details (i.e., T, K, Y, etc., joints applicable for an offshore platform) exhibit a wide variety of joint configurations and details. The S-N curves for tubular joint details do not account for hot spot stresses, requiring the application of stress concentration factors (SCFs) on computed nominal stresses.

Cumulative Fatigue Damage

A relatively simple approach used to obtain fatigue damage requires dividing of stress range distribution into constant amplitude stress range blocks, assuming that the damage per load cycle is the same at a given stress range. The damage for each constant stress block is defined as a ratio of the number of cycles of the stress block required to reach failure. The most often used Palmgren-Miner linear damage rule defines the cumulative damage as the sum of fatigue damage incurred at every stress block.

2.2.2 Analysis Methods

A suitable fatigue analysis method depends on many parameters, including structure configuration, fatigue environment, operational characteristics and the design requirements. A fatigue analysis method may be deterministic or probabilistic. A fully probabilistic method accounting for uncertainties in defining stresses due to random loads, scatter in S-N data and randomness of failure is suited to marine structures. However, less complex deterministic methods are primarily used to analyze the fatigue lives of marine structures.

A deterministic method is sometimes identified as probabilistic analysis as the randomness of the ocean environment is accounted for by incorporating the wave spectra. Thus, depending on how the loads are generated, the fatigue analyses method may be identified as:

- Deterministic - Single Wave
- Spectral - Regular Waves in Time-Domain
- Spectral - Regular Waves in Frequency-Domain
- Spectral - Irregular Waves in Time-Domain
- Spectral - Wind Gust

Further discussion on fatigue analyses parameters and analysis sequence is presented in Sections 3 and 4, respectively.

2.3

SIGNIFICANCE OF FATIGUE FAILURE

An improper design may lead to an unacceptable catastrophic fatigue failure, resulting in loss of life and damage to the environment.

Non-catastrophic fatigue failures are also unacceptable due to difficulty and cost of repairs as well as the need to increase costly inspection and maintenance intervals.

Numerous marine structures of different configurations are in operation. As illustrated on Figure 2-3, these structures may be grouped as "mobile" or "stationary", depending on their functional requirement. Although mobile vessels/structure can be moved to a shipyard for repairs, the total cost of the repair includes downtime. Stationary offshore vessel/structure inspections and repairs are extremely costly due to on-location work and their operating environment, yet the effectiveness of repairs is often uncertain. Thus, for both mobile and stationary marine structures, it is essential to consider avoidance of fatigue failure at every phase of design and fabrication.

FATIGUE FAILURE AVOIDANCE

Fatigue failure avoidance is not just a motto, but a goal that can be achieved with relative ease if the fatigue design is an integral part of the original design program.

Despite their diversity, most marine structures are designed to meet established functional requirements, environmental criteria and rules and regulations. The design process is executed through several stages to optimize structure configuration and operational performance. Since the objectives identified to achieve optimization are not necessarily compatible, various trade-offs become necessary. To ensure that fatigue failure avoidance strategy is compatible with the overall design objectives an interactive design sequence is essential.

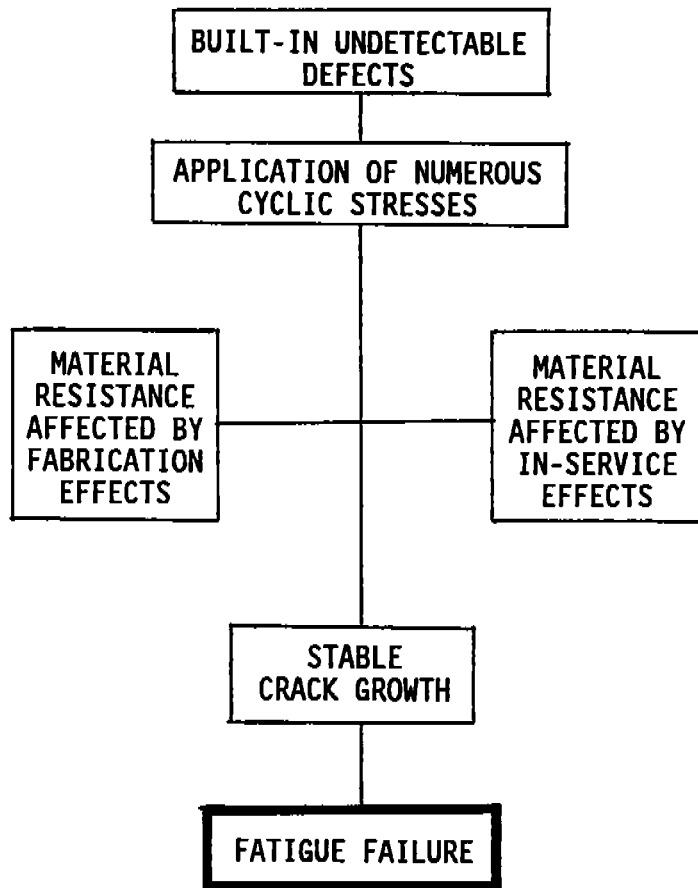


Figure 2-1 Fatigue Phenomena Block Diagram Summary

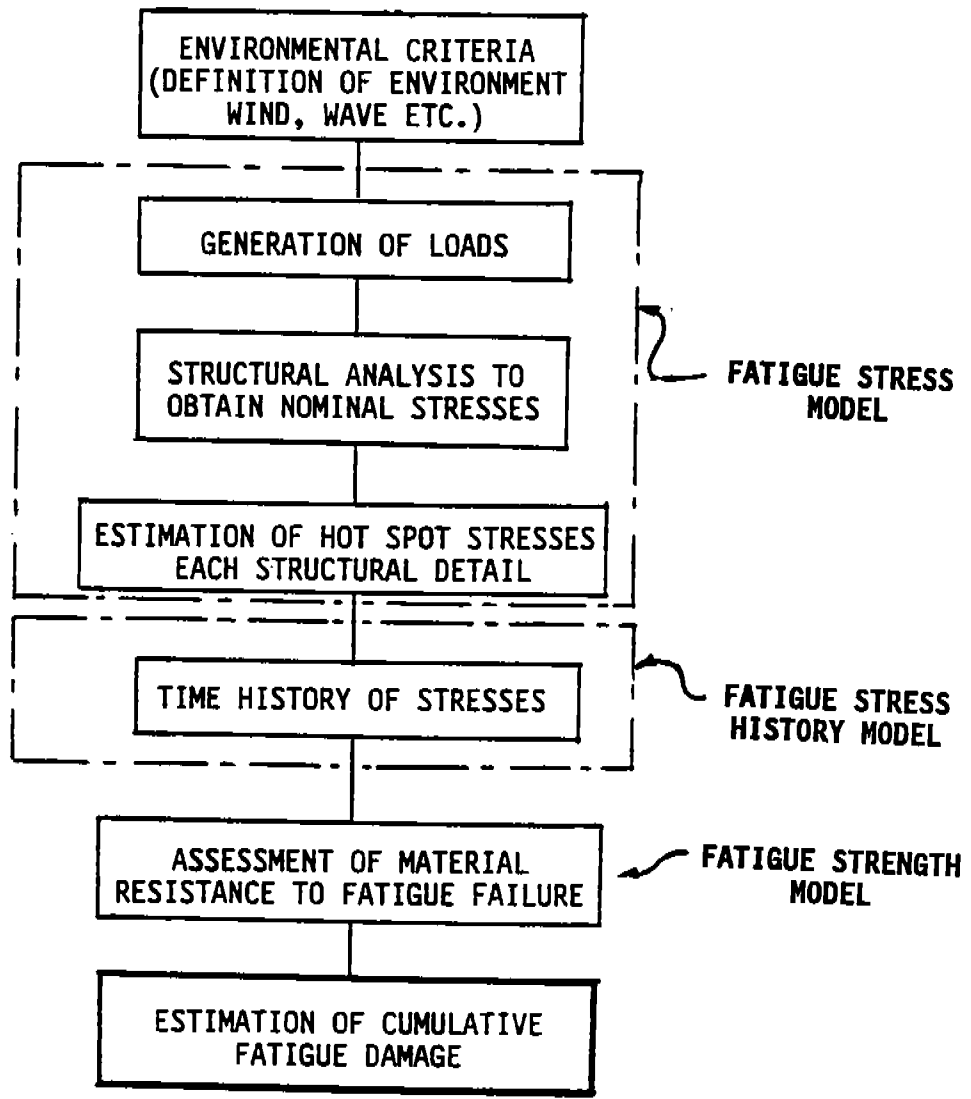


Figure 2-2 Fatigue Analysis Block Diagram Summary

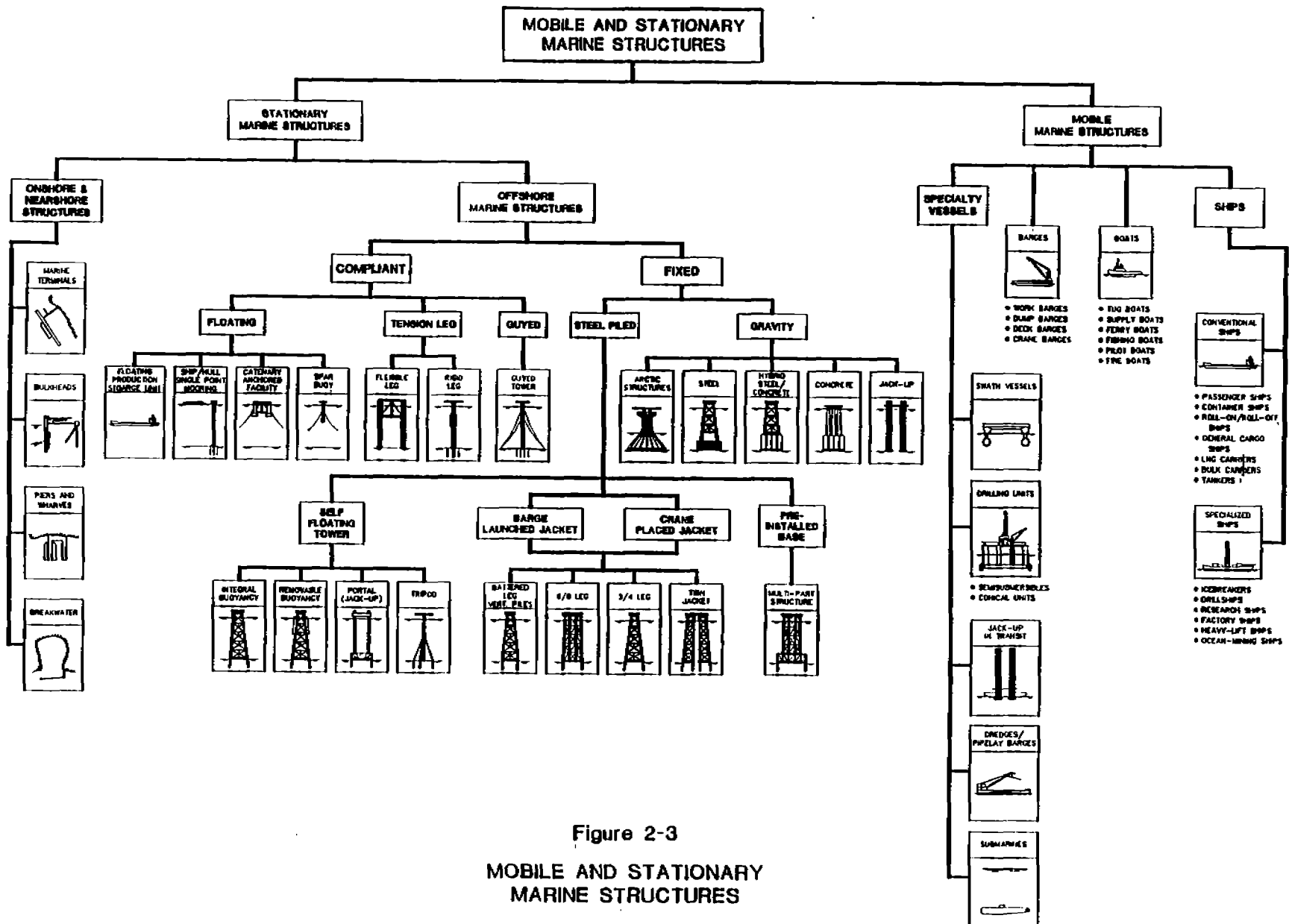


Figure 2-3

MOBILE AND STATIONARY MARINE STRUCTURES

W
W

(THIS PAGE INTENTIONALLY LEFT BLANK)

3. **FATIGUE DESIGN AND ANALYSIS PARAMETERS**

One approach to assess the variables, parameters and assumptions on fatigue is to separate the design from analysis. Fatigue design parameters do affect the fatigue performance and they can be revised during the design process to optimize the structure.

Fatigue analysis parameters and assumptions affect the computed fatigue life of the structure. The analyses approach selected should be compatible with the structure configuration and its fatigue sensitivity. Both fatigue design and analyses parameters are summarized on Figure 3-1 and discussed in the following sections.

3.1 REVIEW OF FATIGUE DESIGN PARAMETERS

All of the parameters affecting fatigue performance of a marine structure and its components can be grouped into three categories based on both function and chronological order. The three groups are:

- Design parameters
- Fabrication and post-fabrication parameters
- In-Service parameters

The parameters in these three groups actually dictate crack initiation, crack propagation to a critical size and exceedance of cracked weldment residual strength. While these parameters are assessed and incorporated into a design program to qualitatively enhance fatigue performance, quantitative analyses are necessary to verify that the structure's components have satisfactory fatigue lives. Fatigue analysis parameters and analysis sequence are discussed in Sections 3.2 and 3.3, respectively.

3.1.1 Design Parameters

There are numerous parameters that can be incorporated into a design to enhance fatigue performance. These parameters are grouped into four general categories:

- Global configuration
- Component characteristics and structural details
- Material selection
- Fabrication procedures and specifications

The effect of these parameters are summarized on Figure 3-2 and discussed as follows.

Global Configuration

The overall configuration of every marine structure, mobile or stationary, should be reviewed to ensure that the applied environmental forces will be minimized. Trade-offs are often necessary to ensure that the extreme environment and operating environment loadings are both as low as possible (although it may be that neither is minimized) to ensure overall optimum performance.

Planned redundancy is extremely beneficial to fatigue performance because alternative load paths are provided to accommodate a fatigue failure. Such redundancies prevent catastrophic failures, and also provide ample time for repair of local failures.

Component Characteristic and Structural Details

Wherever possible, a component's arrangement and stiffness should be similar to that of adjacent components to ensure a relatively uniform load distribution. Nominal stresses at a given detail will be amplified because of the geometry of the detail. The ratio of the peak or hot spot stress to the nominal stress, known as the stress concentration factor (SCF), is affected by many variables, including component member load paths, interface plate thicknesses

and in-plane/out-of-plane angles, and stub-to-chord diameter ratios (for tubular members).

The arrangement of structural details is very important from a standpoint of their configuration (affecting SCFs) and access (affecting quality of work). Shiphull stiffeners are often arranged with these considerations in mind. Similarly, tubular interfaces of less than 30 degrees are not desirable in order to ensure reasonable access for assembly and inspection.

Material Selection

Steel material is selected not only for strength but also for its other characteristics, including weldability and durability. Thus, the material selected should have both the chemical composition and the mechanical properties to optimize its performance. The use of higher strength steel requires specification of higher material toughness requirements to meet the limits on fabrication flaws. Since the material with higher toughness can tolerate larger loads for a given flaw without brittle fracture during its service life, such a material is preferred.

Impurities in steel (including Carbon, Nitrogen, Phosphorus, Sulphur and Silicon) can cause temper embrittlement, thereby decreasing notch toughness during the cooling of quenched and tempered steel. Desirable notch toughness (Charpy) and Crack Tip Opening Displacement (CTOD) test results are not always achieved at the fabrication yard. Inspection of the welded joint root, weld material and the heat-affected zone (HAZ) may show degradation of root toughness, sometimes extending into the parent material beyond the HAZ.

Studies carried out by Soyak et al (Reference 3.1) to assess fracture behavior in a low toughness HAZ indicated that a small low-toughness area in the HAZ can be masked by the higher-toughness area surrounding it. Thus, Soyak et al recommend requiring testing of

not three but five Charpy specimens from the low-toughness HAZ region to more accurately predict brittle fracture.

On the other hand, crack-toughness levels implied in the impact tests required in design guidelines may be overly conservative. Pense's work (Reference 3.2) indicates that the ship hull strain rates during crack initiation, propagation and arrest are lower than those estimated, confirming higher levels of crack-toughness.

Fabrication Specifications and Procedures

Degradation of root toughness extending into the parent material beyond the HAZ can be caused by procedures used in the fabrication yard. Loosely specified fabrication tolerances often result in fabrication and assembly distortions and may cause strain aging embrittlement. Unnecessarily tight tolerances could result in repair work that might contribute to degradation of material.

Fabrication procedures contribute to the pattern of local weldment defect distribution, residual stress pattern in the HAZ, and material properties. Since these factors in turn directly affect crack growth, fabrication procedures should be carefully developed for each design.

3.1.2 Fabrication and Post-Fabrication Parameters

Activities in the shipyard or fabrication yard directly impact the fabricated marine structure. These activities can be categorized as either fabrication or post-fabrication parameters (Figure 3-3).

Fabrication Parameters

The primary fabrication parameters can be defined by the questions who, what, when and how. Each of these parameters affects the fabrication quality, in terms of residual stresses, defects, repairs and post fabrication processes. These variables, which determine

the general quality of fabrication, also affect specifics such as the rate of crack growth and corrosion.

The four primary fabrication parameters are:

- Who is Doing the Work? (i.e. personnel qualification)
- What are the Work Requirements? (i.e., defining the program)
- When is the Work Done? (i.e., sequence/timing of activity)
- How is the Work Done? (i.e., following the specifications)

Post-Fabrication Parameters

Both the design parameters and fabrication parameters directly affect fatigue performance of a fabricated component, thereby influencing the post-fabrication processes. The post-fabrication processes discussed here are activities that enhance the fatigue performance of the structure component.

The toe of the weld and the weld root often contain geometric imperfections and high localized stresses and therefore they are often the site of fatigue crack propagation. To enhance fatigue performance, modification of both the weld geometry and the residual stress is recommended. The weld geometry can be improved by weld toe grinding, which is often specified to obtain a smooth transition from weld to the parent material. This process should improve fatigue life locally both by removing small defects left at the toe during welding and by reducing the stress concentration at the weld toe due to elimination of any notches. Weld toe remelting (by TIG or plasma dressing) and the use of special electrodes for the final pass at the toe can also improve fatigue performance.

Post-weld heat treatment (PWHT) is recommended to relieve residual stresses introduced in welding thick sections, typically defined as having a wall thickness in excess of 2.5 in (63 mm) in U.S. (less

elsewhere). Both thermal stress relief and weld material straining to set up desirable compressive stresses at the weld toe are used. Typically, a node subjected to PWHT experiences both stress and strain relief and should exhibit improved fatigue performance. However, the efficiency of PWHT needs further verification. Some experts in the field consider it difficult to justify any improvement of fatigue performance as a result of stress relief.

Corrosion protection is necessary to ensure as-designed performance of the structure, including achieving the desired fatigue life. Post fabrication work on corrosion protection systems varies from installation of anodes for cathodic protection to coating and painting.

3.1.3 In-Service Parameters

The environment in which fatigue cracks initiate and grow substantially affects fatigue life. The environment affects corrosion and crack growth due to both the nature of the environment (i.e., sea water properties, including conductivity, salinity, dissolved oxygen, pH and temperature) and the magnitude and frequency of the applied loading (i.e., wind, wave and current characteristics).

Environmental loads that cause reversal of stress on a marine structure component are primarily caused by wave and wind action. While the loading directionality and distribution is often carefully accounted for, the sequence of loading usually is not. The other in-service parameters reflect inspection, maintenance and repair philosophy and have a major influence on corrosion and the rate of crack growth. The in-service parameters are summarized on Figure 3-4.

3.2 REVIEW OF FATIGUE ANALYSIS PARAMETERS

3.2.1 Fatigue Analysis Criteria

Fatigue analysis criteria for marine structures are developed in conjunction with the overall design criteria. The structure type, environmental conditions and the scope of the overall design effort all affect the fatigue analysis criteria. A fatigue life that is twice as long as the structure's design life is routinely specified to ensure satisfactory fatigue performance. Larger safety factors are often used for critical components where inspection and/or repairs are difficult.

For many marine structures the use of a probabilistic fatigue analysis, based on a probabilistic simulation of applied forces, residual stresses, defects and imperfections, crack growth and failure, appears to be desirable. This true probabilistic method may be considered an emerging technology and the time and cost constraints often require alternative methods to develop a design that meets the fatigue criteria.

Although the following sections refer to both "deterministic" and "probabilistic" fatigue methods, essentially the discussions cover deterministic methods. The probabilistic methods defined only refer to probabilistic treatment of the ocean environment.

3.2.2 Interacting Parameters

Fatigue design and analysis is carried out in conjunction with other activities that ensure proper design of the structure to meet all pre-service and in-service loading conditions. The structure and its component members must have sufficient strength to resist the extreme loads for a range of conditions, and these conditions are often interdependent.

The design is an iterative process in which the general configuration gradually evolves. Thus, the fatigue design and

analysis process is often initiated after the initial structure configuration has been defined, but while its components are still being designed and modified.

3.2.3 Stress Model Parameters

A generalized stress model represents all of the steps necessary to define the local stress ranges throughout the structure due to the structure's global response to excitation loads. These parameters are as follows:

Motions (Hydrodynamics) Model

A motions (hydrodynamics) model includes various models necessary to determine the applied excitation forces, response of the structure to these forces, and the resultant loads on the system. The choice of a model primarily depends on the structure configuration. While a continuous finite element model may be used for ship-shaped structures or semisubmersibles with orthotropically stiffened plate system (i.e. continuous systems), a discrete space frame consisting of strut members are typically used for the analyses of an offshore platform.

Floating structures, whether ship-shaped, twin-hulled or of another configuration, may require the use of diffraction analyses to define the hydrodynamic coefficients. Diffraction pressures generated are transformed into member wave loads while the radiation pressures are transformed into added mass and damping coefficients. This approach is valid to obtain hydrodynamic coefficients for non-conventional geometries, the motion analysis utilizing hydrodynamic coefficients does account for the effects of member interaction and radiation damping components.

Bottom-supported structures are generally made up of small-diameter tubulars, and their drag and inertia coefficients can be defined based on previous analytical and model basin work on tubulars. However, some components are frequency-dependent for a range of wave

frequencies of interest, requiring definition of frequency dependency.

Thus, some of the more important parameters to be considered in the development of a hydrodynamics model are:

- Structure configuration (continuous versus discrete systems).
- Structure size and irregularity of shape.
- Structure component member dimensions (with respect to both the structure and the wave length).
- Component member arrangement (distance from each other).
- Component member shape, affecting its hydrodynamic coefficients.

Analysis Techniques

Analysis techniques, or the approaches used to generate and apply environmental loads, fall into two categories: deterministic analysis and spectral analysis. Deterministic analysis is based on the use of wave exceedance curves to define the wave occurrences. Spectral analysis (also referred to as probabilistic analysis of the ocean environment only) is based on the use of wave spectra to properly account for the actual distribution of energy over the entire frequency range.

The five approaches can be defined in these two categories:

- Selected Wave(s) - Deterministic

A closed-form deterministic analysis procedure recommended by Williams and Rinne (Reference 3.3) is often used as a screening process. This approach may be considered a marginally acceptable first step in carrying out a fatigue

analysis of a fixed platform. As discussed in Section 3.2.4 under Stress History Parameters, wave scatter diagrams are used to develop wave height exceedance curves in each wave direction and used to obtain the stress exceedance curves. Considering both the effort needed and the questionable level of accuracy of selecting wave heights to represent a wide range of wave heights and periods, it may be better to initiate a spectral fatigue analysis directly.

- Regular Waves in Time Domain - Spectral

Because a spectral fatigue analysis is carried out to properly account for the actual distribution of wave energy over the entire frequency range, a sufficient number of time domain solutions is required to define the stress ranges for sufficient pairs of wave heights and frequencies. A result of this procedure is development of another characteristic element of spectral fatigue analysis, namely, the stress transfer functions, or response amplitude operators (RAOs).

For each wave period in the transfer function, a sinusoidal wave is propagated past the structure and a wave load time history is generated. The equations of motion (structure response) are solved to obtain a steady state response. A point on the transfer function at the wave period is the ratio of the response amplitude to the wave amplitude. A sufficient number of frequencies is required to incorporate the characteristic peaks and valleys.

- Random Waves in Time Domain - Spectral

The use of random waves avoids the necessity of selecting wave heights and frequencies associated with the regular wave analysis.

- Regular Waves in Frequency Domain - Spectral

This method, based on the use of regular waves in the frequency domain, requires linearization of wave loading. Approximating the wave loading by sinusoidally varying forces, and assuming a constant sea surface elevation does contribute to some inaccuracies. However, these approximations also allow equations of motion to be solved without having to carry out direct time integration, thereby greatly facilitating fatigue analysis work.

The approach chosen should depend on the structure type and the environment. For most "rigid body" inertially driven floating structures, frequency-domain spectral fatigue analysis is recommended. However, for tethered structures such as a TLP, and for structures in areas where large waves contribute substantially to cumulative fatigue damage, the effects of linearization and inundation are substantial. In these cases the preferred approach may be time-domain spectral fatigue analysis. Even time-domain solutions at several frequencies may be sufficient to compare the RAOs obtained from a frequency-domain solution and to calibrate them as necessary.

- Wind Gust - Spectral

Most marine structures are designed to resist extreme wind loadings, but they are rarely susceptible to cyclic wind gusts that cause fatigue damage. Some structures, such as flare towers or radio towers, support negligible equipment and weights; as a result, they are often made up of light and slender members, making them susceptible to wind-caused fatigue damage.

As with analysis of the wave environment, structures subjected to wind turbulence can be analyzed by quantifying cyclic wind forces and their associated frequencies. The total applied

wind loading on a structure is due to mean and cyclic components. The loads are computed and statically applied on the structure and then converted to harmonic loads for dynamic analysis.

The stresses obtained at each frequency are unitized by dividing them by the corresponding cyclic wind speeds. Application of wind spectra to define the occurrence of wind speeds and gust spectra to define the energy content of the gust on unitized stress ranges yields the stress spectrum. Further discussion wind loading is provided in Sections 6 and Appendix D.

Structural Analysis Model

A floating structure is by definition in equilibrium. The applied loads and inertial response from the motions analysis provide a balance of forces and moments for the six degree of freedom system. To obtain a stiffness solution, the structure model may be provided with hypothetical supports. A typical solution should yield close to zero loads at those hypothetical supports. The deformations obtained from stiffness analysis at member joints are transformed into stresses.

A single- or a dual-hulled structure is a continuous system with large stiffened members/components. Applied loads on the structure necessitate determination of hull girder bending moments in vertical and horizontal axes and local internal and external pressure effects. The use of beam elements may be appropriate when local pressure effects are small and stress distribution patterns are well understood. Since the local pressure effects are substantial for ship structures and the local stress distributions rapidly change as a function of several parameters, a finite element analysis is the generally recommended approach to determine the local stress distributions.

The finite element models of increasing mesh refinement are often used to obtain accurate stress range data locally in fatigue sensitive areas. Thus, an overall coarse mesh model of the structure used in the first stage of analyses is modified by increasing mesh refinement in various fatigue sensitive areas. The finite element models are typically built from membrane plate elements, bending plate elements, bar elements and beam elements and further discussed in Section 5.

Because the individual joints and members define the global structure, the boundary conditions should also reflect the true response of the structure when subjected to the excitation loads. For a bottom-supported structure, individual piles can be simulated by individual springs. Whatever the support characteristics, a foundation matrix can be developed to represent the foundation-structure interface at the seafloor. It should be noted that the foundation matrix developed for an extreme environment would be too flexible for a milder fatigue environment. Thus, the foundation matrix developed should be compatible with the applicable load range.

Stress Response Amplitude Operators (RAOs)

The stress RAOs or stress transfer functions are obtained by unitizing the stress ranges. If the wave height specified is other than the unit wave height (double amplitude of 2 feet or 2 meters), stress ranges at each frequency are divided by the wave heights input to generate the loads. Similarly, wind loads computed based on cyclic wind velocities at each frequency are divided by the respective velocities to obtain the unitized stress ranges.

Stress Concentration Factors (SCF) and Hot Spot Stresses

The stresses obtained from a stiffness analysis, and the RAOs generated, represent nominal or average stresses. However, the load path and the detailing of orthotropically stiffened plate or an intersection of tubular members will exhibit hot-spot or peak

stresses several times greater than the nominal stresses. The fatigue test results for a wide variety of ship hull stiffener geometries can be used directly with the nominal stresses.

At an intersection of a tubular brace and chord, depending on the interface geometry, the maximum hot-spot stresses often occur either on the weld toe of the incoming brace member or on the main chord. The ratio of the hot-spot stress to the nominal stress is defined as the stress concentration factor (SCF).

$$SCF = \sigma_{\max} / \sigma_n$$

The SCF value is probably the most important single variable that affects the fatigue life of a detail/joint, necessitating accurate determination of SCFs.

There are several practical approaches for determining SCF values. The first approach is to develop an analytical model of the detail/joint and carry out a finite element analysis (FEA). When modeled correctly, determination of SCFs by FEA is a very reliable approach. The second approach is to test a physical model and obtain the hot-spot stresses from measurements. Whether a strain-gauged acrylic model or other alternatives are used, the accuracy of hot-spot stresses largely depends on the ability to predict hot-spot stress locations and obtain measurements in those areas.

Although reliable and recommended for obtaining SCFs, these two methods are time consuming and expensive. Thus, a third approach, based on applying empirical formulations to determine SCFs, has been extensively accepted for fatigue analysis of marine structures. A set of empirical formulae developed by Kuang (Reference 3.4) were derived by evaluating extensive thin-shell finite element analyses results. The formulae proposed by Smedley (Reference 3.5) and Wordsworth (Reference 3.6) of Lloyds Register were derived from evaluating the results of strain-gauged acrylic models.

The stress model parameters discussed above are summarized on Figure 3-5. A summary of empirical equations, parametric study results obtained by using applicable empirical equations for T, K and X joints, and an illustrative finite element analyses results for a complex joint are presented in Appendix C.

3.2.4 Stress History Model Parameters

The wave scatter diagram and wave directionality data are necessary whether a deterministic or a spectral analysis technique is used. In a deterministic analysis wave exceedance curves are generated in each wave direction and used with the hot-spot stresses to obtain the stress exceedance curves.

For a spectral fatigue analysis, a scatter diagram and the directional probability is used with wave or wind spectra to obtain the stress spectrum from hot-spot stresses. These parameters are summarized on Figure 3-6. Stress History Models are discussed further in Section 6.

3.2.5 Fatigue Damage Computation Parameters

Many parameters affect the fatigue life computation. Some, such as stress sequence, maintenance and repairs, lapses in corrosion protection, etc., are not accounted for in fatigue damage computation. Fatigue damage is characterized by an accumulation of damage due to cyclic loading, with fatigue failure occurring when the accumulated damage reaches the critical level. To evaluate the damage, the stress-time history is broken into cycles from which a distribution of stress ranges is obtained. The variable-amplitude stress range distribution is divided into constant-amplitude stress range blocks, S_{rj} , to allow the use of constant-amplitude S-N curves.

Selection of S-N Curve

The S-N curve defines the relationship between a constant-stress amplitude block and the number of cycles necessary to cause the failure of a given detail/joint. Such S-N curves are largely derived by testing models of simplified detail/joint components with subjecting constant amplitude stress reversals in a laboratory environment. The laboratory environment is substantially different from the typical marine environment. Similarly, the laboratory models are idealized while actual marine structure details/joints incorporate fabrication residual stresses and substantial welding defects.

The S-N curve defining a particular type of detail/joint and material properties is derived by obtaining the mean of the test data and then defining the mean minus two standard deviations. S-N curves were first developed for fillet-welded plate details and some small scale-tests on tubular joints. Later tests provided data on more complex details and thicker plate sections. The S-N curves for continuous system details (i.e., ship hull stiffening) are typically reduced by the ratio of hot spot-to-nominal stresses and can be used directly with shiphull nominal stresses to determine fatigue damage. The S-N curves for discrete system joints represent the failure stresses and necessitate multiplication of nominal stresses by SCFs to obtain hot spot stresses.

The choice of an applicable S-N curve depends not only on the material, configuration of the detail/joint and the fabrication effects (residual stresses, weld profile, defects, etc.) but also on the service condition of the structure. The original U.K. Department of Energy (DEn) recommended Q-curve, based on simple thin plate details, has been replaced by a T-curve (Reference 1.6). The American Petroleum Institute (API) recommended X-curve (Reference 1.5) is applicable to a welded profile that merges with the adjoining base material smoothly. If the weld profile is not smooth, then a lower X'-curve is applicable.

While API S-N curves are applicable to stationary marine structures, other S-N curves by DEn and Det norske Veritas (DnV - Ref. 1.7) may be equally applicable to stationary and mobile vessels with tubular and orthogonally stiffened plate construction. The preferred S-N curve should be defined in the design criteria. Typical S-N curves applicable for marine structures are illustrated on Figure 3-7. S-N curves are discussed further in Section 5.

Cumulative Damage

The calculation of cumulative damage is typically performed using the Palmgren-Miner damage rule. In this approach fatigue damage is calculated by dividing stress range distribution into constant amplitude stress range blocks, assuming that the damage per load cycle is constant at a given stress range and equal to:

$$D_{ri} = 1/N$$

where,

D_{ri} is the damage, and

N is the constant-amplitude number of cycles to failure at a given stress range.

Another key assumption of the Palmgren-Miner damage rule is that damage is independent of order in which loads are applied. Accordingly, for the case of a stress history with multiple stress blocks, S_{ri} , each block having n_i cycles, the cumulative damage is defined by:

$$D = \sum_{i=1}^k \frac{n_i}{N_i} < 1.0$$

This is the Miner-Palmgren formula, where:

D is the cumulative damage,

k is the number of stress blocks,

n is the number of stress cycles in stress block i with constant stress range, and

N is the number of cycles to failure at constant stress range.

Although the linear Palmgren-Miner damage rule is extensively used, the significance of constant-amplitude loading and the sequence of loading (i.e., large stress blocks during the beginning rather than toward the end of design life) may be important to correct assessment of fatigue damage. This subject is discussed further in Section 7.

Fatigue Life Evaluation

Fatigue damage and fatigue life should be determined at all critical hot-spot stress areas. While one or two areas may be targeted on a plate and stiffener interface, at least eight points are recommended on a tubular member. If eight points, spaced at 45 degree intervals around the circumference, are chosen, relatively accurate hot-spot stresses and fatigue damage data will be obtained. Typically, fatigue damage (D) is calculated on an annual basis. The fatigue life (L) is then determined by taking the inverse of the accumulated damage ratio (D).

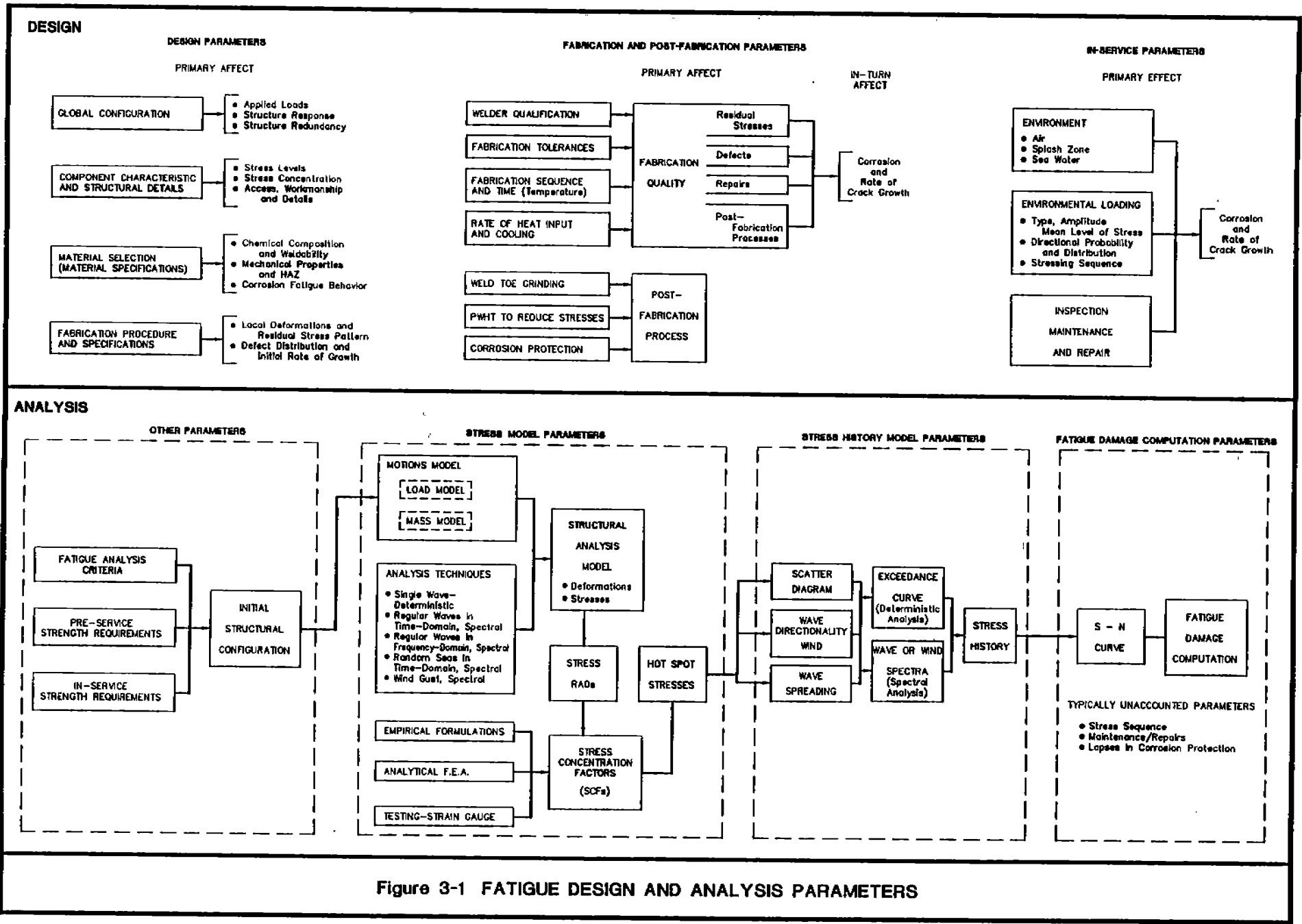


Figure 3-1 FATIGUE DESIGN AND ANALYSIS PARAMETERS

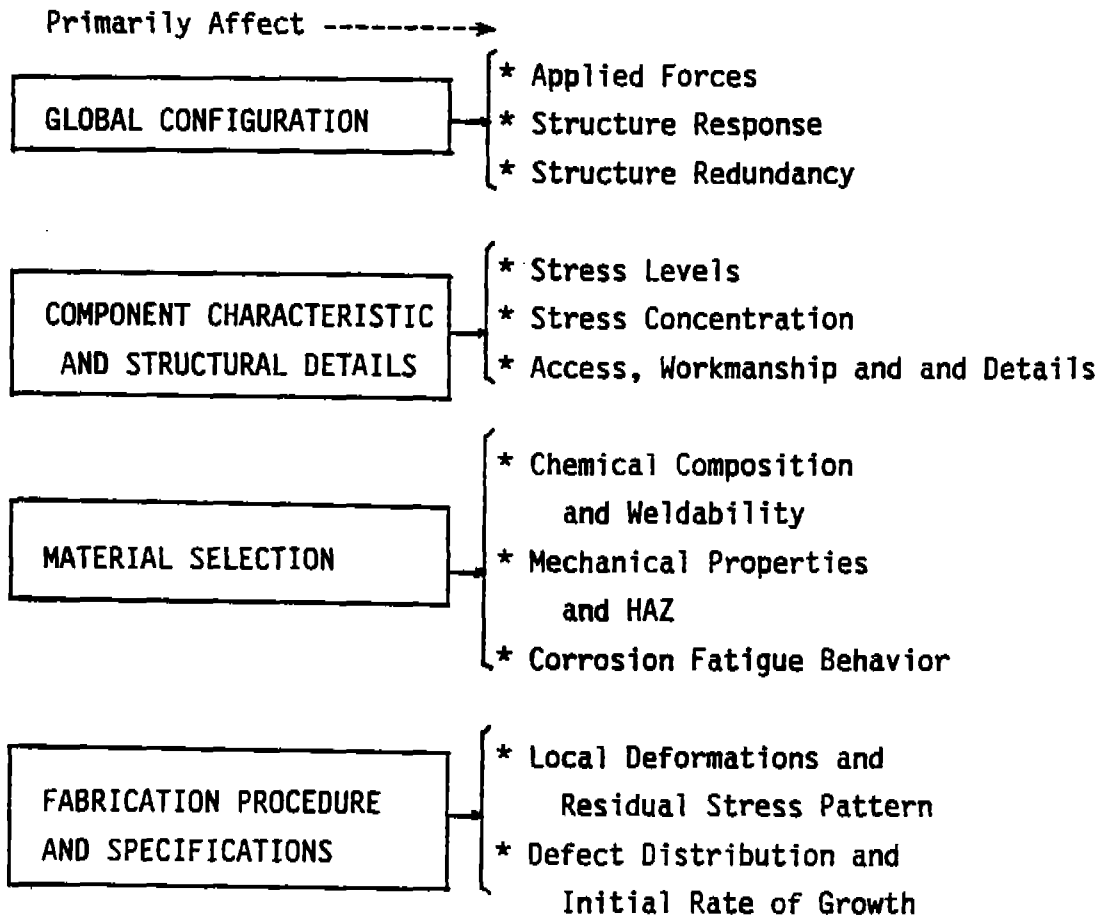


Figure 3-2 Design Parameters

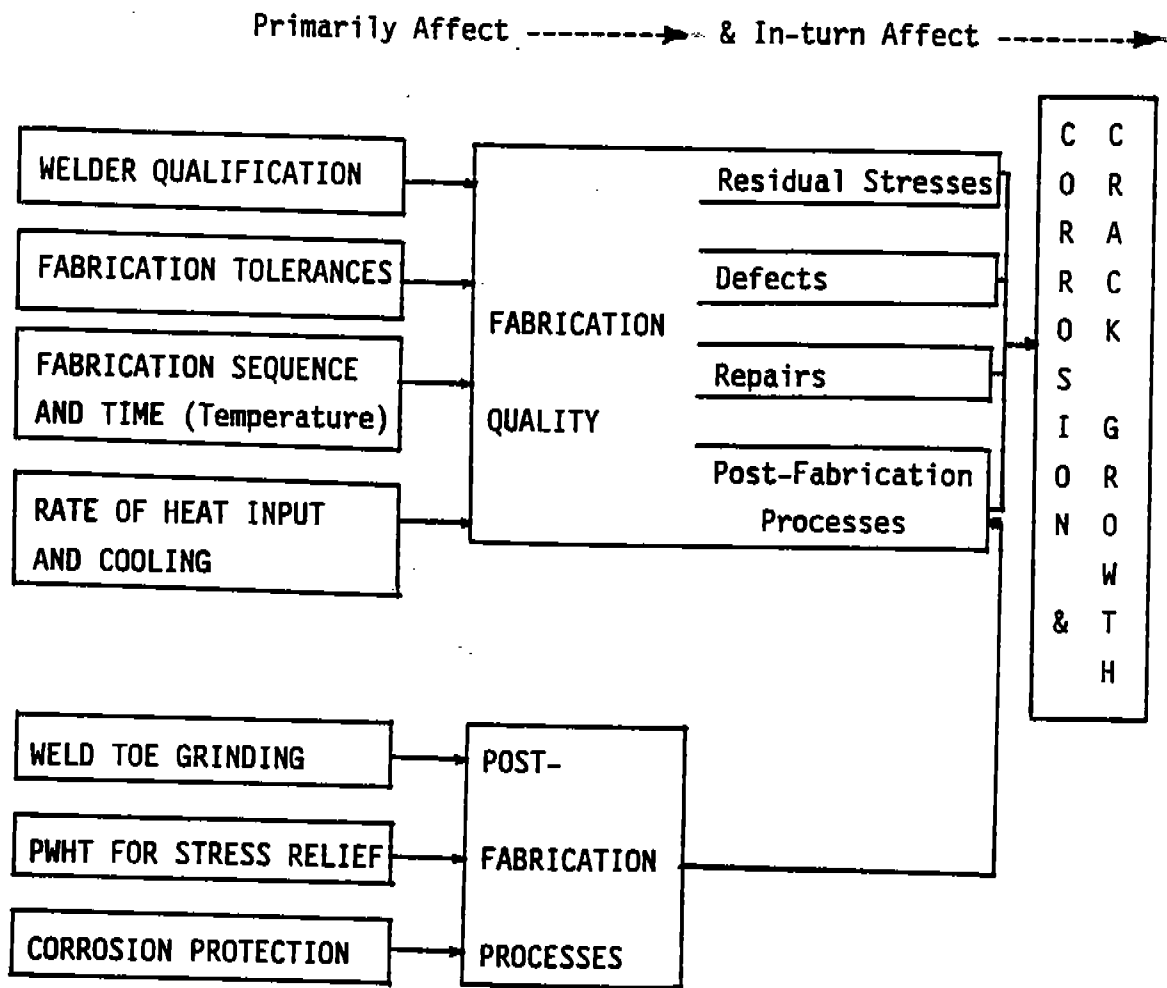


Figure 3-3 Fabrication and Post-Fabrication Parameters

Primarily Affect ----->

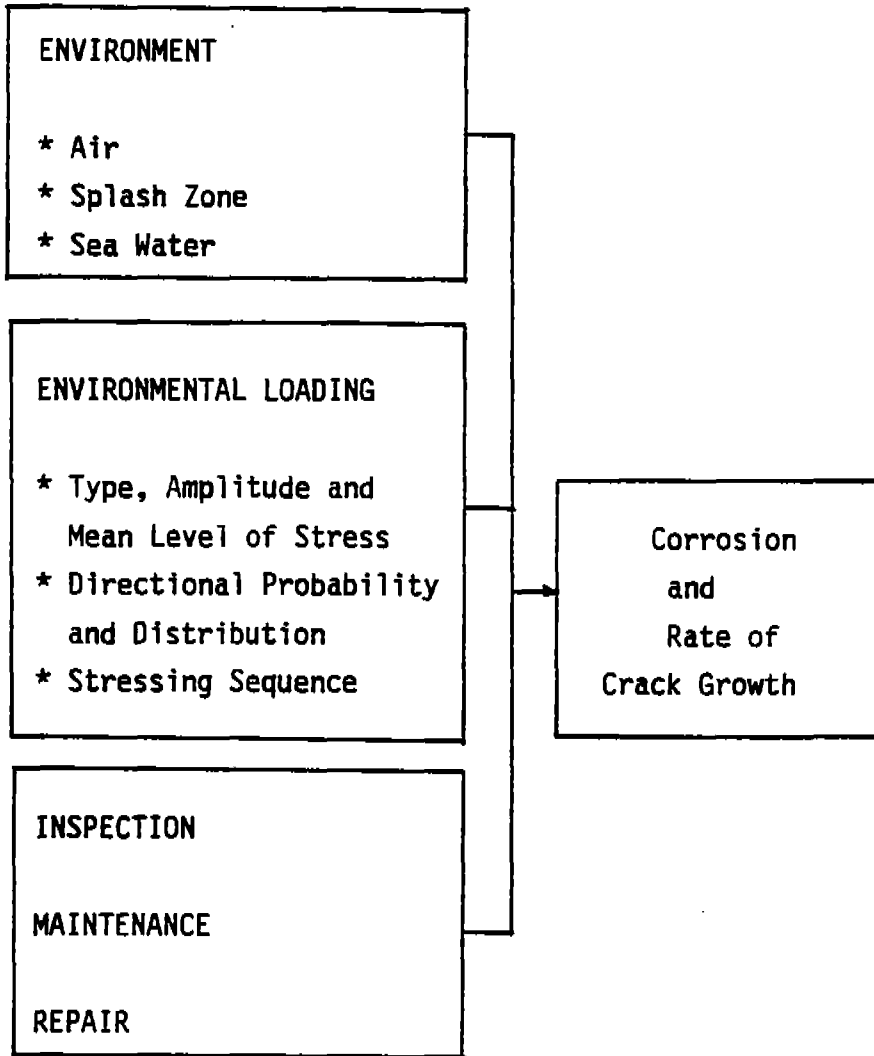


Figure 3-4 In-Service Parameters

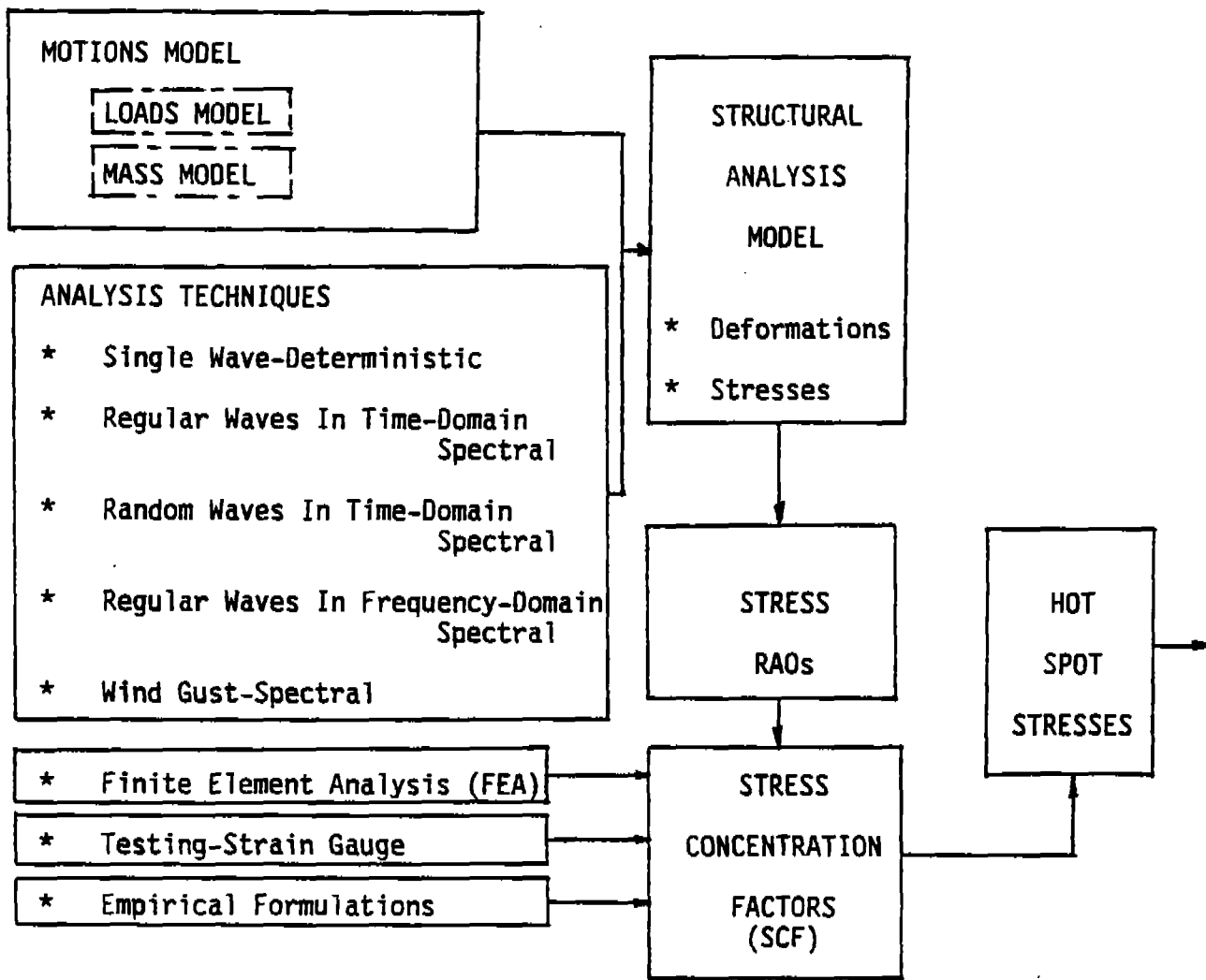


Figure 3-5 Stress Model Parameters

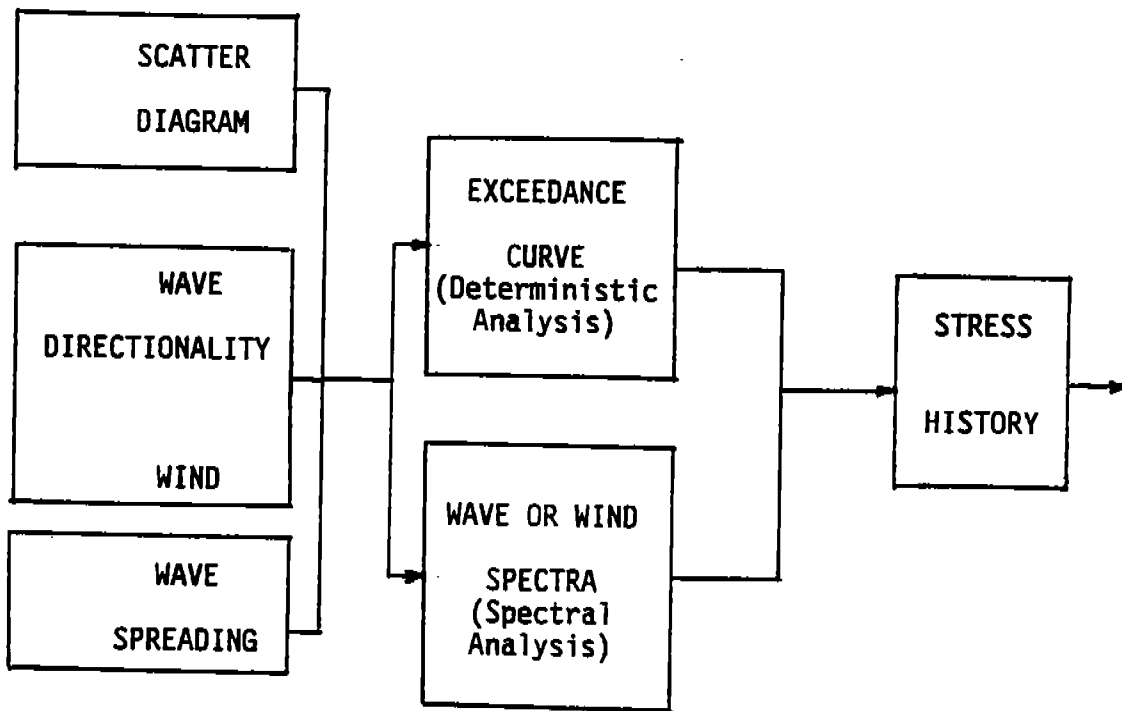


Figure 3-6 Time History Model Parameters

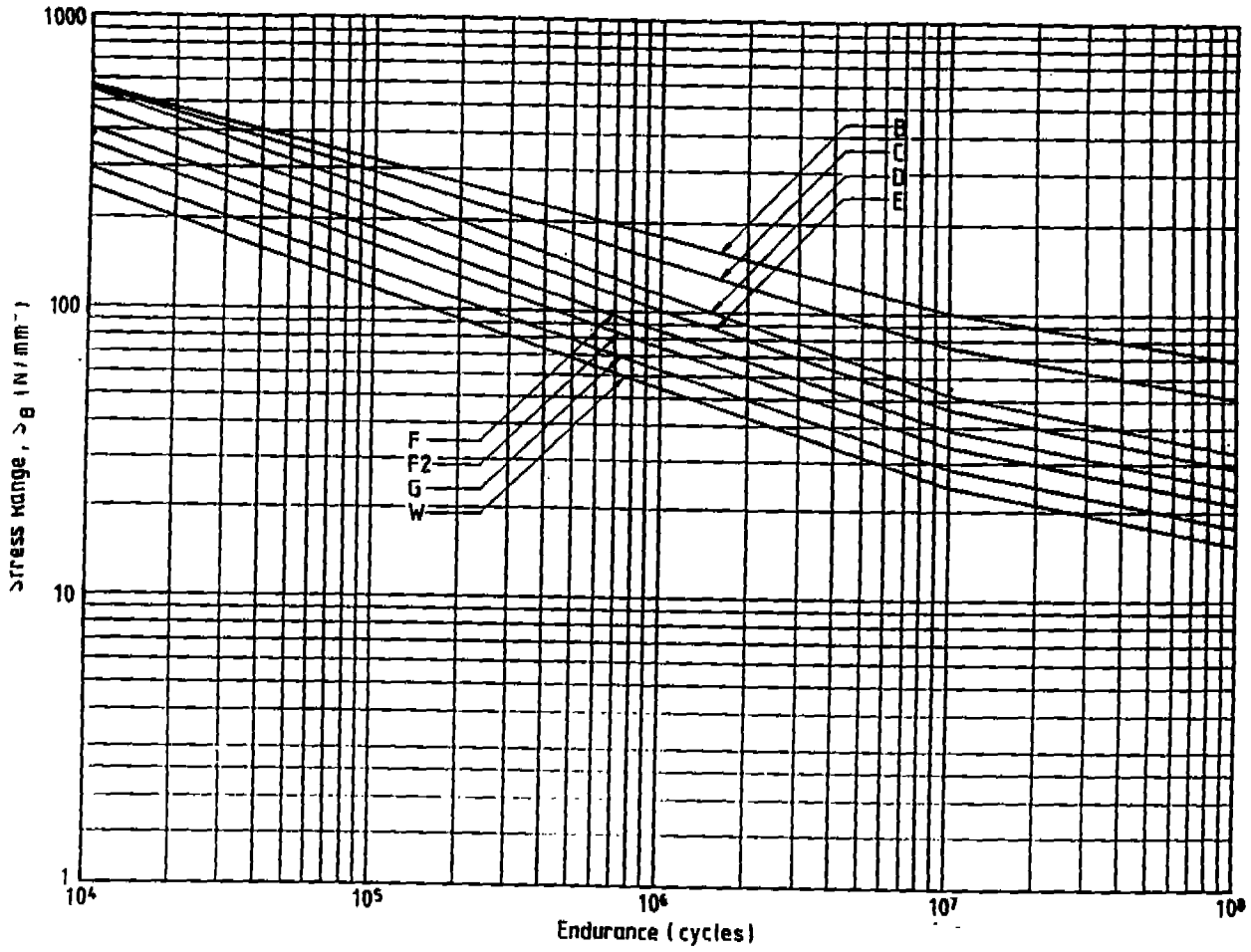


Figure 3-7 Typical S-N Curves

57

(THIS PAGE INTENTIONALLY LEFT BLANK)

4. GLOBAL REVIEW OF FATIGUE

4.1 APPLICABLE ANALYSIS METHODS

4.1.1 Background

Analysis and design of marine structures in the past often did not include explicit treatment of fatigue. With the installation of offshore platforms in deeper water increased emphasis was placed in fatigue design. An experience-based allowable stress methods developed were soon complemented with detailed analyses methods.

Ship structure design often did not incorporate explicit treatment of fatigue through analysis. However, with the increasing use of higher strength steels, the cyclic stress ranges also increased, necessitating fatigue analysis of more structures. Although the allowable stress methods developed are used in the design of majority of ship structures, more and more of the new designs incorporate detailed analysis methods.

Several methods may be applicable and acceptable for the fatigue analysis and design of a marine structure. The most suitable method depends on many parameters, including structure configuration (shape, redundancy, details/joints, etc.), fatigue environment, operational characteristics/constraints, and the design requirements. The complexity and cost of this analysis and design effort should be compatible with available design information and the desired degree of accuracy of the analysis and design.

The design and analysis parameters discussed in Sections 3.1 and 3.2 are summarized on Figure 3-1. The four dotted-line boxes around the analysis parameters illustrate a typical analysis sequence. Although the methods used in obtaining the hot-spot stress (stress model), stress spectrum (stress history model), and the fatigue life may differ, the general sequence shown is usually followed. A different sequence is applicable for a simplified analysis and design method. An allowable stress approach is one such example.

The different methods and their application sequences are discussed in the following sections.

4.1.2 Simplified Analysis and Design Methods

The simplified analysis and design methods applicable to ship structures and offshore structures are based largely on both theoretical knowledge and past experience and account for the environment likely to be encountered. Typically, ship hull girders are designed to resist maximum bending moments due to still water plus a wave-induced condition derived from harsh North Atlantic wave data (Reference 4.1). The basic hull girder, designed for the extreme environment loading, is intended to have ample cross-sectional area and moment of inertia to keep the magnitude of stress reversals low and exhibit low susceptibility to fatigue damage. The minimum plate and scantling sizes specified and the detailing developed are intended to keep the nominal and peak stress ranges low to prevent fatigue failures in the secondary members. In addition, steel is specified to ensure that its chemical composition and mechanical properties will make it less susceptible to fatigue failure.

Similarly, offshore platform joints are designed to resist maximum punching shear and crushing stresses. The joint details are developed to minimize the SCFs and cyclic stress ranges to make them less susceptible to fatigue failure. Such an indirect approach to fatigue design should be supplemented by an empirical approach based on constant stress range cycle fatigue life test data.

Ship Structures

An allowable stress method for ship structure design should be used to assess applied stresses against allowable stresses. The objective of applying the method is to identify those conditions that require no further fatigue assessment and those conditions that require more comprehensive fatigue analyses.

An allowable stress method, also considered a screening process, relies on both theory and experience. The procedure developed should be calibrated against available fatigue failure data and typically incorporates the following steps:

1. Computation of wave-induced loads
2. Determination of applied stress levels
3. Determination of allowable stress levels
4. Adjustment of allowable stress levels
5. Assessment of various components/details for susceptibility to fatigue failure.

The wave-induced loads are computed using simplified formulae, where the long-term distribution of fatigue loading is represented by a single characteristic value. The vertical bending moment is computed as a function of the vessel length, breadth and block coefficient along the longitudinal axis. The applied (nominal) cyclic stress amplitude is determined by using beam theory and dividing the vertical bending moment at any point along the longitudinal axis with hull girder section modulus.

The allowable stresses depend on many variables. For a simplified method an allowable stress may be defined as a function of location (deck, side shell, etc.) and detail geometry (local stress factor). Typically, such a method is based on a 20-year service life, standard corrosion effects and a nominal geographic area. Thus if specific service life or routing information is available, the allowable stress levels are adjusted. Two of the of the simplified analysis methods are:

1. ABS' Allowable Stress Method

This allowable stress method by Thayamballi (Reference 4.2) is primarily intended for use in fatigue screening of tankers. The simplified formulae presented allow calculation of several types of loading on a tanker due to wave-induced motions. The loading types and their relevancy are:

- Vertical bending moment - needed to determine stresses along the longitudinal axis
- Internal tank load - needed to determine stresses at tank boundaries
- External pressure load - needed to determine stresses at outer hull

Each of these component loads are applied to the structure independent of one another. The method implements beam theory to obtain nominal stresses, except for special cases where ABS Steel Vessel Rules require special consideration. ABS Rules requiring structural analysis also provide substantial flexibility for engineering judgement. The fatigue sensitive areas of the deck, tanks and the hull shell, where the stresses are to be determined, are illustrated on Figure 4-1.

Although the method is intended to provide allowable stress levels for normal operating routes, the allowable stress levels can be adjusted. Thus, a vessel operating in harsh geographic regions can still be screened for fatigue by reducing the allowable stress levels as function of the severity of the environment. The structural components of a vessel having stress levels meeting the reduced allowable stress levels may not require a detailed fatigue analysis.

2. Munse's Method

This allowable stress method for determining ship hull performance by Munse et al (Reference 4.3) is a practical method of designing ship hull structural details for fatigue loading.

The method is considered reliable, as it is based on a study of measured fatigue failure (S-N curves) data for 69 structural details. The design method also incorporates the

results of work covering assessment of 634 structural configurations (from References 4.4 and 4.5). It establishes the basis for selecting and evaluating ship details and developing a ship details design procedure. This method accounts for three of the most important parameters that affect fatigue life of a ship detail:

- Mean fatigue resistance of local fatigue details (S-N curve)
- Application of a "reliability" factor to account for S-N data scatter and slope
- Application of a "random load" factor to account for the projected stress history

Munse's design method can also be used to estimate fatigue life based on actual or assumed stress history and a reliability factor. A study carried out at the American Bureau of Shipping (ABS) (Reference 4.6) to evaluate fatigue life predictions utilized several methods, including Munse's. The study, based on stress histories derived from strain measurements of containership hatch-corners, provided good comparative results. Although Munse's method neglects the effect of mean stress, the fatigue lives computed compared well with lives that are computed using other methods.

Munse's design method is an acceptable fatigue design procedure for all vessels. This design method allows proper selection of design details and provides for design of a cost-effective vessel appropriate for the long term environmental loadings. Vessels that are considered non-standard due to their configuration and/or function (such as a tanker with internal turret mooring or a drillship) should be further analyzed, including a thorough spectral fatigue analysis. Munse's design procedure is summarized in the block diagram on Figure 4-2.

Offshore Structures

Offshore structures such as a semisubmersible drilling vessel is a continuous system, typically having orthogonally stiffened members. While a simplified method, such as Munse's, may be an applicable screening method, such structures have very specialized configurations, response characteristics and structural details. Thus, each structure should be considered unique, requiring a detailed fatigue analyses.

An offshore platform is made up discrete members and joints. Since each structure is unique, a detailed fatigue analysis is recommended. However, a simplified method may be applicable if such a method can be developed based on a large number of similar structures in a given geographic region. Such a method was developed for the Gulf of Mexico by American Petroleum Institute (Reference 1.5) and discussed further.

The simplified API method (Section 5.1.1 of Reference 1.5) is based on defining the allowable peak stresses as a function of water depth, design fatigue life, member location and the applicable S-N curve. Although the approach can be modified to apply to other geographic areas, it was developed by calibrating previously completed fatigue analyses of fixed offshore platforms. The maximum allowable stress method is applicable to typical Gulf of Mexico platforms with structural redundancy, natural periods less than three seconds, and the water depths of 400 feet or less.

This API allowable stress method is intended for use as a simplified fatigue assessment procedure for Gulf of Mexico platforms subjected to long-term cyclic stresses considered small relative to the extreme environment stresses. The method attempts to predict fatigue behavior as a function of the design wave event for a generalized platform. It should be noted that the applied force levels can vary substantially with platform geometry. The relative importance of extreme design waves and operating environment fatigue waves changes with both the water depth and the actual member/joint

location. Thus, the method should be used with caution. Detailed discussion on this method and the calibration effort is presented by Luyties and Geyer (Reference 4.7).

4.1.3 Detailed Analyses and Design Methods

The detailed analyses and design methods applicable to ship structures and offshore marine structures generally follow the same analyses sequence and incorporate the variables associated with strength model, time history model and damage computation. The differences among the various types of detailed analyses are largely in the methodology implemented to obtain hot-spot stresses, to develop the stress spectrum and to compute the fatigue life.

A detailed fatigue analysis is recommended for all marine structures susceptible to fatigue failure. While simplified design methods are valid in determining the viability of structural details/joints of typical ships/tankers built from mild steel or offshore platforms in shallow waters of Gulf of Mexico, a detailed fatigue analysis is often necessary for other structures. Projected fatigue lives of a marine structure subjected to cyclic stresses should then be determined at all critical areas. The uncertainties in fatigue design and analysis parameters require that more emphasis be placed on the relative fatigue lives computed than on the absolute lives obtained. As a result, fatigue analysis is considered to be a systematic process to identify details/joints susceptible to failure, and to modify those susceptible areas to yield fatigue lives substantially in excess of the design life. The following are some detailed analyses options that apply to ship structures and to fixed and mobile marine structures.

Ship Structures

A ship that fails to meet simplified fatigue analysis requirements will not necessarily have fatigue failures. It only implies that a more detailed fatigue analysis is required. Typically, detailed

analysis is likely to be required when one or more of the following are applicable:

- The ship structure configuration has unique characteristics.
- The structure is built from high strength steel.
- The use of high strength steel allowed reduction of scantling sizes based on strength requirements and due consideration for fatigue phenomena was not given.
- The operational routes for the vessel are more severe than typical, making the structural components more susceptible to fatigue failure.

The detailed fatigue analysis sequence for ship structures is similar to fatigue analyses of other marine structures and includes all of the analyses parameters shown on Figure 3-1. However, the ship geometry, appreciable forward speed and the varying operational routes require a special effort to determine the ship motions, applied loads, stress distribution of loads and the long term distribution of fatigue stresses. Typically, a detailed fatigue analysis is a spectral fatigue, requiring determination of long term fatigue stress distribution for each case, accounting for each seastate and the applicable duration for that seastate.

Although very different from simplified fatigue analyses described in Section 4.1.2, when the spectral fatigue analysis approach is modified to represent the long term fatigue stress distribution with a shape factor (i.e. Weibull approach), it is sometimes identified as a simplified fatigue analyses.

Some of the characteristics of a spectral fatigue analysis and an alternate Weibull approach are as follows:

1. Spectral Fatigue Analysis

Although spectral fatigue analyses for ship structures and other often stationary offshore structures are similar, the methods used to determine loads and stresses are different. A ship structure requires determination of hull girder bending moments in vertical and horizontal axes along the entire longitudinal axis (i.e., hull length). In addition, local internal and external pressure effects need to be determined.

Most often the applied wave loads are computed with the use of linear ship motion theory for wave crestline positions at 90 degree phase angle separation (i.e. in-phase and out-of-phase components of wave). Since the fatigue damage occurs largely due to normal operating sea states the use of linear ship motion theory is considered appropriate for large majority of spectral fatigue analyses. However, some vessels may have unique configurations, move at high speeds or be susceptible to extreme loading fatigue damage. For such vessels the ability to predict wave nonlinearities and vessel hogging, sagging and racking effects accurately may become important. In such instances a non-linear ship motion theory may be preferred over linear ship motion theory. Further discussion on the specifics of global and local load determination is presented in Section 5.

The structural analyses needed to convert the in-phase and out-of-phase components of the load transfer function varies largely with the characteristics of the structure configuration. The beam elements used in the structural stiffness analyses of a discrete system, such as an offshore platform, may be appropriate for standard ship structures where other detailed analyses and experience allow reasonably accurate estimation of local stress distribution. This approach may be appropriate if loading is largely due to hull girder bending moments in vertical and horizontal axis. However, secondary girder bending moments due to external

dynamic loads on vessel bottom may be appreciable. In addition, vessels containing cargo such as oil, iron ore etc., will have inertial loads on internal tank walls/transverse bulkheads.

The secondary bending, when appreciable, does affect the magnitude of local stress distribution. The geometric complexities also contribute to the difficulty in estimating local stress distribution. Since the fatigue life estimate is function of stress range cubed, the accuracy of fatigue life estimate is very much a function of the accuracy of local stress distribution. Thus, a finite element analysis is the generally recommended approach to determine the local stress distributions for continuous system such as ships and tankers.

The stress range transfer functions are obtained to define response of the ship structure for all sea states covering a range of frequencies. Thus, in-phase and out-of-phase loads at each frequency and for each wave direction must be determined to define the stress range transfer function. In practice, the effort can be curtailed. A careful review of load transfer functions should allow selection of several important frequencies and determination of stresses for those frequencies.

The number of constant amplitude stress range cycles to reach failure is empirically defined as an S-N curve that may or may not include the effect of localized stress peaking. Thus, in addition to selecting an S-N curve appropriate for the structural detail and operating environment, the S-N curve and the structural analyses should be consistent. The stress range histogram developed and the S-N curve selected for the location allows determination of fatigue damage per year and fatigue life by using Miner's linear cumulative damage rule.

2. Weibull Approach

The Weibull shape factor is a stress range distribution parameter. The Weibull shape factor used with the characteristic stress range allows carrying out of a fatigue analyses with a relatively few structural analysis cases. Since the Weibull approach differs from detailed spectral fatigue analysis only in how the stress range is obtained, the accuracy of fatigue lives obtained with this approach largely depends on the validity of Weibull shape factor.

The Weibull shape factor may vary between 0.8 and 1.2. If information on structure and route characteristics are not available, a shape factor of 1.0 may be used. Shape factors obtained by calibrating the characteristic stress range against a spectral fatigue approach indicate that single most important variable affecting the shape factor is the environment. In severe North Atlantic and Pacific wave loadings, the shape factor is higher; the shape factor is also generally lower for those ship structures with longer hulls.

Although the shape factor may be somewhat different for different parts of the structure (i.e. bulkheads, bottom) and it may also depend on the number of cycles to failure, further work is necessary to document those effects.

Fixed and Mobile Marine Structures

The structures referred to in this section are both floating and bottom-supported steel structures. Most organizations that issue recommendations, rules, regulations and codes distinguish between floating and fixed structures because of the differences in their configurations and the resulting differences in applied loads, structure response, redundancy and accessibility for inspection and repairs. The requirements vary substantially in scope and detail from one document to another, but efforts to provide consistent yet flexible fatigue analysis requirements have been successful.

In general, the minimum requirement for fatigue analysis is defined as the need to ensure the integrity of the structure against cyclic loading for a period greater than the design life. Some documents, such as the ABS MODU rules (Reference 4.8) state that the type and extent of the fatigue analysis should depend on the intended mode of operation and the operating environments. Thus, the designer, with the Owner's input and concurrence is responsible for developing the design criteria, methodology and analysis documentation for certification of a design that meets the fatigue requirements. Further discussion on fatigue rules and standards is presented in Section 4.2

Fixed Structures

As illustrated on Figure 3-5, there are several alternative approaches to determining the hot-spot stress, stress history and fatigue life. A flowchart shown on Figure 4-3 illustrates a deterministic analysis applicable for a fixed platform in a moderate water depth site subjected to relatively mild fatigue environment. The method relies on obtaining hot-spot stresses for one or two selected regular waves and generation of wave exceedance curves from the scatter diagram to obtain the stress history. Although this method requires substantial computer use and is considered to be a detailed analysis, it is also considered to be a screening method and useful in initial sizing of the structure components.

A more desirable alternative approach to a deterministic analysis is to carry out a spectral fatigue analysis. The applied wave loads on a structure can be generated in the time domain and in the frequency domain. A structure, such as a flare boom, may be subjected to wind loading only. For such structures wind gust loads can be similarly generated to evaluate wind-induced fatigue loading. The stress spectrum is then generated from hot spot stresses, scatter diagram and specific wave or wind spectra.

One variable in defining the stress spectrum is whether or not to account for wave spreading. The purpose for distributing the wave

energy about the central direction by using a "spreading function" is to represent the nature more realistically. Considering the uncertainties and complexity of implementation, wave spreading is not generally incorporated into design. While it is a valid parameter that can be used to more accurately determine the fatigue lives of an as-designed or as-built structure (see Section 6.1.4 for definition of spreading function), it is often unconservative to neglect it when dynamics are significant.

It is also necessary to assess the significance of short-term density functions developed from statistical parameters. The joint probability of significant wave height and characteristic period (i.e., each sea state) is used to develop short-term probability density function of the stress range. This function is often idealized by a Rayleigh distribution and can be further improved. This improvement, incorporation of a rainflow correction factor, is discussed by Wirsching (Reference 4.9). Fatigue damage is then typically computed for each sea state by using the S-N curve and the Miner-Palmgren cumulative damage formulation. An alternative to this approach is based on weighting and summing the probability density functions to obtain a long-term probability density function. Total damage can then be computed based on either numerical integration or the use of Weibull shape parameter and a closed form solution. Chen (Reference 4.10) offers a short-term closed form method that facilitates spectral fatigue analysis. Spectral fatigue analysis is discussed further in Sections 5, 6 and 7.

Mobile and Stationary Vessels

Both conventional single-hull and twin-hull mobile and stationary vessels differ from fixed structures in the characteristics of applied environmental forces and the response of the structure to these forces. Thus, fatigue analysis of these vessels differs from that of fixed structures primarily in generation of applied forces and determination of stresses. Those vessels going from port-to-

port are also subjected to different environments, necessitating the use of scatter diagrams applicable for each route.

While a diffraction analysis method may be used to develop the excitational forces directly, it is often used to compute equivalent hydrodynamic coefficients. These coefficients are then used in Morison's formulation to generate wave forces. A typical spectral fatigue analysis sequence, including generation of dynamic inertial response loads compatible with excitational forces, is illustrated on Figure 4-4.

In the past conventional single-hull vessels were generally designed conservatively to meet both strength and fatigue requirements. Following initiation of monitoring programs to obtain wave loading and stress histories of selected cargo ships and tankers, fatigue design criteria were further improved. One reason for the preference of this design approach over the analysis approach is that most vessels are mobile and subjected to multitude of site and time specific environment over their design lives, necessitating certain conservatism in their design. The use of vessels for specialized functions, such as bow-moored storage tanker or a drill-ship with a large opening (moonpool) to facilitate drilling, necessitated detailed fatigue analyses to evaluate the other fatigue sensitive areas throughout the structure.

The detailed fatigue analysis, carried out on increasing number of floating structures, follow the basic steps shown on Figure 4-4. While both space frame models with beam elements and finite element models are used to analyze twin-hull structures, finite element models are almost exclusively used for single-hull vessels.

4.1.4 Other Methods

Complete Probabilistic Methods

A reliability-based fatigue analysis is ideally suited to account for various uncertainties associated with fatigue parameters.

Although considered to be an emerging technology and necessitate time consuming effort, probabilistic methods have been effectively utilized in some fatigue analyses. Typically, such a method accounts for:

- Inaccuracies in defining stresses due to random loadings
- Uncertainties and observed scatter in S-N data
- Randomness of failure in the use of simplified models

A probabilistic method recommended by Wirsching (Reference 4.11) utilizes a full distributional procedure and the variables discussed above are assumed to have a log-normal distribution.

A detailed analysis and design method, based on the use of a finite element model, to determine environmental loading, vessel response and load and stress distribution does not need to be a complete probabilistic method. Daidola and Basar (Reference 4.12) discussing lack of statistical data on ship strengths and stresses recommend development of a semiprobabilistic analysis method which does not require a distribution shape.

Fracture Mechanics Methods

A fracture mechanics method addresses the relationship between defect geometry, material, and the stress history. The defect geometry can be accurately modeled with finite elements. Stress intensity factors characterizing the defect behavior and the fatigue crack growth laws allow determination of defect growth characteristics. Thus, a hypothetical or an actual defect is used as the basis for determining the fatigue life and identifying the necessary corrective measure.

The initial defect size and location and the stress intensity are very important parameters in determining crack growth period to failure. The fracture mechanics approach is a useful tool to assess

the sensitivity of fabrication defects in determining the fitness-for-purpose of the component. This concept, first described by Wells (Reference 4.13), allows engineering assessment of weld defects to determine those defects that require repair as well as those that are considered fit-for-purpose without a repair.

4.2

FATIGUE RULES AND REGULATIONS

The primary objective of the various recommendations, rules, regulations and codes applicable to marine structures is to ensure that the design and analysis process results in construction of marine structures that can resist both extreme loads and cyclic operating loads and have adequate fatigue lives.

Rules and recommendations issued by classification societies and certifying agencies may represent the minimum requirements based on research and development. The hull girder design criteria given by each of the four leading classification societies (American Bureau of Shipping, Lloyd's Register of Shipping, Bureau Veritas and Det Norske Veritas) is very similar and differs only in some of the details. While the design basis primarily addresses stillwater and wave-induced bending moments, some discussion on dynamic stress increments and fatigue life assessment is often provided. Recent research and development efforts have produced several recommended fatigue design guidelines. Rules and recommendations on offshore structures are very specific on fatigue design. Guidelines are provided to carry out both simplified and detailed analyses. Commentary to such guidelines also provide background for the development of fatigue design methods.

Fatigue design methods chosen vary depending on several factors, including the owner's design philosophy. Most fatigue design methods are variations of a method based on application of S-N curves representing the fatigue strength of similar details/joints. A basic S-N curve applicable for a given detail/joint also requires adjustments to incorporate the influence of variables. Although

many design rules implement this approach, the recommended S-N curves are often different from each other.

Assessment of defects detected during fabrication, or cracks discovered while the structure is in service, is best accomplished using fracture mechanics and crack growth laws. Fitness-for-purpose considerations will then directly affect repair programs and inspection schedule.

The recommendations, rules, regulations and codes that apply to fatigue design have evolved over the past 20 years, and several have been revised or reissued in the last five years. These documents are discussed briefly below as they apply to vessels and other marine structures.

The American Welding Society (AWS) and American Institute for Steel Construction (AISC) fatigue design specifications (Reference 4.15) provide the basis for approximate fatigue design based on S-N curves. However, unless the method developed accounts for the most likely loads and other uncertainties, various critical and non-critical fatigue cracks are likely to occur.

Most documents on fatigue provide substantial flexibility in carrying out comprehensive fatigue design and analysis, while also incorporating extensive guidelines. Various DnV documents on specific types of structures such as Steel Ships (Reference 4.16), Tension Leg Platforms (Reference 4.17, Part 3, Chapter 6) and Fixed Steel Platforms (Reference 4.17, Part 3, Chapter 4) provide general guidelines and refer to a comprehensive document on fatigue analysis (Reference 1.7). The UEG Recommendations (Reference 1.8) are similar to U.K. DEn Guidance Notes (Reference 1.6), differences largely limited to the revisions introduced in the latest (fourth) edition of Guidance Notes.

4.2.1 Applicable Methods

Simplified Analysis Methods:

ABS provides a simplified allowable stress method, suitable for fatigue screening of tankers. As discussed in Section 4.1.2, the method allows substantial flexibility for engineering judgement.

Both DnV (Reference 1.7) and API (Reference 1.5) provide for simplified fatigue assessment of fixed offshore platforms. The API approach requires that the peak hot-spot stresses for the fatigue design wave do not exceed the allowable peak hot-spot stresses. This simplified approach is based on detailed fatigue evaluation of typical Gulf of Mexico jackets in less than 400 feet water depth, with natural periods less than 3 seconds. Variations in structure geometry, and in the approximations introduced, make the simplified analysis best suited for screening of similar structures for sensitivity to fatigue loadings.

The simplified DnV fatigue analysis is useful if the long-term stress distribution for a given area is not known. This simplified method provides an empirical relationship to determine the maximum allowable stress range during a 20-year life as a function of S-N curve parameters, long-term stress distribution as function of a Weibull parameter and the complete gamma function. This method is quite useful as a design parametric tool because it allows assessment of joint configurations for weld type and plate thicknesses and facilitates selection of details least susceptible to fatigue failure. However, since it is difficult to define accurately and/or conservatively the long-term stress distribution as a function of a Weibull parameter, the computed fatigue lives should be used cautiously.

Detailed Analysis Methods

The detailed fatigue analysis sequence for ship structures is similar to fatigue analyses of other marine structures. While appreciable forward speed and ship motions complicate determination of cyclic stress distributions, finite element based spectral fatigue analyses approaches recommended by classification societies are similar to those recommendations applicable to offshore structures.

The recommendations and rules applicable to fixed offshore platforms are generally quite flexible in the use of applicable analysis methods. To ensure structural integrity, all cyclic loads that will cause appreciable fatigue damage must be considered, including those due to transportation and all in-service loading for stationary structures. Several methods of determining the applied loads are acceptable to DnV (Reference 1.7), API (Reference 1.5) and the DEn (Reference 1.6). For fixed platforms, both deterministic and spectral methods can be used to generate the applied loads and determine the hot-spot stresses. However, a spectral analysis approach is often recommended to properly account for the wave energy distribution over the entire frequency range.

Comparative studies carried out on a benchmark API platform, utilizing four separate approaches (one deterministic and three spectral), yielded large scatter of fatigue lives due to inherent differences from one analysis approach to another. Such results justify the philosophy conveyed in most recommendations and rules, including API (Reference 1.5) and DEn Guidance Notes (Reference 1.6), that the fatigue analysis be treated as a systematic parametric analysis, requiring determination of the sensitivity of various parameters that affect fatigue lives.

SCFs, S-N Curves and Cumulative Damage

Stress Concentration Factors (SCFs)

It is desirable that the discontinuities that result in high stress concentrations be evaluated by laboratory testing or finite element analysis. But because these methods of obtaining stress concentration factors (SCFs) are often not practical, empirical formulations are widely used to determine the SCFs. Most recommendations and rules provide general guidelines on the use of SCFs and refer other reference documents. Lloyd's Register was responsible for carrying out extensive strain-gaged acrylic model tests and developing SCF formulas. These empirical formulas are incorporated into Lloyd's Register Rules (Reference 4.18). Assessment of various SCF formulas is discussed further in Section 5.4 and Appendix C.

S-N Curves

For the purposes of defining fatigue strength as a function of constant amplitude stress and the number of cycles to reach failure, welded joints are divided into several classes. DnV (Reference 1.7) provides an S-N curve identified as "T-curve" for all tubular joints and eight other classes to define other joints, depending upon:

- The geometrical arrangement of the detail
- The direction of the fluctuating stress relative to the detail
- The method of fabrication and inspection of the detail

API provides two S-N curves to define the tubular joints. The X-curve presumes welds that merge with the adjoining base metal smoothly (i.e., profile control), while the X'-curve is applicable for welds that do not exhibit a profile control. The API X-curve was originally based on the 1972 AWS test data and has been upgraded based on later editions of AWS D1.1 (Reference 4.14).

The DnV X-curve and the DEn Guidance Note Q-curve of 1977 were also based on the original AWS test data and the recommended S-N curve. Recent experimental work carried out in Europe has provided additional data on fatigue strength of tubular joints. Statistical evaluation of these test results provided the basis for revision of both the DnV (Reference 4.17) X-curve and the DEn Guidance Notes (Reference 1.6) Q-curve. As illustrated on Figure 4-5, the slope of the new T-curve is steeper and typically results in lower lives, often necessitating an increase in wall thickness. The DEn Guidance Notes recommended T-curve is identical to the DnV T-curve up to 10 million cycles for cathodically protected areas.

The basis for the revision of the S-N curves by both DnV and DEn is primarily due to evaluation and assessment of test data. While the AWS data are based on some plate and some small-diameter thin-wall sections, the European data are obtained mostly from larger diameter tubulars with 5/8 inch and 1-1/4 inch (16 mm and 32 mm) wall thicknesses. It appears that an inverse log-log slope of 3.0 (versus 4.38 for the API X-curve) was chosen for the T-curve because of the scatter of data and to ensure consistency with the British Standards BS 5400. Based on statistical evaluation of test data and Gurney's (Reference 4.19) analytical studies on plate thickness, the T-curve is adjusted due to changes in plate thickness.

Although the DnV (Reference 4.17) document states that all tubular joints are assumed to be of Class T, an X-curve is also considered acceptable, provided weld profiling is carried out. The comparison of the API X-curve and the T-curve (Figure 4-5) shows that the two curves intersect at about 500,000 cycles and would yield similar lives for a plate thickness of 1-1/4 inch (32 mm). However, for plate thicknesses greater than 1-1/4 inches the use of a T-curve in the computation of fatigue lives will result in shorter lives.

Cumulative Damage

The use of the Palmgren-Miner linear damage rule is considered appropriate by all of the recommendations, regulations and rules. A cumulative sum of the number of cycles at each constant stress divided by the number of cycles to failure should always be less than 1.0 for the desired service (design) life. While this value is directly tied to the S-N curve selected, the desirable ratio (i.e., safety factor) of fatigue to service life is not always specified. The API recommended fatigue life is at least twice the service life. For critical members that may affect structure redundancy and integrity, API recommends the use of higher fatigue to design life ratios.

The DEn Guidance Notes recommend additional safety factors to account for structural redundancy and the implications of fatigue failure on the structure. However, no specific safety factor is recommended.

4.2.3 Fatigue Analysis Based on Fracture Mechanics

The fatigue crack propagation analysis is typically used to assess crack growth and fitness-for-purpose of defects discovered at the fabrication yard. Test data on crack growth can also be used to determine fatigue lives. The DnV CN 30.2 document (Reference 1.7) provides a crack growth rate data and fracture mechanics-based procedure for fatigue analysis and design.

Whether the welded joint details have surface or root defects, the growth of such defects into fatigue cracks depends on several factors, including joint connection geometry, cyclic stress range history, weld profile and defect size. The equations provided to solve for the number of cycles to reach fatigue failure contain many parameters and allow evaluation of various joint and defect geometries. As an example, butt weld toe defects in a connecting plate whether in air or seawater, can be assessed with and without

bending restrictions. Cruciform and tubular joint defects can be similarly assessed. The DnV CN 30.2 document provides standard crack growth parameters to facilitate a fatigue analysis based on fracture mechanics. Lotsberg and Andersson (Reference 4.20) further discuss fracture mechanics-based fatigue analysis and illustrate the approach with several examples of crack growth calculation.

4.3 CURRENT INDUSTRY PRACTICES

Current industry design practices for marine structures are significantly more advanced than the design practices of only 20 years ago. The extensive use of ever more powerful computers and the development of a wide range of software packages has facilitated the design and analysis of marine structures. Research work on long-term ocean environment, model basin studies on structure motions, structure component member testing for stress distribution, buckling, yielding and fatigue failure all have been instrumental in developing better and more effective means of designing marine structures. Structural reliability research has also provided the means to incorporate the large number of uncertainties into the analysis and design effort.

Fatigue analysis and design is perhaps the part of the overall analysis and design effort that benefits the most from these developments. Since the hot spot stress is a primary variable influencing fatigue life, analytical and experimental programs have been carried out to help develop details/joints with lower hot spot stresses. Good design detailing without fabrication quality is not adequate. Thus, parameters affecting fabrication quality are incorporated into current design practices and fabrication specifications. It is feasible to analyze each joint of a discrete system such as a fixed platform. However, a continuous system, such as a ship, has thousands of details/joints and lends itself to a selective analysis. Current industry practice is to select number of cross-sections along the hull and analyze a dozen or more details/joints at each cross-section.

Although additional research is needed to expand the available data, the industry has the ability to incorporate most sophisticated analysis procedures into fatigue design. The degree of sophistication needed to design a marine structure that has fatigue life in excess of its design life depends both on the structure and its operating environment. Thus, the effort necessary may be grouped into ordinary and special designs.

4.3.1 Ordinary Designs

All marine structures can be designed effectively by ordinary means if those structures are not going to be subjected to any appreciable fatigue environment. For example, offshore platforms in relatively shallow waters may be susceptible to typhoon/hurricane loading but less susceptible to cyclic loadings that cause fatigue, eliminating the need for comprehensive fatigue analyses. Such structures can be designed for other loading conditions and checked against fatigue by approximate allowable stress procedures.

The design of ships still is largely based on design rules (such as ABS, Reference 4.1) developed by combining theoretical knowledge and design experience. Most ships in-service are designed to meet these rules and other fatigue design procedures (References 1.2 and 4.3) to ensure that the component details meet fatigue requirements. This approach has been quite satisfactory for most ships. Recently built vessels, especially large tankers built in the last several years have exhibited substantial fatigue problems. These problems may be largely attributed to the use of high strength steel, resulting in the use of lower plate thicknesses and yielding higher stress levels. As a result, detailed fatigue analysis and design procedures are implemented on more and more vessels.

4.3.2 Specialized Designs

Those vessels with specialized functions and/or configurations, or which are likely to be moored in a specific area for an extended

period, are also designed to meet the rules and other fatigue design procedures. However, such vessels also require spectral fatigue analysis to define the loadings, response and stress distributions. Often, model basin tests are also carried out to validate the applied loadings and motions.

Stationary marine structures are generally unique and have specialized functions. Since the design criteria and functional requirements dictate the general configuration of such structures, each structure must be analyzed thoroughly to generate the loads, to determine the response to these loads, and to determine its susceptibility to fatigue. Most specialized structures require spectral fatigue analysis.

4.4

SENSITIVITY OF FATIGUE PARAMETERS

Fatigue design and analysis parameters discussed in Sections 3.1 and 3.2 illustrate the general interaction of these parameters. The specific interactions and the actual sensitivities of these parameters depend largely on the structure's global configuration, joint configuration and details, material characteristics, fabrication quality and the design requirements other than fatigue. Therefore, fatigue analysis and design efforts often incorporate flexibility to carry out parallel studies to assess the sensitivity of major parameters that affect fatigue life.

Although the parameters illustrated on Figure 3-1 are all important, some of the more important parameters for fatigue life improvement are:

- Enhance fabrication quality and minimize defects
- Minimize applied loads and motions to minimize nominal cyclic stress ranges
- Optimize the design for uniform load distributions

- Optimize the design details to minimize SCFs

Another parameter that is not important to the actual fatigue life but very important to the computed fatigue life is the analysis method and the assumptions used in the analysis. Although there is no substitute for experience, comparative studies carried out by others should be utilized and the analysis method selected and the assumptions made should be applicable to the marine structure being designed.

4.5 FATIGUE DESIGN AND ANALYSIS CRITERIA

Fatigue design and analysis criteria are generally covered in one chapter of the structural design basis document. Fatigue criteria may also be jointly prepared by the engineer and the owner as a separate design brief to document the fatigue design and analysis basis.

4.5.1 Basis for the Preparation of Criteria

The design and analysis criteria serve the purpose of clearly defining the work to be undertaken. Three primary variables that affect the fatigue design and analysis criteria are:

- The owner's requirements for work scope and schedule
- The engineer's assessment of the marine structure's sensitivity to fatigue and the required level of analysis
- The role of classification societies

The owner, engineer and classification society all agree that the design and analysis should lead to quality fabrication and ensure the structural and operational integrity of the marine structure throughout its design life. To accomplish these goals, a design should provide a balance between efficiency and redundancy and also

incorporates inspection strategy (References 4.21, 4.22 and 4.23). As a result, the design effort must incorporate consideration of global response, alternate load paths, local stress distributions, structural detailing, material selection, fabrication procedures, etc., to ensure that the structure's fatigue sensitivity is minimized. However, the extent of the fatigue analysis is a function of cost as well as technical considerations. A marine structure costing \$1 million and another costing \$50 million will not be analyzed to the same extent. In lieu of extensive analysis, approximate analysis combined with greater safety factors is appropriate for less costly structures.

A fatigue criteria document may be very general, stating the design and analysis objectives and the classification and/or certification requirements. It can also list every method to be implemented and every assumption to be made in the execution of fatigue analysis. Most often the document will specify the scope of work, define overall methodology, and provide the data necessary for fatigue analysis.

A typical fatigue design and analysis criteria table of contents contains the following elements:

1. INTRODUCTION
 - 1.1 Objectives
 - 1.2 Scope
 - 1.3 Third Party Inputs
2. MODELLING
 - 2.1 Loads Model
 - 2.2 Mass Model
 - 2.3 Stiffness Model
3. OCEAN ENVIRONMENT
 - 3.1 Applicable Sea States
 - 3.2 Recommended Wave Theories
 - 3.3 Wave Directionality and Distribution
 - 3.4 Wave Scatter Diagrams and Recorded Data
 - 3.5 Wave Spectra
4. PRELIMINARY ANALYSIS
 - 4.1 Applicable Method
 - 4.2 Accuracy of Results

5. DETAILED ANALYSIS
 - 5.1 Structure Motions and Loading
 - 5.2 Calibration of Loading
 - 5.3 Nominal Stresses
 - 5.4 Applicable SCF Formulations
 - 5.5 S-N Curve and Fatigue Damage Calculation
6. FATIGUE SENSITIVITY STUDIES
 - 6.1 Study Parameters
 - 6.2 Areas Selected and Extent of Study
7. REFERENCES
8. APPENDIXES

4.5.2 Applicable Software

The analysis method chosen has to be compatible with the computer softwares available. Since a wide range of computer software is available, the analyses method and the software should be chosen based on structure configuration, applicable environmental loads, structural response to applied loading, stress distribution patterns and susceptibility to fatigue failure.

The software packages necessary to carry out the analysis and design functions should facilitate determination of:

- Ocean environment loads
- Structure motions
- Structural analyses and stress distributions
- Stress history and fatigue damage evaluation

While there are special-purpose software programs such as SEALOAD (Reference 4.24) to generate wave loads and SHIPMOTION (Reference 4.25) to determine motions, these and other software programs are often a component of larger generalized systems. A large system will facilitate execution of all functions from wave load generation to fatigue damage assessment within the system, eliminating the need for external data transfers.

There are numerous finite element programs well-suited for detailed analyses and design of continuous structures such as ships, semisubmersibles and TLPs. The best known of these programs in public-domain are ANSYS, NASTRAN, SAPIV, DAISY and SESAM. Mansour and Thayamballi (Reference 4.26) provide a survey of computer software and they discuss programs specifically developed for the marine industry.

4.5.3 Fatigue Versus Other Design and Scheduling Requirements

Fatigue analysis and design is only one of many aspects of the overall analysis and design effort. Because the final as-designed structure must meet many varied pre-service and in-service requirements, the fatigue design effort reflects the necessary interactions among various activities. The design criteria typically include specific assumptions and procedures to coordinate such activities. As an example, some of these interactions for a fixed offshore platform design project are as follows:

- A computer model used to generate extreme environment loads is also used for fatigue analysis, with changes in hydrodynamics coefficients and foundation matrix as necessary.
- A computer analysis model used for stiffness analysis should not account for the effect of thickened brace stubs, but the stress ranges used for fatigue analysis should account for the increased thickness.

The overall design schedule often dictates that fatigue design and analysis be carried out immediately after the structure's general configuration is finalized. But the fatigue design must incorporate flexibility, to allow for significant configuration revisions during the detailed design, which will affect both the applied loads and the stress ranges. The desired flexibility is often obtained by carrying out parametric studies to identify the effects of changes,

and by providing sufficient margin when determining the desirable fatigue lives.

LOCATIONS OF FATIGUE CRACKS

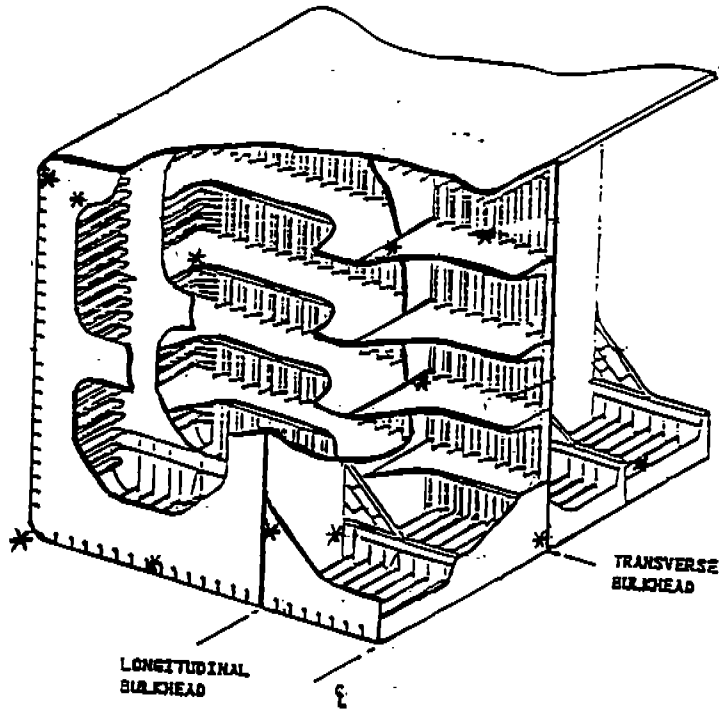


Figure 4-1 Typical Fatigue Sensitive Ship Structure Details

Design Procedure

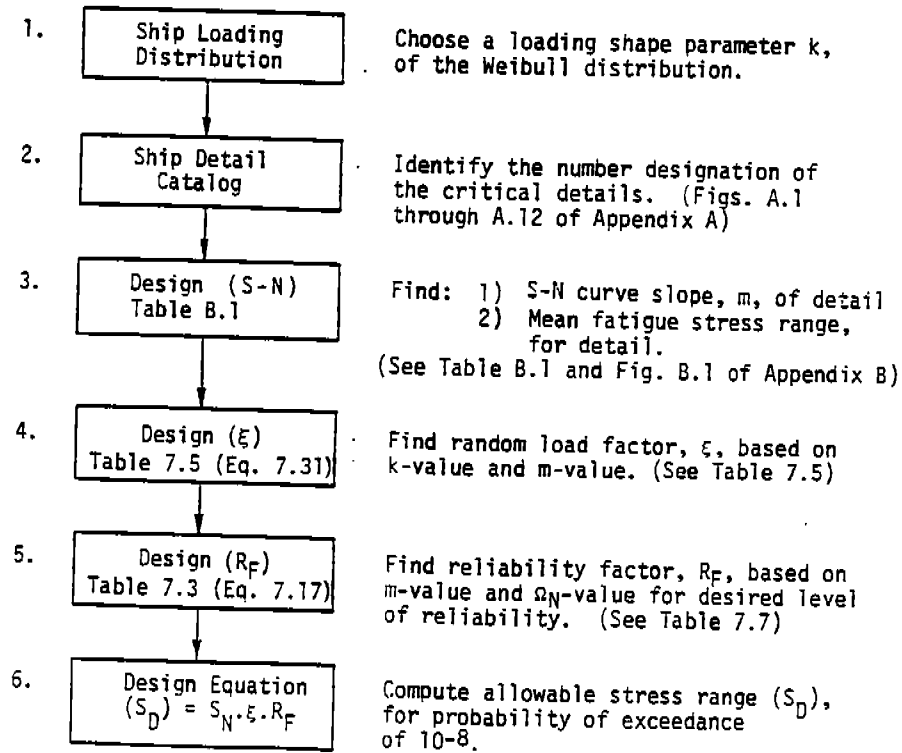


Figure 4-2 Munse's Ship Details Design Procedure

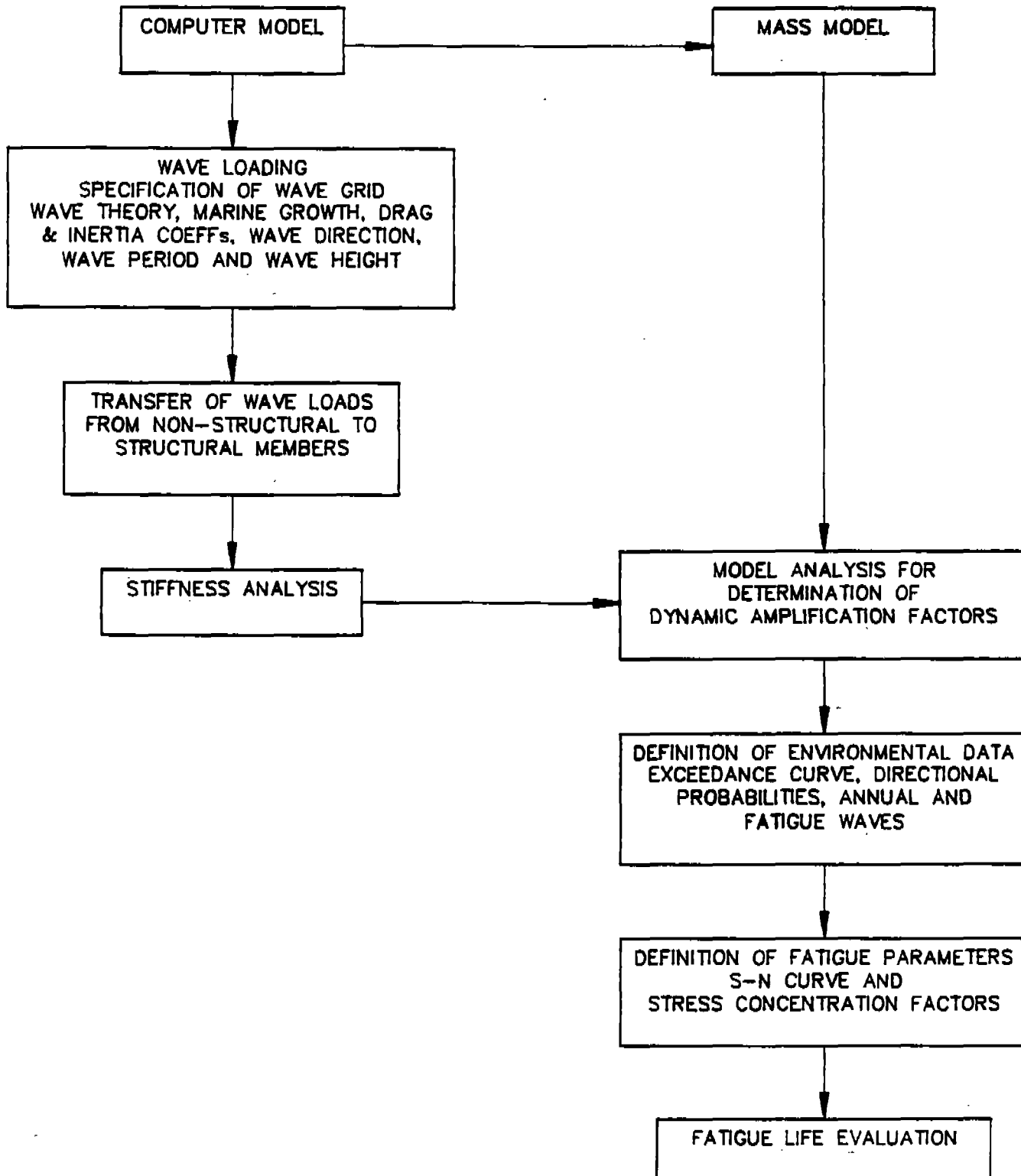


Figure 4-3 A Typical Deterministic Fatigue Analysis Flow Chart

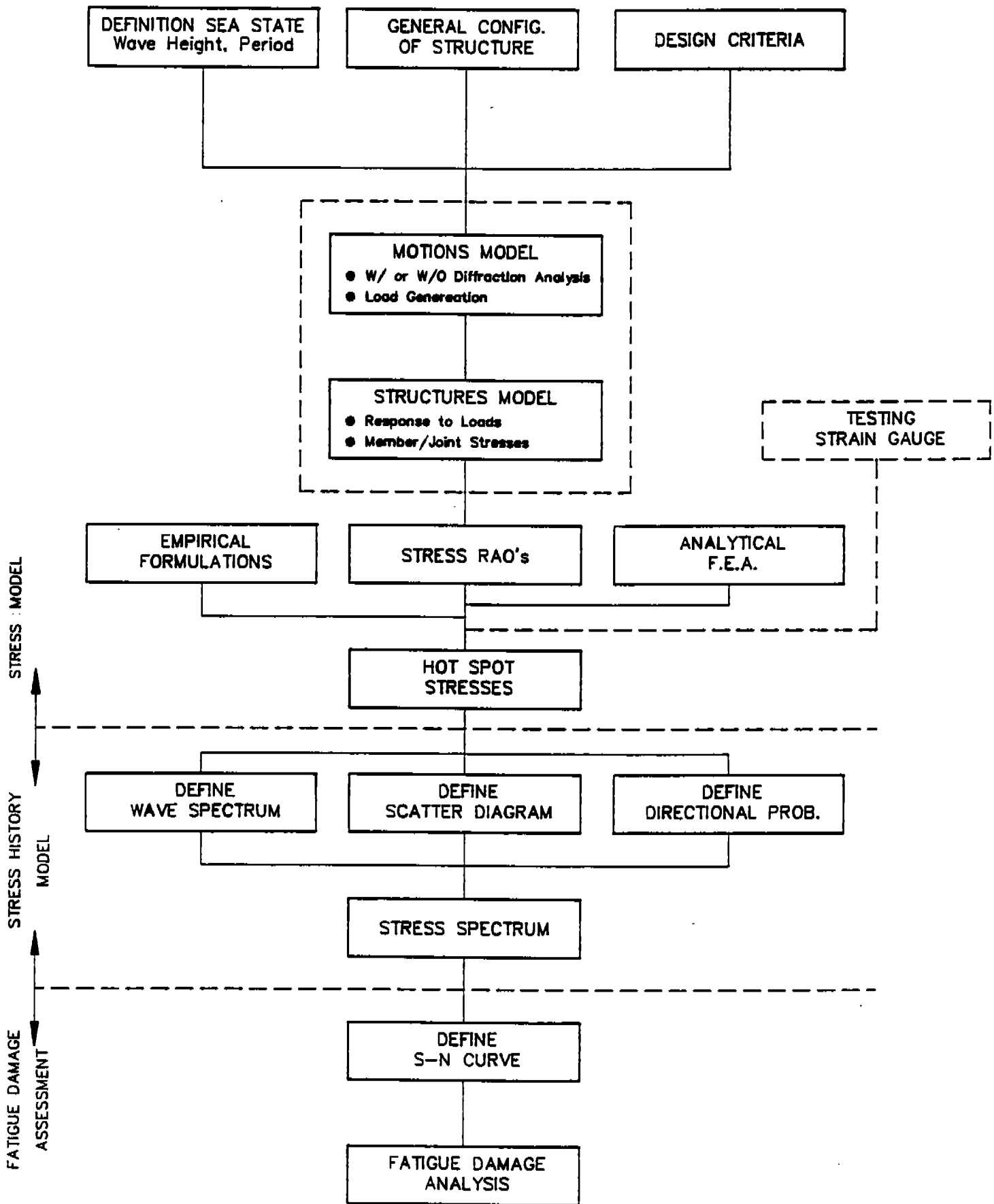


Figure 4-4 A Typical Spectral Fatigue Analysis Flow Chart

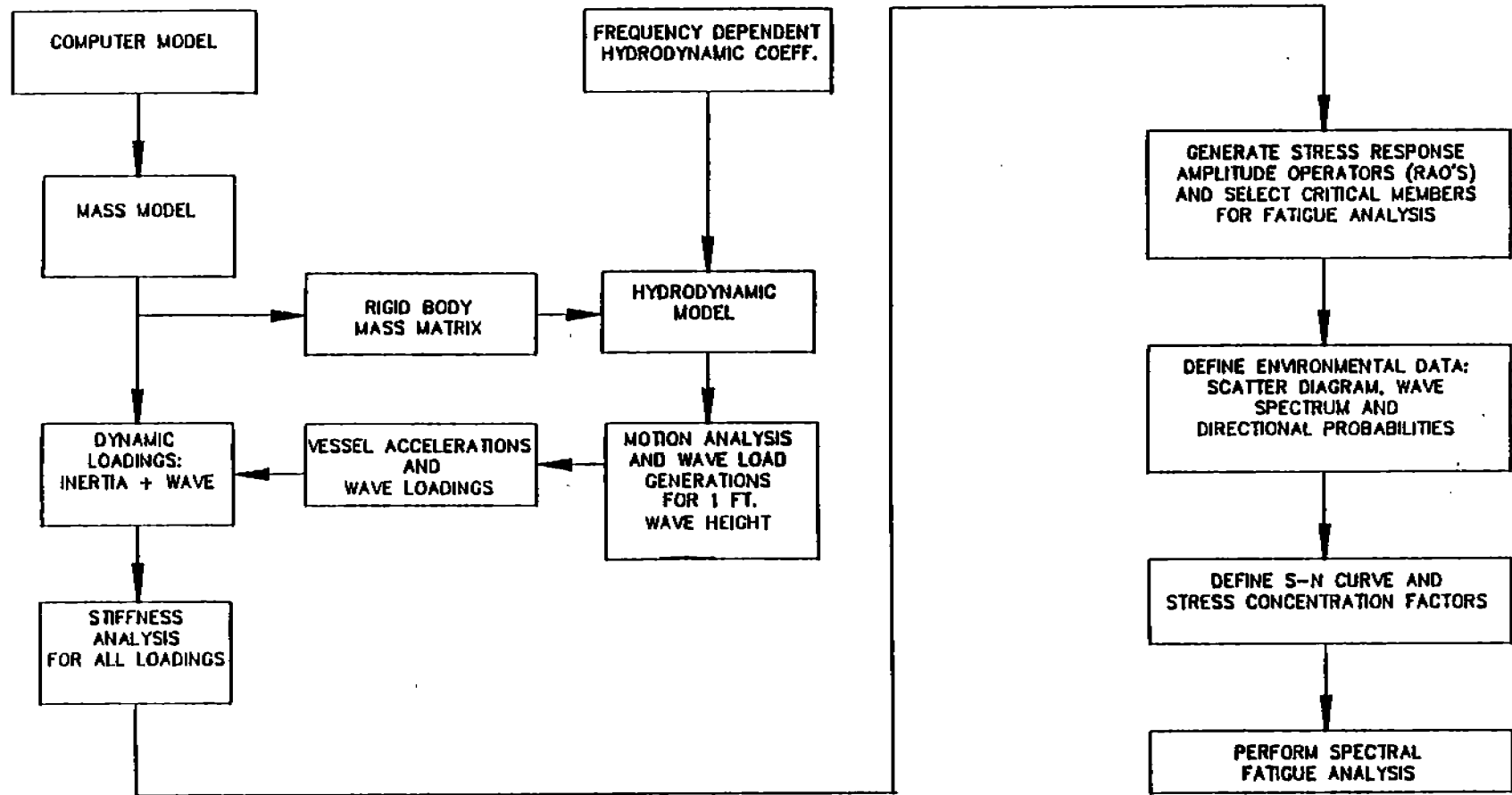
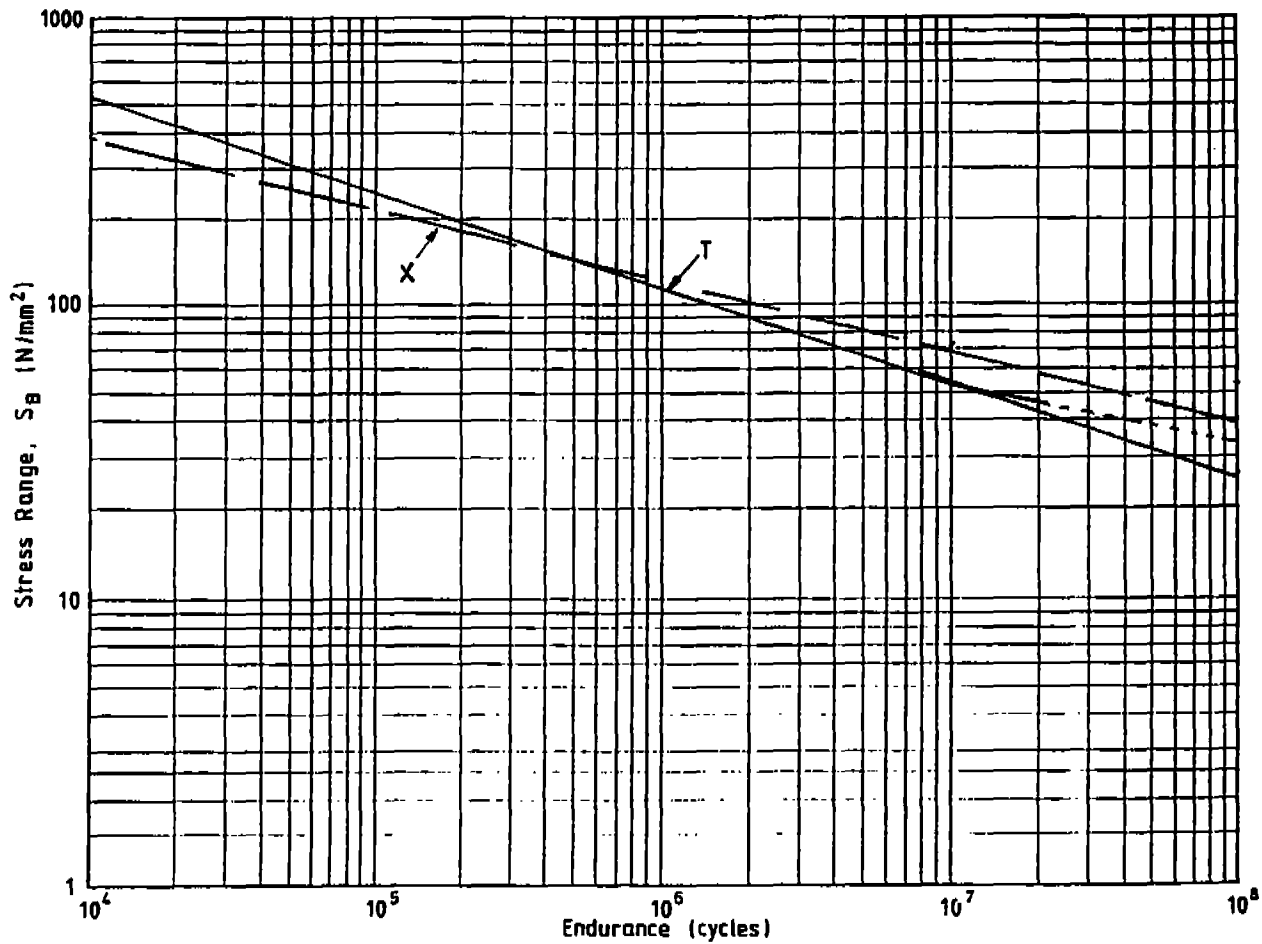


Figure 4-4 A Typical Spectral Fatigue Analysis Flow Chart



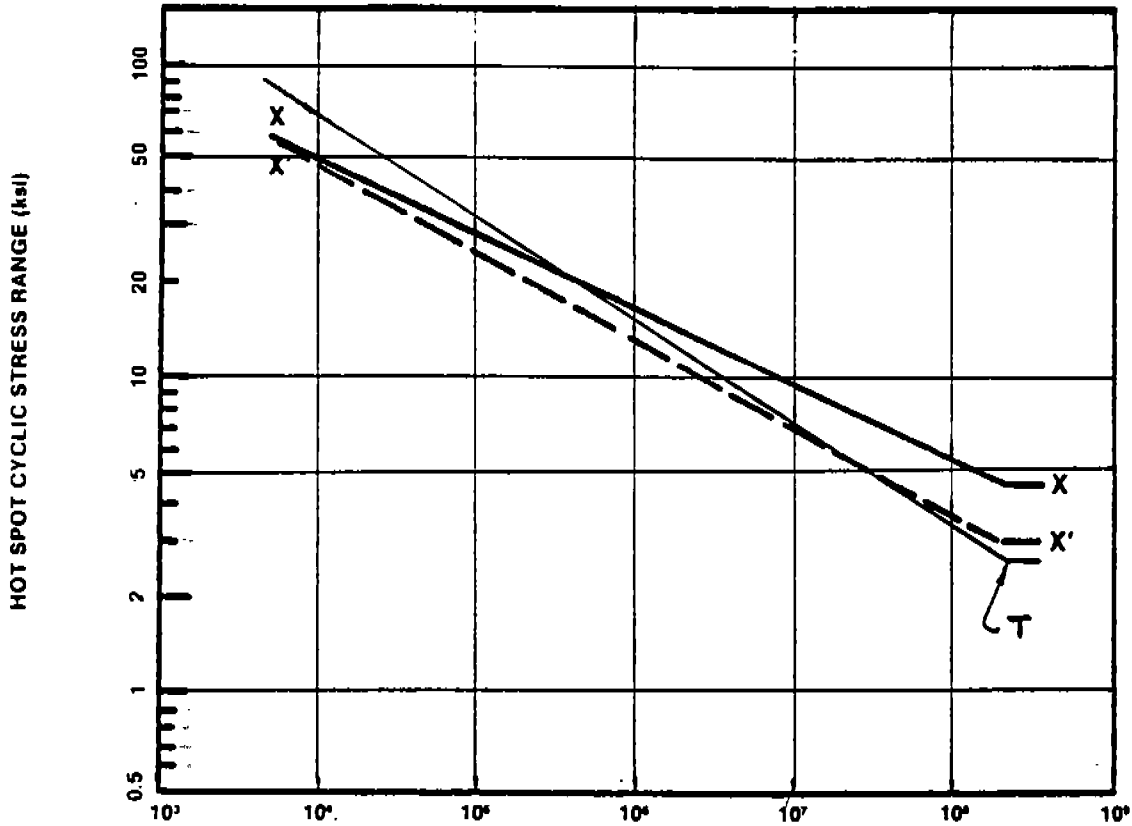
Details of basic S-N curves

Class	K_1	K_1		m	Standard deviation		K_2	S_0
		\log_e	\log_e		\log_{10}	\log_e		
B	2.343×10^{15}	15.3697	35.3900	4.0	0.1821	0.4194	1.01×10^{15}	100
C	1.082×10^{14}	14.0342	32.3153	3.5	0.2041	0.4700	4.23×10^{13}	78
D	3.988×10^{12}	12.6007	29.0144	3.0	0.2095	0.4824	1.52×10^{12}	53
E	3.289×10^{12}	12.5169	28.8216	3.0	0.2509	0.5777	1.04×10^{12}	47
F	1.289×10^{12}	12.2370	28.1770	3.0	0.2183	0.5027	0.63×10^{12}	40
F2	1.231×10^{12}	12.0900	27.8387	3.0	0.2279	0.5248	0.43×10^{12}	35
G	0.566×10^{12}	11.7525	27.0614	3.0	0.1793	0.4129	0.25×10^{12}	29
W	0.368×10^{12}	11.5662	26.6324	3.0	0.1846	0.4251	0.16×10^{12}	25
T	4.577×10^{12}	12.6606	29.1520	3.0	0.2484	0.5720	1.46×10^{12}	53*

* Idealized hot spot stress

For example the T curve expressed in terms of \log_{10} is:
 $\log_{10}(N) = 12.6606 - 0.2484d - 3\log_{10}(S_B)$

Figure 4-5 The DnV X- and the New T-Curves



PERMISSIBLE CYCLES OF LOAD N

NOTE — These curves may be represented mathematically as

$$N = 2 \times 10^6 \left(\frac{\Delta\sigma}{\Delta\sigma_{ref}} \right)^{-m}$$

where N is the permissible number of cycles for applied cyclic stress range $\Delta\sigma$, with $\Delta\sigma_{ref}$ and m as listed below.

<u>CURVE</u>	<u>$\Delta\sigma_{ref}$ STRESS RANGE AT 2 MILLION CYCLES</u>	<u>m INVERSE LOG-LOG SLOPE</u>	<u>ENDURANCE LIMIT AT 200 MILLION CYCLES</u>
X	14.5 ksi (100 MPa)	4.38	5.07 ksi (35 MPa)
X'	11.4 ksi (79 MPa)	3.74	3.33 ksi (23 MPa)

Figure 4-6 API X- and X'-Curves and DnV T-Curve

TOPIC	U.K. DEPARTMENT OF ENERGY (DEn) GUIDANCE NOTES	AMERICAN PETROLEUM INSTITUTE API RP 2A
<p><u>GENERAL CONSIDERATIONS</u></p> <ul style="list-style-type: none"> o Fatigue Life o Fatigue Loading o Fatigue Analysis/Design <ul style="list-style-type: none"> - Simplified Method - Detailed Analysis 	<p>Life \geq Service Life All cyclic loads (Ref. 21.2.10c)</p> <p style="text-align: center;">No</p> <p style="text-align: center;">Recommended</p> <p>* Life should not be <20 years and an additional factor on life is recommended when structural redundancy is inadequate (Ref. 21.2.10f)</p>	<p>Life > 2 x Service Life (Ref. 5.2.5)</p> <p>Yes, allowable stress method applicable to Gulf of Mexico (GOM) (Ref. 5.1.1)</p> <p>Recommended for:</p> <ul style="list-style-type: none"> - water depth \geq 400 ft (122m), or - platform period > 3 sec, or - environment harsher than GOM (Ref. 5.1.2)
<p><u>DETERMINATION OF STRESSES</u></p> <ul style="list-style-type: none"> o Objective o Modeling o Analysis 	<p>To determine cyclic stress ranges (i.e., mean stresses are neglected - Ref. 21.2.11)</p> <p>No specific reference</p> <p>A detailed fatigue analysis allowing each critical area to be considered.</p>	<p>To determine cyclic stresses properly accounting actual distribution of wave energy over entire frequency range, spectral analysis techniques are recommended.</p> <p>Space frame analysis to obtain structural response and stress distribution (including dynamic effects)</p> <p>Typically, spectral analysis to determine stress response for each sea state.</p>

Figure 4-7 Comparison of Recommendations
U.K. Guidance Notes and API RP 2A

97

TOPIC	U.K. DEPARTMENT OF ENERGY (DEn) GUIDANCE NOTES	AMERICAN PETROLEUM INSTITUTE API RP 2A
<p>o Hot Spot Stress</p>	<p>Range is the product of the nominal stress range in the brace and the SCF. It incorporates the effects of overall joint geometry but omits the stress concentrating influence of the weld itself.</p>	<p>Range is obtained by multiplying the nominal stress range at tubular joint by SCF.</p>
<p><u>STRESS CONCENTRATION FACTORS (SCFs)</u></p>		
<p>o SCF</p>	<p>No references given</p>	<p>SCFs defined are based upon modified Kellogg formulas (for chord) and Marshall formula (for brace) (Ref. C5.1, Table 5.1.1-1)</p>
<p>o Simple Joints - Nodal</p>	<p>None defined</p>	<p>SCFs define hot spot stresses immediately adjacent to the joint intersection ($0.25''$ to $0.1\sqrt{RT}$ from weld toe, Ref. C 5.4)</p>
<p>o Empirical Equations</p>	<p>None defined</p>	<p>K, T, Y and X joints defined for axial, in-plane and out-of plane loading</p>
<p>Other Joints</p>		<p>Recommends a brace SCF ≥ 6 (Ref. 5.5)</p>
<p><u>STRESS HISTORY</u></p>		
<p>o Wave Climate</p>		<p>Wave climates may be derived from both recorded data and hindcasts. Aggregate of all sea states to be expected over the long term condensed into representative sea states. A sea state, characterized by wave energy spectrum and probability of occurrence, may be defined by: o Two parameter scatter diagrams o Directional scatter diagrams o Directional scatter diagrams with spreading</p>

Figure 4-7 Comparison of Recommendations
U.K. Guidance Notes and API RP 2A

86

TOPIC	U.K. DEPARTMENT OF ENERGY (DEn) GUIDANCE NOTES	AMERICAN PETROLEUM INSTITUTE API RP 2A
<p><u>FATIGUE STRENGTH</u></p> <ul style="list-style-type: none"> o Defined by S-N curves based on experimental data o Tubular Joints <ul style="list-style-type: none"> - Recommended - Alternate o Other Joints o Other Parameters Affecting S-N Curves <ul style="list-style-type: none"> - Environment 	<p>Mean-minus-two-standard deviation curves (Ref. 21.2.10.f) $\log(N) = \log(K_1) - d \sigma - m \cdot \log(S_p)$ A slope of $m=3$ adopted based on data</p> <p>Full penetration welds - T curve (Ref. 21.2 - 12a)</p> <p>Partial penetration welds - W curve</p> <p>One of 8 classes: B, C, D, E, F2, G & W, depending on geometry, stress direction and method of manufacture and inspection</p> <p>Cathodically protected joints in Sea Water equivalent to joints in air. Unprotected joints in seawater require S-N curve to be reduced by a factor of 2 on 11fe (Ref. A21.2.13a)</p>	<p>The long-term wave height distribution may be represented by the sum of two Weibull distributions one for normal and another for hurricane conditions (Ref. Fig. C5.2.1)</p> <p>X curve is sufficiently devalued to account for thickness/size effect.</p> <p>Smooth weld metal merging with parent metal - X curve, otherwise X' curve (Ref. C5.4)</p> <p style="text-align: center;">Not Covered</p> <p>Refers to AWS D1.1</p> <p>S-N curves (X' and X) presume effective cathodic protection. Fatigue provisions of AWS D1.1 apply to members and joints in atmospheric service.</p>

Figure 4-7 Comparison of Recommendations
U.K. Guidance Notes and API RP 2A

109

TOPIC	U.K. DEPARTMENT OF ENERGY (DEn) GUIDANCE NOTES	AMERICAN PETROLEUM INSTITUTE API RP 2A
<p>- Plate Thickness</p> <p style="padding-left: 40px;">nodal joints</p> <p style="padding-left: 40px;">non-nodal joints</p> <p>- Weld Improvement</p>	<p>Basic S-N curve for $t_B=32$ mm (T curve) Correction $S = S_B (32/t)^{1/4}$</p> <p>Basic S-N curve for $t_B \leq 22$ mm (B-G curve) Correction $S = S_B [t_B/t]^{1/4}$ (Ref. Figure A.21.2.13b)</p> <p>30% in strength (2.2 factor on life) by controlled machining or grinding of weld toe (Ref. Figure A.21.8)</p> <p>Note: Required a smooth concave profile at weld toe with min. 0.5 mm penetration into the plate.</p>	<p>Does not recommend further reduction of S-N curve for free corrosion (FC) based on test data on both FC and cathodic protection (CP). (Ref. C 5.5)</p> <p style="text-align: center;">Not covered</p> <p style="text-align: center;">Not covered</p> <p>Profiling allows the use of X-curve rather than X'-curve</p>
<p><u>FATIGUE DAMAGE COMPUTATION</u></p> <p>Recommended Method</p>	<p>Cumulative damage by Miner's Rule (Ref. 21.2.14)</p>	<p>Cumulative damage by Miner's rule where stress responses for each sea state are combined into the long term stress distribution, which should then be used to calculate the cumulative damage ratio. Alternatively, the damage ratio may be computed for each seastate and combined to obtain the cumulative damage ratio, (Ref. 5.2.4)</p>

Figure 4-7 Comparison of Recommendations
U.K. Guidance Notes and API RP 2A

100

TOPIC	U.K. DEPARTMENT OF ENERGY (DEn) GUIDANCE NOTES	AMERICAN PETROLEUM INSTITUTE API RP 2A
<u>OTHER COMPONENTS</u>		
Cast or Forged Steel	Covered (Ref. 21.2.15)	Not covered
<u>OTHER CONSIDERATIONS</u>		
Fatigue sensitivity and consequence of failure studies.	Recommends identification of critical joints/members and developing a selective inspection program compatible with both fatigue sensitivity and failure consequence (Ref. 21.2.10e)	
PWHT	Beneficial reduction in the level of tensile residual stress. However, no benefits assumed on fatigue life. (Ref. 21.2.11)	Considered beneficial as residual stresses influence crack initiation. However, no benefits assumed on fatigue life.
Treatment of low stress cycles	Non-propagating stress at $N = 10^7$ (Ref. A21.2.13c)	Non-propagating stress at $N = 200 \times 10^6$
Treatment of high stress cycles	T curve extrapolated back to stress range $S_B = 2.2\sigma_f$ (Ref. A. 21.2.13d)	Endurance limits = 5.07 ksi (35 MPa) for X-curve 3.33 ksi (23 MPa) for X'-curve

Figure 4-7 Comparison of Recommendations
U.K. Guidance Notes and API RP 2A

101

(THIS PAGE INTENTIONALLY LEFT BLANK)

5. FATIGUE STRESS MODELS

5.1 REVIEW OF APPLICABLE MODELING STRATEGIES

The structure configuration essentially dictates the modeling strategies and the analysis methodologies. Various strip methods are used to determine the wave loadings on long, slender bodies such as ships. The strip theory can account for the effect of diffracted and radiated waves. The hydrodynamic loadings on ships, as well as semisubmersibles, can be obtained from three-dimensional diffraction analysis.

Discrete systems, such as bottom-supported fixed platforms, are substantially different from continuous systems, such as ships and semisubmersibles, in the characteristics of the applied loadings, their response to these loads, and the resulting stress distribution. Although the components of the strength model are similar for both systems, the specifics and the related uncertainties are different. Thus, fatigue stress models for bottom-supported and floating marine structures are discussed separately in Sections 5.2 and 5.3, respectively.

5.1.1 Modeling Strategies

Analytical models are developed to determine excitational loads, motions/response, and deformations/stresses. The level of desirable model complexity depends on many variables, including:

- The desired level of accuracy of results.
- The accuracy of variables/assumptions input into the analysis.
- The effect of modeling complexity on modeling errors and on the interpretation of results.

- The effect of modeling complexity on analysis schedule and cost.

The current state-of-knowledge provides us with the tools necessary to develop and analyze models. The desirable level of modeling sophistication, different for each structure, is thus determined based on tradeoffs among some of the variables given above.

The goal of a modeling strategy should always be to achieve realistically accurate results consistently and without excessive complexity. The analysis assumptions and the modeling strategy is very important in minimizing modeling accuracy/error. Most engineers rely on previous work and engineering judgement to reduce the level of modeling errors, typically defined as the ratio of actual-to-predicted results. Such a subjective approach can be supplemented by statistical methods to define the modeling uncertainty. The mean value of the modeling error, X_{me} , is defined as the "bias." While the modeling uncertainty is referred to as the random component of the modeling error. The modeling uncertainty, given by its coefficient of variation, $(C.O.V.)_{X_{me}}$ is meaningful only if sufficient data is available.

5.1.2 Comparison of Structures

A discrete system composed of numerous members and joints (such as an offshore platform) is modeled as a 3-D space frame. Individual members of the system are modeled as stick elements, with correct dimensions (diameter, net length) and hydrodynamic coefficients. The two basic premises affecting the accuracy of wave loadings are:

- The hydrodynamic forces are typically computed based on water particle kinematics along each member centerline. When the wave length-to-cylinder diameter ratio is less than about 10, the wave force computed based on a stick model centerline is too conservative.

- The water particle kinematics are assumed to be unaffected by the presence of such members. When the cylinders are spaced so that they are at least 3 or 4 diameters apart, the wave inertia forces on one cylinder are relatively unaffected by the presence of the other cylinders as the radiation effects are small.

Since platform member diameters are typically less than 3 feet (2.0m) for braces and less than 6 feet (2.0 m) for legs, the two basic premises are valid. Even if a 10 foot (3.0 m) diameter leg is utilized, for a wave period of 6 seconds the wave length-to-leg diameter ratio is in excess of 18. Thus, diffraction effects are small.

However, a 45 foot (14 m) diameter column of a tension leg platform will have a wave length-to-column diameter ratio of only about 4 for a wave period of 6 seconds. The columns are likely to be only 3 to 4 diameters apart. The column spacing is even less for a semisubmersible having three columns on each pontoon. Thus, the two premises are not applicable for structures made up of large members. The water particle kinematics at member centerlines are no longer valid for small wave periods and the presence of such members in the proximity of others affects the water particle kinematics.

Although the stick model of a platform can be modeled from one joint node to another, the applied loads could be in error by 2% to 3% because the loadings on member ends within the chord are computed more than once due to member overlaps. Most software packages include an option to define the member ends within the chord, preventing multiple computation of the applied loads, buoyancy and weight at each joint.

Accurate definition of a ship's deck strength is important to define the box-girder-like response of the entire hull. If a strip method is not used, the plate elements of the model used in a diffraction analysis (for loads) and the finite element analysis (for stresses)

shall have sufficiently fine mesh and member properties to ensure accuracy of the results. On other floating structures, such as the TLP and a semisubmersible, the diaphragm action of the deck plating can be represented either by shear plates or by equivalent beams.

5.2 FLOATING MARINE STRUCTURES

Both mobile and stationary marine structures are discussed in this section. The overall discussion is applicable to configurations ranging from ships and barges to semisubmersibles and tension leg platforms (TLPs).

The floating marine structure configuration and the mode of operation (mobile versus stationary) are the primary variables affecting the development of an appropriate "loads" or "hydrodynamics" model. The problems encountered and the technique applied to determine the wave loads are different for ships and other stationary marine structures for several reasons:

- While ships are treated as slender bodies, most offshore structures other than FPSOs, FOSs and drillships can not be treated as slender bodies.
- The three-dimensional flow calculation technique can be applied to typical stationary structures but cannot be applied to ships that have a constant forward speed.
- Steady-state response of a stationary structure to excitational wave loads allows determination of relative water particle velocities and accelerations and assessment of structure compliancy (net loading). These excitational loads have less influence on ships in-motion (i.e., near-complete compliancy).
- Stationary floating marine structures are moored/tethered and are subjected to low-frequency drift forces, which, due to the

"radiation pressure" of waves, significantly affect the mooring/tethering system design.

5.2.1 Ship Structures

Determination of Loads

Seakeeping and wave loads on ship structures are determined largely based on two-dimensional solutions of flow problems for plane sections. Combinations of various plane section solutions provide an approximate loading for the entire hull. Approaches based on utilizing the plane sections of slender hulls are identified as "strip methods." Typically, a strip method utilizes a linear relationship between wave amplitude and response in a frequency-domain solution. However, non-linear responses in a time domain can be also solved.

A two-dimensional flow problem is often analyzed for a range of variables. Typically, solutions are obtained for one wave direction and a number of frequencies. Then other wave directions, defining an angle of encounter between the wave and the ship, are chosen and solutions obtained. The study results are interpolated to determine the ship response amplitudes. Although eight wave directions should be considered for stress analysis (head and following seas, beam seas, bow quartering and stern quartering), several directions can be disregarded (global effects of port and starboard quartering seas are similar) for motions analysis.

Typically, strip methods disregard the longitudinal forces due to surge motions of the ship. Longitudinal forces are small and the use of Froude-Krilof forces and hydrostatic head appears to be satisfactory to determine the hull longitudinal stresses. However, work carried out by Fukusawa et al (Reference 5.1) indicates that the deck longitudinal stresses of a fully loaded tanker may be increased appreciably due to longitudinal wave forces.

The ship motion and wave action result in truly complicated interaction of variables affecting the loading on the hull structure. The loads due to incident, diffracted and radiated waves and due to ship forward motions may be approximated for various sections of the hull by the use of strip theory. Loads due to diffraction and radiation can be also directly obtained from a three-dimensional flow solution. Work carried out by Liapis and Beck (Reference 5.2) provides a very good comparison of various 3-D flow solutions, strip theory solution and experimental results. The added mass and damping coefficients plotted against frequency on Figure 5-1 indicate that the coefficients obtained by Liapis and Beck are quite close to those obtained based on both strip theory and experimental work. Actually, over the range of applicable frequencies, the three sets of coefficients based on 3-D solutions show larger scatter.

Considering the difficulties of applying 3-D solutions and the proven reliability of good strip methods, a strip method is likely to remain the preferred approach to determine the applied loads in most ships. Ships with special characteristics, including supertankers, navy vessels, drillships, etc., are the likely candidates for application of 3-D flow solutions. It should be emphasized that whichever solution method is chosen, substantially greater inaccuracies are introduced into the hull loading due to:

- Uncertainties on wave height and period (wave statistics)
- Uncertainties regarding ship routing and the correlation with wave environment
- The variable nature of ship cargo and ballasting
- Inaccuracies in hull response to applied loads

The preceding discussion covers wave loading on ships susceptible to cumulative fatigue damage. A linear theory is applicable to determine the applied loading for fatigue analyses and design. In an extremely harsh environment, wave nonlinearities have substantial

influence on the applied loading. However, a linear theory can still be used in a harsh environment to produce approximate loadings as harsh environment generally contributes very little to the cumulative fatigue damage.

If an appreciable portion of fatigue damage is due to harsh environment loading, some of the important variables not accounted for in linear theory should be evaluated:

- Wave steepness
- Wave slamming
- Viscous effects
- Hydrostatic effects (due to flaring ship sections)
- Hydrodynamic effects (due to flaring ship sections)

These primary and other secondary nonlinearity effects on ship loading can be accounted for by perturbation and simulation methods. Second-order perturbation methods are relatively simple and they are used to solve the wave action/ship motion problem in the frequency domain. A detailed discussion of second order perturbation methods is presented in References 5.3 and 5.4.

Another approach to determine the non-linear effects is the integration over time of the applied forces on the structure. A detailed discussion of such simulation methods, including principles of effective computer simulations, is presented by Hooft (Reference 5.5).

Motions Model and Analysis Techniques

Since the linear ship motion theory is considered appropriate for large majority of spectral fatigue analyses, the modeling and analysis technique is further discussed.

Typically, a standard ship or a tanker has two distinct drafts, one for laden and another for ballast condition. The pre-analyses effort usually covers the following:

- Preparation of a table of offsets for the vessel, defining the geometry with stations (20 or more) along the longitudinal axis and points (15 or more) at each station (i.e. describing the transverse section).
- Preparation of weight distribution to define structure (steel) and variables (ballast, cargo, fuel, etc.).
- Utilization of table of offsets and weight distribution to compute bending moments and shear forces at each station.

The shear force and bending moment diagrams developed along the length of the vessel facilitate equilibrium checks.

The vessel motion analysis requires definition of vessel hydrodynamic properties. For a linear strip theory based ship motion computer program, the hydrodynamic properties defining vessel added mass and damping coefficients may be input based on available data on similar vessels. Conformal mapping approach is also used to define the added mass and damping coefficients. However, if the vessel configuration is unique, a 2D or 3D diffraction analysis is recommended to define the hydrodynamic properties.

The linear strip theory based ship motion program, utilizing the hydrodynamic coefficients, is used to generate equilibrium solutions for vessel motions in six degrees of freedom. Then, the transfer functions can be defined for vertical and lateral bending, torsional moments, vessel accelerations and hydrodynamic pressures at each station along the vessel longitudinal axis.

Finite Element Stiffness Model

The load transfer function, both in-phase and out-of-phase components, are used in the stress analyses to obtain corresponding stress range transfer functions. The computer model and the structural analysis used is very important to define local stress ranges. Fatigue is a local phenomena and it is important to define

their function, selecting appropriate element aspect ratios (less than 1:2) will contribute both to better accuracy and a better model.

5.2.2 Stationary Marine Structures

Determination of Loads

Stationary marine structures have various configurations and exhibit a wide range of compliancy. A substantial effort is desirable to minimize the fatigue loadings on stationary structures. For a moored tanker FPSO the smallest functional size exhibiting a minimum silhouette is desirable. For structures composed of columns and pontoons, the column spacing, column water plane area, displacement of pontoons affecting overall center of buoyancy and the total displacement are some of the interacting parameters that affect not only the magnitude and character of the applied loading but also the response of the structure to applied loading (see Reference 5.6 for structure configuration optimization).

While the hydrodynamic forces on a slender stationary body can be determined based on strip method or diffraction theory, a structure made up of columns and pontoons can be determined either by Morison's equation or by diffraction theory. As discussed in Section 5.1, large diameters disturb the flow, leading to diffraction which is highly frequency dependent. There are two benefits of using diffraction theory:

- Diffraction usually causes a reduction in the wave loads.
- Viscosity can be ignored and thus, treating the flow as irrotational, potential flow theory may be used.

The hydrodynamic loads acting on a structure are typically generated using a combination of three-dimensional diffraction theory, i.e., a source-sink distributed potential theory (Reference 5.7) and a conventional Morison's equation. Although a two-dimensional

analysis program can be used, a three-dimensional program facilitates overall analysis effectiveness.

To analyze, the structure surface is divided into panels, much like a finite element model and the potential flow problem is solved over each panel and yields diffraction and radiation pressures on these panels. While the diffraction pressures are transformed into member wave loads, the radiation pressures are transformed into added mass coefficients. Hydrodynamic drag forces on these members and both the drag and potential forces on smaller members (simulated by stick elements) are generated using Morison's equation. Diffraction effects are strongly dependent on frequency, so a range of frequencies must be addressed.

Mass Model

Typically the deck structural members are modeled by using equivalent members to represent the deck structure mass and stiffness. All other members subjected to hydrodynamic loading are modeled, with appropriate mass distribution. The accuracy of structure mass and its distribution directly affect the accuracy of structure motions.

Motions Model and Analysis Techniques

The mass model discussed above allows determination of a structure's inertial response to the applied excitational environmental loads by obtaining solutions to the six-degree-of-freedom equilibrium equations. Considering the rigid-body motions, the dynamic force equilibrium on a structure can be expressed using the following system of six simultaneous equations:

$$[[M] + [M_a]] \{ \ddot{X} \} + [[C_R] + [C_V]] \{ \dot{X} \} + [K_H] \{ X \} = \{ F_D \} + \{ F_I \} + \{ F_{DF} \} \quad 5-1$$

This equation differs from that in Section 5.3.3 in that (1) primary damping is due to wave radiation and viscous effects, (2)

hydrostatic stiffness is introduced and (3) the make-up of applied forces differs.

The terms given represent:

- [M] = 6x6 structure mass matrix
- [M_a] = 6x6 added mass matrix
- [C_R] = 6x6 wave radiation damping matrix
- [C_V] = 6x6 linearized viscous damping matrix
- [K_H] = 6x6 hydrostatic stiffness matrix
- (F_D) = 6x1 linearized wave drag force vector
- (F_I) = 6x1 wave inertia force vector
- (F_{DF}) = 6x1 diffracted wave inertia force vector
- {x}, {ẋ}, {ẍ} = 6x1 structure displacement, velocity and acceleration

If a structure such as a TLP is tethered to the seafloor, the stiffness matrix is modified from:

$$[K_H] \{x\} \text{ to } [[K_H] + [K_T]] \{x\}$$

where, the [K_T] represents 6x6 tether stiffness matrix.

As discussed in previous sections, the structure configurations and the motion characteristics (i.e., steady state harmonic motion) facilitate the 6 x 6 motions equations solution over the frequency domain.

It is recommended that the significant wave height in the wave scatter diagram that is likely to contribute most to the fatigue damage be chosen to linearize the drag forces for all wave frequencies.

The basic approach discussed here has been utilized frequently in recent years, and is discussed herein as it was implemented on the design and analysis of a TLP by Sircar et al (Reference 5.8). The

approach, also called "consistent method" differs from the conventional analyses method only in the generation of hydrodynamic loads. The hydrodynamic loads for a conventional analysis are typically generated based on a method by Hooft (Reference 5.5) with a modified form of Morison's equation. Although the conventional method also yields reliable results in most cases, it should be noted that the hydrodynamic interaction among component members of the structure is neglected. Figure 5-2 shows that the applied heave and pitch loadings based on both consistent and conventional methods are very similar for wave periods (4 to 8 sec.) that contribute largely to fatigue damage. For larger wave periods (9 to 15 sec.) representing less frequent larger waves, the consistent method provides more reliable results.

Stiffness Model

Typically the hydrodynamic model, mass model and stiffness model are all developed from the same structural model. The stiffness model incorporates correct member cross-sectional areas and stiffness properties, joint releases and boundary conditions to allow correct distribution of structural member loadings and stresses.

The stiffness analysis is performed for each wave period and direction to obtain in-phase and out-of-phase member stresses. It is necessary that nominal stresses computed are realistic. Thus, if stick members are used to represent large members with internal chords and bulkheads, additional finite element study of such areas may be necessary. By using the loads from stick model analyses as the applied loads on a detailed finite element model of a joint, accurate stress distribution can be obtained to define the nominal stresses in each sub-component of such complex joints.

5.2.3 Overview and Recommendations

Although allowable stress methods may be used to size the component members of marine structures and to develop better details, a detailed fatigue analysis is recommended for each structure. Each

structure is unique and an allowable stress method based on typical structures and a typical environment will only provide information on relative susceptibility of various joints/details to fatigue failure. In addition, newer vessels are often constructed from high strength steel, allowing the use of thinner plates. Ship structure scantling sizes are based on strength requirements and any reduction in scantling sizes without due consideration for fatigue phenomena is likely to make the allowable stress method unconservative. Therefore, allowable stress methods can be used as a "screening process" and a detailed fatigue analysis is recommended to ensure integrity of the design.

Ship Structures

The use of a linear ship motion theory is appropriate for fatigue analysis of most vessels. For most vessels structural dynamic amplifications, wave nonlinearities, and effects such as springing due to high forward speeds have negligible effect on overall fatigue lives. However, some vessels operating in harsh environments may be subjected to appreciable fatigue damage due to harsh environment loading. For such vessels the ability to predict wave nonlinearities and vessel hogging, sagging and racking effects accurately may become important. In such instances, a non-linear ship motion theory may be preferred over a linear ship motion theory.

Fatigue is a local stress phenomena and it necessitates accurate definition of stresses for very complex geometries. In addition to primary hull girder bending in horizontal and vertical axis, substantial secondary girder bending moments will occur due to external dynamic loads on vessel bottom and internal inertial loads due to vessel contents. Thus, a beam theory based nominal stresses due to primary hull bending are inaccurate both due to complexity of geometry and the local load effects. A finite element model should be developed to represent the behavior of the vessel and to determine the local stress distributions accurately.

For each load component (in-phase and out-of-phase) at each frequency of a given wave direction the finite element model is used to generate local stress distributions. The stress range transfer functions are then generated for each wave direction. Although current computers are well suited to compute large problems, the number of frequencies necessary to define the transfer function may be small. Using the predominant load transfer function as guide a limited number of frequencies (say 4 to 6) may be adequate to define the other transfer functions. The use of a stress range distribution parameter allows carrying out of a fatigue analysis with relatively few structural analyses cases. The accuracy of fatigue lives obtained largely depends on the validity of the Weibull shape factor used.

The shape factors obtained by calibrating the characteristic stress range against spectral fatigue approach indicate that the single most important variable affecting the shape factor is the environment. While the shape factor may vary from 0.8 to 1.2, depending on the route characteristics and on structure geometry, a factor of 1.0 may be used when such information is not available.

Stationary Marine Structures

The accuracy of stress transfer function for a joint/detail of a stationary marine structure depends on many variables, including the accuracy of applied loads, motion response characteristics and the stress distribution. Hydrodynamic forces may be determined by either Morison's equation or by diffraction theory. Since the wave length-to-member sizes are small for most floating (i.e. semisubmersibles, TLPs) structures, diffraction effects should be accounted for.

A 2D or 3D diffraction analysis can be used to generate the hydrodynamic coefficients. Then, utilizing these coefficients, Morison's equation can be used to generate the applied loads. As an alternative, diffraction analysis can be used to generate the wave

loads directly. Since the diffraction effects are strongly dependent on frequency, a wide range of frequencies must be used.

The response of the floating structure to applied wave loadings depends on its own geometry, stiffness and mass properties. Water plane area and its distribution (i.e., hydrostatic-stiffness) and mass properties directly affect the natural periods and the heave, pitch and roll response amplitudes. For a tethered structure, such as a TLP, tether stiffness will predominate hydrostatic stiffness. Tether pretensions will control surge and sway natural periods and response amplitudes. The primary damping is due to wave radiation and viscous effects.

It is recommended that the "consistent approach" discussed in Section 5.2.2 is used to accurately generate hydrodynamic loads. A finite element model of the structure can be used to obtain the solution to the motions analysis and determine the stress distributions. As an alternate, a stick model may be used to obtain solutions to the equations of motion and to define global deformations and forces. Then, additional finite element models of various interfaces will be necessary to determine local stress distributions accurately. The boundary conditions for the finite element models will be the stick model deformations.

5.3 BOTTOM-SUPPORTED MARINE STRUCTURES

This section discusses bottom-supported marine structures that are represented by three-dimensional space frames and composed of cylindrical shells. The dynamics of a large gravity-type bottom supported structure dynamics are somewhat similar to those of a fixed platform. However, the characteristics of excitational loads on gravity structures have more in common with floating structures.

5.3.1 Load or Hydrodynamics Model

A wave force acting on a single stationary element is due to both the acceleration of water particles (inertial force) and the kinetic

energy of the water particle (drag force). These forces are given by Morison's equation as:

$$\begin{aligned}
 F &= F_I + F_D \\
 &= \frac{\pi}{4} \rho C_m D^2 \dot{u}_w + \frac{1}{2} \rho C_d D u_w |u_w|
 \end{aligned}
 \tag{5-2}$$

where:

F = hydrodynamic force vector per unit length acting normal to the axis of the member

F_I & F_D = inertia and drag components of F

ρ = density of water

C_m = inertia force coefficient

C_d = drag force coefficient

D = diameter of a tubular

u_w = component of the velocity vector of the water normal to the axis of the member

$\dot{u}_w = \frac{du_w}{dt}$ = component of the acceleration vector of the water normal to the axis of the member

$| |$ = denotes absolute value

An appropriate approach to estimate the wave forces with reasonable accuracy is to assess the load model in its entirety, and for its component elements.

The element diameter should reflect any geometric variations, including marine growth. The C_d and C_m values applied may range

typically from 0.6 to 0.8 and 1.5 to 2.0, respectively. Very comprehensive experimental data obtained from full-scale measurements of the second Christchurch Bay Tower (References 5.9, 5.10 and 5.11) validate the coefficients in use today. As illustrated on Figure 5-3, the C_d and the C_m values applicable for most cylindrical members near the water surface (Level 3) are 0.66 and 1.8, respectively. Although these values are applicable for Keulegan-Carpenter (K_e) number in excess of 30, even when K_e is reduced to 5, the inertia coefficient, C_m , value reaches 2.0, while the drag coefficient, C_d , gradually increases to unity at K_e equal to 10.

These coefficients also decrease with the distance from the water surface. However, because the uncertainties in marine growth (which directly affects the surface roughness and therefore the drag coefficient) and the additional effort necessary to input, check and justify different coefficients, it is advisable to use one set of C_d and C_m values.

The use of conventional Morison's equation and the wave kinematics for regular two-dimensional waves has proven to be valid for jacket structures in moderate water depths. Assessment of measured wave force data (Reference 5.12) for extreme wave loading associated with directionally spread seas in a hurricane environment in the Gulf of Mexico compares quite well with those analytically computed.

Morison's equation is also valid to compute forces on non-cylindrical members by applying appropriate C_d and C_m values and equivalent diameters. Suitable values of C_d and C_m for different cross-sections may be obtained from a Det norske Veritas (DnV) document (Reference 4.16.)

If the extreme loadings are to be computed, an applicable wave theory, compatible with the wave steepness, water depth, etc., must be used. The applied total load on a structure composed of many members is then the cumulative sum of loads computed on each member

for a pre-defined wave height, wave period and crestline position. This conventional regular wave method produces applied hydrodynamic loads that has been validated by an extensive performance record of structures in shallow-to-moderate water depths. However, such a method is not advisable for structures in deeper water and exhibiting dynamic response. More rigorous approach to represent the true response characteristics is necessary (References 5.13 and 5.14).

5.3.2 Mass Model

For a bottom-supported structure in relatively shallow water, a mass model may or may not be necessary. Such a rigid structure has natural periods that are less than about 3 seconds and exhibits little dynamic response when subjected to long-period waves associated with a harsh environment. For such an environment the static forces obtained due to water particle kinematics can be increased slightly to account for the dynamic response predicted (i.e., computation based on estimated natural periods). However, most of the fatigue damage is likely to occur due to short-period waves, necessitating determination of platform dynamic response to a wide range of wave periods.

Whether platform dynamic response is to be determined or not, the dynamic amplification factors (DAF) used in a deterministic fatigue analysis require an accurate estimate of natural periods and the use of a mass model is recommended to obtain an eigenvalue solution. For a spectral fatigue analysis, only the use of a mass model allows determination of platform dynamic response and direct generation of structure inertia loads that are compatible with the excitation loads due to waves.

A mass model of a three-dimensional space frame should incorporate all structural members. The mass will be accurately defined if the weight of all structural and non-structural members, deck equipment, ballast, hydrodynamic mass, etc., are accounted for correctly and in their respective locations. Ideally, all member weights should

therefore be defined uniformly along the member lengths. However, considering the cost of modal analysis, most structural member weights are input as lumped masses at member ends that attach to applicable joints.

5.3.3 Motions Model and Analyses Techniques

The mass model discussed above allows determination of a structure's initial response to applied excitational environmental loads by the use of equilibrium equation solutions. The dynamic force equilibrium on a structure can be expressed using the following system of six simultaneous equations:

$$[[M] + [M_a]] \{X\} + [C] \{\dot{X}\} + [K] \{X\} = \{F_D\} + \{F_I\} \quad 5-3$$

where:

[M]	=	6 x 6 structure mass matrix
[M _a]	=	6 x 6 added mass matrix
[C]	=	6 x 6 structure damping matrix
[K]	=	6 x 6 structure stiffness matrix
{F _D }	=	6x1 wave drag force vector
{F _I }	=	6x1 wave inertia force vector
{X}, { \dot{X} }, {X}	=	6x1 structure displacement, velocity and acceleration

The terms on the right hand side of the dynamic equilibrium equations represent external forces applied to the structure. Following solution of the equilibrium equations, the structure dynamic response can be moved to the right hand side of the equation to define the resultant loading.

Thus, the net loading using Morison's equation given in Section Eqn. 5-2 can be rewritten as:

$$F_{net} = \frac{\pi}{4} \rho D^2 [C_m \dot{u}_w - (C_m - 1) \dot{u}_s] + \frac{1}{2} \rho C_d D u |u|$$

where:

- u = defined as the net velocity vector component $\equiv u_w - u_s$
- u_w = the component of the velocity vector of the water
- u_s = the structure velocity
- u_w = the component of the acceleration vector of the water
- u_s = the structure acceleration
- C_m = added mass coefficient is often taken to be a variable ranging from 1.5 to 2.0. It is recommended that C_m be taken as 2.0, which is consistent with the potential flow solution for added mass.

It is necessary to choose an appropriate method or analysis technique that is compatible with fatigue design parameters such as the structure configuration and its susceptibility to fatigue and the environment. If the structure dynamics are negligible, and a deterministic analysis, based on the use of wave exceedence curves, may be appropriate for initial sizing of platform components. However, for most structures, the dynamic response should be incorporated into the fatigue analyses as illustrated in the above given equilibrium equations.

A rigorous analysis using a time integration method to determine platform global and local dynamic responses at each wave height and period is time consuming and costly. Therefore, it is desirable to have an alternative analysis procedure. One such alternative proposed by Serrahn (Reference 5.15) consists of a hybrid time and frequency domain analysis method. The analysis flow chart on Figure 5-4 summarizes this analysis methodology.

Global spectral static and dynamic responses (e.g. base shear and overturning moment) are determined at selected discrete wave heights and periods. The static response is determined based on an applied

load analysis of a detailed three-dimensional model of the platform. An eigenvalue (modal) analysis is also performed on the same model to determine platform natural periods and mode shapes. The platform global dynamic responses are determined by separating each applied static wave loading into its Fourier series components and solving directly for the dynamic response (This method of solution is detailed in Appendix E of Ref. 5.15). Spectral analyses for both the static and dynamic responses are then performed and the spectral inertial load calculated. Inertial load sets are then developed from the modal results of the previous eigenvalue analysis which produce the calculated global spectral inertial response (This method of inertial load development is detailed in Appendix F of Ref. 5.15).

Such analyses can be repeated for various wave spectra, structural damping, platform period, etc. at a relatively nominal increase in analysis time and computer cost. Therefore, this method facilitates parametric studies to assess fatigue sensitivity of the platform.

Of the three spectral analysis options available to define the wave loading, the frequency-domain solution, providing member and joint in-and out-of-phase wave loads is most frequently used due to its simplicity. For an iterative design process, an analysis approach utilizing random waves or regular waves in time domain is appropriate but not frequently used due to both time and cost constraints. Thus, a hybrid time and frequency domain method is well suited for spectral fatigue analysis of a bottom-supported structure. Figure 5-5 illustrates the scatter of fatigue lives as a function of the analysis method chosen.

Another appropriate procedure to define hydrodynamics and wave-force model, proposed by Kint and Morrison (Reference 5.16), is based on a short extract from a random simulation substituted for a design wave. The proposed procedure offers a valid and a relatively simple alternative to the conventional regular wave analysis. Inertial loads due to structure response can be obtained and dynamic amplification factors (DAFs) determined by performing a number of

simulations of random waves. The basic DAF approach, allowing combination of inertial loads compatible with static loads, is further discussed by Digre et al (Reference 5.17). Typically, simulation of the response is performed, the ratio of dynamic-to-static loads determined (i.e. DAF), and the process is repeated until the DAF stabilizes. Larrabee (Reference 5.18) also provides further discussion on the logic behind DAF approach.

5.3.4 Stiffness Model

The load and the stiffness models are essentially the same. Typically, a three-dimensional space frame model of the structure is made up of individual joints and members, each defining the joint and member incidences, coordinates, hydrodynamic coefficients, etc. that are necessary for generation of environmental loads. The loads model, provided with member cross-section areas and stiffness properties, joint releases, and boundary conditions, transforms into a stiffness model. The structure mass model incorporates the correct member sizes, joint coordinates and boundary conditions, and can be considered a stiffness model. Static stiffness analysis solution follows standard structural analysis technique. Dynamic analysis is typically based on a modal (eigenvalue) analysis solution; two modal analysis solution techniques may be used:

- The subspace iteration technique is a Ritz-type iteration model used on a lumped mass system that produces eigenvectors and eigenvalues for a reduced set of equations. This is the method of choice for most fixed offshore structures since only a relatively small number of modes are required to adequately model the total structure response.
- The Householder tridiagonalization technique first tridiagonalized the dynamic matrix, then computes all eigenvectors and eigenvalues by inverse iteration. This technique is most appropriate for structures with a small number of degrees of freedom, for structures where all modal

responses are required , or where consistent mass modeling has been used.

Once eigenvectors and eigenvalues have been determined, specific dynamic analyses under load (such as wave loading) may be performed. As previously mentioned, rigorous time integration analyses may be undertaken, evaluating the dynamic response of the platform over many cycles of wave loading until steady state response is achieved. However, the previously recommended approach of expressing the applied loading as a Fourier series and solving and superimposing the response of each platform mode to each Fourier sinusoidal component allows direct determination of platform dynamic response without time consuming and costly time integration analyses.

The global analysis carried out is often intended to analyze the three-dimensional space frame lateral deformations and ensure that all components of the structure meet fatigue requirements. An emphasis should also be placed on plan-level components near the water surface and subjected to vertical (out-of-plane) deformations.

5.3.5 Overview and Recommendations

Small structures in shallow-to-moderate water depths and in relatively mild environments are typically not analyzed for fatigue. Often, stress levels are evaluated and API's simplified allowable stress method is used to verify the integrity of design.

Other structures are designed for a wide range of pre-service and in-service design conditions, including fatigue. Since a fatigue analysis is carried out to ensure that the design has adequate safety against damage due to fatigue during the planned life of the structure, it should address the variables affecting fatigue appropriately. Modeling and analysis variables (stiffness and mass models, loading coefficients, stress RAOs, SCFs, etc.), affecting the strength model, and the wave climate (scatter diagram, directional probability, wave spectrum), affecting the time history model, incorporate substantial uncertainties.

The analysis effort must be kept comparatively flexible and manageable and the level of effort should be compatible with design objectives and available information.

It is recommended that a simplified allowable stress approach or a deterministic fatigue analyses be limited to initial sizing of members, if considered desirable. A thorough spectral fatigue analysis is recommended to identify fatigue sensitive components/details of a structure and to take corrective measures.

Considering its relative ease of application a spectral frequency-domain method is well suited for design. A time-domain method is better suited to determine the response of a bottom-supported structure. Since it is time consuming and costly to determine global and local dynamic response of the platform for each wave height and period, an alternate less time consuming method is desirable. Several methods (References 5.15 and 5.16) are appropriate. A hybrid time- and frequency-domain analysis method (Reference 5.9), also facilitates carrying out of extensive parametric studies to assess fatigue sensitivity of structure components for a wide range of variables and is recommended for fatigue analyses and design.

5.4 DEVELOPMENT OF HOT-SPOT STRESSES

5.4.1 Nominal Stresses and Stress RAOs

The stresses obtained from a stiffness analysis, and the response amplitude operators (RAOs) generated, represent nominal or average stresses. In general, correct input of member cross-sectional areas and section properties allow determination of nominal stresses quite accurately.

More complex joints, incorporating bulkhead and diaphragm sub assemblies, require careful evaluation to determine the realistic load paths. To determine the nominal stresses at complex joints,

either multiple stick elements (for each load path) or a finite element model should be utilized.

5.4.2 Stress Concentration Factors and Hot-Spot Stresses

Background

The locations at which maximum stresses occur are called hot spots. Hot spots usually occur at discontinuities such as the stiffener edge or a cutout. On tubular member intersections, they usually occur on either the weld toe of the incoming tubular (brace) or of the main tubular (chord), depending on the geometry of the joint. The stress concentration factor (SCF) is evaluated by taking the ratio of the hot-spot principal stress to the nominal principal stress. The hot-spot stress used in fatigue life assessment is raised to a power of the inverse of the slope of the S-N curve used. Since the inverse of the slope of S-N curve is usually between 2.5 and 4.0, the choice of SCF can have approximately a cubic effect on damage. Thus the SCF value is probably the most important variable affecting the applicable stress ranges through the life of a structure and thus the fatigue life of joints.

There are several practical approaches for determining SCF values:

- Develop an analytical model of the detail/joint and carry out a finite element analysis (FEA).
- Test a physical model and obtain hot-spot stresses from measurements.
- Use empirical formulations.

The use of FEA is the most reliable and reasonably cost-effective approach for complex joints. When modeled correctly, the SCFs obtained by FEA are very reliable and depend largely on the mesh sizes used in the analysis. Whether the physical model used to determine the hot-spot stresses is an acrylic model or another

alternative, the accuracy of hot-spot stresses depends largely on the ability to predict hot-spot stress locations in advance and obtain measurements in those areas.

Since the use of both FEA and the physical model requires substantial investment of time and cost, they can be used only on a selective basis. Thus, most structure hot-spot stresses must be defined based on the application of empirical formulations.

Joint Geometry

The primary variables affecting the magnitude of stress concentration are weld profile and joint geometry. The weld profile is accounted for in the S-N curve. The joint geometric characteristics determine the magnitude of stress concentration. For most simple structural details, typically a wide range of plate and stiffener joints, the nominal stresses can be used directly to compute fatigue lives as the effect of SCFs are incorporated in the S-N curves.

The joint geometries of tubular members are quite complex and the S-N curves are used with the hot spot stresses, requiring definition of SCFs for each joint geometry and loading. The SCFs are determined for axial load, in-plane moment and out-of-plane moment. Typically, a peak SCF is determined and conservatively applied to eight points around the intersection. For the crown and saddle points shown on Figure 5-7 separate SCFs can be determined. At other locations, the SCFs are then interpolated between the crown and saddle positions.

Joint Definition

When tubular members frame into one another, they form a tubular joint, with the largest diameter or thickest member being the through member or chord and all other members being braces.

Braces may have stubs or cones, which are the part of the brace member welded to the chord. Typically, both the stubs and the cones are thicker than the brace members.

To facilitate the development and use of empirical equations several parameters are used in defining the characteristics of a joint. The chord diameter and thickness are referred to as D and T respectively. The brace or stub diameter and thickness are referred to as d and t . The angle from the chord to the brace is defined as theta θ . The ratio of the brace diameter to chord diameter is defined as beta, β . The ratio of chord radius to chord thickness is defined as gamma, γ . The ratio of brace thickness to chord thickness is defined as tau, τ . The empirical equations used to determine SCFs utilize the parameters $\theta, \beta, \gamma, \tau$. The terminology used in defining a simple joint is shown in Figure 5-7.

Joint Type and Classification

Joints are classified into types based on geometry and loading. The joint type usually looks like the letter formed from the brace and chord intersection. Four basic joint types exist in offshore structures:

- 1) T or Y joint
- 2) K joint
- 3) KT joint
- 4) X joint

Figure 5-8 shows the four common joint types.

Although the joint type usually looks like the letter formed from the brace and chord intersection, the joint is actually classified according to load distribution. If the axial load is transferred between the brace and chord by shear, then the joint is classified as a T or Y joint. If the load is transferred between the braces at a joint, without traveling through the joint, then the joint is

classified as a K joint. If the load is transferred by some combination of shear through the joint and brace-to-brace, then the joint is classified as a KT joint.

If the load is transferred through one side of the chord to another, then the joint is classified as an X joint. Figure 5-9 shows joint classification by load distribution.

5.4.3 Empirical Equations

Prior to the discussion of empirical equations it is beneficial to briefly discuss the available data on SCFs. Review of various published data (References 1.8, 5.19, 5.20, 5.21 and 5.22) indicate that substantial scatter of SCFs is observed. Variations in SCFs occur in both nominally identical joints and in symmetrical locations of joints where one would expect little variations in SCFs. Material and fabrication imperfections contribute to the SCF variations. Lalani et al (Reference 5.23) point out that the parameters contributing to these variations can be grouped into two:

- Experimental error, including modeling, gauge position and measurements and the loading.
- Expected variations due to material and fabrication imperfections, including variations in weld profile, size and imperfections.

The use of empirical formulations has been extensively accepted for fatigue analysis of marine structures. A set of empirical formulae developed by Kuang (Reference 3.2) were derived by evaluating extensive thin-shell FEA results. The formulae proposed by Smedley (Reference 3.3) and Wordsworth (Reference 3.4) of Lloyd's Registry were derived from evaluating the results of strain-gauged acrylic models. Other empirical equations published include those by as a T or Y joint. If the load is transferred between the braces at a joint, without traveling through the joint, then the joint is

Whatever the basis for an empirical formula, the formula has an applicable range of parameters and the level of conservatism varies not only with the formulation but also within the applicable range of parameters. The use of SCFs also requires judgement not only on the applicability of an empirical formula but also on assessment of implications of in-plane and out-of-plane loadings/stresses.

The parametric equations developed by Kuang, Smedley-Wordsworth, and Smedley consist of different relationships defined by the joint variables D, T, d, t, L, g, and θ .

Different equations are applicable for different joint types. Presently, the joint types and the applicable equations most often used are listed below:

<u>Joint Type</u>	<u>Applicable Equations</u>
T or Y	Kuang, Smedley-Wordsworth, & Efthymiou
K	Kuang, & Smedley-Wordsworth
KT	Smedley-Wordsworth
X	Smedley-Wordsworth, & Smedley

The empirical equations given by UEG (Reference 1.8) are based on an extensive database and relate to Woodworth equations. Modification of Woodworth equations and the extension of the validity ranges allow the application of UEG equations to joints with extreme geometries. Comparison of various empirical equations show that UEG equations yield generally conservative values of SCFs and are considered to be most reliable. On the otherhand none of the equations appear to allow accurate determination of K-joint SCFs subjected to axial loading.

An excellent overview and reliability assessment of SCF empirical equations are provided by Ma et al (Reference 5.20), Tolloczko et al (Reference 5.22) and Lalani et al (Reference 5.23). Further discussion on SCFs and the predicted chord SCF for the different equations for T and K joints are presented in Appendix C.

Details of Equations

The details of some of the equations are given in Appendix C. The equations are given in simple terms of joint geometry: D , T , d , t , L , g , and r . The Kuang brace SCFs have been modified for the Marshall reduction. The Smedley-Wordsworth chord SCFs have been modified for the recommended d/D limitation.

The parametric equations should not be used outside of their assigned limits without justification. Near the assigned limits, the SCFs rapid decrease should be noted to determine if the calculated SCF is unconservative. The Smedley-Wordsworth effects revised for d/D limitation can dramatically increase SCFs for d/D ratios near 1.0.

Minimum Stress Concentration Factor

The minimum stress concentration factor for all modes of loading should be 2.0. This is generally accepted as an industry lower bound. However, acrylic model tests from the Tern project in United Kingdom showed a SCF of 1.6 could be used as a lower bound.

5.4.4 Illustration of a T-Joint SCFs

A typical T-joint with an assumed applied axial load is used to illustrate the application of empirical equations.

The joint shown on Figure 5-10 is classified by load path and the joint variables are specified in order to determine an SCF according to Kuang and Smedley-Wordsworth criteria. The Kuang brace SCF includes a Marshall reduction factor, Q_r . The Smedley-Wordsworth chord SCF calculation uses the d/D limitation.

5.4.5 Overview and Recommendations

Uncertainties

The SCF equations currently in use for simple tubular joint design are based on results of acrylic model tests and finite element (FE) analysis. Lloyd's Register has recently studied these empirical questions and assessed their reliability when compared against steel specimen test data. Although the empirical equations are considered reasonably reliable, substantial uncertainties exist as the SCF equations:

- Sometimes do not properly account for relative brace loads
- Sometimes do not properly represent the stress at the brace and chord connection of interest
- Axial SCF value for crown and saddle is not constant

The FE analysis of SCFs yield substantially different values depending on both the modeling techniques and the computer program used. The use of a thin or a thick element, modeling of the weld and the definition of chord length substantially influence the computed SCFs.

SCF equations for a T or a Y joint typically contain a term for chord length. Since the appropriate length for a chord is not defined, most designers use the chord can length. While this is conservative, the use of the half of the bay length to represent the chord could be very unconservative.

Substantial work carried out in Europe need further assessment and analyses. An API Task Group will be formed in 1991 to review the SCF equations in detail, to identify their validity and limitations and to recommend preferred SCF equations for specific joint types and load components.

An API initiated joint industry project (JIP) is proposed to summarize the computer programs used and modeling strategies implemented to investigate variables affecting the SCF (including chord length) and to develop guidelines on obtaining SCFs by the use of FE analysis.

Screening Process

For a preliminary design of a structure it is common practice to use a blanket SCF of 5.0 or 6.0 for all joints, depending upon dynamic effects. If the structure is susceptible to dynamic amplification the higher blanket SCF should be used. Once the fatigue sensitive joints are identified during this screening process, the SCFs for these joints should be determined.

In the determination of SCFs a parametric study of variables d/D and t/T should be considered. The joint fatigue life is a function of nominal brace stress and SCF. To increase joint fatigue life, the nominal brace stress or the SCF should be reduced. An increase in brace diameter can dramatically reduce nominal brace stress without a significant increase in SCF. This is particularly true for brace members intersecting large diameter legs. However, where members are more similar in size, an increase in brace diameter also requires an increase in chord diameter.

By increasing the brace diameter rather than increasing the brace thickness, a more effective section can be used and prohibitively low diameter to thickness ratios can be avoided. Increasing the brace diameter may be the easiest way to increase joint fatigue life during preliminary design. The chord diameter may also have to be increased to offset the SCF increases if the brace area and section modulus are increased.

Comprehensive Design

Once the member diameters are finalized a comprehensive fatigue analysis and design may be carried out. The parameter most easily modified during this stage is the member thickness. An increase in brace thickness increases brace axial and bending section properties, which will reduce brace nominal stress. However, as stated above, the chord thickness should be increased accordingly. Otherwise the brace nominal stress reduction will be offset by the joint SCF increase, resulting in marginal difference in fatigue

life. During the comprehensive design the best parameter to increase is brace thickness while keeping t/T constant.

Further improvements in fatigue lives may be obtained by determining the SCF through the use of finite elements analysis or models tests. Another alternative to lower the SCF is to stiffen the joints with rings and thus reduce the SCFs to the lower bound values. However, considering the increased fabrication costs of stiffened joints, the use of rings should be considered the least desirable option to lower the SCFs and improve the fatigue lives.

The validity of SCF equations and their sensitivities to various geometric parameters are illustrated in Appendix C. It is recommended that the tables and figures provided are studied to determine an acceptable approach compatible with the specific problem on hand. A finite element study results are also included in Appendix C to illustrate the range of SCFs for a typical complex joint. Since empirical equations are applicable for only simple joints, a FEA is recommended for determination of complex joint SCFs.

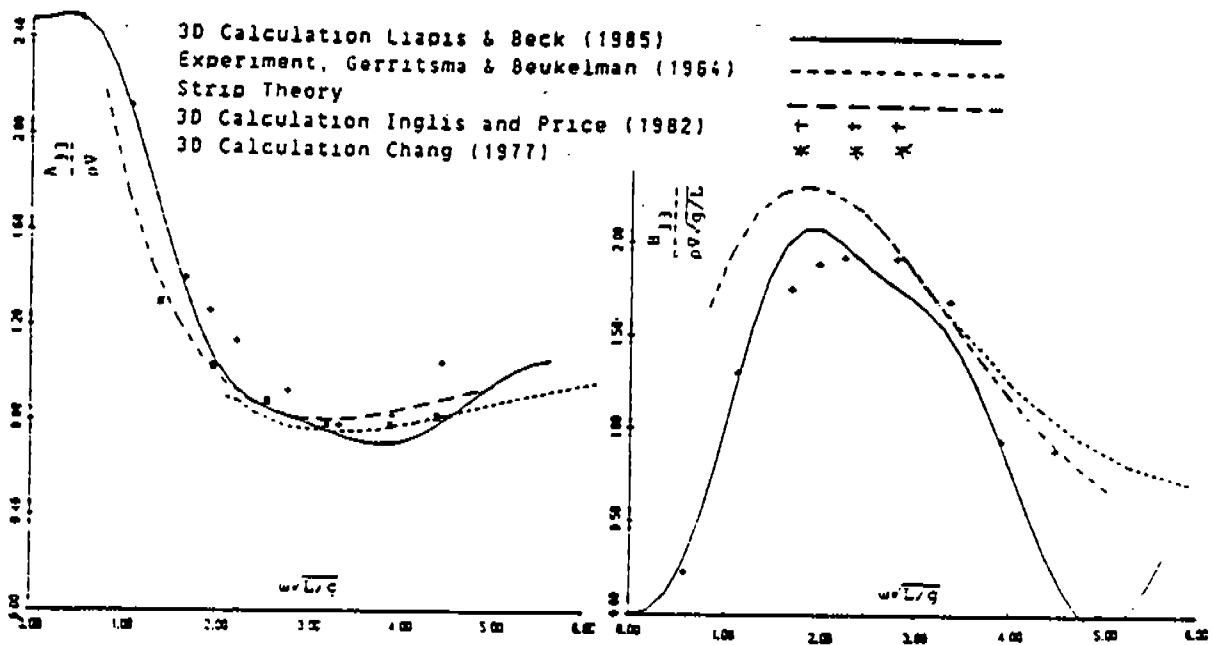


Figure 5-1 Comparison of Heave Added Mass and Damping Coefficients Based on Different Methods
(From Reference 5.2)

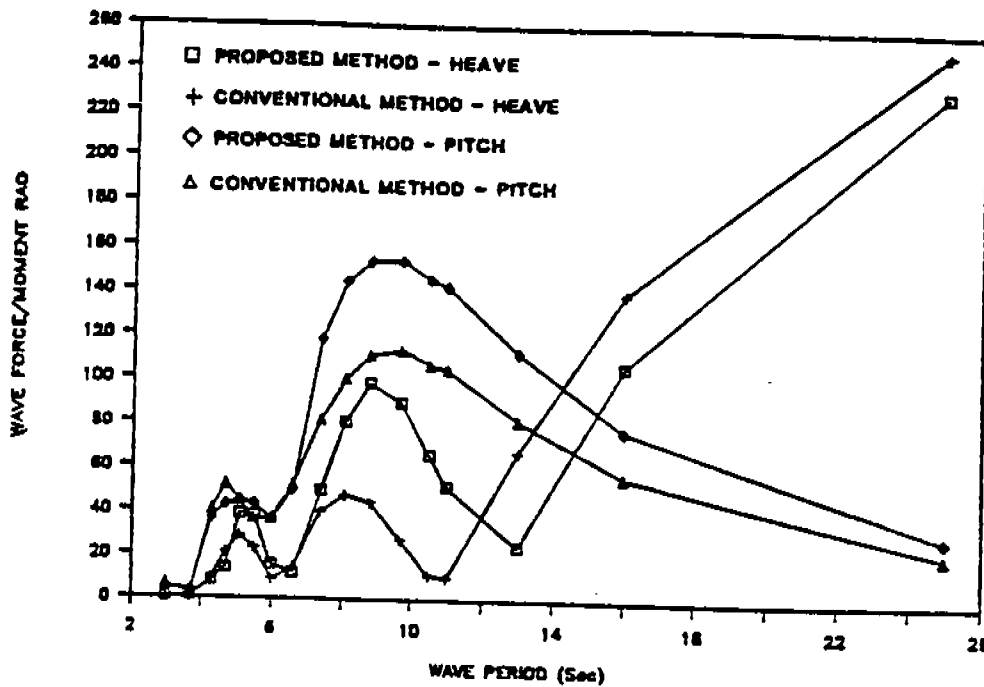


Figure 5-2 Comparison of Wave Loading Based Conventional and Consistent Methods
(From Reference 5.8)

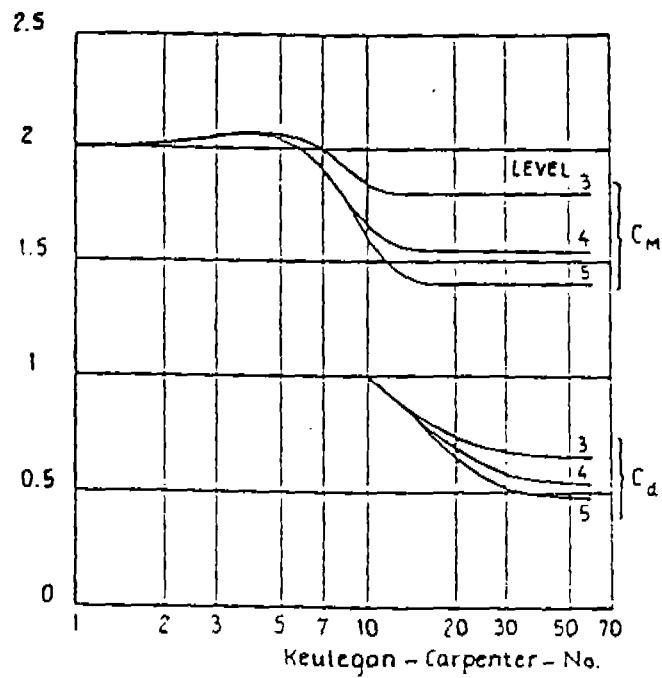


Figure 5-3 Comparison of Mean C_d and C_m Values for Christchurch Bay Tower
(From Reference 5.9)

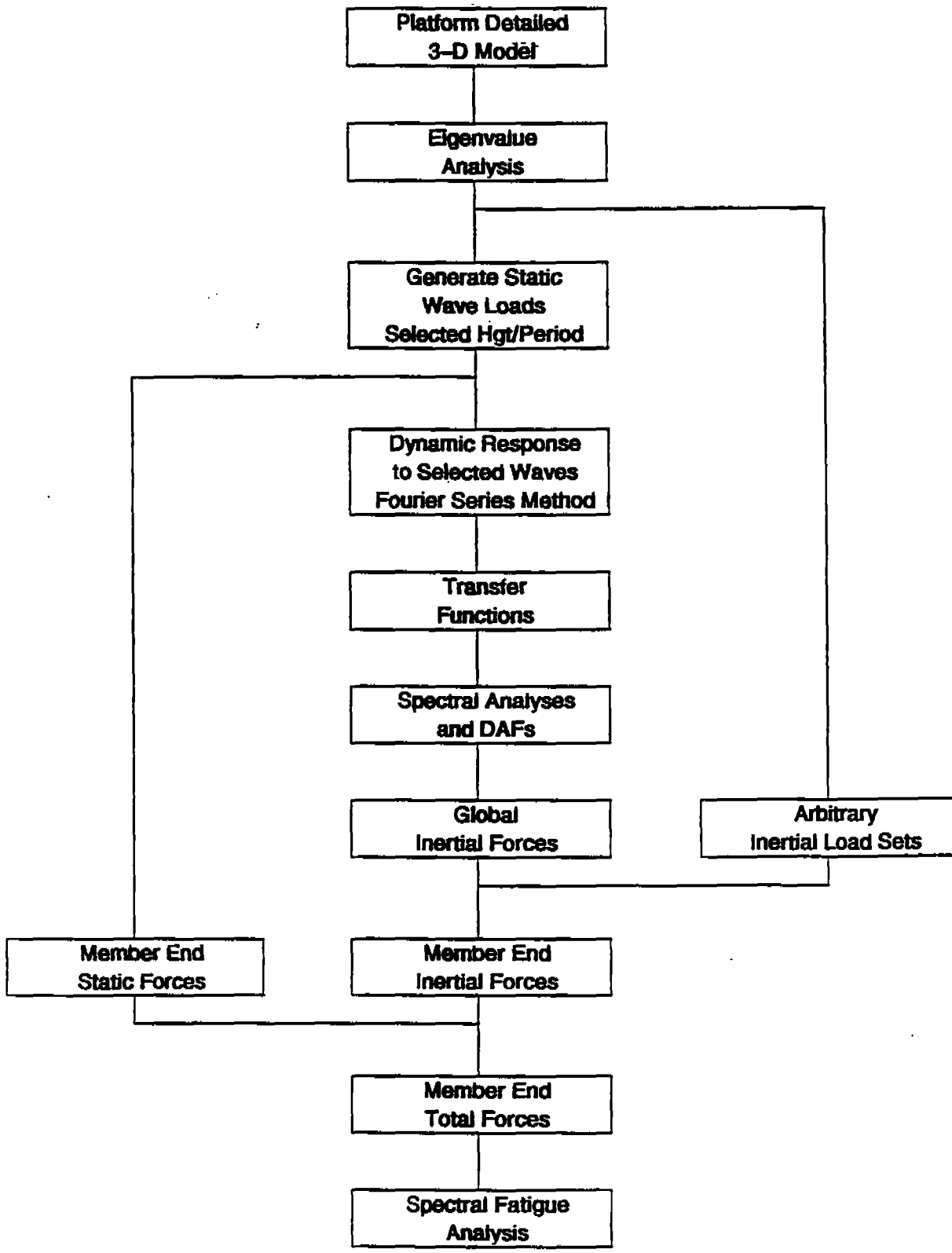
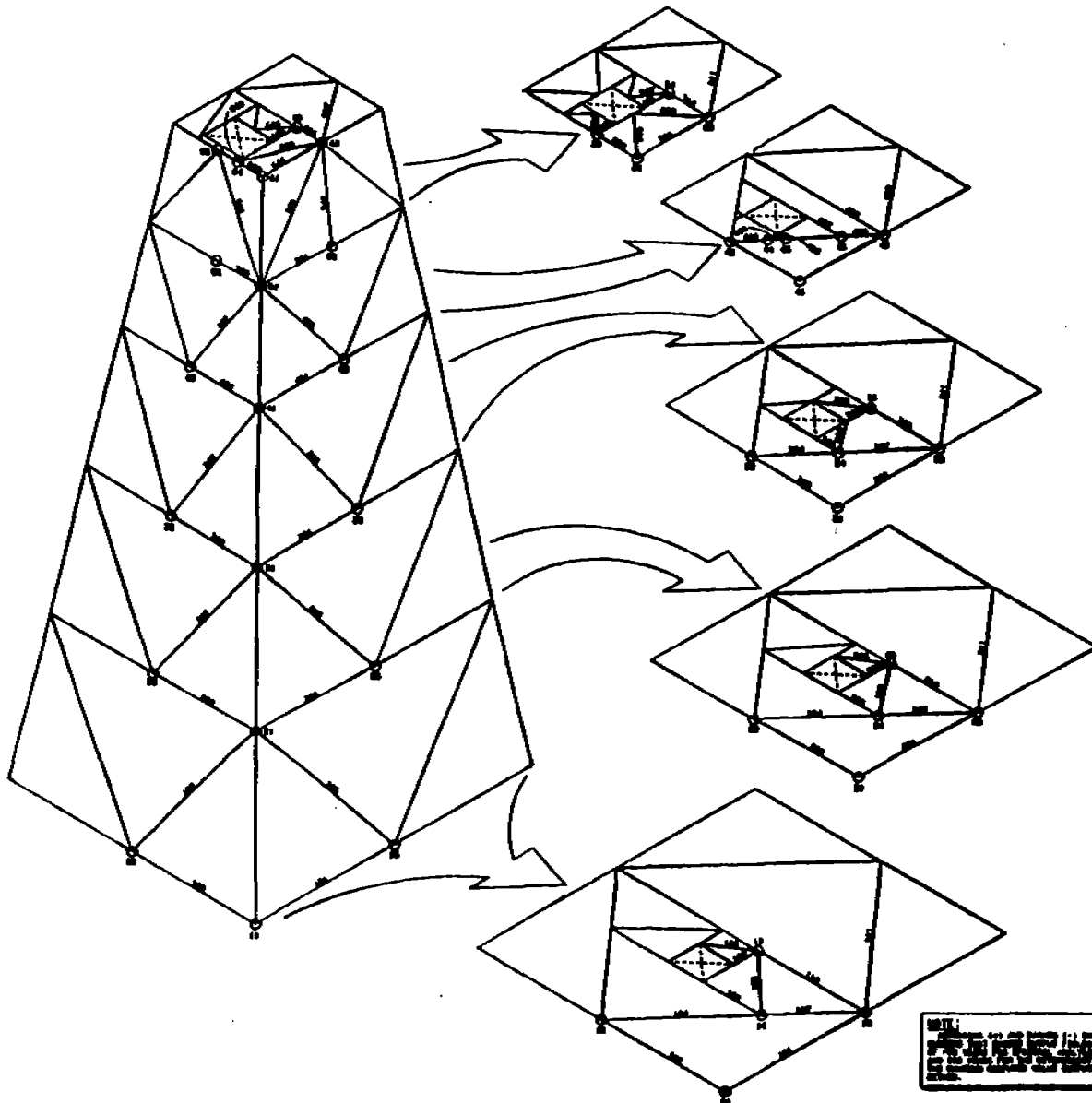


Figure 5-4 Dynamic Wave Load Analysis Methodology

FATIGUE DESIGN CRITERIA

TABLE A
COMPARISON OF DETAILED FATIGUE ANALYSES

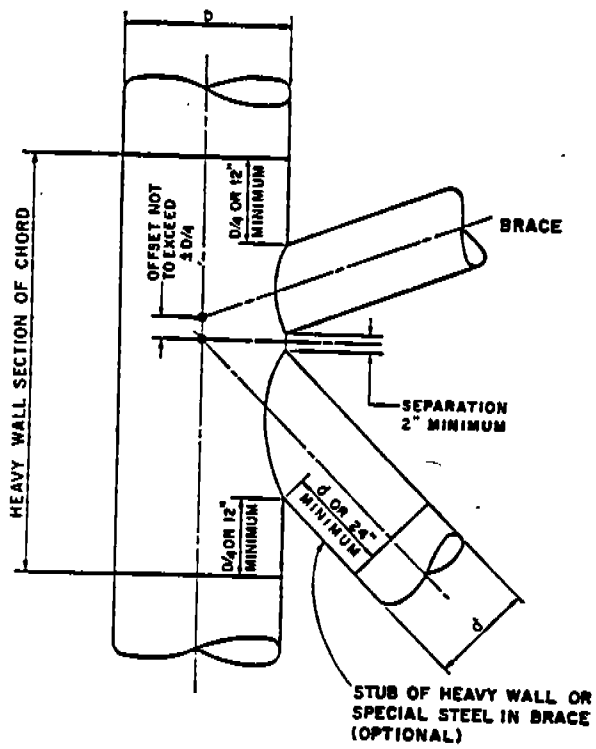


JOINT	MEMBER	COMPUTED STRESS (TENSILE OR COMPRESSIVE) IN THE MEMBER	METHOD OF ANALYSIS (STRESS IN TENSILE OR COMPRESSIVE MEMBER)		
			STRESS ANALYSIS USING AVERAGE STRESS IN THE MEMBER	STRESS ANALYSIS USING PEAK STRESS IN THE MEMBER	STRESS ANALYSIS USING RANGE OF STRESS IN THE MEMBER
11	100	354	354	354	354
12	100	313	309	371	359
13	100	300	300	371	357
14	100	300	300	371	357
15	100	300	300	371	357
16	100	300	300	371	357
17	100	300	300	371	357
18	100	300	300	371	357
19	100	300	300	371	357
20	100	300	300	371	357
21	100	300	300	371	357
22	100	300	300	371	357
23	100	300	300	371	357
24	100	300	300	371	357
25	100	300	300	371	357
26	100	300	300	371	357
27	100	300	300	371	357
28	100	300	300	371	357
29	100	300	300	371	357
30	100	300	300	371	357
31	100	300	300	371	357
32	100	300	300	371	357
33	100	300	300	371	357
34	100	300	300	371	357
35	100	300	300	371	357
36	100	300	300	371	357
37	100	300	300	371	357
38	100	300	300	371	357
39	100	300	300	371	357
40	100	300	300	371	357
41	100	300	300	371	357
42	100	300	300	371	357
43	100	300	300	371	357
44	100	300	300	371	357
45	100	300	300	371	357
46	100	300	300	371	357
47	100	300	300	371	357
48	100	300	300	371	357
49	100	300	300	371	357
50	100	300	300	371	357
51	100	300	300	371	357
52	100	300	300	371	357
53	100	300	300	371	357
54	100	300	300	371	357
55	100	300	300	371	357
56	100	300	300	371	357
57	100	300	300	371	357
58	100	300	300	371	357
59	100	300	300	371	357
60	100	300	300	371	357
61	100	300	300	371	357
62	100	300	300	371	357
63	100	300	300	371	357
64	100	300	300	371	357
65	100	300	300	371	357
66	100	300	300	371	357
67	100	300	300	371	357
68	100	300	300	371	357
69	100	300	300	371	357
70	100	300	300	371	357
71	100	300	300	371	357
72	100	300	300	371	357
73	100	300	300	371	357
74	100	300	300	371	357
75	100	300	300	371	357
76	100	300	300	371	357
77	100	300	300	371	357
78	100	300	300	371	357
79	100	300	300	371	357
80	100	300	300	371	357
81	100	300	300	371	357
82	100	300	300	371	357
83	100	300	300	371	357
84	100	300	300	371	357
85	100	300	300	371	357
86	100	300	300	371	357
87	100	300	300	371	357
88	100	300	300	371	357
89	100	300	300	371	357
90	100	300	300	371	357
91	100	300	300	371	357
92	100	300	300	371	357
93	100	300	300	371	357
94	100	300	300	371	357
95	100	300	300	371	357
96	100	300	300	371	357
97	100	300	300	371	357
98	100	300	300	371	357
99	100	300	300	371	357
100	100	300	300	371	357

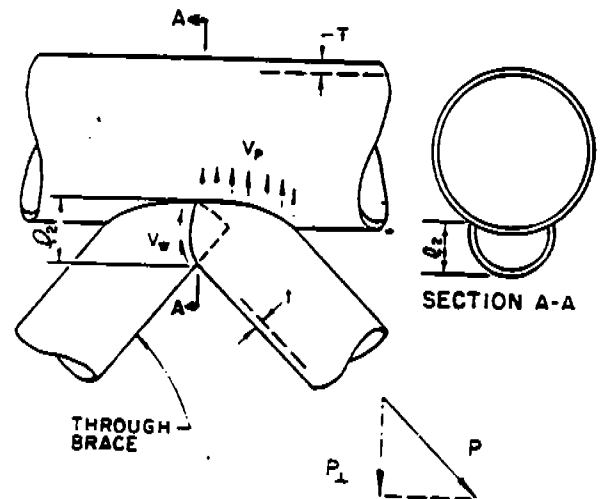
NOTE: THE STRESS ANALYSES WERE MADE USING THE RANGE OF STRESS METHOD.

Figure 5-5 Comparison of Detailed Fatigue Analyses Techniques

oh1



DETAIL OF SIMPLE JOINT



DETAIL OF OVERLAPPING JOINT

Figure 5-6 Joint Geometry (From Reference 1.5)

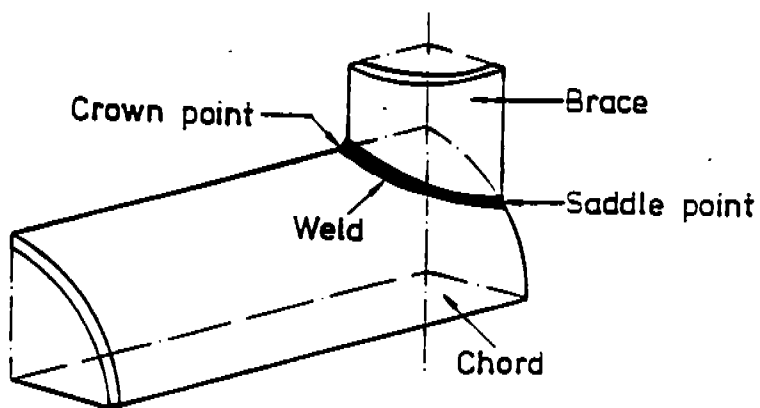
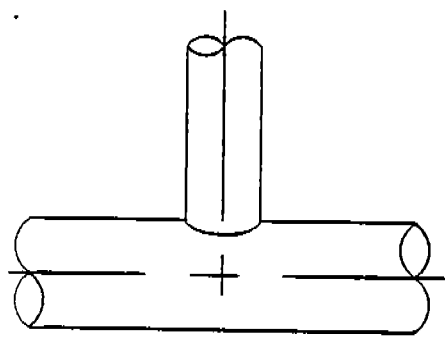
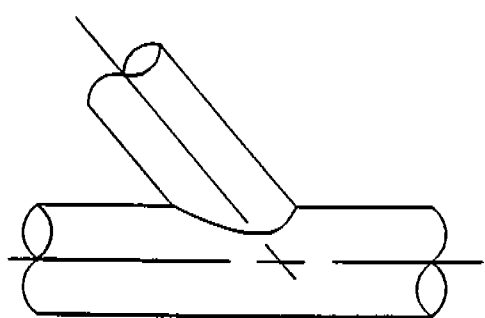


Figure 5-7 Simple Joint Terminology (From Reference 1.6)

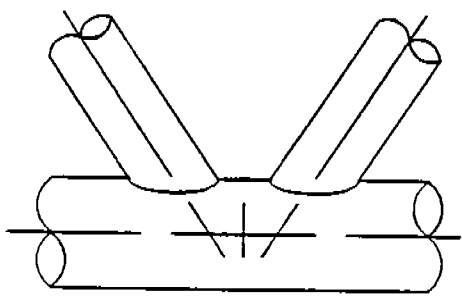


T-JOINT

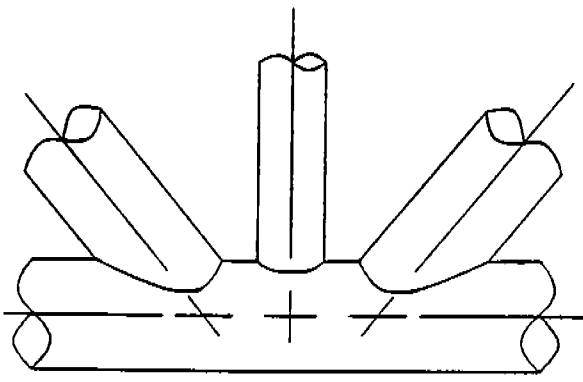


Y-JOINT

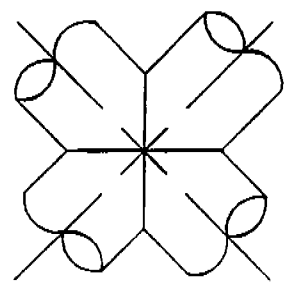
OR



K-JOINT



K-T JOINT



X-JOINT

Figure 5-8 Common Joint Types

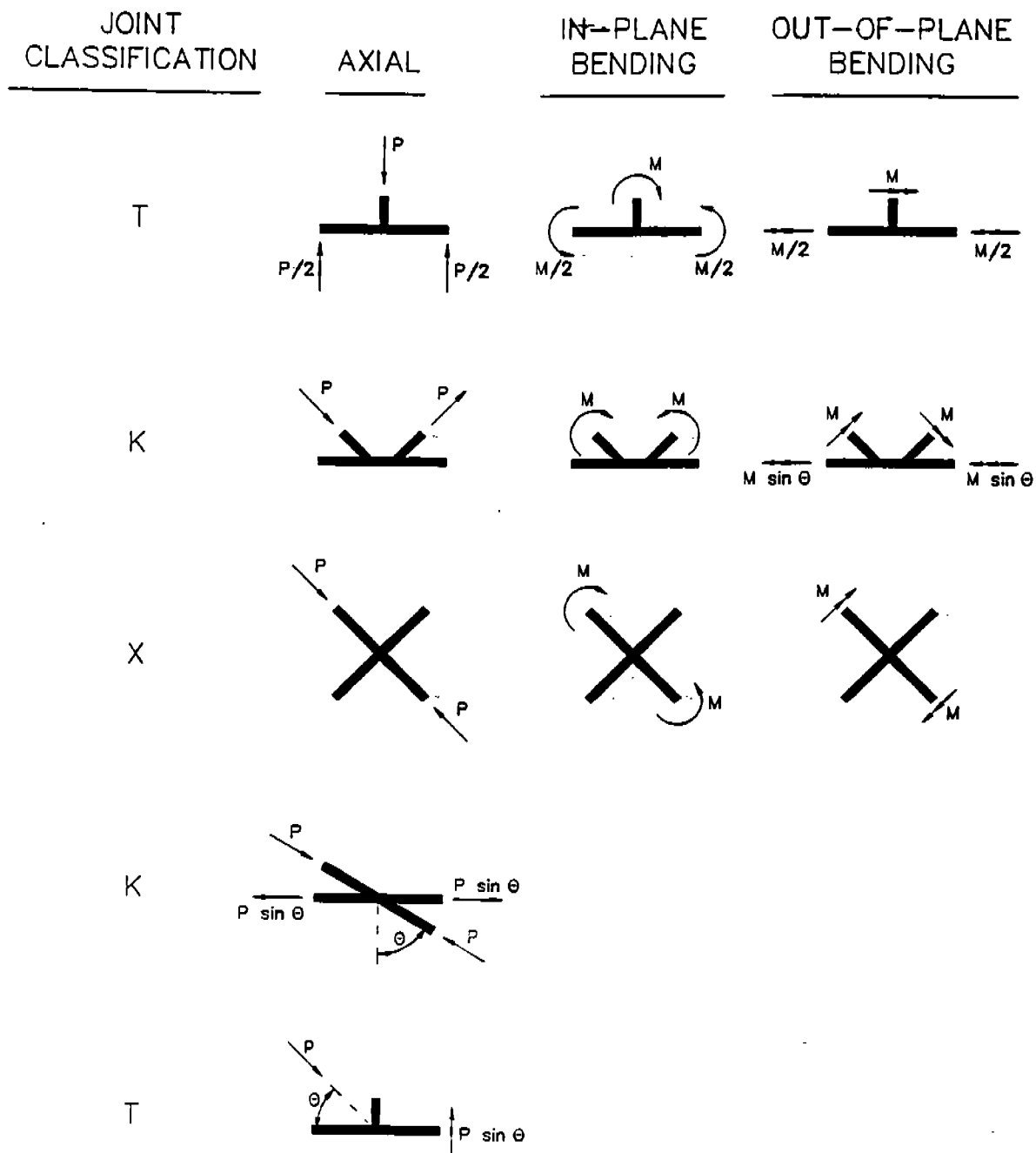


Figure 5-9 Joint Classification by Loading

SMEDLEY-WORDSWORTH

$\beta = \frac{d}{D} = \frac{600}{1200} = 0.500$	$0.13 \leq \beta = 0.500 \leq 10 \quad \checkmark$
$\gamma = \frac{D}{2T} = \frac{1200}{2(40)} = 15.0$	$12 \leq \gamma = 15.0 \leq 32 \quad \checkmark$
$\tau = \frac{t}{T} = \frac{20}{40} = 0.500$	$0.25 \leq \tau = 0.500 \leq 1.0 \quad \checkmark$
$\alpha = \frac{2L}{D} = \frac{2(21,000)}{1200} = 35.0$	$8 \leq \alpha = 35 \leq 40 \quad \checkmark$
$\theta = 90^\circ$	$30^\circ \leq \theta = 90^\circ \leq 90^\circ \quad \checkmark$

VALIDITY CHECK

AXIAL SCF CHORD

$$\text{SADDLE SCF} = \gamma \tau \beta (6.78 - 6.42 \beta^{0.5}) \sin^{(1.7+0.7\beta^3)\theta} = \underline{8.40}$$

$$\text{CROWN SCF} = [0.7+1.37\gamma^{0.5}\tau(1-\beta)][2 \sin^{0.5\theta} - \sin^3\theta]$$

$$+ \left[\frac{\tau(2\gamma\beta-\tau)\left(\frac{\alpha}{2}\right)-\beta \sin\theta \sin\theta}{2\gamma-3} \right] \left[1.05 + \frac{309^{1.5}(1.2-\beta)(\cos^4\theta + 1.5)}{\gamma} \right] = \underline{7.16}$$

KUANG

$\beta = \frac{d}{D} = \frac{600}{1200} = 0.500$	$0.30 \leq \beta = 0.500 \leq 80 \quad \checkmark$
$\gamma = \frac{T}{D} = \frac{40}{1200} = 0.0333$	$0.015 \leq \gamma = 0.0333 \leq 0.060 \quad \checkmark$
$\tau = \frac{t}{T} = \frac{20}{40} = 0.500$	$0.20 \leq \tau = 0.500 \leq 0.80 \quad \checkmark$
$\alpha = \frac{D}{L} = \frac{1200}{21000} = 0.0571$	$0.05 \leq \alpha = 0.0571 \leq 0.30 \quad \checkmark$
$\theta = 90^\circ$	$30^\circ \leq \theta = 90^\circ \leq 90^\circ \quad \checkmark$

AXIAL SCF CHORD

$$\text{SCF} = 1.177\gamma^{-0.808} e^{-1.2\beta^3} \tau^{1.333} \alpha^{-0.057} \sin^{1.694\theta} = \underline{7.40}$$

Figure 5-10 Sample Evaluation of a T-Joint

6. FATIGUE STRESS HISTORY MODELS

Creation of the fatigue stress history model requires determination of the fatigue environment and application of the environment to the structure to produce stresses. The environment can be applied to the structure by either a spectral analysis or by a time-domain analysis. The spectral analysis derives the stress range and an average N number of cycles from the statistical properties of the stress response spectrum. A true time-domain analysis sorts the stress ranges and accumulates the stress range counts as the stress time history is being generated. For practical reasons a hybrid time-domain method is often used to generate stress history.

6.1 DETERMINATION OF FATIGUE ENVIRONMENTS

To evaluate the fatigue life of a fixed structure or a floating vessel a representative fatigue environment must be modeled. For a fixed structure the fatigue environment will be the typical wave and wind conditions for the surrounding area. For a ship the fatigue environment will be the typical environmental conditions along various routes.

6.1.1 Data Sources

The types of environmental data range from actual wave and/or wind records to recreated (hindcast) data. The wave and wind records may be raw recordings (not generally available) or condensed summary reports produced by government agencies or environmental consultants. Hindcast data are generated by various computer models using environmental information available for the area or nearby areas.

Wave Records

Older wave and wind information has come from voluntary observations by ship personnel and from measurements by weather ships and coastal weather stations. The most likely source of current wave records are from government agencies such as the National Oceanographic and Atmospheric Administration (NOAA), obtained through various means, including weather platforms and weather buoys. Newer techniques using measurements from satellites provide more comprehensive wave records. Hoffman and Walden (Reference 6.1) discuss environmental wave data gathering in detail.

While majority of the published wave data is from the North Atlantic, much of the data applicable to the Pacific were published in Japanese and Chinese. Several recent publications (References 6.2, 6.3 and 6.4) in English provide additional description of wave environment in Asia - Pacific.

The older wave and wind data has the advantage that it covers many years (decades), but the disadvantages are that the wave heights were visually estimated, the wave periods were crudely timed, and the wind measurements were likely biased by the vessel speed. Various data analysts have devised formulas to correct the "observed" data. For example, Hogben and Lumb (Reference 6.5) developed the equations to correlate the significant wave height (H_S) and the mean zero upcrossing period (T_Z) with the observed data:

$$H_S = (1.23 + 0.44 * H_{ows}) \quad (\text{meters})$$

$$T_Z = (4.7 + 0.32 * T_{ows}) \quad (\text{seconds})$$

H_{ows} is the wave height and T_{ows} is the period reported by observers on weather ships.

Actual recorded wave elevation data is the most accurate information available. However, wave records are only available for a few locations, and typically the time spans of available recorded wave data are less than 10 years. Even recorded data may not be complete. The most serious fault in recorded data is that measurement techniques cannot detect the higher frequency waves. Wave rider buoys measure wave slope and wave heights are derived from the slope records. The resolution of these slope measurements are limited by the dimensions and motion properties of the buoy. The recorded data does not readily allow detection of the very long period waves and subsequent data analyses "filter" out the long period information. Filtering is used to separate "sea" and "swell" wave spectra. The sea/swell filtering technique is often a simple truncation of the measured spectrum above and below a selected frequency. Thus, the higher frequency "sea" part of the spectrum loses its longer period wave information.

Wind Data

The sources of wind data are the same as for wave data. Older data tends to be voluntary observations from ships and newer data comes from measurements on platforms or from weather buoys. Satellites may provide information on high altitude winds by tracking clouds or from lower level winds by tracking weather balloons.

The older observations are logged anemometer readings and are typically only the mean wind speed. The height above water at which the wind speed was measured may be unknown. Various analysts have devised methods to correlate observed wind data to actual measured data.

Existing oil platforms allowed gathering of extensive wind records, including gust readings which can be analyzed to derive wind spectrum information. The presence of the platform has some effect upon the measured wind velocity, and the location of the anemometer is very important to the accuracy of the measurements.

In many cases wind information may be available from transmitting ships or nearby coastal weather stations for areas where wave data is either skimpy or questionable. For these cases various equations have been developed to estimate or verify the wave information. Example equations to relate wind speed to wave height can be as simple as the "25% Rule",

$$H_s = 0.25 * U$$

where H_s is the significant wave height in feet and U is the observed wind speed in feet/sec. More involved equations include the wind "fetch" and the wind duration. The wind fetch is the distance over water that the wind acts. Appendix B presents the equations developed by Bretschneider to calculate wave height and period based on wind speed, duration and fetch.

Hindcast Data

Elaborate computer models have been developed to "hindcast" or recreate weather (wind and wave) records. The hindcast models may be for a region (such as the North Sea), or the models may be oceanic or even global. One important consideration in the development of hindcast models is the sensitivity of these models to interaction of various parameters. Using available wind and wave data to correlate the hindcast results can improve the accuracy of hindcast models.

The hindcast models derive wind information from pressure and temperature information. Pressure measurements are fairly accurate, and the techniques of combining the pressure readings from many measurement stations to produce isobar plots allows determination of the pressures over a large region without making measurements at each grid point. The temperatures measured at coastal weather stations surrounding the area of interest along with whatever temperature measurements available from the area can be used to identify temperature gradients, fronts, etc.

Wave information is calculated from wind, accounting for direction, duration and fetch. By integrating the weather conditions over small time steps, a wind and wave history can be built. The resulting records can be analyzed in a manner similar to that used with actual wind and wave records to produce wave scatter diagrams and wave exceedence curves.

6.1.2 Wave and Wind Spectra

Wave and wind spectra define the energy that is being applied to a structure or vessel. There are many wave spectra formulations and some of these are discussed in Appendix A. The most general and therefore most useful wave spectrum formulation is the General JONSWAP. The General JONSWAP spectra include the Bretschneider spectra which in turn include the Pierson-Moskowitz spectra. Reference 6.6 presents a summary of the various wind spectra. The spectrum recommended in Reference 6.6 is defined as follows:

JONSWAP Wave Spectrum

The JONSWAP (Joint North Sea Wave Project) spectrum was derived from wave measurements in the southern North Sea and is based on older spectra formulations, Pierson-Moskowitz/Bretschneider/ISSC Modified P-M. The Mean JONSWAP spectrum has fixed parameters and represents the waves measured during the project. The General JONSWAP parameters can be varied so that the spectrum can represent either fully developed seas or developing seas.

The formula for the JONSWAP spectrum is as follows:

$$S(f) = a (g^2/f^5) \text{EXP}[-1.25(f/f_m)^{-4}] q^a$$

where $a = \text{EXP}[-.5 (f-f_m)^2/(s f_m)^2]$

The Mean JONSWAP is defined with the following parameters.

$$\begin{aligned}
q &= 3.3 \\
s &= 0.07, \text{ for } f < f_m \\
s &= 0.09, \text{ for } f > f_m
\end{aligned}$$

The Bretschneider spectrum is a subset of the General JONSWAP; setting the gamma parameter to 1.0 converts the JONSWAP spectrum into the Bretschneider or ISSC Modified P-M spectrum. Also setting the alpha parameter to 0.0081 converts the JONSWAP spectrum into the Pierson-Moskowitz spectrum.

As a guideline, the JONSWAP spectrum with gamma = 2 would be an applicable spectrum for confined regional areas. The Bretschneider spectrum (JONSWAP with gamma = 1) would be applicable for open ocean (Pacific or Atlantic) areas.

Ochi-Shin Wind Spectra

Ochi and Shin reviewed six wind spectra formulations currently in use and have created an average wind spectrum to represent the variation (gusts) of the wind about the mean value. The wind spectrum represents the average of measured spectra and was deliberately devised to accurately represent the low frequency portion of the wind spectrum. The equation has three forms depending upon the frequency range.

$$S(f^*) = \begin{cases} 583 f^* \\ 420 f^{*0.70} / (1+f^{*0.35})^{11.5} \\ 838 f^* / (1+f^{*0.35})^{11.5} \end{cases}$$

with $f^* = f z / U_z,$

where f = frequency in Hz,
 z = height above sea level in meters, and
 U_z = mean wind speed at height z in meters/sec.

6.1.3 Scatter Diagram

Wave scatter diagrams show the occurrences of combinations of significant wave height and average zero-upcrossing period over many years.

Significant Height vs Zero-crossing Period

Irregular waves do not have any consistent pattern of height or period, but exhibit complete randomness. Irregular wave heights and periods are usually defined by the statistical properties of the wave record or by the properties of the energy spectrum which represents the random sea. The significant wave height is taken to be four times the standard deviation of the recorded water surface elevations, or if the sea is represented by a half-amplitude energy spectrum, the significant wave height is four times the square-root of the area under the spectrum. The average zero-upcrossing period is the average of the time intervals between negative to positive sign changes in the recorded water surface elevations, or is the square-root of the area under the spectrum divided by the square-root of second moment of the spectrum (frequency in H_z).

The wave height and period distribution over time can be obtained by actual wave measurements. The heights and periods of all waves in a given direction are observed for short periods of time at regular intervals. A short time interval of several hours may be considered constant. For this sea state, defined as "stationary", the mean zero-upcrossing period, T_z , and the significant wave height, H_s , are calculated. The H_s and T_z pairs are ordered, and their probabilities of occurrence written in a matrix form, called a wave scatter diagram. A typical wave scatter diagram, presenting statistical data on the occurrence of significant wave height and zero-upcrossing period for one direction is shown on Figure 6-1 and further discussed in Appendix B.

Seasonal Variation

The annual wave scatter diagram is often separated out into monthly or seasonal (spring, summer, fall and winter) scatter diagrams. Because a fatigue environment covers many years, the seasonal or monthly scatter diagram cell values may be added to produce the annual diagram.

Directional Variation

Sometimes the wave scatter diagram is separated out by direction. This may be important for fixed structures, because waves from one direction may cause a different stress distribution than waves from another direction.

Sea and Swell

Sometimes the wave scatter diagrams are separated into "sea" and "swell". The sea scatter diagram shows the significant wave heights and zero-upcrossing periods defining sea spectra. The swell scatter diagram usually shows the heights and periods of long period regular waves. This separated information can be helpful in analyzing the structure, because the swell may be present a large percentage of the time, and the swell is likely to be from a different direction than the higher frequency waves producing unique stress distributions.

6.1.4 Directionality and Spreading

The directions that have been referred to up to now have been the "central" direction of the sea. Irregular waves are often idealized as two-dimensional with wave crests parallel in the third dimension and all waves moving forward. Such an irregular sea is called long crested. In reality, storms occur over a finite area and the wave heights diminish due to lateral spreading. If such waves meet other waves from different directions, a more typical "confused" sea is observed. A confused sea is referred to as a short-crested sea. The

waves in a short crested sea approach from a range of directions centered about the central direction.

Directionality

For a fixed structure the direction of the sea will affect the stress distribution within the structure. Most fatigue analyses are performed for four or eight wave directions. When directional wave scatter diagrams are available the sea direction can be matched to the analysis direction, and the fatigue damage accumulated. If the data available do not include wave directionality, directions can be estimated on the basis of wind roses or hindcasting.

Spreading

In order to model a short crested sea a "spreading function" is used to distribute the wave energy about the central direction. In typical analyses the short crested sea is represented by a set of long crested spectra coming from directions spread over -90 deg to +90 deg from the central direction and having a total energy equal to the specified short-crested sea spectrum.

The directional spreading function as defined by Kinra and Marshall (Reference 6.7) is often used in the following form.

$$D(\theta) = C_n \cos^n(\theta)$$

where n is a positive integer and is measured from the central direction. The coefficient C_n should satisfy the following:

$$\int_{-\pi/2}^{\pi/2} D(\theta) d\theta = 1$$

A typical n value for wind-driven seas would be 2, while an appropriate value for a limited fetch (restricted spreading) may be

4. Şarpkaya (Reference 6.8) provides further discussion on spreading.

A significant effect of short crested seas is that they can cause response in a direction orthogonal to the central direction, i.e. a ship may develop considerable roll motion even though the vessel is headed into the waves.

In the design and analysis of typical offshore platforms (i.e., conventional structures in shallow or moderate waterdepths) spreading is generally neglected. However, for both typical and nonconventional structures such as the tripod or an extended base platform (see Figure 6-2) spreading may be significant. A platform with very different response characteristics in two orthogonal axes, such as the extended-base platform, may be susceptible to larger dynamic response in one axis. Even a typical platform, with a natural period coinciding with the wave force cancellation frequency, will be subjected to higher wave loading at the cancellation frequency and neglecting of spreading may not be conservative.

6.2 STRESS SPECTRUM

A stress spectrum is the stress energy distribution resulting from loading the structure with a particular sea spectrum.

6.2.1 Stress RAOs

In order to derive the stress statistics a stress response spectrum is developed. The stress response spectrum is the product of the wave spectrum ordinates times the stress response amplitude operators squared. The stress response amplitude operators (RAOs) are the stresses representing a "unit amplitude" regular wave, obtained by normalizing the input wave heights.

The stress responses to a set of regular waves covering the complete frequency (or period) range and the complete direction range are

evaluated as explained in Section 5. For a vessel global effects of port and starboard quartering seas are identical, allowing reduction of applied loading cases. Similarly, for a platform with two planes of symmetry several of the eight loading cases (45 deg. intervals) may be combined.

6.2.2 Response Analysis

The response analysis squares the stress RAOs; multiplies them by the spectrum ordinate; multiplies that product by the spreading function; and sums/integrates over directions the results to produce the stress spectrum.

The stress range spectra is integrated to allow determination of various statistical parameters, including the zero-upcrossing frequency, the mean squared value, etc., from which the short-term probability statistics are constructed. The "Rayleigh" distribution can be used to idealize the stress range associated with a particular cell (H_s and T) in the scatter diagram. Then, the fatigue damage associated with each block can be computed, the cumulative damage thus incorporating the weighting effect of the joint probability of wave scatter diagram. Since the damage for each cell is computed numerically, this approach is generally defined as the "short-term numerical method."

The typical loading response exhibits smaller stress cycles interspersed among larger stress cycles, making it difficult to identify the number of cycles contributing to fatigue damage. Rainflow counting is the name of a large class of stress cycle counting methods often applied to upgrade the short-term statistics. The rainflow parameter, introduced by Wirsching (Reference 6.9) is frequently used in upgrading stress spectra statistics.

The stress range associated with a particular block of the wave scatter diagram is random in nature and governed by a probability density function. Such a density function, covering the fatigue

Life of a structure, cannot be defined by a closed-form mathematical function. Most often a numerical long-term density function of the stress range is used to determine the fatigue damage and the method is identified as the "long-term numerical method". If the long-term stress range density function is idealized, an approximate density function can be used. "Weibull" distribution is one commonly accepted shape parameter used to describe the long-term stress density function. The fatigue damage computed is closed form. Incorporating the Weibull shape parameter is generally referred to as the "Long-Term Closed-Form Method".

6.2.3 Uncertainties and Gaps in Stress Spectrum Development

There are several important variables contributing to the uncertainties in the development of the spectrum.

Analysis assumptions substantially influence the calculated results. The most important of these is the selection of scatter diagram blocks. While a typical scatter diagram has 40 to 60 blocks (each representing the joint probability of H_s and T), these blocks are often arbitrarily grouped into 10 to 15 super blocks to facilitate analyses. In addition to the uncertainties introduced due to lumping of these blocks, validity of Rayleigh distribution is also jeopardized due to limited number of blocks defining the entire environment.

Other analyses uncertainties result from the use or omission of various parameters (rainflow counting, Weibull distribution) and their validity for the problem at hand.

Work carried out by various investigators have helped enhance the reliability of spectral fatigue analysis. Chen and Murakami (Reference 6.10) offer a close form spectral fatigue analyses method that eliminates some of the uncertainties due to analyses assumptions and computational procedures. The computer program developed, incorporating the self-contained algorithm, appears to minimize the uncertainties due to analytical assumptions (i.e.,

judgement errors) and facilities carrying out of a cost-effective spectral fatigue analysis.

Some studies show that full-scale service stress data match the predicted design stresses reasonably well. However, it should also be noted that full-scale service stress data may substantially differ from those predicted during design. This may be especially true for ships and both the short-term and the long-term service stress data require a careful scrutiny. Evaluation of full-scale service stress data on three different ship types (a high-speed containership, a bulk carrier and a VLCC) by Dalzell et al (Reference 6.11) shows that short-term wave-induced bending moment do not reasonably fit the Rayleigh distribution. The combined dynamic stress distributions for two of the three ship types did not fit the Rayleigh or the exponential distributions. Dalzell et al recommend that additional response calculations are carried out for different ship types utilizing Rayleigh and broad-band distributions. Comparison of response calculations with experimental and/or full-scale results should indicate the magnitude of error and advisability of corrective measures.

6.2.4 Decompose into Stress Record

To obtain a stress histogram from the response statistics, the stress response spectrum for each wave spectrum in the scatter diagram can be decomposed into a finite Fourier series. In order to produce a realistic stress record, the number of frequencies required will be on the order of 100. Each component will have an amplitude defined by the differential stress energy in the neighborhood of the frequency. Each component will be given a random phase. By summing the components at each time step, a stress value is obtained. The stress value is then accumulated into the stress histogram, according to the probability of occurrence of the particular wave spectrum. The stress histogram can then be used to evaluate the fatigue life at the hot spot.

Nonlinear effects, such as submersion/ immersion, velocity squared drag, mean drift offset, etc., may have a noticeable influence upon the stresses of a structure. When the nonlinear effects are substantial, the stresses may be directly calculated from a time-domain analysis. For a time-domain analysis a discrete set of regular waves are selected to represent the typical sea spectrum. The structure response and the stress responses are evaluated by stepping the waves past the structure in small time increments. At each time step the Newtonian laws are satisfied.

The regular waves may be selected at equal frequency increments. Each wave will be the same frequency difference away from its neighbors, but each wave will have a different height corresponding to the energy within its frequency increment. Typically, wave period increments should not be greater than 2 seconds to correctly define the effects of wave period variability. Wave heights in 3 ft (1m) increments are considered acceptable.

Alternatively, the regular waves may be selected so that they each have the same energy (height). The area under the sea spectrum is decided into bands of equal area. Either the centroid frequency (first frequency moment divided by area) or the zero-upcrossing frequency (square-root of the second frequency moment divided by area) of the frequency band is used as the regular wave frequency. Regardless of the selection technique, each regular wave is assigned a phase using some randomizing method. A number of waves, on the order of 100, should be selected to insure that the random wave record does not repeat itself during the "sampling" time.

Since any "bin" in the scatter diagram is characterized by a characteristic wave height and a characteristic period, another alternative technique may be used to facilitate the work. "Bins" of unequal period (frequency) may also be used to help prevent repetition of the random wave record.

6.3.1 Stress Statistics

The resulting stress records are then processed to find the stress statistics. The significant stress can be determined as four times the standard deviation of the stress values. Stress histograms can also be derived from the records.

6.3.2 70 Percentile Spectra

Time-domain analyses tend to be computation intensive, and they often require costly computer runs. Therefore, the number and extent of time-domain analyses must be kept within reason by selecting one or a few representative sea spectra for evaluation. Selecting the representative sea spectrum and the regular waves to model it will have an effect upon the resulting fatigue life.

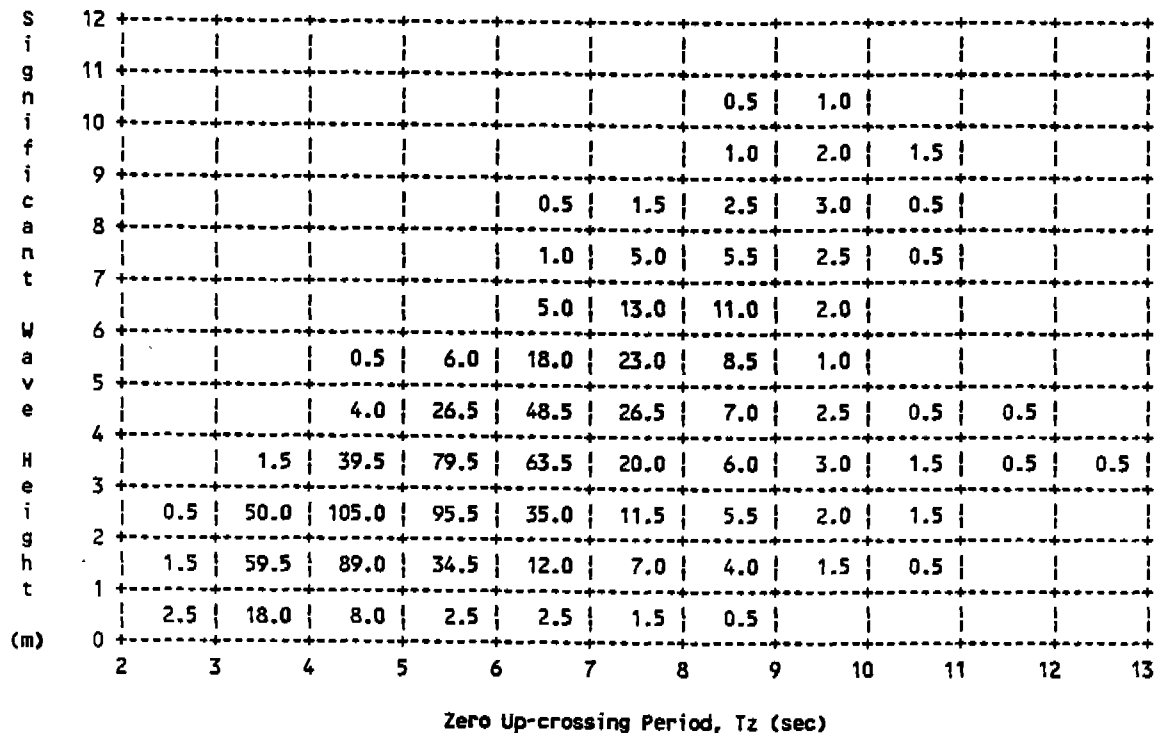
Because the fatigue damage is an accumulation over many years of exposure to mostly mundane sea conditions, the selected (representative) sea state must be an average or mean condition, with a slight hedge toward conservatism. A recommended selection is a spectrum along 70 percentile wave height line, i.e. from a cell in the scatter diagram below which lie 70% of the scatter diagram probabilities. The zero-upcrossing period would be near the median on the 70 percentile line with a slight offset to the side that is expected to produce the greater stresses.

6.4 OVERVIEW AND RECOMMENDATIONS

The long term wave environment, as defined by a wave scatter diagram, is usually based on measurements and hindcasting. Measurements should be reviewed as to the extent of area covered, the time length of coverage, and the measurement system. Typically, measurements are made for limited time spans. Accelerometers of a measurement system may have limitations, preventing accurate description of wave energy content in all frequency ranges and in all directions.

The wave environment definitions based on hindcast models are quite reliable. However, modeling parameters should be carefully reviewed to ensure accuracy of the data. The environment is defined by multiple "bins" in the scatter diagram, each "bin" representing a significant wave height and a zero upcrossing period. Each "bin" is used to generate a specific wave spectra, defining that seastate. Since wind fetch and geographic parameters differ from one area to another, mathematical formulations developed to define wave spectra in one area may not be applicable to another area. Thus, as discussed in Section 6.1 and in Appendix B, P-M, Bretschneider, ISSC, JONSWAP, etc. wave spectra should be carefully reviewed as to their applicability to a given geographic area.

Sample Wave Scatter Diagram



SUM of Occurances 999.5

Figure 6-1 Typical Wave Scatter Diagram

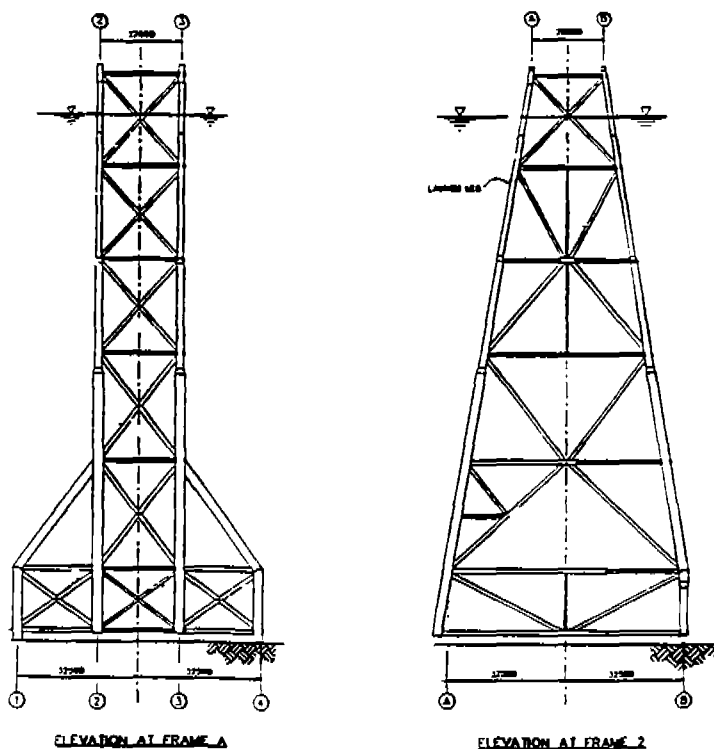


Figure 6-2 Platform with Different Dynamic Response Characteristics in Two Orthogonal Axis

161

(THIS PAGE INTENTIONALLY LEFT BLANK)

7. FATIGUE DAMAGE ASSESSMENT

7.1 BASIC PRINCIPLES OF FATIGUE DAMAGE ASSESSMENT

Fatigue damage of marine structures is typically determined using S-N curves and the linear cumulative damage rule known as Miner's rule. The S-N curves are usually provided in design standards, where each curve is applicable to specific joint configurations. The S-N curves applicable to details with complex stress patterns, such as tubular joint interfaces, require amplification of the nominal stresses by stress concentration factors (SCFs). The S-N curves applicable to details with simple stress patterns, such as hull scantlings, often include geometric effects and therefore can be used directly with nominal stresses.

Application of Miner's rule typically implies that the long-term distribution of stress range is replaced by a stress histogram consisting of a number of constant amplitude stress range blocks. Thus, for a stress history covering many stress ranges, each with a number of cycles (N), damage for each stress block is added to produce cumulative fatigue damage. An alternative to this approach is based on weighting and summing the probability density functions to obtain a long-term probability density function. Total damage can then be computed based on either numerical integration or the use of Weibull shape parameter and a closed form solution. Chen (Reference 4.10) offers a short-term closed form method that facilitates spectral fatigue analysis. Further discussion on this subject is presented in Section 6.2.

As discussed in Section 4.1, various recommendations, rules and standards differ in defining desirable fatigue lives and the specifics and applications of S-N curves. However, these recommendations, rules and standards (References 1.5, 1.6, 1.7 and 4.14) generally adhere to the following basic principles of fatigue damage determination:

- Fatigue test data should be carefully evaluated and S-N curves should be generated by statistical means to allow estimation of failure probability and incorporation of conservatism into the design. Separate S-N curves should be applicable to different weld details and in some applications to different profiles.
- S-N curves include a level of fabrication effects that should not be exceeded.
- The cumulative fatigue damage computation should be based on Miner's rule, and should consider the damaging effects of all loadings (both global and local).

Fatigue damage assessment technology has benefitted from the application of fatigue crack growth data and fracture mechanics analysis of defects. In addition to predicting fatigue life, fracture mechanics analysis allows better understanding of various parameters that affect the behavior of welded joints. In turn, experimental data and fracture mechanics analysis have allowed upgrading of recommended S-N curves (References 1.5, 1.7) including Gurney's work on the influence of plate thickness (Reference 7.1).

7.2

S-N CURVES

The S-N curves recommended by various rules, recommendations and codes are based on the application of constant amplitude stress cycle on various detail/joint geometries in the laboratory until fatigue failure. Most S-N curves for simple details (stiffener, cutout, etc.) account for the local notch stress and can be used with the member nominal stresses. Tubular joints of offshore structures exhibit a wide variety of joint configurations and details. Therefore, while the S-N curves account for several parameters (plate thickness, weld profile), they do not account for peak stresses, requiring the application of SCF's on computed nominal stresses to obtain peak (hot-spot) stresses.

The S-N curves that can be used directly with the nominal stresses most often apply to ship structure details. Munse's SSC-318 report (Reference 1.3) documents the S-N curves for 69 ship structure details and refers to earlier work by Jordan and Cochran (Reference 7.2) on in-service performance of ship structure details.

Tubular offshore components have more complex geometries and are subjected to corrosive ocean environment, requiring careful assessment of all parameters contributing to fatigue failure and selection of appropriate S-N curves.

Many design, fabrication and in-service factors affect the fatigue lives of details/joints. Fatigue cracks in welded joints often initiate at weld discontinuities introduced during fabrication. Weld quality problems that contribute to the degradation of fatigue strength include:

- Planar defects in the body of the weld
- Incomplete penetration
- Imperfect weld root quality
- Imperfect weld toe profile
- Development of an embrittled heat affected zone (HAZ)

Fatigue assessment requires definition of the number of applied stress cycles (N). Welded details/joints subjected to repeated cyclic stresses will go through several stages of crack growth. For each hot-spot stress range (s), failure is assumed to go through three stages:

- First discernable surface cracking (N_1)
- First through-wall cracking (N_2)
- Extensive cracking and end of testing (N_3)

Ideally, cracks should be large enough to detect, yet not large enough to cause failure and alteration of load path. To ensure that cracks are repairable, the number of cycles to failure in fatigue

assessment is typically identified as the number required to produce through-wall cracking (N_2), which can often be visually detected in a laboratory environment. To ensure accuracy of results tubular joints being tested in a laboratory are sometimes pressurized and the number of cycles to N_2 is tied to the first drop in pressure.

Tests are carried out for numerous stress range blocks to determine the number of stress cycles needed to reach failure, allowing development of an S-N curve. An S-N curve is also based on idealized laboratory conditions that may not fully represent the actual fatigue life in a marine environment. As discussed in Section 4.2.2, the S-N data for offshore components are based on testing of fillet-welded plates and small-scale tubular joints. The test data on Figure 7-1 indicate substantial scatter and allow development of S-N curves for a 99% confidence level or a 95% confidence level (representing the characteristic strength at two standard deviations).

The use of an S-N curve based on strictly small specimen data is not advisable. Small test specimens usually do not depict welded offshore component details accurately as full-scale component fabrication residual stresses are substantially different from test specimen residual stresses. Further discussion on size effect of welded joints is presented by Marshall (Reference 7.3).

It is also necessary to consider definition of hot spot stress levels. API recommended X and X'-curves (with and without smooth transition of weld profile at weld toe) are derived from hot spot stresses obtained from strain gages placed within 0.25 inch (6 mm) to 0.1Rt of the weld toe. The hot spot stresses as obtained are less severe than the local stress concentrations at the weld toe, but the S-N curve developed accounts for this difference. DEN Guidance Notes (Reference 1.6) defines the hot spot stress as "that which is as near the weld as possible without being influenced by the weld profile".

The primary factors that influence the fatigue life assessment are discussed as follows:

7.2.1 Design Parameters

The design is optimized to ensure effective resistance of marine structures to both extreme and operating fatigue loads. Typically the structure and joint/detail configurations should be developed to minimize stress concentrations and stress levels, and arranged to provide easy access to help maintain welding quality. The material should be selected to have an acceptable chemical composition to ensure weldability and satisfactory mechanical properties to ensure notch toughness.

Fabrication specifications should permit only minimized mismatch tolerances, thereby reducing SCF's and residual stresses. They should also control the quantity and quality of repair work, thereby ensuring allowable defects in weldments comply with specifications. These design parameters are discussed in Section 3. and described in more detail below.

Material Strength

Fatigue strengths of marine structure components are sometimes assumed to be affected by material strength. Cast steel node or forged components of a structure have significant fatigue crack initiation periods and material strength may have an effect on fatigue lives. However, material strength does not affect the fatigue life of welded components of marine structures. As-welded joints of marine structures contain inherent flaws and Maddox (Reference 7.4) has shown that the fatigue life of such joints is largely expended in crack propagation. While increased material strength retards crack initiation, the rate of crack growth has been shown to be insensitive to material strength. Experimental work carried out by Hartt et al (Reference 7.5) on high strength steel (HSS) specimens in a corrosive ocean environment indicated fatigue

damage accumulation similar to that of structural steel. Gurney (Reference 7.6) indicates that increased material tensile strength does not increase fatigue resistance and implies that a fatigue design approach incorporating material tensile strength is not valid for welded marine structures.

The effect of initial flaw size on fatigue life and the parameters affecting crack propagation should be understood. An initial flow size estimating procedure by Grover (Reference 7.7) is quite helpful in assessing fatigue crack growth.

Plate Thickness

Current S-N curves recommended by DnV (Reference 1.7), DEn (Reference 1.6) and AWS (Reference 4.13) incorporate a thickness correction factor. DnV and DEn recommendations largely reflect early work by Gurney (Reference 7.1) and many test programs corroborating plate thickness effect corrections proposed by Gurney. Class B, C, D, E, F, F2, G and N curves are applicable to non-tubular (including tube-to-plate) joints based on detail geometry, stressing pattern and method of fabrication/inspection. While these eight classes are applicable without correction to plate thickness up to 7/8 inch (22 mm), class T curve (for tubular joints) is applicable to 1-1/4 inch (32 mm) plate.

The UK DEn Guidance Notes recommend specific size effect (i.e., plate thickness) correction factors in the following form:

$$S = S_b (32/t)^{1/4} \quad 7-1$$

where

$$S = \text{fatigue strength of a joint under consideration} \\ (\text{N/mm}^2)$$

1/68

S_b = fatigue strength of a joint applicable to T curve
for 32 mm wall thickness (N/mm^2)

t = wall thickness of a joint under consideration (mm)

Although the tubular joint test data available may be insufficient to document the size effect throughout the range of plate thicknesses in use, the data available has been grouped, analyzed and relative fatigue strength data documented. Tolloczko and Lalani (Reference 7.8) report that size effect is adequately represented in the Guidance Notes (Reference 1.6) and that none of the more than 300 datapoints fall below the applicable S-N curves.

Test results show that plate thickness or scale increases can adversely affect fatigue strength, perhaps due to increase in weld toe stresses with an increase in plate thickness. S-N curves modified to account for thickness-effect of thick plates often substantially affect the fatigue lives computed. Some experts consider the applicable plate thickness correction to be mild for typical nodes. However, additional work by Maddox (Reference 7.9) indicates that thickness correction may be too severe if only the primary plate thickness is increased. His work on cruciform-type joints (Figure 7-2) indicates that the joint proportions ratio (L/B) has greater effect on fatigue strength than does the primary plate thickness.

While Maddox's encouraging results are applicable to joints subjected to axial tension, increased primary plate thickness subjected to bending stresses still adversely affects the fatigue life. A typical joint in most marine structures is likely to be subjected to substantial bending stresses. Thus, before any relaxation of plate thickness effect on the S-N curves is attempted further data are necessary for a range of geometries and combined loading conditions.

Fabrication Restrictions

Fabrication specifications and drawings often attempt to minimize the conditions that may adversely affect fatigue strength of a detail/joint. Fatigue tests performed on various types of joints, and fracture mechanics analysis carried out by Maddox (Reference 7.10), indicate that the fatigue life of a joint does not change appreciably due to attachment of a backing bar on a plate. Fatigue strength also has been shown to be unaffected by poor fit-up between the backing bar and the plate or by the configuration of the backing bar. However, it should be emphasized that fatigue strength not changing appreciably due to attachment of a backing bar or a poor fit-up may have more to do with the root condition without backing bar.

7.2.2 Fabrication and Post-Fabrication Parameters

Fabrication parameters cover all of the fabrication activities that affect the quality of welded details/joints. These parameters, ranging from welder qualification to heat input and cooling rates, were identified on Figure 3-3 and discussed in Section 3.1.2.

Misalignments

Misalignments adversely affect the fatigue strength of a detail/joint. When a misalignment between two elements is large, both elements may have to be improperly deformed to align them prior to welding. Such joints incorporate substantial residual stresses. If the misalignment between two elements is small, they may be welded as-is, but the misalignment causes a stress concentration due to the resulting secondary bending.

Because misalignment increases the stress at the weld toe of joints loaded axially, the stress magnification factor (K_c) can be correlated to fatigue damage. Fatigue test results for different levels of misalignment in plate joints and tubulars carried out by

Maddox (Reference 7.11) provide the basis for assessment of misalignments.

Weld Quality

A significant scatter of fatigue life test data is expected and appropriately accounted for. A characteristic strength representing a 95% confidence level in test data may be used to assess data points falling substantially below the S-N curve. Such data points are likely to be due to a problem with the welding procedure or the welder qualification. Weld quality degradation (and therefore fatigue life degradation) due to incomplete penetration and poor weld root quality can be minimized by developing a welding specification applicable to the specific configuration and closely adhering to it during fabrication. Weld quality degradation due to undercut at the weld toe can be similarly minimized.

Weld Toe Profile

The significance of weld profiles on joints subjected to fatigue loading is controversial. Substantial time and expenditures are necessary to prepare a favorable weld profile, and weld profiling may increase welding costs by as much as 20%. Thus, weld profiling is limited to specific tubular joints of discrete marine systems.

While API RP2A does not recognize and quantify plate thickness effects, the API S-N curves recognize and quantify weld profile. As illustrated on Figure 4-3 in Section 4.1.2, API (Reference 1.5) recommends the use of an X-curve for welds with a favorable profile while the X'-curve is recommended for welds without such a profile. As illustrated on Figure 7-3, substantial preparation, weld bead shape, application of extra weld beads and grinding may be necessary to allow the use of an X-curve.

Fatigue strength of a tubular joint is shown to improve due to weld profiling (References 7.12 and 7.13). Weld profiling (including grinding of weld toe) has two primary benefits:

- It can minimize the potential for crack propagation by removing inherent crack-like flaws.
- It can reduce stress concentrations by improving local weld profile.

However, grinding to remove flaws and to provide a smooth transition between the weld and parent material is not universally accepted as quantifiable benefit unless the weld toe undercut is sufficient. Both AWS and API do not require a corrective measure if the undercut of weld toe is less than 0.01 in. (See Figure C 10.7.5, Reference 4.14). DnV (Section 3.3.1 , Reference 1.7) states, "the effect of weld profiling giving the weld a smooth concave profile compared with the typical triangular or convex shape may improve the fatigue properties." Although DnV accepts the use of an X-curve (in lieu of a T-curve) provided weld profiling is carried out, it also stipulates that the effect of profiling on the S-N curves will be considered for each case separately.

The weld profiles applicable to API X and X' S-N curves are shown on Figure 7-3. However, to ensure that the flaws at weld toe are removed, grinding or AWJ process should result in sufficient undercut at the weld toe. The minimum undercut recommended by the DEn Guidance Notes (Reference 1.6) is shown on Figure 7-4.

Further discussion and an excellent overview of the effects of weld improvement techniques is provided by Bignonnet (Reference 7.14).

7.2.3 Environmental Parameters

The environment in which fatigue cracks initiate and propagate substantially affects fatigue life. The amplitude, distribution and

frequency of loading identify severity of the fatigue environment. Although a structure's configuration can be optimized to reduce the stress range, the site-specific environmental loading controls the choice of fatigue design and analyses method.

An environmental parameter that affects fatigue is either air or seawater. Because of the adverse effects of seawater corrosion on fatigue strength, a design factor is often applied for fatigue life in a seawater environment. However, an effective cathodic protection system will reduce or prevent seawater corrosion, and if such a system is used, the design factor may be deemed unnecessary. This approach (and its inclusion in various rules, recommendations and standards) is based on corrosion fatigue test data on welded plate specimens with and without cathodic protection.

Environmental effects on welded flat plates have been assumed to be the same as those on tubular joints. However, Wylde et al (Reference 7.15) have indicated that the corrosive effect of seawater on tubular joints may be greater than the effect on flat plate specimens. Although difficult to document, tubular joints may be more susceptible to environmental effects than small welded flat plates due to scale effects, including initial flaws. Flat plates may have longer fatigue lives as substantial time will be expended in initiation of flaws.

7.3

FATIGUE DAMAGE COMPUTATION

State-of-the-art methodology for determining fatigue lives and designing structures with fatigue lives in excess of the design lives is primarily based on S-N curves and the cumulative damage rule. The cumulative damage rule is an approach used to obtain fatigue damage by dividing the stress range distribution into constant amplitude stress blocks, assuming that the damage per load cycle is the same at a given stress range.

Current recommendations, rules and standards uniformly allow the use of Miner's rule to compute the cumulative damage. Applicable cumulative damage rules are discussed in this section, followed in Section 7.4 by a discussion of stress spectrum in the context of fatigue damage computation.

7.3.1 Miner's Rule

The damage for each constant stress block is defined as a ratio of the number of cycles of the stress block required to reach failure. Thus, the Palmgren-Miner linear damage rule defines the cumulative damage (D) for multiple stress blocks as equal to:

$$D = \sum_{i=1}^k \frac{n_i}{N_i} < 1.0$$

As briefly discussed in Section 3.2.5, Miner's rule can either overpredict or underpredict the cumulative damage.

One source of inaccuracy regarding cumulative damage is the application of constant amplitude stress blocks; it may be important to be able to predict the fatigue damage due to variable amplitude loading. Another source of inaccuracy is the sequence of loading; while Miner's rule cannot account for the loading sequence, occurrence of large amplitude loads early in fatigue life can accelerate the rate of crack growth. Another source of inaccuracy for wide band processes is the choice of cycle counting method, which is further discussed in Section 7.4.

Despite these sources of potential inaccuracy, Miner's rule is used to compute fatigue damage because of its simplicity as well as its ability to predict fatigue damage conservatively most of the time. Other uncertainties in determining wave environment, wave loading and hot-spot stresses contribute far more to the inaccuracy of

fatigue damage predictions. Fatigue analysis assumptions also contribute to the inaccuracy of fatigue damage predictions. As an example, 10 to 15 stress blocks, each representing a significant wave height and a zero-crossing point, may be used in the fatigue analyses. The use of 40 to 50 stress blocks is desirable, but often considered impractical for most analyses.

7.3.2 Alternative Rules

The ability to use servohydraulic testing machines and to apply computer-controlled loads has allowed testing of a substantial number of specimens subjected to variable amplitude loading (References 7.16, 7.17, 7.18 and 7.19). Gerald et al (Reference 7.20) provide an excellent overview on variable amplitude loading. Some analytical work carried out and many of the test results show that Miner's rule is realistic and conservative. However, some of the test results also show that Miner's rule may lead to underprediction of fatigue damage.

One source of discrepancy may be crack growth fluctuations. Stress block procedures used in tests result in the application of high tensile stresses, which can retard crack growth. Test specimens subjected to random loadings are less likely to have similar high tensile stresses. Another source of discrepancy is the counting of stress cycles. Gurney (Reference 7.17) and Trufiakov (Reference 7.21) conclude that small fluctuations superimposed on each stress cycle add substantially to fatigue damage.

Miner's rule is the accepted method for fatigue damage computation. However, since alternatives to Miner's rule have been proposed it is beneficial to review one such rule.

Gurney proposes a damage rule by expressing the applied stress spectrum in terms of the maximum stress range (S_{max}), the number of cycles (n_i) applied at proportions (p_i) of S_{max} , and its length ($\sum n_i$) defined as the block length. Gurney's rule states:

$$N_B = \prod_{i=1}^n \left[\frac{N_{Ei-1}}{N_{Ei}} \right]^{p_i} \cdot N_C$$

where:

- N_B = predicted life in blocks
- N_C = constant amplitude life at S_{max}
- N_{Ei} = number of cycles per block $\geq p_i S_{max}$
- i = 1 to n

This product rule can be compared to Miner's

$$N_B = \frac{N_C}{\sum_{i=1}^n p_i n_i^m}$$

where m is the slope of the S-N curve expressed as $S^m N = \text{constant } K$

It should be noted that Gurney's rule may also result in underprediction of fatigue damage. Study of spectrum shape and block length (Reference 7.22) indicates that for long block lengths Gurney's rule may be unsafe.

7.4 STRESS HISTORY AND UPGRADED MINER'S RULE

7.4.1 Background

Miner's linear cumulative damage rule can be used safely, provided some of the wave environment uncertainties (including counting of cycles and evaluating the stress ranges compatible with cycles) are properly accounted for.

Typically, the sea state represented by joint probabilities of significant wave heights and characteristic periods (scatter diagram) is applied to the transfer function to produce the stress range spectrum. Integration of the spectra provides a number of statistical parameters, such as the bandwidth, the zero-upcrossing frequency, etc., allowing development of short-term probability density functions.

The short-term probability density function of the stress range for each significant wave height and its characteristic period is generally defined by using a Rayleigh distribution. For this assumption to be valid, (1) a large number of sea states must be used, and (2) the stress cycles can be considered narrow-banded. Individual stress cycles are considered narrow-banded when they are readily identifiable and there is no ambiguity in counting the stress cycles. The wide-banded loadings exhibit smaller stress cycles interspersed among larger stress cycles. Because it is difficult to define the stress cycles, different cycle counting methods result in different fatigue damage predictions.

Rainflow counting is the name of a large class of stress cycle counting methods, including the original rainflow method, Hayes method, range-pair counting, range-pair-range counting, ordered overall range counting, racetrack counting and hysteresis loop counting.

Rainflow counting and other alternatives are briefly discussed in Sections 7.4.2 and 7.4.3, respectively, to illustrate the options available to upgrade Miner's rule. However, it should be noted that two very important variables affecting fatigue life computation should be addressed in any attempt to upgrade Miner's rule:

- (1) S-N curves are based on constant amplitude stress blocks and should be compared against variable amplitude results.

- (2) Damage computation does not account for stress sequence and may overpredict fatigue lives of joints/details subjected to large stress amplitude ranges early on, accelerating crack propagation.

7.4.2 Miner's Rule Incorporating Rainflow Correction

The rainflow counting procedure is more accurate than other counting methods because the rainflow procedure is based on counting the reversals in accordance with the material stress-strain response.

Modified Miner's rule uses the rainflow cycle counting procedure but does not require the stress process to be simulated.

$$D = \frac{n}{K} E(S^m)$$

where:

- n = total number of cycles
- K = constant, equal to $S^m N$
- $E(S^m)$ = the mean value of S^m
- S = a random variable denoting fatigue stress cycles

If the process is stationary, Gaussian and narrow band, the damage D can be shown that:

$$D = \left(\frac{n}{K}\right) (2/2 \sigma)^m \Gamma\left(\frac{m}{2} + 1\right)$$

where:

- σ = RMS of the process
- $\Gamma()$ = gamma function

When the structure response yields narrow-banded stress cycles, the choice of counting method is immaterial. Even for moderately wide band stress cycle histories, the various cycle counting methods produce similar fatigue damage predictions. The choice of counting method becomes significant only for wide band stress histories with an irregularity factor equal to or less than 0.5. The irregularity factor is a measure of the band width, defined as the ratio of mean crossings with positive slopes to the number of peaks or valleys in the stress history.

7.4.3 Other Alternatives

An alternative approach to predicting fatigue damage under wide-band stresses is to use the narrow-band stress approach and apply an adjustment factor. Assuming a narrow band fatigue stress with the same RMS, and the same expected rate of zero crossings, f_0 , as the wide band stress, a damage estimate can readily be carried out.

Given the spectral density of the stress $w(f)$, the k th moment of spectral density function m_k is equal to:

$$m_k = \int_0^{\infty} f^k w(f) df, \text{ while the}$$

RMS (Std dev.) = $\sigma = \sqrt{m_0}$, and the expected rate of zero crossings

with slope

$$f_0 = \sqrt{m_2/m_0}$$

With this equivalent narrow band process, the fatigue damage can be predicted by the following closed form solution:

$$D_{NB} = (f_0 T/K) (2\sqrt{2} \sigma)^m \Gamma \left(\frac{m}{2} + 1 \right)$$

where

$$\begin{aligned} n &= f_0 T \\ T &= \text{design life} \end{aligned}$$

Wirsching (Reference 7.23) proposes that the fatigue damage be expressed as:

$$D = \lambda D_{NB}$$

where λ is the adjustment factor to fatigue damage predicted based on a narrow-band stress. Thus, the rainflow counting effect to fatigue damage can be incorporated directly if λ is known. An empirical formula proposed by Wirsching is as follows:

$$\lambda(\epsilon, m) = a(m) + [1 - a(m)] (1 - \epsilon)^{b(m)}$$

$$\begin{aligned} \text{where} \quad a(m) &= 0.926 - 0.033 m \\ b(m) &= 1.587m - 2.323 \end{aligned}$$

Thus the fatigue damage obtained by incorporating the narrow-band adjustment factor, λ provides a closed-form formulation. The empirical formula allows fatigue damage predictions quite close to those obtained by incorporating the direct rainflow method.

The λ parameter introduced by Wirsching is an equivalent rainflow adjustment factor intended to correct the slight conservatism of the Rayleigh distribution. Whether a closed-form or a numerical integration is carried out, short-term statistics and the probability density function allow obtaining of partial damage, weighting and summing of all damages.

Following the weighting of the short-term density functions, the long-term density functions for the structure's design life are obtained. While the cumulative damage may be computed through numerical integration, an approximation is introduced to allow application of a closed-form solution. Typically, a Weibull shape parameter (Weibull distribution) is used in predicting cumulative fatigue damage based on the long-term, closed-form method. This subject is discussed further in Section 6 and in a comprehensive paper by Chen and Mavrakis (Reference 7.24).

7.5 OVERVIEW AND RECOMMENDATIONS

7.5.1 Application of S-N Curves

The S-N curves used in determining fatigue damage computations should be compatible with structural details investigated. The S-N curve including the effect of peak stresses should be used together with nominal stresses at the detail, while the S-N curve uninfluenced by the weld profile should be used with nominal stresses increased by appropriate SCFs.

Scatter in fatigue test data should also be appropriately accounted for. One primary parameter affecting scatter of S-N data may be plate thickness. As plate thickness increases higher localized stresses will occur near plate surface, accelerating propagation of fatigue cracks. Considering that small specimen S-N data need to be adjusted for scale effects and a reasonable confidence level should be achieved, S-N curves may be obtained assuming 95% to 97.5% confidence level and a log normal distribution.

There are other parameters that are difficult to assess yet they affect the crack growth and fatigue failure, causing substantial scatter of S-N data points. One important consideration is the size of initial flaw (crack) and another is the number of flaws. Although further work is necessary, Morgan's (Reference 7.25) findings on

interaction of multiple fatigue cracks provide valuable insight into scatter of S-N data points.

Additional parameters contributing to the fatigue life uncertainties are the effects of corrosive sea water environment and the implications of long-life regime. Although cathodically protected offshore structure components in sea water are assumed to have the same fatigue resistance as those components in air, the basis for this assumption is the test data for simple plate specimens. Some large scale tubular joint tests indicate (Reference 7.15) that the corrosive effects of seawater on tubular joints may be greater than the effect on small flat specimens. More test data is necessary to quantify corrosive effects.

There are limited number of test data in long-life regime. As a result, some codes do not provide endurance limit, some have a changing slope and some have a definite plateau at different number of cycles. These and other uncertainties require further research work to upgrade current S-N curves. Current research efforts on fatigue resistance are summarized in Section 9.

The S-N curves recommended by API, DEn and DnV (References 1.5, 1.6 and 1.7) may be used in the computation of fatigue damage. While most early S-N curves were based on AWS data, current DEn curves are largely based on work at the Welding Institute (primarily Gurney and Maddox). DEn Guidance Notes also provide tables, allowing the selection of S-N curves for specific details. For ship structure details, appropriate DEn S-N curves can be selected based on judgement in assessing the details and tables. Earlier works by Munse (Reference 1.3) and Jordan and Cochran (Reference 4.4) can be used directly or in comparison of component test data for ship structure details.

The S-N curves given in DEn Guidance Notes are applicable to a base case plate thickness of 7/8 inch (22 mm), requiring an adjustment of the S-N curves for thicker plates. Considering further validation of

thickness effect is necessary and the ship structure plate thicknesses are not excessive, the correction factor may be neglected.

The S-N curves recommended by API for offshore platforms may be used in the computation of tubular component fatigue damage. The API X-curve and the DEn T-curve (identical to DnV T-curve up to 10 million cycles for cathodically protected areas - see Section 4.2.2) intersect at about 500,000 cycles and would yield similar lives for a plate thickness of 1-1/4 inch (32 mm). Most tubular chord and stub thicknesses are likely to be greater than 1-1/4 inches and the application of corrected DEn or DnV T-curves to compute fatigue lives will result in shorter lives and considered to be appropriate.

Considering the effects of plate thickness, weld profile and undercut on fatigue strength and the S-N curves it may be prudent to reassess the hot spot stress range concept. Tolloczko et al (Reference 7.8) recommend modifying the definition of hot spot stress range to reflect weld toe defects. Then, the S-N curves will reflect only the size effects.

7.5.2 Fatigue Damage Computation

Fatigue lives determined based on S-N curves and Miner's cumulative damage rule are uniformly acceptable to certifying and classification agencies. The national and international standards allow the use of simple cumulative damage rule for the computation of damage. Large number of test results as well as the in-service performance records of marine structures indicate adequacy of this approach.

Alternative rules to compute fatigue damage and methods to upgrade Miner's rule have been proposed. Although necessary to evaluate possible benefits of such alternatives, additional complexity and the cost should also be considered. Since the S-N curves are developed based on constant amplitude stress ranges, the effect of variable

amplitude loading and loading sequence on fatigue life is a valid concern.

The results obtained from a substantial number of specimens subjected to variable amplitude loading show that Miner's rule is appropriate and generally conservative. Dobson et al (Reference 7.26) studied loading histories of containerships based on recorded service data. When the stress intensity ranges were expressed as the root-mean-square, the crack growth of laboratory specimens subjected to constant-amplitude loading history compared quite well with those specimens subjected to constant amplitude loading.

Fatigue damage computation is based on stress ranges and number of cycles and does not account for stress sequence. Since welded structure fatigue lives are largely expended in crack propagation, application of sufficient number of large stress amplitudes early in fatigue life is likely to accelerate crack propagation and overpredicting of fatigue life. The uncertainty of stress sequence, aside, the use of rainflow counting procedure, based on counting the reversals in accordance with the material stress-strain response, may enhance accuracy of damage computation. However, improvement in accuracy is significant only for wide band stress histories with an irregularity factor equal to or less than 0.5. When the structure response yields narrow-banded stress cycles, the choice of counting method is immaterial. Even for moderately wide band stress cycle histories, the various cycle counting methods produce similar fatigue damage predictions. Although further research is necessary, especially on the effect of stress sequence, the use of S-N curves and Miner's cumulative fatigue damage rule is appropriate.

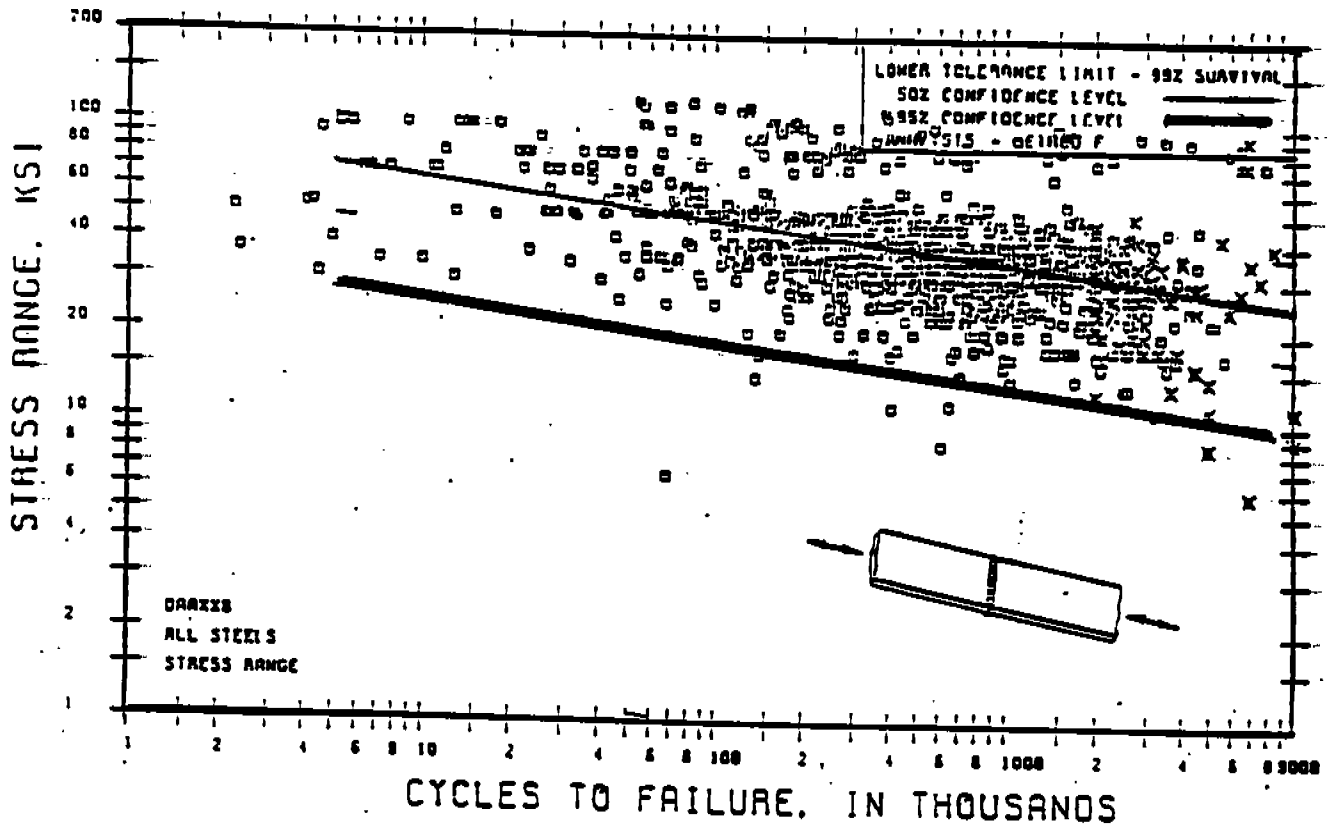


Figure 7-1 S-N Curve for a Transverse Butt Weld and Test Data

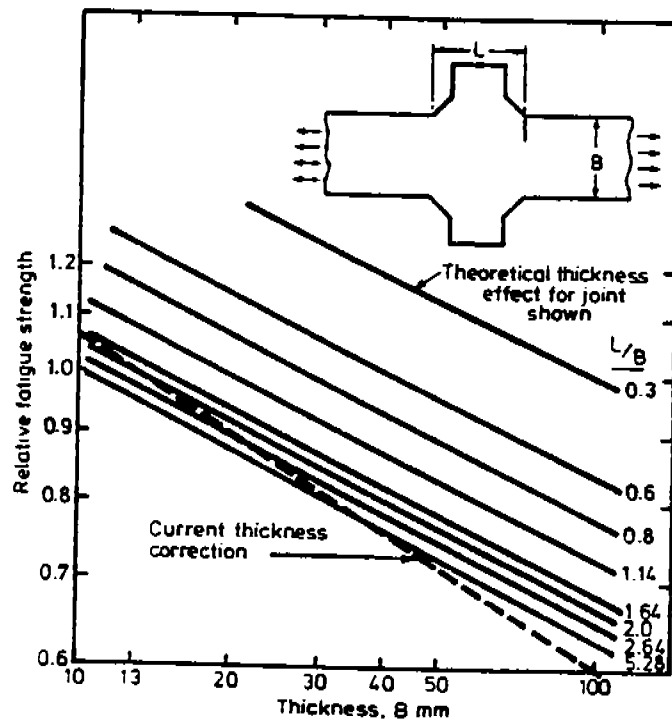


Figure 7-2 Theoretical Thickness Effect for a Cruciform Joint
(From Reference 7.9)

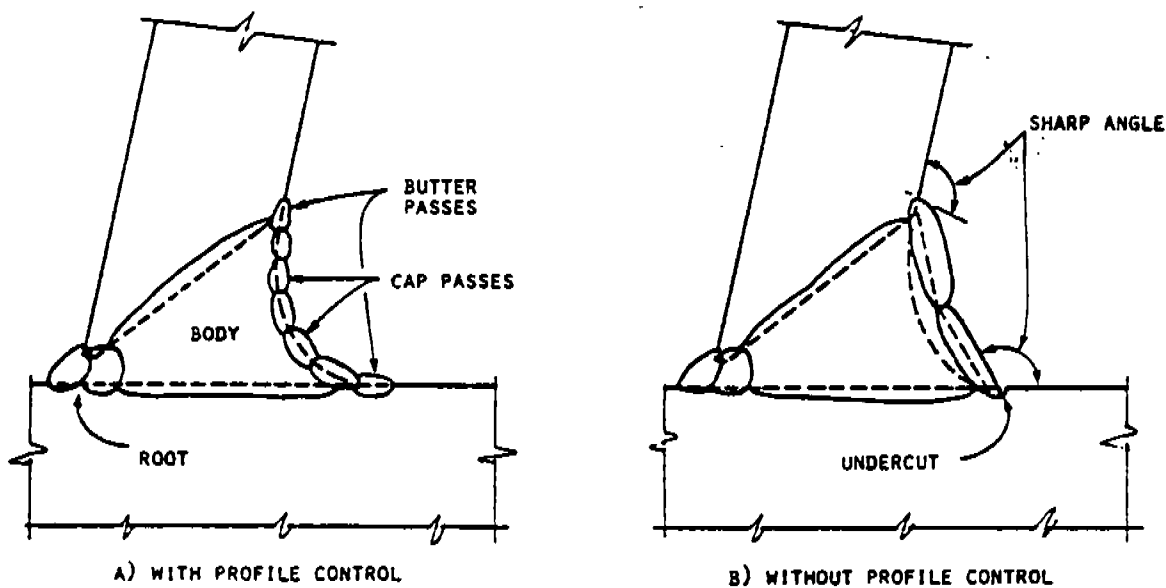
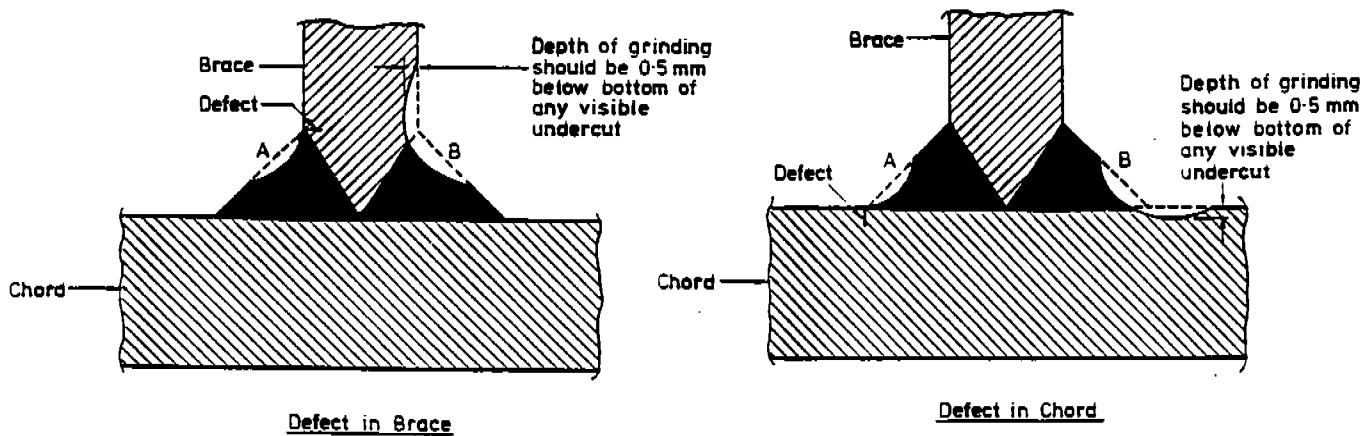


Figure 7-3 Weld Profiles for API X and X' S-N Curves
(From Reference 1.5)



Grinding a weld toe tangentially to the plate surface as at A, will produce little improvement in strength. Grinding must extend below the plate surface, as at B, in order to remove toe defects.

Figure 7-4 DEn Guidance Notes Recommended Weld Profiling and Undercut
(From Reference 1.6)

8. FATIGUE DUE TO VORTEX SHEDDING

This section specifically addresses fatigue due to vortex shedding. Fatigue due to vortex-induced vibrations is different from other forms of fatigue discussed in previous sections only in its loading characteristics. Generally, relatively small number of slender members are susceptible to vortex-induced fatigue. However, response to vortex shedding cannot be predicted using conventional dynamic analyses techniques because the problem is non-linear. In compliance with project objectives, a brief discussion is presented on vortex shedding phenomena, analysis and design, damage assessment and avoidance. A comprehensive discussion, including example problems, is presented in Appendix D.

8.1 VORTEX SHEDDING PHENOMENON

8.1.1 Background

A member exposed to fluid flow may be subjected to unsteady drag and lift forces caused by shedding of vortices. While the vortices shed are most often due to steady wind or current flow, the phenomena can occur due to combined wave and current action. Depending on the member's natural frequency and the velocity of fluid flow, the member may experience sustained vibrations.

Many structure members may be susceptible to vortex induced vibrations (VIV). Relatively large diameter cylindrical brace members of a fixed offshore platform can be designed to avoid VIV. Component members of a cargo boom on a ship or the flare structure on production units (FPSO, platform, etc.) are relatively slender and can not be readily designed to avoid VIV. Then, they need to be either designed to have adequate fatigue strength to resist the VIV over the design life of the structure or provided with devices or spoilers to modify the vortex shedding and/or member natural frequencies.

It should be pointed out that the effect of wind-induced vibration is often not adequately addressed during design. The basis for the issuing of an offshore Safety Notice 7/87 by the U.K. DEN to all North Sea Operators for reassessment of platform flare boom structural adequacy was the discovery of fatigue cracks in the flare boom struts. Bell and Morgan (Reference 8.1) report that the original design documents revealed relatively low fatigue stresses and high fatigue lives. Reanalyses of the flare boom joints indicated that the extensive cracking observed may be due to the combined effect of poor weld quality in the joints and the larger-than-expected stress cycles due to vortex-induced vibrations.

8.1.2 Vortex Induced Vibration (VIV)

At low fluid velocities (expressed as Reynold's numbers) the flow across the cylindrical member remains stable. As the fluid velocity increases (i.e., higher Reynold's numbers) the innermost part of the shear layer adjacent to the cylinder moves more slowly than the outer part of the layer. As a result, the shear layers "roll-up" into discrete swirling vortices. These vortices are shed periodically, either in pairs (in-line flow) or sequentially (cross-flow) from two sides of the cylinder, generating unsteady and very complex pressure distribution. As illustrated on Figure 8-1 (from Reference 8.2), the laminar boundary layer goes through several stages of vortex turbulence with increasing Reynold's numbers. A detailed discussion on vortices and pressure distribution is presented by Marris (Reference 8.3).

If the cylindrical member natural frequency (f_n) is close to the vortex shedding frequency, vibrations of the cylinder may affect the vortices shed. The vortex shedding frequency (f_v) will no longer be dependent on the Strouhal number (S_t), and is likely to become equal to the natural frequency of vibration. If this "lock-in" effect materializes, further increases in the vibration amplitudes will be observed. To prevent the occurrence of critical velocity (f_c), where the member natural frequency is equal to the vortex shedding

frequency (i.e. $f_c = f_n = f_v$), member stiffness and mass may be modified. The maximum amplitude of oscillation for the critical velocity is an important variable, directly affecting the stress amplitudes. The maximum amplitude of oscillation of a member depends on member support conditions and the K_s value, reaching a value approximately equal to member diameter for simply supported boundary conditions. To prevent the lock-in effect, it is desirable to keep the member natural frequencies to less than 70% or more than 130% of the vortex shedding frequency, whenever practical.

8.2 ANALYSES AND DESIGN FOR VORTEX SHEDDING

The interactive nature of the vortices shed and the vibration of the cylinder makes analytical prediction of response to vortex induced vibration (VIV) extremely difficult. Empirical formulations (References 8.5, 8.6 and 8.7) have been developed to reflect the state-of-the-art with respect to VIV technology. These empirical approaches incorporate various parameters and are based on the comparison of specific parametric values with experimental results.

Empirical formulations can be effectively used to avoid VIV, but they are less reliable at predicting the occurrence of VIV and determining the response amplitudes.

8.2.1 Susceptibility to Vortex Shedding

Cylindrical members may experience either in-line or cross flow oscillations for a range of flow velocity and member response characteristic ratios. To define susceptibility of a member to VIV, a reduced velocity (V_r) term is introduced:

$$V_r = \frac{V}{f_n d}$$

where:

V = flow velocity normal to the cylinder axis
 f_n = fundamental frequency of the member (Hz)
 d = diameter of the member

Susceptibility of a member to VIV in air is different than in water due to the density of air flowing around the member being different than the density of water. Susceptibility of a member is defined for in-line and cross-flow oscillations in both environments.

In-line VIV may occur when:

$1.2 \leq V_r < 3.5$ in an Ocean Current Environment
 and $K_s \leq 1.8$
 $1.7 < V_r < 3.2$ in a Wind Environment

Cross-flow VIV may occur when:

$3.9 \leq V_r < 9$ in an Ocean Current Environment
 and $K_s \leq 16$
 $4.7 < V_r < 8$ in a Wind Environment

The stability parameter (K_s) and other pertinent variables that affect susceptibility of a member to vortex shedding are discussed further in Sections D.2 and D.3 of Appendix D.

The response of cylindrical members to wave-induced vortex shedding has not been investigated in depth. Often, it is considered to be less critical than current-induced vortex shedding because wave water particle velocities continually change both in magnitude and in direction. Wave-induced vortex shedding is discussed in detail in a comprehensive paper by Zedan, et al (Reference 8.8).

8.2.2 VIV Response and Stresses

A strategy based on avoidance of VIV is quite feasible for most marine structures. Primary structural members are usually designed to be sturdy enough that they are not susceptible to VIV. However, some secondary or non-structural members may be susceptible to VIV in water and in air. An empirical approach proposed by DnV (Reference 8.7) does not account for the nonlinear relationship between response and damping, thereby yielding conservative response amplitudes and stresses. To predict response amplitudes more reliably an approach based on Hallam et al (Reference 8.9) is recommended.

Cross-flow oscillations due to wind action may not always be preventable, requiring the members to have sufficient resistance. An empirical formulation based on a procedure by Engineering Sciences Data Unit ESDU (Reference 8.6) that accounts for interaction between vortices shed and forces induced is recommended. This procedure and the basis for estimating maximum bending stresses for different boundary conditions are discussed in Sections D.4 and D.5 of Appendix D.

8.3 FATIGUE DAMAGE ASSESSMENT

All members susceptible to VIV should be assessed for fatigue damage. First, the fatigue damage due to VIV is calculated. Then a global fatigue analysis is performed and fatigue determined for all critical members. The total fatigue damage is equal to the sum of local (VIV) and global fatigue damage on each member.

Step-by-step determination of both local and global fatigue damage is discussed further in Section D.6 of Appendix D. Application of the procedure could indicate that the fatigue life is expended after relatively small number of oscillations, requiring corrective measures to be taken either in the design process or during fabrication (devices, spoilers, etc.).

8.4

METHODS OF MINIMIZING VORTEX SHEDDING OSCILLATIONS

Because the environmental factors that cause vortex-induced oscillations (wave, current and wind) cannot be controlled, minimizing the oscillations depends primarily on the physical characteristics of the structure.

There are several ways to solve the problem of vortex-induced oscillations:

- Control of structural design (length, diameter, end fixity) to obtain member natural periods to avoid the critical velocity.
- Control of structural design to have sufficiently high values of effective mass and inherent damping to avoid the critical velocity.
- Altering the pattern of the approaching flow to modify vortex shedding frequency.

Further discussion on this subject is presented in Section D.8 of Appendix D.

8.5

RECOMMENDATIONS

Fatigue damage due to vortex shedding is best prevented during the design of the structure by sizing the members (length-to-length ratio, rigidity, damping, etc.) to ensure that critical velocity values are avoided. If geometric, design schedule or economic constraints preclude resizing of members susceptible to VIV, the total fatigue damage due to local (VIV) and global response should be computed and the integrity of those members verified. If a limited number of members are found to be susceptible to fatigue failure, the flow around such members may be modified through the use of devices and spoilers.

Verification of a member's structural integrity due to VIV fatigue is difficult due to the interactive nature of the vortices shed and the vibration of the member. State-of-the-art procedures developed to determine the response amplitudes of a member incorporate several approximations. It is recommended that some of the more important of these approximations are carefully considered before starting a VIV analyses:

- Experimental data used to correlate parameters in the development of empirical procedures are limited. Published data is not available for in-line VIV in uniform oscillatory flow.
- Accurate determination of structural damping ratios in air and in water is difficult. The damping ratios directly affect the stability parameter and may contribute to either underestimation or overestimation of the vibration amplitudes and stresses.
- Tubulars extending over multiple supports need to be evaluated by considering support sleeve tolerances and spanwise correlation of varying lengths and fixity prior to the determination of natural frequencies.

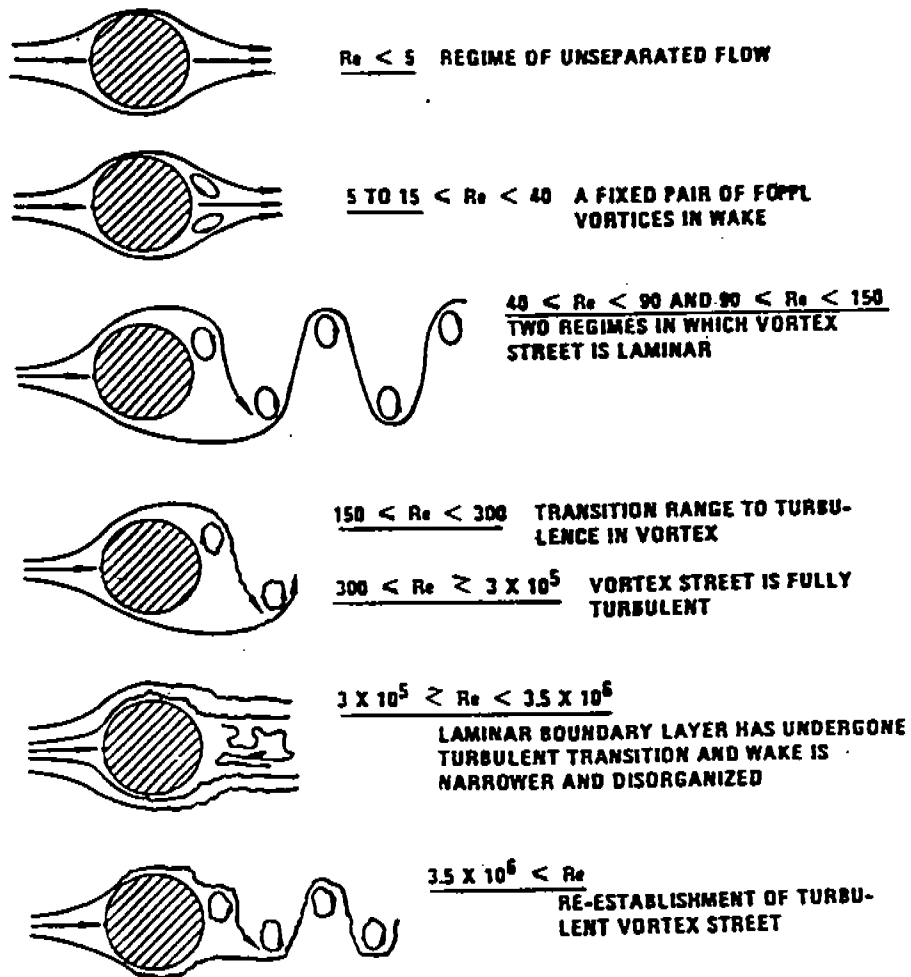


Figure 8-1 Regimes of Fluid Flow Across Circular Cylinders
(From Reference 8.2)

9. FATIGUE AVOIDANCE STRATEGY

Most marine structures are designed and analyzed to resist extreme loadings. Some structures, including offshore structures and ships with special features, are also checked for fatigue. This approach may be valid for structures in environments not susceptible to fatigue loadings. A good overall design of marine structures susceptible to fatigue loading (large ships and tankers, stationary fixed and floating structures, etc.) can be achieved when fatigue is given an equal emphasis to stability, strength and other considerations during design, long before steel is ordered.

Fatigue design should be both an integral part of an overall design effort and a part of a strategy covering the entire design life of the structure. Thus the design, fabrication, inspection and operational maintenance should be treated as interactive parameters that affect fatigue avoidance strategy.

While most offshore structures susceptible to fatigue were properly analyzed and designed to prevent fatigue failures, ship-shaped vessels were seldom analyzed and designed for fatigue. The use of high strength steel in recently constructed vessels proved that an indirect fatigue design (i.e. member sizing, detailing) is not sufficient to prevent fatigue failures. As a result, large number of vessels constructed by reputable firms now incorporate detailed finite element analysis and design to prevent fatigue failures.

9.1 REVIEW OF FACTORS CONTRIBUTING TO FAILURE

Mobile vessels and stationary structures differ not only in their general configuration but also in the nature of applied environmental loading. A stationary structure's site-specific environment usually determines the stress ranges and the number of stress cycles, and is a major variable affecting fatigue life. The next most important variables are the parameters affecting design and fabrication quality. While maintenance may not be important early in design life, it assumes a major role as the structure

ages. The designer has no control over the environment, but other factors can be addressed to enhance fatigue quality.

The factors that affect fatigue quality can be reviewed in four groups. It appears reasonable to assume that each of these four groups contributes equally to fatigue failure:

- Design
- Fabrication
- Maintenance
- Operational Loads

The fatigue life of a vessel is similarly affected by the activities undertaken during design, fabrication, maintenance work and severity of operational loads. Skaar (Reference 9.1) reports that a survey to assess the approximate importance of design, fabrication, maintenance and operations indicated that each contributes about equally to overall quality.

9.2 BASIC FATIGUE AVOIDANCE STRATEGIES

9.2.1 Basic Premises

Review of fatigue failures shows that while relatively few failures threaten structural integrity, repairs are costly and the cost of continuous inspection and maintenance is appreciable. A survey of design configurations and structural details shows that designers who have access to operational feedback on inspection, repair and maintenance, generally develop more reliable designs. To ensure a functional, high-quality structure (i.e., with structural integrity) that is cost-effective, both capital expenditures (CAPEX) and operating expenditures (OPEX) should be addressed simultaneously.

The review of marine structures indicate several design philosophies:

- An indirect fatigue design where the design for extreme loading and experience-based detailing are intended to provide ample fatigue resistance. This approach may be valid for structures subjected to negligible cyclic loadings.
- Simplified allowable stress methods based on in-service data and valid theoretical developments. This approach is valid as a design tool to size structure components.
- Comprehensive fatigue analyses and design methods with appropriate fatigue strength and stress history models. This approach, including finite element analyses to accurately determine the stress distributions, should be used in the design of all structures susceptible to fatigue failure.
- Comprehensive fatigue analyses and design methods, taking the lifetime inspection and maintenance strategies into account. This is the valid approach to implement a cost-effective fatigue avoidance strategy.

Design, inspection and maintenance are thus logically treated as interdependent parts of an overall process contributing to the quality of a structure.

The other basic premises affecting fatigue avoidance strategies can be summarized as follows:

- The fatigue life is usually taken as twice the design life. The target fatigue lives can be chosen to be about five to ten times the design life with very little increase in steel. The additional expenditures caused by the slight increase in steel cost can be offset many times over by savings in operating expenditures associated with inspection, repair and maintenance.
- Service experience is of utmost importance in the design of marine structures. The designer should have an access to

failure data on various structures, including continuous system stiffening details (i.e., orthotropically stiffened hullplate).

- Typically, stiffening detail failures cause serviceability problems, affecting the extent of a structure's repair work and cost. Unrepaired, they may cause buckling, flooding and progressive collapse, thereby, resulting in the pollution of the environment and the loss of structural integrity.
- Typical tubular interface failures of stationary structures can cause substantial degradation in structural integrity. Repairs on location, especially underwater, are extremely costly and are not always entirely successful.

9.2.2 Fatigue Avoidance Strategies

Fatigue avoidance strategies for ships and tankers are both similar and dissimilar to those for fixed and floating stationary structures. The primary components of continuous systems (ship longitudinal girder, semisubmersible column, etc.) are designed to provide ample strength, and the redundant load paths provided by multiple stiffeners make fatigue more a serviceability problem. A discrete system such as a fixed platform may have redundancy to prevent major degradation of the structure, yet redistribution of load paths will accelerate crack growth in adjacent areas and can cause failures in these areas. To prevent additional failures, repair work should not be postponed beyond a reasonable period.

The basic fatigue avoidance strategies are best addressed as the factors that affect design and maintenance:

Design

- Global Configurations

A design strategy that provides a global configuration with redundancy and minimizes both the applied loads and the response will enhance structure fatigue life and reduce maintenance costs.

Both continuous system and discrete system global configurations can be optimized to various degrees to minimize the effect of applied loads and the response of the structure to these applied loads. The dynamic response of the structure can contribute to substantial cyclic stress (i.e. both global and local dynamics, including vortex induced vibrations) and should be minimized.

- Joint/Weld Details

The structural joint/weld details should be developed based on operating experience, analytical studies and assessment of the impact of actual fabrication yard work to minimize the stress concentrations, adverse fabrication effects and stress levels.

The joint/weld details should be designed to prevent large stress concentrations. Review of typical joint/detail failures and analytical parametric studies should be used to identify both "desirable" and "undesirable" details. Review of some of the published data on structural detail failures (References 9.2, 9.3, 4.2 and 4.3) also illustrate that such fatigue failures can be significantly decreased by avoiding magnification of stress patterns on a structure detail. Jordan and Cochran (Reference 9.2) surveyed 3,307 failures in over 50 ships and presented their findings by grouping the structural details into 12 families. The review of details within each family (twelve families: beam brackets, tripping brackets, non-tight collars, tight collars, gunwale

connections, knife edge crossings, miscellaneous cutouts, clearance cuts, deck cutouts, stanchion ends, stiffener ends, and panel stiffener ends) should provide an invaluable operational feedback to the designer in understanding relative susceptibility of different details to fatigue failure.

- Material and Fabrication

The material selected, procedures specified and fabrication specifications issued should be compatible with each other and meet the requirements of the intended function of the structure.

The design effort should ensure selection of material with chemical composition and material properties applicable for the structure's intended function. Welding material and procedures should be compatible with the structural material selected. Overall fabrication specifications, covering fabrication tolerances, repair procedures, etc., should be developed to meet the target objectives. Specifications should reflect a balance between cost and fit-for-purpose approach to quality.

Maintenance

Stationary structures may require a higher degree of design conservatism than mobile structures to minimize the cost of maintenance, inspection and repair. Maintenance and inspection programs should be developed during design to reflect both design conservatism and functionality of the structure and its components.

Maintenance, inspection and repair are interactive in-service parameters. The maintenance and inspection of continuous systems differs from discrete systems largely in degree of accessibility. Most continuous systems (such as interiors of hulls, columns and pontoons) can be routinely inspected and maintained. Such units can be brought to shipyards for scheduled or unscheduled repairs.

Fatigue avoidance strategy for mobile vessels should consider both the consequence of limited degradation due to fatigue failure and the relative ease of routine maintenance and scheduled repairs.

Most discrete systems, such as offshore platforms, are stationary and their components are generally not accessible for internal inspection. Thus, inspection is carried out externally, both above and below water. Any repair work undertaken is costly and may be only partially successful. Where regulations impose comprehensive inspection and maintenance programs, such as in the North Sea, a fatigue design philosophy addressing the inspection and maintenance issues also facilitates certification of design. Typically, redundancy and consequence of failure dictate the inspection intervals. Those areas known to be susceptible to fatigue failure will require more frequent inspection intervals. Similarly, inspection results should be the basis for altering the recommended inspection schedule as necessary.

Analysis

Analytical assumptions and the methodology implemented for fatigue life computations have dramatic effects. The choice of fatigue analyses appropriate for a specific project depends on the information available, research gaps, and sensitivity of structure to fatigue failure. Because fatigue analysis approach is not truly an avoidance strategy, it is discussed separately in Section 9.4.

9.3

FATIGUE STRENGTH IMPROVEMENT STRATEGIES

Fatigue strength improvement and fatigue avoidance strategies benefit from application of an appropriate design philosophy that allows development of structure and component integrity, and that facilitates quality of construction. The specific methods discussed in the section are remedial measures for fatigue strength improvement.

9.3.1 Fabrication Effects

The fatigue strength of welded joints/details is lower than the parent material due a wide range of fabrication effects. Some of the primary causes for the degradation of fatigue strength are due to:

- Increase in peak stresses due to geometrical effects and discontinuities (stress amplification) and mismatch tolerances (bending stress) introduced.
- Residual stresses introduced due to welding, forced fit, excessive heat input, etc.
- Defects introduced in the weld material, and undercut at the edge of welds.

Adverse fabrication effects are minimized by addressing the issues during design and specification writing. Both experience (operational and design) and parametric studies allow development of "desirable" details to minimize the local increase of stresses. Fabrication specifications are prepared to optimize fabrication quality without excessive expenditures.

9.3.2 Post-Fabrication Strength Improvement

Numerous post-fabrication processes can partially or totally counter the fabrication effects that contribute to degradation of fatigue strength. However, post-fabrication processes may be costly and should not be incorporated in the design process routinely.

The development of fatigue cracks depends largely on the geometry of the joint detail and often develop at the weld toe. Any mismatch of parent plates will facilitate propagation of the crack through the weld until a failure across the throat is observed. Deposition of extra weld metal in the throat area to decrease the shear stress can

improve the fatigue strength. The methods available to improve fatigue strength can be grouped into two:

- Modification of weld toe profile
- Modification of residual stress distribution

Some of the methods in each category are identified on Figure 9-1 and discussed in this section.

Modification of Weld Profile

Both contour grinding of the weld profile and the local grinding of the weld toe area are recommended to improve fatigue strength. The two key objectives in the modification of weld toe profile are:

- Remove defects at the weld toe.
- Develop a smooth transition between weld material and parent plate.

By applying either local grinding or remelting techniques to remove defects and discontinuities, the fatigue life is increased as a function of time required for crack initiation. Some applicable methods are as follows:

- Grinding

Full-profile burr grinding, toe burr grinding or localized disc grinding can be carried out. Considering the time required for grinding, local-weld toe grinding has become one of the most frequently used grinding methods. Careful and controlled local grinding of the weld toe improves the fatigue strength of a specimen in air by at least 30%, equivalent to an increase in fatigue life by a factor greater than 2.

However, to obtain such a benefit the grinding must extend about 0.04 inch (1 mm) beneath the plate surface. Typical defects and corrective measures are shown on Figure 9-2.

- Controlled Erosion

An alternate weld toe modification technique uses a high-pressure water jet containing grit. Under carefully controlled conditions the weld toe area can be eroded as though it were being ground. Work carried out on fillet welds with abrasive water jetting (AWJ) by Maddox and Padilla (Reference 9.4) and King (Reference 9.5) indicate that fatigue life improvement due to AWJ erosion and toe grinding are comparable. The S-N curve improvements obtained due to weld toe abrasive water jet erosion are illustrated on Figure 9-3. This approach does not require heat input and can be carried out quickly, offering an advantage over alternative methods.

- Remelting Techniques

Remelting weld material to a shallow depth along the weld toe results in removal of inclusions and helps achieve a smooth transition between the weld and the plate material. Tungsten-inert-gas (TIG) and plasma welding are not practical techniques for routine use, but TIG and plasma dressing can be used to improve the fatigue strength of selective areas.

TIG welding is based on a stringer bead process. TIG dressing is performed on welds made by other processes where the toe region is melted to a shallow depth without the use of a filler material. Slag particles in the remelted zone are brought to the surface, leaving the weld toe area practically defect free. A high heat input should be maintained to obtain a good profile and a low hardness. A low hardness in the heat-affected zone (HAZ) may be also achieved by a second TIG pass.

Plasma dressing requires remelting the weld toe using the plasma arc welding technique. It is very similar to TIG dressing, but plasma dressing uses a wider weld pool and higher heat input. This technique is relatively insensitive

to the electrode position, so the strength improvements are better than the improvements obtained from TIG dressing.

Although overall weld profiling is considered desirable for tubular intersections, rules and recommendations other than API do not allow improvement in fatigue strength of a joint unless weld profiling is accompanied by weld toe grinding.

The fatigue strength increase of welded joints due to weld toe grinding in air is considered equally applicable to cathodically protected welded joints in seawater. However, in the absence of cathodic protection, a corrosive environment helps to initiate fatigue cracks. Thus, without cathodic protection, fatigue strength improvement due to weld toe grinding cannot be justified.

The fatigue strength increase in welded joints due to weld toe grinding is based on simple plate specimens tested in air and in seawater (with and without cathodic protection). However, extension of welded plate specimen test data to tubular joints may not be correct. Work carried out by Wylde et al (Reference 9.6) indicates that additional research is necessary because:

- 1) The corrosive effect of seawater appears to be greater on tubular joints than on flat plates.
- 2) Cathodic protection appears to be less effective on tubular joints than on flat plates.

Modification of Residual Stress Distribution

A wide range of residual stress techniques are available to redistribute the fabrication stresses at a welded joint. If large residual tensile stresses are present at a welded joint, the applied stress cycle near the weld toe can remain wholly tensile. Thus,

after a given number of stress cycles, the stress range to cause failure is practically constant for a wide range of mean stresses.

The undesirable tensile residual stresses at the weld can be modified by the following methods to set up desirable compressive stresses at the weld toe:

- Stress Relief

Various fatigue tests on simple plate specimens indicate that an improved fatigue strength can be obtained by stress relief due to post-weld heat treatment (PWHT). However, plate and stiffening elements of continuous systems rarely require stress relief. Thick tubular joints with residual stresses as a result of fabrication work can often benefit from stress relief. Yet, it is not clear that a complex joint with built-in constraints can be effectively stress relieved. It is likely that substantial residual strains and stresses will remain at a joint assembly after PWHT.

Localized stress relief may be very beneficial in an embrittled heat-affected zone (HAZ). Typically, high localized heat input in a HAZ alters the material properties and causes reduced fatigue life due to unstable fracture. A PWHT carried out to improve toughness of the HAZ may partially restore the fatigue strength of welded joints, as the residual stresses have an influence in the development of fatigue cracks. Previous investigations on this subject (Reference 1.8) document influence of PWHT on fatigue.

- Compressive Overstressing

Compressive overstressing is a technique in which compressive residual stresses are introduced at the weld toe. Experimental results and analytical work demonstrate effectiveness of prior overstressing, but the procedure to be implemented does not appear to be practical for most marine

structures. A comprehensive discussion of strength improvement techniques by Booth (Reference 9.7) is recommended for further review of compressive overstressing.

- Peening

Peening is a cold working process intended to produce surface deformations to develop residual compressive stresses. When impact loading on the material surface would otherwise cause the surface layer to expand laterally, the layer underneath prevents such surface layer expansion, creating the compressive residual stresses at the surface. Typical peening methods are hammer peening, shot peening and needle peening. Further discussion on peening techniques and their relative benefits is provided by Maddox (Reference 9.8).

9.3.3 Comparison of Strength Improvement Strategies

Strength improvement techniques are time consuming and costly and they should be applied selectively. Comparison of different techniques allows assessment of their effectiveness and cost. The recommended strength improvement strategy depends on the characteristics of the structure (global and local) and the preference for one technique over others based on effectiveness, cost and fabrication yard characteristics.

Some of the more important comparisons of various approaches available to improve fatigue strength of weld details subjected to a wide range of stresses are as follows:

- Full profile burr grinding is preferable to toe burr grinding only, or disc-grinding only, because it results in higher fatigue strength even at a substantial cost penalty.

Disc grinding requires the least time and cost. However, it produces score marks perpendicular to the principal stress direction, making this technique less effective than others.

A second pass with polishing disc is considered advisable. A complete chapter on weld toe grinding by Woodley (Reference 9.9) provides a detailed discussion on grinding techniques.

- Using a high-pressure abrasive water jet (AWJ) process for controlled erosion of the weld toe area can be as effective as grinding. Its simplicity, speed and non-utilization of heat make controlled erosion very promising. Work carried out by King (Reference 9.5) indicate that AWJ process is suitable for a range of material removal applications, including weld toe dressing, gouging and weld edge preparation.
- A wider weld pool makes plasma dressing less sensitive to the positioning of the electrode relative to the weld toe, compared with TIG dressing. Therefore, the fatigue strength improvement obtained from plasma dressing is generally better than that obtained from TIG dressing.

Both methods are suitable for automation and cost-effective application.

- Review of grinding, remelting and peening techniques indicate substantial scatter of fatigue strength improvements. Typically the best fatigue strength improvements are achieved by TIG dressing and hammer peening. Toe disc grinding is the least effective technique. Figure 9-4, obtained from Reference 9.7, provides a good comparison of various fatigue strength improvement techniques.

9.4 FATIGUE ANALYSIS STRATEGIES

9.4.1 Review of Uncertainties, Gaps and Research Needs

There are many uncertainties in a fatigue analysis, carried out to determine the fatigue lives of marine structure components. To ensure validity of analysis the first objective is to accurately predict the stress-history for the lifetime of the structure. The

second objective is to accurately evaluate the fatigue strength of the structure components and to calculate the cumulative fatigue damage based on stress-history and fatigue strength. While some of the uncertainties occur in nature, others are caused by shortcomings in simulating the actual behavior.

Uncertainties in Predicting Stress History

It is necessary to model the actual structure as closely as possible to determine the applied loads and the response of the structure to these applied loads. Since marine structures are typically indeterminate structures, stresses are strongly dependent on the structural configuration, necessitating careful simulation of actual member and joint behavior.

a) Hydrodynamic Loads Model

The ship structure loads model allows the use of strip methods or 3-D flow solutions to determine the wave loads. The accuracy of the wave load determination depends on the ability to accurately define the wave force coefficients, marine growth, wave steepness, hydrostatic effects and hydrodynamic effects.

The loads on a stationary semisubmersible or fixed platform are typically determined from Morison's equation. Fixed platform loads are largely affected by the accuracy of wave inertia and drag force coefficients, wave steepness, marine growth and the shielding effect of component members. The use of a stick model is valid for a fixed platform, the use of a stick model for a structure made up of large members will result in inaccurate loads.

Because large members will disturb the flow, leading to highly frequency dependent diffraction, a three-dimensional diffraction theory is often used to determine the wave force components to directly account for the effect of one member on

others. Extensive analytical and experimental work provides validation of techniques used to generate the loads.

For standard vessels with a forward speed, strip methods often provide the desirable accuracy. Although the diffraction methods are still considered largely a research tool by many, they are now used as an analyses and design tool by others.

Limited amount of available data on wave-induced and dynamic impact (i.e. slamming) loading on vessels and the vessel response do not facilitate calibration of analyses models. It is necessary to obtain sufficient data for various vessel types for an extended period. Boylston and Stambaugh (Reference 9.10) recommended program to obtain loading computer records, based on vessel strains for at least three vessel types over a five-year period, should provide sufficient data on probabilistic loadings and the vessel response.

b) Mass, Motions and Stiffness Models

There are few uncertainties in developing an accurate mass model. The motions model, however, is largely affected by the assumptions made to define the motions and stiffness models and the analyses techniques chosen. The uncertainties built into these models that allow the definition of nominal stresses are:

- linearization of drag term
- definition of joint releases, complexity of joint, joint flexibility etc.
- definition of strongbacks and global versus local distribution of loads
- added mass
- appurtenances modelling
- structural damping (for bottom-supported structures)
- foundation matrix (for bottom-supported structures)

- relative slippage between jacket legs and piles.

Additional uncertainties introduced due to assumptions made on analyses techniques, are:

- application of regular or random waves
- application of time-domain or frequency domain solutions
- use of deterministic versus spectral analyses

While some of the uncertainties relate to analytical simulation of actual conditions, others reflect the uncertainties in both the nature and in simulation. Most analysis and modeling uncertainties can be minimized, and the current state-of-knowledge and tools available facilitate obtaining accurate nominal stress distributions.

Since the structure dynamic responses (both global and local, including vortex induced vibrations) contribute substantial cyclic stresses, it is extremely important to minimize the uncertainties in simulating structure responses.

c) Hot Spot Stresses

Peak stresses can be reasonably well defined by the use of physical models and finite element analyses. However, for most analysis and design work the time and cost constraints necessitate the use of empirical formulations to obtain the SCFs and define the hot-spot stresses.

All empirical formulations have application limits and the accuracy of the SCFs computed depend on several variables. More finite element work is required to define the interaction of parameters for a wide range of joint geometries to upgrade existing empirical formulations.

d) Stress Spectrum

Hot-spot stresses combined with the long-term effects of the environment allow development of the stress spectrum. Randomness of ocean environment makes both the short and long-term prediction of sea states quite difficult. The uncertainties of nature that influence the life-time stress history of a stationary structure are:

- Use of full scatter diagram of Hs and T
- Variations of T
- Percentage of occurrence estimates
- Wave directionality
- Interaction of wave and current

For some site-specific stationary structures, a good existing database may allow comprehensive hindcasting studies to predict both short- and long-term environment with a reasonable certainty. A reliability-based full probabilistic fatigue analysis allows selection of the degree of reliability that affects the fatigue life, such as the environmental loading, size and distribution of defects, fatigue strength, etc. However, even commonly used spectral fatigue analyses, which is deterministic, (i.e. application of only probabilistic environmental conditions), the desirable level of uncertainty for the environment can be chosen to be compatible with the other factors that affect the computed fatigue life.

For oceangoing ships which move through various site-specific environments in a single route, the stress history is very difficult to define. A full probabilistic reliability analysis, or the use of conservative upper bound conditions, is necessary to account for the many different routes over the the uncertainties regarding the use of very different routes over the life of the vessel as well as route changes due to extreme environmental conditions.

Uncertainties in Predicting Fatigue Strength and Cumulative Fatigue Damage

Fatigue strength is not analyzed but determined from laboratory test specimens. The experimental work that allows the definition of fatigue strength and the S-N curves require substantial further work. Some of the basic variables contributing to the uncertainty of fatigue strength include the effects of:

- Geometry (weld profile, toe discontinuity, etc.)
- Defect type, size and location
- Definition of fatigue failure (N1, N2) in S-N data
- Size on S-N data
- Assumption of a linear model and log normal distribution for N
- Environment (corrosion, cathodic protection, etc.)
- Load amplitude and sequence
- Fabrication residual stresses
- Post-fabrication procedures to increase fatigue strength

Due to large uncertainties in each of the items listed, the fatigue strength data show a very large scatter, requiring the use of somewhat conservative S-N curves. The available test data on high stress range-low cycle fatigue failure is limited. Thus, the S-N curves for the 1000 to 10,000 cycle range are less reliable than the high cycle ranges.

While additional work is necessary to better define geometric variations, the recent research has shown that there are also some uncertainties regarding the:

- Beneficial effect of weld profile without weld toe grinding or remelting
- Assumption of cathodically protected joints in sea water having the same fatigue strength in air
- Classification of joints based on geometry rather than load pattern

Cumulative fatigue damage computations have been and still are based on Miner's linear cumulative damage rule. Alternative stress cycle (rainflow) counting methods have allowed reduction of uncertainties for wide-band loading. Gurney's rule provides an alternative to Miner's rule. However, the most important research gap in the computation of fatigue damage is the sequence of loading. The wave loading, which is of stochastic nature, have been simulated by Markow matrix (Reference 9.11) to carry out fatigue test of plates under stochastic and constant amplitude loading (Reference 9.12). These initial tests indicate fatigue strength properties for constant amplitude and spectrum loading may be different. Until more research is carried out on loading sequence it should be presumed that a certain number of large amplitude stress cycles during the beginning of a structure's life would be likely to accelerate the fatigue crack growth of most defects. A series of tests being carried out at Technical University of Denmark (Reference 9.13) should provide more definitive conclusions on fatigue life of welded joints subjected to spectrum loading under various corrosive conditions.

9.4.2 Recent Research Activities

Extensive fatigue research activities were carried out in the 1980s. A large percentage of these activities were carried out in Europe, addressing the parameters affecting fatigue life of joints/details in the extreme North Sea environment. Other research activities carried out in the United States and elsewhere indicate that the research activities are often complementary and generally avoid duplication of effort.

The fatigue research activities are generally carried out in two or three phases over multiple years. While some research activities were completed, others will continue into early 1990s. These research activities may be grouped into following areas and the relevant activities are summarized on Figure 9-5.

- Stress concentration factors; including collating of existing data, calibration of SCF equations and development of parametric equations.
- Fatigue analysis and design methods; including finite element analysis procedures and application of fatigue design rules.
- Fatigue resistance; including simple plate S-N curves and complex details, S-N curves for stiffened joints and S-N curves for different materials.
- Effect of various parameters on fatigue life; including the effect of cathodic protection in seawater, plate thickness and weld profile effects.
- Fatigue life improvement techniques.
- Fatigue life determination; including review of cumulative damage, assessment of random loading and low cycle fatigue.

9.4.3 Cost-Effective Analysis Strategies

A cost-effective analyses strategy is relatively easy to develop for any marine structure. First, the structure configuration and the likely marine environment should be assessed to determine susceptibility of the structure to fatigue. Second, structure configuration and operational response characteristics should be assessed to determine the desirable analyses techniques to generate the loads and to determine the response of the structure.

Although computer cost is an important variable in developing an analysis strategy, computer cost should be assessed in conjunction with engineering time and effort as well as the time available to complete the fatigue analysis and design. Most important, design is an iterative process and structural changes will invariably occur during fatigue analysis. Thus, fatigue analysis should be treated

as a parametric study intended to identify the fatigue-susceptible areas for improvement.

Considering that small increases in steel used can appreciably increase fatigue lives, it is recommended that the target fatigue lives (at least for a screening effort) be taken as five to ten times the design life while most rules and recommendations specify a factor of two between fatigue and design life. Then, changes introduced during design that has an impact on applied loads and stress distributions can be readily accommodated.

9.5

RECOMMENDATIONS

Fatigue avoidance strategies adopted and the design tools used have served as well. However, further efforts are necessary in carrying out more research, in developing further improvements in analyses and design, and in upgrading the rules and regulations to incorporate the research results.

Recommendations presented in Section 5 through 8 provided the basis for further in-depth discussions in Section 9. Applicable references in each section are listed in Section 10. Some of the primary recommendations are listed as follows:

- Although "allowable stress" methods may be used as a "screening process," a detailed fatigue analysis is often necessary.
- Assessment of various empirical equations indicate that the UEG equations yield conservative prediction of SCFs for a wide range of geometry. However, empirical equations provided by UEG, Efthymiou, Kuang and others should be reviewed for joint geometry and loading condition to allow selection of most appropriate equation.
- The long-term wave environment definitions based on hindcast models are quite reliable. However, modeling parameters

should be carefully reviewed and the model calibrated to ensure the reliability of data.

- The S-N curves used in determining fatigue damage computations should be compatible with structural details investigated.
- Considering the effect of size, weld profile and undercut on fatigue strength and S-N curves, it may be prudent to reassess the hot spot stress range concept. The definition of hot spot stress range can be modified to reflect the weld toe defects.
- The use of Miner's cumulative fatigue damage rule with the S-N curves is appropriate. Further research, especially on the effects of stress sequence and counting of stress reversals, is considered necessary.

9.5.1 Research Priorities

Whether designing a supertanker or an offshore platform, significant failure modes can be identified, environmental loads generated, structure response characteristics determined, and stress superpositions compatible with the environment and the failure modes computed. Although strength statistics for these structures can be expressed in terms of means and variance, lack of sufficient statistical data on loads, stresses and strength prevent full probabilistic fatigue analyses. A development of a semi-probabilistic analysis approach applicable to various structures and that does not require a distribution shape is desirable.

While a typical fatigue damage assessment is based on fatigue strength data yielding S-N curves, such an assessment can also be made based on fracture mechanics and crack growth laws. While the damage assessment is based on propagation of individual crack, work carried out by Morgan (Reference 9.14) has indicated possible interaction of multiple cracks. Thus, further work is necessary to obtain data on interaction of cracks as well as interaction of parameters affecting development of S-N curves.

Additional areas requiring further research are summarized as follows:

- Parallel study of weld profile and weld toe defects. Analytical study of existing data for weld toe defect stress levels and through-thickness stress levels.
- Identification of the type and magnitude of the errors introduced in laboratory work and development of appropriate means to normalize test data.
- Further assessment of empirical equations. Available test data should be further evaluated, incorporating necessary correction of data, and reliability and limitation of equations revised, as necessary.
- Carrying out of additional tests in both air and in ocean environment to fill the gaps in existing research.
- Development of NDE methods to quantify residual stresses introduced during fabrication.
- Further study of long-term wave environment.
- Further assessment of stress sequence on fatigue life.

9.5.2 Rules and Regulations

Existing rules, regulations and codes are adequate and generally conservative. However, differences exist between various rules, regulations and codes, including omissions and inconsistencies. Research data obtained in the 1980s was the basis for revisions introduced into the 4th Edition of Guidance Notes (1990). Similar effort has been initiated to revise API RP 2A. Some of the recent studies published (References 7.8 and 5.20) follow a deliberate format to facilitate extraction of data to upgrade existing rules

and regulations. These and other study results should prove valuable in revision and upgrading of rules and regulations.

GROUP	Modification of Weld Profile	Modification of Residual Stress Distribution
METHOD	<ul style="list-style-type: none"> a. Local and Contour Grinding b. Controlled Erosion c. Remelting Techniques <ul style="list-style-type: none"> - TIG Dressing - Plasma Dressing 	<ul style="list-style-type: none"> a. Stress Relief b. Compressive Overstressing <ul style="list-style-type: none"> - Local Compression - Spot Heating c. Peening <ul style="list-style-type: none"> - Shot Peening - Hammer Peening - Needle Peening

Figure 9-1 Typical Methods to Improve Fatigue Strength

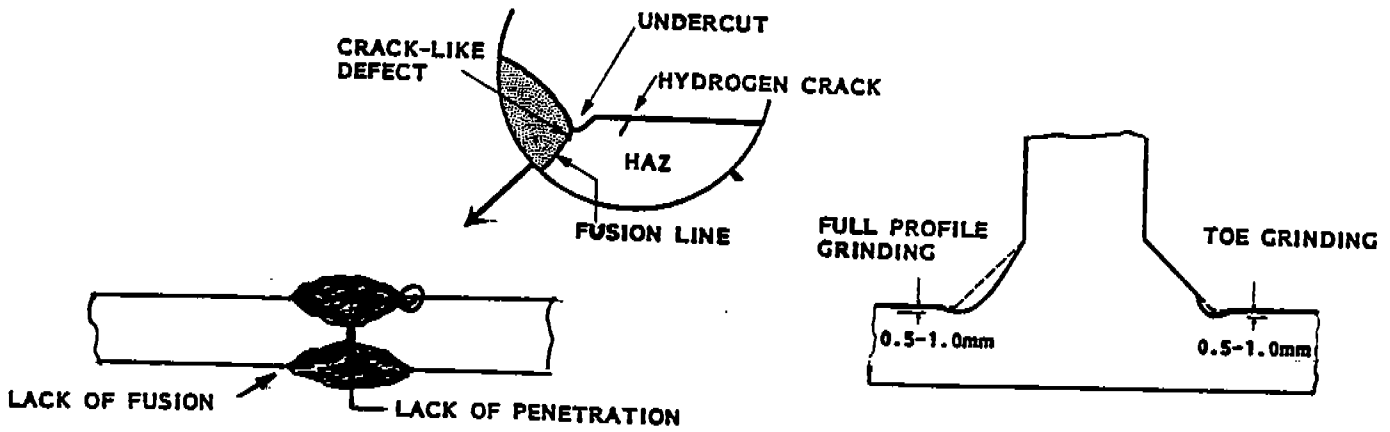


Figure 9-2 Typical Weld Toe Defects and Corrective Measures

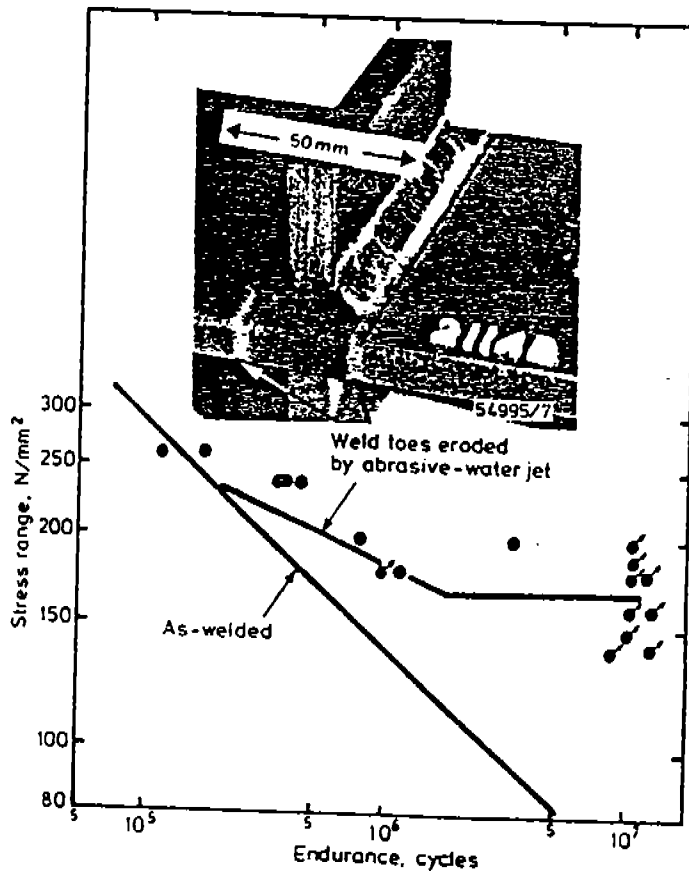


Figure 9-3 Fatigue Life Improvement Due to Weld Toe Abrasive Water Jet Erosion (From Reference 9.4)

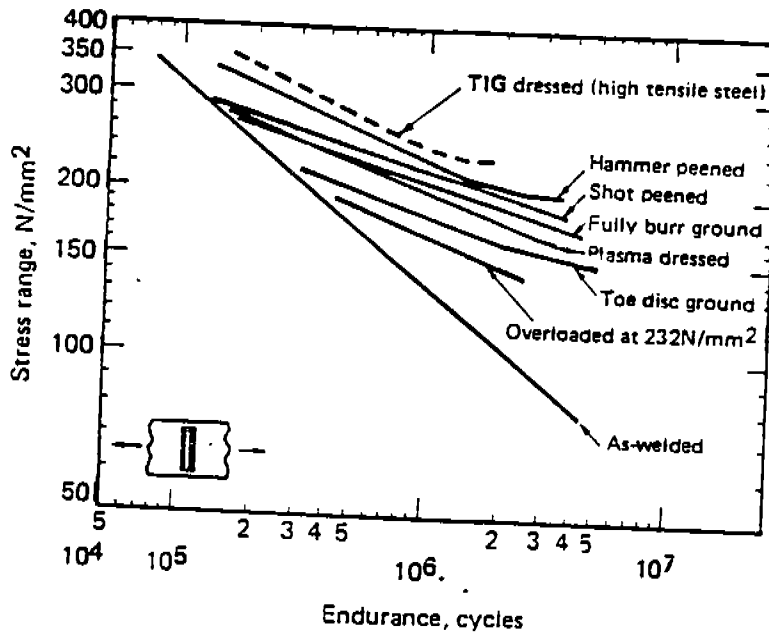
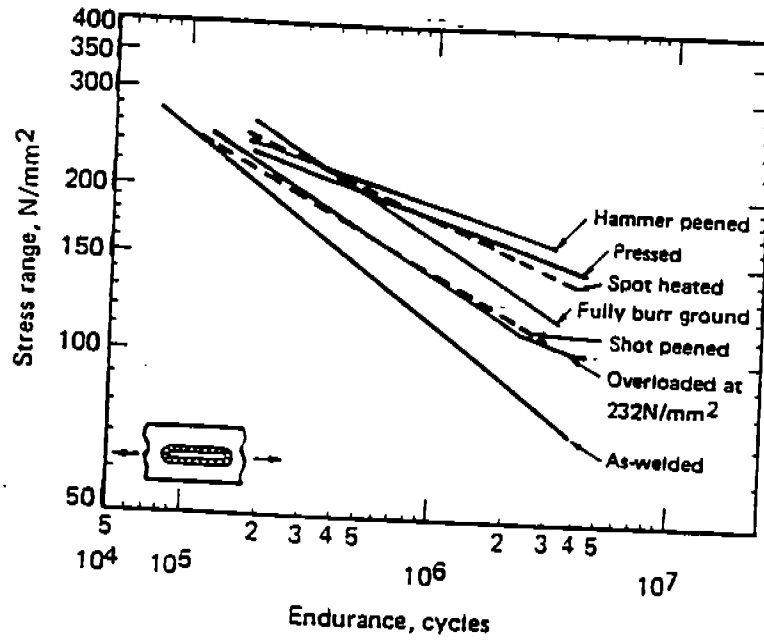


Figure 9-4 Comparison of Fatigue Strength Improvement Techniques (From Reference 9.7)

SOME OF THE RELEVANT FATIGUE RESEARCH PROJECTS

TOPIC	SUBJECT	INVESTIGATOR	COMPLETION & COMMENTS
STRESS CONCENTRATION	Calibration of various SCF equations with simple tubular joint test data	Lloyd's Registry	1988
STRESS CONCENTRATION	Development of SCF equations for internally stiffened complex tubular joints	Lloyd's Registry	1990
STRESS CONCENTRATION	Development of SCF equations for multiplanar joint CHS and RHS sections	Univ. of Delft	1992
FATIGUE STRENGTH	Assessment of S-N curve for internally-stiffened tubular joints	TWI/NEL & Lloyd's	1990
FATIGUE STRENGTH	Development of S-N curve for single-sided closure welds on tubulars	TWI/Glasgow University	1989
FATIGUE STRENGTH	Extend the range of hot spot stress approach to low cycle fatigue	University of Delft	1989
PARAMETERS AFFECTING FATIGUE LIFE	Study of the chord plate thickness and other geometric parameters	TWI	1992
PARAMETERS AFFECTING FATIGUE LIFE	Study of the plate thickness and weld profile effects on fatigue life	Florida Atlantic University	1990
PARAMETERS AFFECTING FATIGUE LIFE	Study of the weld profile effects and assessment of AWS/API requirements	TWI/EWI	1989
PARAMETERS AFFECTING FATIGUE LIFE	Study of cathodic protection effect on tubular joint fatigue	TWI/SSNTEF	1991

Figure 9-5 Summary of Relevant Research Activities
Page 1 of 2

223

TOPIC	SUBJECT	INVESTIGATOR	COMPLETION & COMMENTS
PARAMETERS AFFECTING FATIGUE LIFE	Study of the effect of seawater on thick welded long-life joints	TWI	1992
PARAMETERS AFFECTING FATIGUE LIFE	Application of fatigue life improvement techniques	TWI	?
FATIGUE ANALYSIS	Correlation of simple plate S-N curves for complex details and F.E. analyses procedures	EWI/TWI	Non-tubular details only; through 1992
FATIGUE ANALYSIS	Development of SCF, S-N curves and materials data for cast steel nodes	Wimpey	1988
FATIGUE ANALYSIS	Review of cumulative damage of welded joints	TWI	?
FATIGUE ANALYSIS	Fatigue of welded joints under random loading and implications on the accuracy of Miner's Rule	TWI	1990
FATIGUE ANALYSIS	Effect of loading sequence on fatigue life	Technical Univ. of Denmark	1991

Figure 9-5 Summary of Relevant Research Activities
Page 2 of 2

229

REFERENCES

- 1.1 Fatigue Handbook - Offshore Steel Structures, Edited by A. Almar-Naess, Tabin Publishers, Trondheim, Norway, 1985.
- 1.2 Fatigue Analyses of Tankers, Technical Report No. RD-89020F, Research and Development Department, American Bureau of Shipping, December 1989.
- 1.3 Munse, W.H., Wilbur, T.W., Tellaliar, M.L., Nicoll, K., and Wilson, K., Fatigue Characterization of Fabricated Ship Details for Design, Ship Structure Committee Report SSC-318, 1983.
- 1.4 Wirsching, P.H., "Probability Based Fatigue Design Criteria for Offshore Structures," Final Project Report on API PRAC 81-15, University of Arizona, Tucson, 1983.
- 1.5 Recommended Practice for Planning, Designing and Constructing Fixed Offshore Platform, API Recommended Practice 2A (RP 2A), Eighteenth Edition, American Petroleum Institute, Sept. 1989.
- 1.6 Offshore Installations: Guidance on Design, Construction and Certification, U.K. Department of Energy (UK DE) Guidance Notes, Fourth Edition, June 1990.
- 1.7 Fatigue Strength Analysis for Mobile Offshore Units, Classification Notes, Note No. 30.2, Det Norske Veritas, August 1984.
- 1.8 Design of Tubular Joints for Offshore Structures, Underwater Engineering Group, UEG Publication UR33, 1985.

- 3.1 Soyak, J.F., Caldwell, J.W., and Shoemaker, A.K., "Fatigue and Fracture Toughness Characterization of SAW and SMA A537 Class I Ship Steel Weldments," Ship Structure Committee Report SSC-303, 1981.
- 3.2 Pense, A.W., "Evaluation of Fracture Criteria for Ship Steels and Weldments," Ship Structure Committee Report SSC-307, 1981.
- 3.3 Williams, A.K., and Rinne, J.E., "Fatigue Analysis Procedure of Steel Offshore Structures", Proceedings of Institute of Civil Engineers, Part 1, November 1976.
- 3.4 Kuang, J.G., Potvin, A.B., Leick, R.D., and Kahrlich, J.L., "Stress Concentration in Tubular Joints," Journal of Society of Petroleum Engineers, August 1977.
- 3.5 Smedley, G.P., and Wordsworth, A.C., "Stress Concentration Factors of Unstiffened Tubular Joints," European Offshore Steels Research Seminar, The Welding Institute, Cambridge, England, 1978.
- 3.6 Worsworth, A.C., "Stress Concentration Factors at K and KT Tubular Joints," Fatigue in Offshore Structural Steel, ICE, London, 1981.
- 4.1 Rules for Building and Classing Steel Vessels, American Bureau of Shipping, 1988.
- 4.2 Thayamballi, A.K., "Fatigue Screening for Tankers," Report RD 90005, American Bureau of Shipping, Research and Development Division, May 1990.

- 4.3 Munse, W.H., Wilbur, T.W., Tellalian, M.L., Nicoll, K., and Wilson, K., Fatigue Characterization of Fabricated Ship Details for Design, Ship Structure Committee Report SSC-318, 1984.
- 4.4 Jordan, C.R., and Cochran, C.S., "In-Service Performance of Structural Details," Ship Structure Committee Report SSC-272, 1978.
- 4.5 Jordan, C.R., and Cochran, C.S., "Further Survey of In-Service Performance of Structural Details," Ship Structure Committee Report SSC-294, 1980.
- 4.6 Chen, Y-K., Chiou, J-W, and Thayamballi, A.K, "Validation of Fatigue Life Prediction Using Containership Hatch-Corner Strain Measurements," SNAME Transactions, Volume 94, 1986, pp. 255-282.
- 4.7 Luyties, W.H., and Geyer, J.F., "The Development of Allowable Fatigue Stresses in API RP 2A," Nineteenth Annual Offshore Technology Conference, OTC Paper No. 5555, Houston, TX, 1987.
- 4.8 Rules for Building and Classing Mobile Offshore Drilling Units, American Bureau of Shipping, 1980.
- 4.9 Wirsching, P.H., "Digital Simulation of Fatigue Damage in Offshore Structures," Computational Method for Offshore Structures, Editors: H. Armen and S.G. Stiansen, ASME, 1980.
- 4.10 Chen, Y.N., and Mavrakis, S.A., "Closed-Form Spectral Fatigue Analysis for Compliant Offshore Structures," Journal of Ship Research.
- 4.11 Wirsching, P.H., "Probability Based Fatigue Design Criteria for Offshore Structures," Final Project Report on API PRAC 81-15, University of Arizona, Tuscon, 1983.

- 4.12 Daidola, J.C., and Basar, N.S., "Probabilistic Structural Analysis of Ship Hull Longitudinal Stresses," Ship Structure Committee Report SSC-301, 1981.
- 4.13 Wells, A.A., "The Meaning of Fitness-for-Purpose and the Concept of Defect Tolerance," International Conference on Fitness for Purpose Validation of Welded Constructions, The Welding Institute, Volume 1, Paper No. 33, London, 1981.
- 4.14 Structural Welding Code, American Welding Society, AWS D1.1, 1988.
- 4.15 Specifications for the Design, Fabrication and Erection of Structural Steel for Buildings, American Institute of Steel Construction, 1989.
- 4.16 Rules for Steel Ships, Oil Production and Storage Vessels, Det norske Veritas, Part 5, Chapter 9, 1986.
- 4.17 Rules for Classification of Fixed Offshore Installations, Det norske Veritas, January 1989.
- 4.18 Rules and Regulations for the Classification of Fixed Offshore Installations, Lloyd's Register, Part 4, Steel Structures, July 1988.
- 4.19 Gurney, T.R., "The Influence of Thickness of the Fatigue Strength of Welded Joints," BOSS Conference, London, August 1979, Paper No. 41.
- 4.20 Lotsberg, I., and Anderssson, H., "Fatigue in Building Codes Background and Applications," Chapter 11, Fatigue Handbook - Offshore Steel Structures, Edited by A. Almar-Naess, Tapir, 1985.

- 4.21 Weidler, J.B., and Karsan, D.I., "Design, Inspection and Redundancy Investment Versus Risk for Pile-Founded Offshore Structures," Proceedings Of The International Symposium On The Role Of Design, Inspection and Redundancy in Marine Structural Reliability, Williamsburg, VA, November 1983.
- 4.22 Capanoglu, C. "Design of Floating Offshore Platforms," Proceedings Of The International Symposium On The Role Of Design, Inspection and Redundancy in Marine Structural Reliability, Paper No. 19, Williamsburg, VA, November 1983.
- 4.23 ISSC Design Philosophy Committee (1983), Design Philosophy of Marine Structures Report, International Shipbuilding Progress, Volume 30, No. 346, June 1984.
- 4.24 SEALOAD, A Program for Wave, Wind and Current Load Generation, Earl and Wright Developed SEADYN System Component, 1990.
- 4.25 SHIPMOTION, A Program for Ship Motion Analysis, An American Bureau of Shipping Developed ABS/DAISY System Component, 1989.
- 4.26 Mansour, A.E. and Thayamballi, A., "Computer-Aided Preliminary Ship Structural Design," Ship Structure Committee Report SSC-302, 1981.
- 5.1 Fukusawa, T., Fujino, M., Koyanagi, M. and Kawamura, T., "Effects of Axial Forces on Deck Stress in Case of Slamming of Large Bulk Carrier," JSNAJ, Vol. 155, 1984.
- 5.2 Liapis, S. and Beck, R.F., "Seakeeping Computations Using Time-Domain Analysis," 4th International Conference on Numerical Ship Hydrodynamics, Washington, 1985.
- 5.3 Papanikolaou, A., Zaraphonitis, G. and Perras, P., "On Computer-Aided Simulations of Large Amplitude Roll Motions of Ships in Waves and of Dynamic Stability," IMAEM '87, Varna, 1987.

- 5.4 Papanikolaou, A. and Zaraphonitis, G., "On An Improved Near Field Method For the Evaluation of Second-Order Forces Acting on 3D Bodies in Waves," IMAEM '87, Varna, 1987.
- 5.5 Hooft, J.P., "Hydrodynamic Aspects of Semisubmersibles," Doctoral Thesis From Delft Technical University, The Netherlands, 1972.
- 5.6 Capanoglu, C.C., "Design of a Compliant Tension Leg Platform - Naval Architectural and Structural Design Considerations," Marine Technology, Vol. 16 No. 4, October 1979, pp. 343-353.
- 5.7 Garrison, C.J., "Hydrodynamics of Large Displacement Fixed and Floating Structures in Waves," Report No. 80-102, December 1980, C.J. Garrison Associates.
- 5.8 Sircar, S., Rager, B.L., Praught, M.W. and Adams, C.J., "A Consistent Method for Motions, Strength and Fatigue Analysis of TLPs," Proceedings of Seventh International Offshore Mechanics and Arctic Engineering Conference, OMAE, Houston, February 1988.
- 5.9 Bishop, J.R., "Wave Force Investigations at the Second Christchurch Bay Tower," NMI Report R177, 1984.
- 5.10 Bishop, J.R., "Wave Force Data From the Second Christchurch Bay Tower," Proceedings of Offshore Technology Conference, OTC Paper No. 4953, Houston, 1985.
- 5.11 Tickell, R.S. and Bishop, J.R., "Analyses of Wave and Wave Forces at the Second Christchurch Bay Tower," Proceedings of Offshore Mechanics and Arctic Engineering, OMAE, Dallas, 1985.
- 5.12 Bea, R.G., Pawsey, S.F. and Litton, R.W., "Measured and Predicted Wave Forces on Offshore Platforms," Twentieth Offshore Technology Conference, OTC 5787, Houston, TX, 1988.

- 5.13 Rodenbush, G., "Random Directional Wave Forces on Template Offshore Platforms," Proceedings of the Eighteenth Offshore Technology Conference, OTC 5098, Houston, TX, 1986.
- 5.14 Rodenbush, G. and Forristall, G.Z., "An Empirical Model for Random Directional Wave Kinematics Near the Free Surface," Proceedings of the Eighteenth Offshore Technology Conference OTC 5097, Houston, TX, 1986.
- 5.15 API PRAC PROJECT 83-22 Report, "Implementation of a Reliability-Based API RP 2A Format," American Petroleum Institute January 1985.
- 5.16 Kint, T.E., and Morrison, D.G., "Dynamic Design and Analysis Methodology for Deepwater Bottom-Founded Structure," Proceedings of the Twenty-Second Offshore Technology Conference, OTC 6342, Houston, TX, 1990.
- 5.17 Digre, K.A. Brasted, L.K., and Marshall, P.W., "The Design of the Bullwinkle Platform." Proceedings of the Twenty-First Offshore Technology Conference, OTC 6050, Houston, TX, 1989.
- 5.18 Larrabee, R.D., "Dynamics Analysis," ASCE Continuing Education, Structural Reliability of Offshore Platforms, Houston, TX, 1989.
- 5.19 Efthymiou, M. et al, "Stress Concentrations in T/Y and Gap/Overlap K-Joint," The Forth International Conference on Behavior of Offshore Structures, Amsterdam, The Netherlands, 1985.
- 5.20 Ma, S.Y.A. and Tebbet, I.E., "New Data on the Ultimate Strength of Tubular Welded K-Joints Under Moment Loads," Twentieth Annual Offshore Technology Conference, OTC Paper No. 5831, Houston, TX, May 1988.

- 5.21 Gibstein, M.B., "Stress Concentration in Tubular K-Joints with Diameter Ratio Equal to One, "Paper TS 10, Proceedings of the Third International ECSC Offshore Conference on Steel in Marine Structures (SIMS 87), Delft, the Netherlands, 1987.
- 5.22 Tolloczko, J.A., and Lalani, M., "The Implications of New Data in the Fatigue Life Assessment of Tubular Joints," Twentieth Annual Offshore Technology Conference, OTC Paper No. 5662, Houston, TX, May 1988.
- 5.23 Lalani, M. et al, "Improved Fatigue Life Estimation of Tubular Joints, "Eighteenth Annual Offshore Technology Conference, OTC Paper No. 5306, Houston, TX, 1986.
- 5.24 Gibstein, M.B., "Parametric Stress Analysis of T-Joints," Paper No. 26, European Offshore Steels Research Seminar, Cambridge, November 1978.
- 5.25 Wordsworth, A.C., "Aspects of Stress Concentration Factors at Tubular Joints," Paper TS8, Third International ECSC Offshore Conference on Steel in Marine Structures (SIMS 87), Delft, The Netherlands, 1987.
- 6.1 Hoffman, D., and Walden, D.A., "Environmental Wave Data for Determining Hull Structural Loadings, A Report to Ship Structures Committee, SSC-268, 1977.
- 6.2 Bian Jiayi and Yuan Yeli, "Meteo-Oceanographic Study of JHN Blocks 16/06 in South China Sea", China Ocean Technology Company (COTC), Ltd., July 1988.
- 6.3 Meteo-Oceanographic Study of ACT Blocks 16/04-16/08 and Phillips Area 15/11 in South China Sea. A Report Prepared by Snamprogetti for ACT Operators Group, March 1988.

- 6.4 Study of Environmental Design Criteria For JHN's Offshore China Lufeng Project, A Report to Earl and Wright, Shezhen China Ocan Technology Company (COTC), January 1991.
- 6.5 N. Hogben and F.E. Lumb, "Ocean Wave Statistics," Ministry of Technology, National Physical Laboratory, London: Her Majesty's Stationary Office, 1967.
- 6.6 M.K. Ochi and Y.S. Chin, "Wind Turbulent Spectra for Design Consideration of Offshore Structures," Offshore Technology Conference 1988, OTC 5736.
- 6.7 Kinra, R., and Marshall, P., "Fatigue Analyses of Cognac Platform," Journal of Petroleum Energy, SPE 8600, March 1980.
- 6.8 Sarpkaya, T. and Isaacson, M., "Mechanics of Wave Forces on Offshore Structures," Van Nostrand Reinhold Co., 1981.
- 6.9 Wirsching, P.H., "Digital Simulation of Fatigue Damage in Offshore Structures," Computational Method for Offshore Structures, H. Armen and S.G. Stiansen, Editors, ASMB, 1980.
- 6.10 Chen, Y.N., and Maurakis, S.A., "Close Form Spectral Fatigue Analysis of Compliant Offshore Structures," Journal of Ship Research.
- 6.11 Dalzell, J.F., Maniar, N.M., and Hsu, M.W., "Examination of Service and Stress Data of Three Ships for Development of Hull Girder Load Criteria," Ship Structure Committee Report SSC-287, 1979.
- 7.1 Gurney, T.R., "The Influence of Thickness of the Fatigue Strength of Welded Joints," Proceedings of 2nd International Conference on Behavior of Offshore Structures (BOSS '79), London, 1979.

- 7.2 Jordan, C.R., and Cochran, C.S., "In-Service Performance of Ship Structure Details," Ship Structure Committee Report, SSC-272, 1978.
- 7.3 Marshall, P.W., "Size Effect in Tubular Welded Joints," ASCE Annual Structures Congress, Houston, TX, October 17, 1983.
- 7.4 Maddox, S.J., "Assessing the Significance of Welds Subject to Fatigue," Welding Journal, 1070, 53 (9) 401.
- 7.5 Hartt, W.H., Rengan, K. and Sablok, A.K., "Fatigue Properties of Exemplary High-Strength Steels in Seawater," Twentieth Annual Offshore Technology Conference, OTC 5663, Houston, TX, May 1988.
- 7.6 Gurney, T.R., "Fatigue of Welded Structures," Cambridge University Press, 2nd. Edition, 1978.
- 7.7 Grover, J.L., "Initial Flaw Size Estimating Procedures for Fatigue Crack Growth Calculations," International Conference on Fatigue of Welded Constructions, Paper No. 15, Brighton, England, April 1987.
- 7.8 Tolloczko, J.A. and Lalani, M., "The Implication of New Data on the Fatigue Life Assessment of Tubular Joints," Twentieth Annual Offshore Technology Conference, OTC 5662, Houston, TX, May 1988.
- 7.9 Maddox, S.J., "The Effect of Plate Thickness on the Fatigue Strength of Fillet Welded Joints," Welding Institute Report 1987, 7814.01.
- 7.10 Maddox, S.J., "A Study of the Fatigue Behavior of Butt Welds Made on Backing Bars," Proceedings 5th European Conference on Fracture Life Assessment of Dynamically Loaded Materials and Structures," Lisbon, 1984, 197-215.

- 7.11 Maddox, S.J., "Fitness for Purpose Assessment of Misalignment in Transverse Butt Welds Subject to Fatigue Loading," Welding Institute Members Report 279/1985.
- 7.12 Marshall, P.W., "State of the Art in the U.S.A.," Paper PSI of Proceedings of the Third International ECSC Offshore Conference on Steel in Marine Structures (SIMS 87), Delft, The Netherlands, 1987.
- 7.13 Dijkstra, O.D. et al, "The Effect of Grinding and a Special Weld Profile on the Fatigue Behavior of Large Scale Tubular Joints," Seventeenth Annual Offshore Technology Conference, OTC 4866, Houston, TX, May 1985.
- 7.14 Bignonnet, A., "Improving the Fatigue Strength of Welded Structures," Paper PS4 of the Proceedings of the Third International ECSC Offshore Conference on Steel in Marine Structures (SIMS 87), Delft, netherlands, 1987.
- 7.15 Wylde, J.G., Booth, G.S., and Iwasaki, T., "Fatigue Tests on Welded Tubular Joints in Air and in Sea Water," Proceedings of International Conference on Fatigue and Crack Growth in Offshore Structures, I Mech E, 1986.
- 7.16 Gurney, T.R., "Further Fatigue Tests on Fillet Welded Joints Under Simple Variable Amplitude Loading," Appendix A, Welding Institute Members Report 182/1982.
- 7.17 Gurney, T.R., "Fatigue Tests on Fillet Welded Joints Under Variable Amplitude Loading," Welding Institute Members Report 293/1985.
- 7.18 Gurney, T.R., "Some Variable Amplitude Fatigue Tests on Fillet Welded Joints," Paper No. 65, International Conference on Fatigue of Welded Constructions, Brighton, England, 7-9 April 1987.

- 7.19 Niemi, E.J., "Fatigue Tests on Butt and Fillet Welded Joints Under Variable Amplitude Loading," Paper No. 8, International Conference on Fatigue of Welded Constructions, Brighton, England, 7-9 April 1987.
- 7.20 Gerald, J. et al, "Comparison of European Data on Fatigue Under Variable Amplitude Loading," Paper TS48 of the Third International ECSC Offshore Conference on Steel Marine Structures (SIMS 87), Delft, Netherlands, 1987.
- 7.21 Trufiakov, V.I., and Kovalchuk, V.S., "The Estimation of the Fatigue Crack Propagation Rate Under Bicyclic Loading," IIW Document X111-1139-84, 1984.
- 7.22 Gurney, T.R., "The Influence of Spectrum Shape on Cumulative Damage of Plates with Fillet Welded Edge Attachments," Welding Institute Reports 7816.03/86/495.2, 1987 and 7920.01/87/555.1
- 7.23 Wirsching, P.H., "Digital Simulation of Fatigue Damage in Offshore Structures," Computational Method for Offshore Structures, H. Armen and S.G. Stiansen, Editors, ASME, 1980.
- 7.24 Chen, Y.N. and Mavrakis, S.A., "Close Form Spectral Fatigue Analysis for Compliant Offshore Structures," Journal of Ship Research.
- 7.25 Morgan, H.G., "Interaction of Multiple Fatigue Cracks", International Conference on Fatigue of Welded Constructions, Paper No. 35, Brighton, England, April 1987.
- 7.26 Dobson, W.G., Broderick, R.F., Wheaton, J.W., Giannotti, J. and Stambaugh, K.A., "Fatigue Considerations in View of Measured Spectra," Ship Structures Committee Report SSC-315, 1983.

- 8.1 Bell, E.R.G. and Morgan, D.G., "Repair and Analysis of Cracking in the Murchison Flare Boom," Twentieth Annual Offshore Technology Conference, OTC 5814, Houston, TX, May 1988.
- 8.2 Strouhal, V., Uber Eine Besondere Art der Tonerregung, Ann. Physik, Leipzig, 1878.
- 8.3 Marris, A.W., "A Review of Vortex Streets, Periodic Waves and Induced Vibration Phenomena," Journal of Basic Eng., V. 86, 1964, pp 185-194.
- 8.4 Sarpkaya, T., and Isaacson, M., Mechanics of Wave Forces on Offshore Structures, Van Nostrand Reinhold, New York, 1981.
- 8.5 Hunt, R.J., "Practice For Establishing If A Structure Will Undergo Vortex-Induced Vibrations," CONFIDENTIAL SIPM Report, EPD/112, June 1987.
- 8.6 Engineering Sciences Data Unit, "Across Flow Response Due to Vortex Shedding", Publication No. 78006, London, England, October, 1978.
- 8.7 Det Norske Veritas, "Rules for Submarine Pipeline Systems", Oslo, Norway, 1981.
- 8.8 Zedan, M.F., Yeung, J.Y., Ratios, H.J., and Fischer, F.J., "Dynamic Response of a Cantilever Pile to Vortex Shedding in Regular Waves," Proceedings of Offshore Technology Conference, OTC Paper No. 3799, Houston, May 1980.
- 8.9 Hallam, H.G., Heaf, N.J., and Wootton, F.R., "Dynamics of Marine Structures," CIRIA Underwater Engineering Group Report UR8 (2nd Edition), 1977.

- 9.1 Skaar, K.T., "Contributing Factors to Ship Quality", Report of Committee V.3-Service experience - Ships, Proceedings of the Tenth International Ship and Offshore Structures Congress, Volume 2, Lyngby, Denmark, August 1988.
- 9.2 Jordan, G.P. and Cochran, C.S., "In-Service Performance of Structural Details," Ship Structure Committee Report SSC-272, 1978.
- 9.3 Notes on Structural Failure in Ships, Report NO. 19, Lloyd's Register of Shipping, 1962.
- 9.4 Maddox, S.J., and Padilla, J.A., "Fatigue Life Improvement by Water Jet Erosion", Welding Institute Members Report 280/1985.
- 9.5 King, C.G, "Abrasive Water Jetting: A New Aid to Welded Fabrications," OTC Paper No. 5817, 20th Annual Offshore Technology Conference, Houston TX, May 1988.
- 9.6 Wylde, J.G., Booth, G.S., and Iwasaki, T., "Fatigue Tests on Welded Tubular Joints in Air and Sea Water", Proceedings of International Conference on Fatigue and Crack Growth in Offshore Structures, I Mech E, 1986, pp. 155-170.
- 9.7 Booth, G.S., "Chapter 2 - A Review of Fatigue Strength Improvement Techniques", Improving the Fatigue Strength of Welded Joints, The Welding Institute, 1983.
- 9.8 Maddox, S.J., "Improving the Fatigue Strength of Welded Joints by Peening", Metal Construction, 1985, 17(4) pp 220-224.
- 9.9 Woodley, C.C., "Chapter 4 Practical Applications of Weld Toe Grinding", Improving the Fatigue Strength of Welded Joints, The Welding Institute, 1983.
- 9.10 Boylston, J.W., and Stambaugh, K.A., "Development of a Plan to Obtain In-Service Still Water Bending Moment Information for

Statistical Characterization," Ship Structure Committee Report SSC-319, 1984.

- 9.11 Krenk, S. and Gluver, H., "A Markow Matrix for Fatigue Load Simulation and Rainflow Range Evaluation," Symposium on Stochastic Structural Dynamics, Urbana, Illinois, 1988.
- 9.12 Krenk, S. and Thorup, E., "Stochastic and Constant Amplitude Fatigue Test of Plate Specimens with a Central Hole," Report No. R 242, Department of Structural Engineering, Technical University of Denmark, 1989.
- 9.13 Agerskov, H. and Aarkrog, P., "Fatigue Investigation on Offshore Steel Structures Under Spectrum Loading," International Syposium on Offshore Brazil '89, Rio de Janeiro, Brazil, August 1989.
- 9.14 Morgan, G.G., "Interaction of Multiple Fatigue Cracks," International Conference on Fatigue of Welded Constructions, Brighton, England, 7-9 April 1987.

Imp.

239

COMMITTEE ON MARINE STRUCTURES

Commission on Engineering and Technical Systems

National Academy of Sciences – National Research Council

The COMMITTEE ON MARINE STRUCTURES has technical cognizance over the interagency Structure Committee's research program.

Peter M. Palermo Chairman, Alexandria, VA

Mark Y. Berman, Amoco Production Company, Tulsa, OK

Subrata K. Chakrabarti, Chicago Bridge and Iron, Plainfield, IL

Rolf D. Glasfeld, General Dynamics Corporation, Groton, CT

William H. Hartt, Florida Atlantic University, Boca Raton, FL

Alexander B. Stavovy, National Research Council, Washington, DC

Stephen E. Sharpe, Ship Structure Committee, Washington, DC

LOADS WORK GROUP

Subrata K. Chakrabarti Chairman, Chicago Bridge and Iron Company, Plainfield, IL

Howard M. Bunch, University of Michigan, Ann Arbor, MI

Peter A. Gale, John J. McMullen Associates, Arlington, VA

Hsien Yun Jan, Martech Incorporated, Neshanic Station, NJ

Naresh Maniar, M. Rosenblatt & Son, Incorporated, New York, NY

Solomon C. S. Yim, Oregon State University, Corvallis, OR

MATERIALS WORK GROUP

William H. Hartt Chairman, Florida Atlantic University, Boca Raton, FL

Santiago Ibarra, Jr., Amoco Corporation, Naperville, IL

John Landes, University of Tennessee, Knoxville, TN

Barbara A. Shaw, Pennsylvania State University, University Park, PA

James M. Sawhill, Jr., Newport News Shipbuilding, Newport News, VA

Bruce R. Somers, Lehigh University, Bethlehem, PA

Jerry G. Williams, Conoco, Inc., Ponca City, OK

C-3 80107-659

SHIP STRUCTURE COMMITTEE PUBLICATIONS

- SSC-351 An Introduction to Structural Reliability Theory by Alaa E. Mansour
1990
- SSC-352 Marine Structural Steel Toughness Data Bank by J. G. Kaufman and
M. Prager 1990
- SSC-353 Analysis of Wave Characteristics in Extreme Seas by William H. Buckley
1989
- SSC-354 Structural Redundancy for Discrete and Continuous Systems by P. K.
Das and J. F. Garside 1990
- SSC-355 Relation of Inspection Findings to Fatigue Reliability by M. Shinozuka
1989
- SSC-356 Fatigue Performance Under Multiaxial Load by Karl A. Stambaugh,
Paul R. Van Mater, Jr., and William H. Munse 1990
- SSC-357 Carbon Equivalence and Weldability of Microalloyed Steels by C. D.
Lundin, T. P. S. Gill, C. Y. P. Qiao, Y. Wang, and K. K. Kang 1990
- SSC-358 Structural Behavior After Fatigue by Brian N. Leis 1987
- SSC-359 Hydrodynamic Hull Damping (Phase I) by V. Ankudinov 1987
- SSC-360 Use of Fiber Reinforced Plastic in Marine Structures by Eric Greene
1990
- SSC-361 Hull Strapping of Ships by Nedret S. Basar and Roderick B. Hulla 1990
- SSC-362 Shipboard Wave Height Sensor by R. Atwater 1990
- SSC-363 Uncertainties in Stress Analysis on Marine Structures by E. Nikolaidis
and P. Kaplan 1991
- SSC-364 Inelastic Deformation of Plate Panels by Eric Jennings, Kim Grubbs,
Charles Zanis, and Louis Raymond 1991
- SSC-365 Marine Structural Integrity Programs (MSIP) by Robert G. Bea 1992
- SSC-366 Threshold Corrosion Fatigue of Welded Shipbuilding Steels by G. H.
Reynolds and J. A. Todd 1992
- None Ship Structure Committee Publications – A Special Bibliography

C-4 80107-659

U.S. Department
of Transportation

United States
Coast Guard



SSC-367

**FATIGUE TECHNOLOGY
ASSESSMENT AND STRATEGIES
FOR FATIGUE AVOIDANCE IN
MARINE STRUCTURES**

APPENDICES



This document has been approved
for public release and sale; its
distribution is unlimited

SHIP STRUCTURE COMMITTEE

1993

C-1

80117
659

SHIP STRUCTURE COMMITTEE

The SHIP STRUCTURE COMMITTEE is constituted to prosecute a research program to improve the hull structures of ships and other marine structures by an extension of knowledge pertaining to design, materials, and methods of construction.

	RADM A. E. Henn, USCG (Chairman) Chief, Office of Marine Safety, Security and Environmental Protection U. S. Coast Guard	
Mr. Thomas H. Peirce Marine Research and Development Coordinator Transportation Development Center Transport Canada	Mr. H. T. Haller Associate Administrator for Ship- building and Ship Operations Maritime Administration	Dr. Donald Liu Senior Vice President American Bureau of Shipping
Mr. Alexander Malakhoff Director, Structural Integrity Subgroup (SEA O5P) Naval Sea Systems Command	Mr. Thomas W. Allen Engineering Officer (N7) Military Sealift Command	CDR Stephen E. Sharpe, USCG Executive Director Ship Structure Committee U. S. Coast Guard

CONTRACTING OFFICER TECHNICAL REPRESENTATIVE

Mr. William J. Siekierka
SEA O5P4
Naval Sea Systems Command

SHIP STRUCTURE SUBCOMMITTEE

The SHIP STRUCTURE SUBCOMMITTEE acts for the Ship Structure Committee on technical matters by providing technical coordination for determining the goals and objectives of the program and by evaluating and interpreting the results in terms of structural design, construction, and operation.

AMERICAN BUREAU OF SHIPPING

Mr. Stephen G. Arntson (Chairman)
Mr. John F. Conlon
Dr. John S. Spencer
Mr. Glenn M. Ashe

NAVAL SEA SYSTEMS COMMAND

Dr. Robert A. Sielski
Mr. Charles L. Null
Mr. W. Thomas Packard
Mr. Allen H. Engle

TRANSPORT CANADA

Mr. John Grinstead
Mr. Ian Bayly
Mr. David L. Stocks
Mr. Peter Timonin

MILITARY SEALIFT COMMAND

Mr. Robert E. Van Jones
Mr. Rickard A. Anderson
Mr. Michael W. Touma
Mr. Jeffrey E. Beach

MARITIME ADMINISTRATION

Mr. Frederick Seibold
Mr. Norman O. Hammer
Mr. Chao H. Lin
Dr. Walter M. Maclean

U. S. COAST GUARD

CAPT T. E. Thompson
CAPT W. E. Colburn, Jr.
Mr. Rubin Scheinberg
Mr. H. Paul Cojeen

SHIP STRUCTURE SUBCOMMITTEE LIAISON MEMBERS

U. S. COAST GUARD ACADEMY

LCDR Bruce R. Mustain

U. S. MERCHANT MARINE ACADEMY

Dr. C. B. Kim

U. S. NAVAL ACADEMY

Dr. Ramswar Bhattacharyya

STATE UNIVERSITY OF NEW YORK MARITIME COLLEGE

Dr. W. R. Porter

SOCIETY OF NAVAL ARCHITECTS AND MARINE ENGINEERS

Dr. William Sandberg

OFFICE OF NAVAL RESEARCH

Dr. Yapa D. S. Rajapaske

NATIONAL ACADEMY OF SCIENCES - MARINE BOARD

Mr. Alexander B. Stavovy

NATIONAL ACADEMY OF SCIENCES - COMMITTEE ON MARINE STRUCTURES

Mr. Peter M. Palermo

WELDING RESEARCH COUNCIL

Dr. Martin Prager

AMERICAN IRON AND STEEL INSTITUTE

Mr. Alexander D. Wilson

DEPARTMENT OF NATIONAL DEFENCE - CANADA

Dr. Neil G. Pegg

C-2 80117/659

Member Agencies:

*United States Coast Guard
Naval Sea Systems Command
Maritime Administration
American Bureau of Shipping
Military Sealift Command
Transport Canada*



Address Correspondence to:

Executive Director
Ship Structure Committee
U. S. Coast Guard (G-M/R)
2100 Second Street, S.W.
Washington, D.C. 20593-0001
PH: (202) 267-0003
FAX: (202) 267-4677

An Interagency Advisory Committee

May 17, 1993

SSC-367
SR-1324

**FATIGUE TECHNOLOGY ASSESSMENT AND STRATEGIES FOR FATIGUE
AVOIDANCE IN MARINE STRUCTURES**

This report synthesizes the state-of-the-art in fatigue technology as it relates to the marine field. Over the years more sophisticated methods have been developed to anticipate the life cycle loads on structures and more accurately predict the failure modes. As new design methods have been developed and more intricate and less robust structures have been built it has become more critical than ever that the design tools used be the most effective for the task. This report categorizes fatigue failure parameters, identifies strengths and weaknesses of the available design methods, and recommends fatigue avoidance strategies based upon variables that contribute to the uncertainties of fatigue life.

This set of Appendices includes more in-depth presentations of the methods used in modeling the loads from wind and waves, linear system response to random excitation, stress concentration factors, vortex shedding and fatigue damage calculation.

A. E. HENN
Rear Admiral, U.S. Coast Guard
Chairman, Ship Structure Committee

8017
659

1. Report No.		2. Government Accession No.		3. Recipient's Catalog No.	
4. Title and Subtitle FATIGUE DESIGN PROCEDURES				5. Report Date June 1992	
				6. Performing Organization Code	
				8. Performing Organization Report No. SR-1324	
7. Author(s) Cuneyt C. Capanoglu				10. Work Unit No. (TRAIS)	
9. Performing Organization Name and Address EARL AND WRIGHT 180 Howard Street San Francisco, CA 94105				11. Contract or Grant No. DTCG23-88-C-20029	
				13. Type of Report and Period Covered Final Report	
12. Sponsoring Agency Name and Address Ship Structure Committee U.S. Coast Guard (G-M) 2100 Second Street, SW Washington, DC 20593				14. Sponsoring Agency Code G-M	
				15. Supplementary Notes Sponsored by the Ship Structure Committee and its members agencies.	
16. Abstract <p style="text-align: center;"><u>ABSTRACT</u></p> <p>This report provides an up-to-date assessment of fatigue technology, directed specifically toward the marine industry. A comprehensive overview of fatigue analysis and design, a global review of fatigue including rules and regulations and current practices, and a fatigue analysis and design criteria, are provided as a general guideline to fatigue assessment. A detailed discussion of all fatigue parameters is grouped under three analysis blocks:</p> <ul style="list-style-type: none">● Fatigue stress model, covering environmental forces, structure response and loading, stress response amplitude operations (RAOs) and hot-spot stresses● Fatigue stress history model covering long-term distribution of environmental loading● Fatigue resistance of structures and damage assessment methodologies <p>The analyses and design parameters that affect fatigue assessment are discussed together with uncertainties and research gaps, to provide a basis for developing strategies for fatigue avoidance. Additional in-depth discussions of wave environment, stress concentration factors, etc. are presented in the appendixes.</p>					
17. Key Words Assessment of fatigue technology, fatigue stress models, fatigue stress history models, fatigue resistance, fatigue parameters and fatigue avoidance strategies			18. Distribution Statement Available from: National Technical Information Serv. U. S. Department of Commerce Springfield, VA 22151		
19. Security Classif. (of this report) Unclassified		20. Security Classif. (of this page) Unclassified		21. No. of Pages 194 Excl. Appendixes	22. Price

METRIC CONVERSION FACTORS

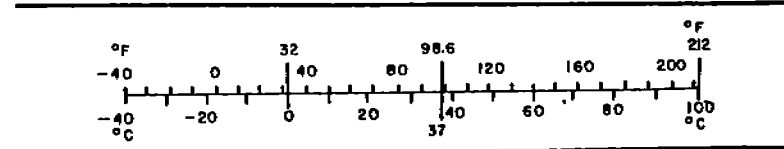
Approximate Conversions to Metric Measures

Symbol	When You Know	Multiply by	To Find	Symbol
LENGTH				
in	inches	2.5	centimeters	cm
ft	feet	30	centimeters	cm
yd	yards	0.9	meters	m
mi	miles	1.6	kilometers	km
AREA				
in ²	square inches	6.5	square centimeters	cm ²
ft ²	square feet	0.09	square meters	m ²
yd ²	square yards	0.8	square meters	m ²
mi ²	square miles	2.6	square kilometers	km ²
	acres	0.4	hectares	ha
MASS (weight)				
oz	ounces	28	grams	g
lb	pounds	0.45	kilograms	kg
	short tons (2000 lb)	0.9	tonnes	t
VOLUME				
tsp	teaspoons	5	milliliters	ml
Tbsp	tablespoons	15	milliliters	ml
fl oz	fluid ounces	30	milliliters	ml
c	cups	0.24	liters	l
pt	pints	0.47	liters	l
qt	quarts	0.95	liters	l
gal	gallons	3.8	liters	l
ft ³	cubic feet	0.03	cubic meters	m ³
yd ³	cubic yards	0.76	cubic meters	m ³
TEMPERATURE (exact)				
°F	Fahrenheit temperature	5/9 (after subtracting 32)	Celsius temperature	°C



Approximate Conversions from Metric Measures

Symbol	When You Know	Multiply by	To Find	Symbol
LENGTH				
mm	millimeters	0.04	inches	in
cm	centimeters	0.4	inches	in
m	meters	3.3	feet	ft
m	meters	1.1	yards	yd
km	kilometers	0.6	miles	mi
AREA				
cm ²	square centimeters	0.16	square inches	in ²
m ²	square meters	1.2	square yards	yd ²
km ²	square kilometers	0.4	square miles	mi ²
ha	hectares (10,000 m ²)	2.5	acres	
MASS (weight)				
g	grams	0.035	ounces	oz
kg	kilograms	2.2	pounds	lb
t	tonnes (1000 kg)	1.1	short tons	
VOLUME				
ml	milliliters	0.03	fluid ounces	fl oz
l	liters	2.1	pints	pt
l	liters	1.06	quarts	qt
l	liters	0.26	gallons	gal
m ³	cubic meters	35	cubic feet	ft ³
m ³	cubic meters	1.3	cubic yards	yd ³
TEMPERATURE (exact)				
°C	Celsius temperature	9/5 (then add 32)	Fahrenheit temperature	°F



*1 in = 2.54 (exactly). For other exact conversions and more detailed tables, see NBS Misc. Publ. 286, Units of Weights and Measures, Price \$2.25, SD Catalog No. C13.10:286.

**FATIGUE TECHNOLOGY
ASSESSMENT AND STRATEGIES
FOR FATIGUE AVOIDANCE IN
MARINE STRUCTURES**

APPENDICES

CONTENTS

APPENDIX A Review of the Ocean Environment

APPENDIX B Review of Linear System Response to Random Excitation

APPENDIX C Stress Concentration Factors

APPENDIX D Vortex Shedding Avoidance and Fatigue Damage Computation

APPENDIX A

REVIEW OF OCEAN ENVIRONMENT

CONTENTS

- A. REVIEW OF OCEAN ENVIRONMENT
 - A.1 IRREGULAR WAVES
 - A.2 PROBABILITY CHARACTERISTICS OF WAVE SPECTRA
 - A.2.1 Characteristic Frequencies and Periods
 - A.2.2 Characteristic Wave Heights
 - A.3 WAVE SPECTRA FORMULAS
 - A.3.1 Bretschneider and ISSC Spectrum
 - A.3.2 Pierson-Moskowitz Spectrum
 - A.3.3 JONSWAP and Related Spectra
 - A.3.4 Scott and Scott-Wiegel Spectra
 - A.4 SELECTING A WAVE SPECTRUM
 - A.4.1 Wave Hindcasting
 - A.4.2 Direct Wave Measurements
 - A.5 WAVE SCATTER DIAGRAM
 - A.6 WAVE EXCEEDANCE CURVE
 - A.7 WAVE HISTOGRAM AND THE RAYLEIGH DISTRIBUTION
 - A.8 EXTREME VALUES AND THE WEIBULL DISTRIBUTION
 - A.9 WIND ENVIRONMENT
 - A.9.1 Air Turbulence, Surface Roughness and Wind Profile
 - A.9.2 Applied, Mean and Cyclic Velocities
 - A.9.3 Gust Spectra
 - A.10 REFERENCES

A. REVIEW OF OCEAN ENVIRONMENT

The ocean environment is characterized by waves, wind and current. The waves are typically irregular (confused or random seas). Some waves are generated locally by the wind, and some waves are generated great distances away. The wind is unsteady, with gusts. The wind varies with height above water. The current is caused by the wind, by waves, by the tide, and by global temperature differences. The current varies with depth. All of these characteristics vary with time.

A.1 IRREGULAR WAVES

Irregular waves (a random sea) can be described as the sum of an infinite number of individual regular (sinusoidal) waves of different amplitude, frequency, and phase (Figure A-1). Therefore, the randomly varying sea surface elevation can be represented by a Fourier series.

$$\eta(t) = \sum_{i=1}^N a_i^* \cos(\omega_i^* t + \phi_i)$$

where $\eta(t)$ is the water surface elevation measured from still water level,

a_i is the amplitude of each component regular wave,

ω_i is the frequency of each component regular wave,

ϕ_i is the phase angle of each component regular wave, and

t is time.

The most distinctive feature of a random sea is that it never repeats its pattern and it is impossible to predict its shape. - Therefore, total energy is used to define a particular sea. The energy (E) in an individual regular wave per unit surface area is,

$$E = \frac{1}{2} \rho g a^2$$

and the total energy of the sea is the sum of the energies of the constituent regular waves.

$$E = \frac{1}{2} \rho g \sum_{i=1}^N a_i^2$$

The total energy of the sea is distributed according to the frequencies of the various wave components. The amount of energy per unit surface area within the small frequency band $(\omega_i, \omega_i + d\omega)$ is,

$$E(\omega_i) = \frac{1}{2} \rho g a_i^2 d\omega$$

The total energy of the sea is then the sum of the energies within the individual wave components. If the sea is made up of an infinite number of waves, the energies of the waves form a smooth curve, and the above summation may be replaced by an integral.

$$E = \rho g \int_0^{\infty} \frac{1}{2} a^2 d\omega$$

The smooth distribution of the wave energy is called the energy spectrum or wave spectrum of the random sea, and is often designated as $S(\omega)$. A wave spectrum is normally depicted as a curve with an ordinate of energy and an abscissa of frequency. A typical wave spectrum has a central peak with a tapered energy distribution either side of the peak.

The recommended form of displaying a wave spectrum is with an ordinate of $\frac{1}{2}a^2$ and an abscissa of ω , radial frequency. However, since the engineer will encounter wave spectra equations in a number of forms, using various bases and units, the applicable conversion factors are provided in the following sections.

Spectrum Basis

The recommended spectrum basis is half amplitude squared or energy. Often spectrum equations having a different basis are encountered. Before any statistical calculations are performed with a spectrum equation, the equation should be converted to the recommended basis.

For a "half amplitude" or "energy" spectrum, the basis is one-half times the amplitude squared.

$$S(\omega) = \frac{1}{2}n^2$$

$$S(\omega)d\omega = E / (pg)$$

where,

S is the spectral ordinate,

ω is the radial frequency,

n is the wave amplitude of the constituent wave of frequency,

E is the energy content of the constituent wave of frequency, ω .

For an "amplitude" spectrum, the basis is amplitude squared.

$$S(\omega) = n^2$$

$$S(\omega) = 2 * (\frac{1}{2} * \eta^2)$$

For a "height" spectrum, the basis is height squared.

$$S(\omega) = h^2$$

$$S(\omega) = 8 * (\frac{1}{2} * \eta^2)$$

where,

h is the height of the constituent wave of frequency, ω .

For a "height double" spectrum, the basis is two times the height squared.

$$S(\omega) = s * h^2$$

$$S(\omega) = 16 * (\frac{1}{2} * \eta^2)$$

The basis of the spectrum must be determined before the spectrum is used in an analysis, because the ordinate of one representation of the spectrum may be as much as 16 times as great as the ordinate of another representation.

Units

The spectrum equation may be expressed in terms of radial frequency, circular frequency, or period. Conversion between circular frequency and radial frequency is accomplished by multiplying by the constant, 2π .

$$\omega = 2\pi * f$$

$$S(\omega) = S(f) / (2\pi)$$

where,

f is the circular frequency.

The conversion between period and radial frequency is more complicated.

$$\omega = 2\pi/T$$

$$S(f) = T^2 * S(T)$$

$$S(\omega) = T^2 * S(T) / (2\pi)$$

where,

T is the period.

When converting between period and frequency, the abscissa axis is reversed. Zero period becomes infinite frequency, and infinite period becomes zero frequency.

Wave spectrum equations may be used with any length units by remembering that the spectrum ordinate is proportional to amplitude squared or height squared.

$$S(\omega)_{\text{meter}} = (0.3048)^2 * S(\omega)_{\text{feet}}$$

The mathematical formulation for the wave spectrum equation will often include the significant height squared or the gravitational constant squared, which when entered in the appropriate units will convert the equation to the desired length units.

A.2 PROBABILITY CHARACTERISTICS OF WAVE SPECTRA

The characteristics of ocean waves are determined by assuming that the randomness of the surface of the sea can be described by two

common probability distributions, the Gaussian (or normal) distribution and the Rayleigh distribution. These probability distributions are used to define the distribution of wave elevations, η , and of wave heights, H , respectively.

A.2.1 Characteristic Frequencies and Periods

For design purposes sea spectra equations are selected to represent middle aged seas that would exist some time after a storm, yet which are still young enough to have a good dispersion of wave frequencies. The primary assumption about the design seas is that the wave elevations follow a Gaussian or normal distribution. Samples of wave records tend to support this assumption. In conjunction with the Gaussian distribution assumption, the wave elevations are assumed to have a zero mean. Digitized wave records tend to have a slight drift of the mean away from zero, usually attributed to tide or instrument drift. The Gaussian distribution assumption is equivalent to assuming that the phase angles of the constituent waves within a wave spectrum, are uniformly distributed.

The Gaussian distribution allows one to calculate statistical parameters which are used to describe the random sea. The mean elevation of the water surface is the first moment of the Gaussian probability density function. The mean-square is the second moment taken about zero, and the root-mean-square is the positive square root of the mean-square. The variance is the second moment taken about the mean value. The standard deviation is the positive square root of the variance. Since the wave elevations are assumed to have a zero mean value, the variance is equal to the mean-square, and the standard deviation is equal to the root-mean-square. In present practice, the area under a random wave energy spectrum is equated to the variance.

In a similar way, the characteristic frequencies and periods of a wave spectrum are defined in terms of the shape, the area, and/or the area moments of the $\frac{1}{2} * a^2$ wave spectrum. Depending upon the

particular wave spectrum formula, these characteristic periods may or may not reflect any real period. The area and area moments are calculated as follows.

Area:

$$m_0 = \int_0^{\infty} \omega^0 S(\omega) d\omega$$

Nth Area Moment:

$$m_n = \int_0^{\infty} \omega^n S(\omega) d\omega$$

The characteristic frequencies and periods are defined as follows.

ω_m : Peak frequency

The peak frequency is the frequency at which the spectral ordinate, $S(\omega)$ is a maximum.

T_p : Peak period

The peak period is the period corresponding to the frequency at which $S(\omega)$ is a maximum.

$$T_p = 2\pi/\omega_m$$

T_m : Modal period

The modal period is the period at which $S(T)$ is a maximum. Since the spectrum equations in terms of frequency and in terms of period differ by the period squared factor, the modal period is shifted away from the peak period.

T_V : Visually Observed Period, or Mean Period, or Apparent Period

The visually observed period is the centroid of the $S(\omega)$ spectrum. The International Ship Structures Congress (ISSC) and some environmental reporting agencies have adopted T_V as the period visually estimated by observers.

$$T_V = 2\pi \cdot (m_0/m_2)^{1/2}$$

T_Z : Average Zero-upcrossing period or Average Period

The average zero-upcrossing period is the average period between successive zero up-crossings. The average period may be obtained from a wave record with reasonable accuracy.

$$T_Z = 2\pi \cdot (m_0/m_2)^{1/2}$$

T_C : Crest Period

The crest period is the average period between successive crests. The crest period may be taken from a wave record, but its accuracy is dependent upon the resolution of the wave measurement and recording equipment and the sampling rate.

$$T_C = 2\pi \cdot (m_2/m_4)^{1/2}$$

T_S : Significant Period

The significant period is the average period of the highest one-third of the waves. Some environmental reporting agencies give the sea characteristics using T_S and H_S , the significant wave height. There are two equations relating T_S to T_p .

$$T_S = 0.8568 \cdot T_p, \quad \text{01d}$$

$$T_s = 0.9457 * T_p, \quad \text{New}$$

The first equation applies to original Bretschneider wave spectrum, and the second is the result of recent wave studies (See Reference A.1).

The peak period, T_p , is an unambiguous property of all common wave spectra, and is therefore the preferred period to use in describing a random sea.

A.2.2 Characteristic Wave Heights

From the assumption that the wave elevations tend to follow a Gaussian distribution, it is possible to show that the wave heights follow a Rayleigh distribution. Since wave heights are measured from a trough to succeeding crest, wave heights are always positive which agrees with the non-zero property of the Rayleigh probability density. From the associated property that the wave heights follow a Rayleigh distribution, the expected wave height, the significant wave height, and extreme wave heights may be calculated. The equation for the average height of the one-over-nth of the highest waves is as follows.

$$H_{1/n} / (m_0)^{1/2} = \frac{2 * [2 * \ln(n)]^{1/2} + n * (2\pi)^{1/2} * \{1 - \text{erf}[(\ln(n))^{1/2}]\}}{n}$$

where:

m_0 is the variance or the area under the energy spectrum,

\ln is the natural logarithm,

erf is the error function, (the error function is explained and tables of error function values are available in mathematics table books.)

The characteristic wave heights of a spectrum are related to the total energy in the spectrum. The energy is proportional to the area under the $\frac{1}{2} * a^2$ spectrum.

H_a : Average Wave Height

The average or mean height of all of the waves is found by setting $n=1$.

$$H_a = 2.51 * (m_0)^{\frac{1}{2}}$$

H_s : Significant Height

The significant height is the average height of the highest one-third of all the waves, often denoted as $H_{1/3}$.

$$H_s = 4.00 * (m_0)^{\frac{1}{2}}$$

H_{max} : Maximum Height

The maximum height is the largest wave height expected among a large number of waves, (n on the order of 1000), or over a long sampling period, (t on the order of hours).

The maximum wave height is often taken to be the average of the 1/1000th highest waves.

$$H_{1/1000} = 7.94 * (m_0)^{\frac{1}{2}} = 1.985 * H_s$$

Using the one-over-nth equation and neglecting the second term gives the following equation.

$$H_{1/n} = 2 * [\ln(n)]^{\frac{1}{2}} * (m_0)^{\frac{1}{2}}$$

or

$$H_{1/n} = 2 \cdot [2 \cdot \ln(n)]^{1/2} \cdot H_S$$

For $n = 1000$, this gives,

$$H_{1/1000} = 7.43 \cdot (m_0)^{1/2} = 1.86 \cdot H_S$$

For a given observation time, t , in hours, the most probable extreme wave height is given by the following equation.

$$H_{\max} = 2 \cdot [2 \cdot m_0 \cdot \ln(3600 \cdot t / T_Z)]^{1/2}$$

The $3600 \cdot t / T_Z$ is the average number of zero up-crossings in time, t .

A.3 WAVE SPECTRA FORMULAS

The Bretschneider and Pierson-Moskowitz spectra are the best known of the one-dimensional frequency spectra that have been used to describe ocean waves. The JONSWAP spectrum is a recent extension of the Bretschneider spectrum and has an additional term which may be used to give a spectrum with a sharper peak.

A.3.1 Bretschneider and ISSC Spectrum

The Bretschneider (Reference A.2) spectrum and the spectrum proposed as a modified Pierson-Moskowitz spectrum by the Second International Ship Structures Congress (Reference A.4) are identical. The Bretschneider equation in terms of radial frequency is as follows.

$$S(\omega) = (5/16) \cdot (H_S)^2 \cdot (\omega_m^4 / \omega^5) \cdot \exp [-1.25 \cdot (\omega / \omega_m)^{-4}]$$

where:

H_s is the significant wave height, and

ω_m is the frequency of maximum spectral energy.

The Bretschneider equation may be written in terms of the peak period instead of the peak frequency, by substituting $\omega_m = 2\pi/T_p$.

$$S(\omega) = (5/16) * (H_s)^2 * [(2\pi)^4 / (\omega^5 * (T_p)^4)] * \exp[-1.25 * (2\pi^4 / (\omega * T_p)^4)]$$

A.3.2 Pierson-Moskowitz Spectrum

The Pierson-Moskowitz (Reference A.4) spectrum was created to fit North Atlantic weather data. The P-M spectrum is the same as the Bretschneider spectrum, but with the H_s and ω_m dependence merged into a single parameter. The frequency used in the exponential has also been made a function of reported wind speed. The equation for the Pierson-Moskowitz spectrum is as follows.

$$S(\omega) = \alpha * g^2 / \omega^5 * \exp[-\beta * (\omega_0 / \omega)^4]$$

where:

$$\alpha : 0.0081$$

$$\beta = 0.74$$

$$\omega_0 = g/U$$

and, U is the wind speed reported by the weather ships.

The Pierson-Moskowitz spectrum equation may be obtained from the Bretschneider equation by using one of the following relations between H_s and ω_m .

$$H_s = 0.1610 * g / (\omega_m)^2$$

or

$$\omega_m = 0.40125 * g / (H_s)^{1/2}$$

An interesting point that may be noted is that if β were set equal to 0.75 instead of 0.74, the ω_0 would be the frequency corresponding to the modal period, T_m .

A.3.3 JONSWAP and Related Spectra

The JONSWAP wave spectrum equation resulted from the Joint North Sea Wave Project (Reference A.5). The JONSWAP equation is the original Bretschneider wave spectrum equation with an extra term added. The extra term may be used to produce a sharply peaked spectrum with more energy near the peak frequency. The JONSWAP spectrum can be used to represent the Bretschneider wave spectrum, the original Pierson-Moskowitz wave spectrum, and the ISSC modified P-M spectrum. The full JONSWAP equation is as follows.

$$S(\omega) = (\alpha_j * g^2 * \omega^5) * \exp[-1.25 * \omega / \omega_m^{-4}] * \gamma^a$$

where:

$$a = \exp \left[-\frac{1}{2} * (\omega - \omega_m)^2 / (\sigma * \omega_m)^2 \right]$$

ω_m is the frequency of maximum spectral energy.

The Joint North Sea Wave Project recommended the following mean values to represent the North Sea wave spectra.

$$\gamma = 3.3$$

$$\sigma = 0.07, \quad \text{for } \omega < \omega_m$$

$$\alpha = 0.09, \quad \text{for } \omega > \omega_m$$

The value of α is found by integrating the spectrum and adjusting ω to give the desired area.

The Bretschneider equation and the ISSC equation can be obtained by setting the following parameter values.

$$\gamma = 1.0$$

$$\alpha = (5/16) * (H_s)^2 * (\omega_m)^4 / g^2$$

The Pierson-Moskowitz equation is obtained from the further restriction that H_s and ω_m are related.

$$H_s = 0.1610 * g / (\omega_m)^2$$

or

$$\omega_m = 0.140125 * (g / H_s)^{1/2}$$

or

$$\alpha = 0.0081$$

When γ is set to one the JONSWAP term is effectively turned off. Without the JONSWAP term, the wave spectrum equation can be mathematically integrated to give the following relationships among the characteristic wave periods.

$$T_p = 1.1362 * T_m$$

$$T_p = 1.2957 * T_v$$

$$T_p = 1.4077 * T_z$$

$$T_p = 1.1671 * T_s$$

For $\gamma = 1$, the fourth area moment is infinite. The crest period, T_c , is therefore zero.

For values of γ other than one, the JONSWAP equation cannot be mathematically integrated. The period relationships as a function of γ can be calculated by numerical integration of the wave spectrum equation over the range from three-tenths of the peak frequency to ten times the peak frequency.

The shape of the JONSWAP spectrum can be further adjusted by changing the values of e . The e values are sometimes varied when the JONSWAP spectrum is used to fit measured wave spectra.

A.3.4 Scott and Scott-Wiegel Spectra

The Scott (Reference A.6) spectrum was also formulated to fit North Atlantic weather data. The Scott spectrum is the Darbyshire (Reference A.7) spectrum with slight modifications to the constants in the equation. The spectrum equation is as follows.

$$S(\omega) = 0.214 * (H_s)^2 * \exp[-(\omega - \omega_m) / \{0.065 * (\omega - \omega_m + 0.26)\}^{1/2}]$$

for $-0.26 < \omega - \omega_m < 1.65$

= 0, elsewhere.

where

H_s is the significant height,

$$\omega_m = 3.15*T^{-1} + 8.98*T^{-2},$$

T is the characteristic period of the waves.

The ω_m is the frequency of the peak spectral energy, but unfortunately, the period, T , used in the equation for ω_m does not correspond to any of the mathematical characteristics of the spectrum. The equation for ω_m was derived as a curve fit to real data.

The Scott-Wiegel spectrum is a Scott spectrum modification that was proposed by Wiegel (Reference A.8). The constants are adjusted to match the equation to a "100-year storm" wave condition. The new equation is as follows.

$$S(\omega) = 0.300*(H_s)*\exp[-(\omega-\omega_m)^{1/2} / \{0.0.353*(\omega-\omega_m + 0.26)\}]$$

The ω_m in this equation is 1.125 times that specified for the Scott equation.

A.4 SELECTING A WAVE SPECTRUM

Information about the random sea characteristics in a particular area is derived by either 'wave hindcasting' or by direct wave measurement. For many areas of the world's oceans, the only data available is measured wind speeds and visually estimated wave heights. Sometimes the estimated wave heights are supplemented by estimated wave periods. For a few areas of intense oil development, such as the North Sea, direct wave measurement projects have produced detailed wave spectra information.

A.4.1 Wave Hindcasting

Wave hindcasting is a term used to describe the process of estimating the random sea characteristics of an area based upon meteorological or wind data. Various researchers (References A.2, A.4, A.6, A.7 and A.8) have attempted to derive a relationship between the wind speed over a recent period of time and the spectrum of the random sea generated by the particular wind. The wind speed data is usually qualified by two additional parameters, the duration that the wind has been blowing at that speed and the fetch or distance over open ocean that the wind has been blowing.

A set of equations as derived by Bretschneider (Reference A.2), which relate wind speed, duration and fetch are as follows.

$$g*H_s/U^2 = 0.283*\tanh[0.125*(g*F/U^2)^{0.42}]$$

$$g*T_s / (2\pi*U) = 1.2*\tanh[0.077*(g*F/U^2)^{0.42}]$$

$$g*t_{min}/U = 6.5882*\exp\{[0.161*\Lambda^2 - 0.3692*\Lambda + 2.024]^{1/2} + 0.8798*\Lambda\}$$

where

U is the wind speed,

F is the fetch,

$\Lambda = \ln[g*F/U^2]$,

t_{min} is the minimum duration for which the fetch will determine the significant height and period, and

\tanh is the hyperbolic tangent.

If the wind duration is less than t_{min} , then the third equation is used to find the fetch which would correspond to $t_{min} = t$.

For a fully arisen sea, the above equations simplify to the following.

$$g*H_s/U^2 = 0.283$$

$$g*T_s/(2\pi*U) = 1.2$$

Other relationships have been developed in the references. Often specialized weather/wave research companies have developed elaborate wave hindcasting models to derive the wave spectra characteristics for particular areas. However, the assumptions incorporated into these models have very profound impact on the outcome.

A.4.2 Direct Wave Measurements

By installing a wave probe or a wave buoy in the ocean area of interest, wave elevation histories may be directly measured. The elevation of the sea at a particular point is either recorded by analog means or is sampled at short time intervals (typically one second) and recorded digitally. The wave elevations are usually recorded intermittently, ie. the recorder is turned on for say 30 min every four hours.

The wave records are then reduced by computer, and the wave characteristics are summarized in various ways. Two common ways of summarizing the data are as a wave scatter diagram and/or as a wave height exceedance diagram.

The wave scatter diagram is a grid with each cell containing the number or occurrences of a particular significant wave height range and wave period range. The wave period range may be defined in terms of either peak period or zero-upcrossing period.

The wave height exceedance diagram is a curve showing the percentage of the wave records for which the significant wave height was greater than the particular height.

A5

WAVE SCATTER DIAGRAM

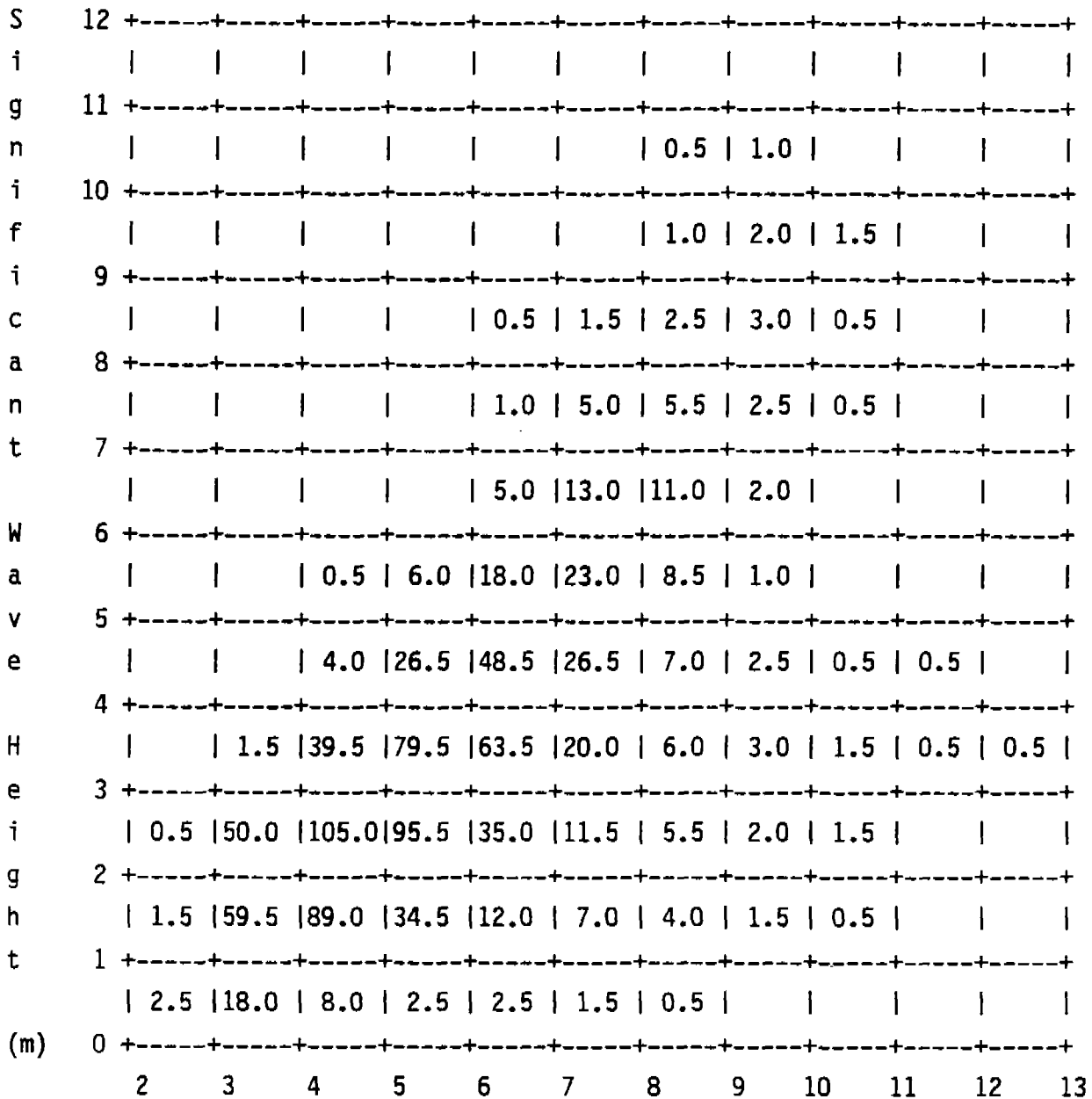
Wave scatter diagrams show the occurrences of combinations of significant wave height and average zero-upcrossing period over an extended time period such as many years.

Wave height distribution over time can be obtained by actual wave measurements. The heights and periods of all waves in a given direction are observed for short periods of time at regular intervals. A short time interval of several hours may be considered constant. For this sea state, defined as "stationary", the mean zero up-crossing period, T_z , and the significant wave height, H_s , are calculated. The H_s and T_z pairs are ordered and their probabilities of occurrence written in a matrix form, called a wave scatter diagram.

Sometimes wave scatter diagrams are available for the sea and for the swell. The sea scatter diagram includes the sea spectra generated locally. The swell scatter diagram contains the swell spectra (or regular waves) generated far from the area, days before. Due to greater energy losses in high frequency waves and the continual phase shifting caused by viscosity, the energy in irregular seas tends to shift toward longer periods, and the spectra becomes more peaked as time passes. The energy in the swell is concentrated about a single long period/low frequency, and often the swell is treated as a single regular wave.

A typical wave scatter diagram, presenting statistical data on the occurrence of significant wave height and zero up-crossing period per wave direction is shown on Figure A-2.

Sample Wave Scatter Diagram



Zero Up-crossing Period, T_z (sec)

Sum of Occurances 999.5

Figure A-2 A Typical Wave Scatter Diagram for the Central North Sea

Using the significant wave height and zero up-crossing period from the wave scatter diagram and selecting a representative sea spectrum formulation, the energy of each sea state can be reconstructed.

A.6 WAVE EXCEEDANCE CURVE

A wave exceedance curve shows the number (percentage) of waves that are greater than a given wave height for consistent wave height intervals. Table A-1 shows the type of data contained on a wave exceedance curve.

Wave Height (ft)	Number of Waves (N)
0	35,351,396
5	3,723,300
10	393,887
15	41,874
20	4,471
25	480
30	51
35	5
40	1

Table A-1 Wave Exceedance Data for Campos Basin
(Number of Waves from Northeast)

This data can be plotted on semi-log paper and closely approximated by a straight line plot. Typically, a wave exceedance H-N curve can be defined with the following equation.

$$H = H_m + m_z * \log N_h$$

where

H_m is the maximum wave height for the design life,

m_z is the slope of the H-log N curve, $-H_m/\log N_h$,

N_m is the total number of waves in the design life, and

N_h is the number of occurrences of waves with height exceeding H .

A.7 WAVE HISTOGRAM AND THE RAYLEIGH DISTRIBUTION

Actual wave height measurements can be plotted to show the number of waves of a given height at equal wave height intervals. The histogram obtained can be defined by a simple curve.

A simple curve that fits most wave histograms is the Rayleigh distribution. Past work have shown that the Rayleigh distribution often allows accurate description of observed wave height distributions over a short term.

The Rayleigh distribution is typically given as,

$$P(H_i) = 2 * H_i * \text{EXP}(-H_i^2/\underline{H}^2) * (1/\underline{H}^2)$$

where

$P(H_i)$ is the wave height percentage of occurrences,

H_i is the wave heights at constant increments,

\underline{H}^2 is the average of all wave heights squared.

A.8 EXTREME VALUES AND THE WEIBULL DISTRIBUTION

For design purposes an estimate of the maximum wave height (extreme value) is required. The Rayleigh distribution provides such an estimate over a short duration. However, in order to estimate the extreme wave that may occur in say 100 years, the Weibull distribution is often used.

The equation for the Weibull distribution is as follows.

$$P(H) = 1 - \text{EXP} [- ((H-\epsilon)/\theta)^\alpha]$$

where

$P(H)$ is the cumulative probability,

H is the extreme height,

ϵ is the location parameter that locates one end of the density function,

θ is the scale parameter, and

α is the shape parameter.

By plotting the wave exceedance data on Weibull graph paper, the distribution can be fit with a straight line and the extreme value for any cumulative probability can be found by extrapolation.

A.9 WIND ENVIRONMENT

The wind environment, source of most ocean waves, is random in nature. The wind speed, its profile and its directionality are therefore best described by probabilistic methods.

A.9.1 Air Turbulence, Surface Roughness and Wind Profile

Air turbulence and wind speed characteristics are primarily influenced by the stability of the air layer and terrain. For extreme wind gusts the influence of stability is small, making

turbulence largely a function of terrain roughness. In an ocean environment, the wave profile makes prediction of wind characteristics more difficult. As the wind speed increases, the wave height also increases, thereby increasing the surface roughness. A surface roughness parameter is used as a measure of the retarding effect of water surface on the wind speed.

A simple relationship developed by Charnock (Reference A.9) is often used to define the surface roughness parameter and the frictional velocity in terms of mean wind speed. Further discussion on surface roughness parameter and drag factor is presented in an ESDU document (Reference A.10).

Full scale experiments carried out by Bell and Shears (Reference A.11) may indicate that although turbulence will decay with the distance above sea surface, it may be reasonably constant to heights that are applicable for offshore structures.

Considering that wind flow characteristics are primarily influenced by energy loss due to surface friction, the mean wind profile for an ocean environment may be assumed to be similar to that on land and to follow this power law:

$$V_{mz} = V_{mz1} (z/z_1)^\alpha$$

where:

V_{mz} = mean wind velocity at height z above LAT

V_{mz1} = mean wind velocity of reference height above LAT

z = height at point under consideration above LAT

z_1 = reference height, 30 ft (10 M), above LAT
(typical)

α = height exponent, typically 0.13 to 0.15.

A.9.2 Applied, Mean and Cyclic Velocities

The random wind velocity at height z can be thought of as a combination of time-averaged mean velocity, V_{mz} , and a time varying cyclic component, $v_z(t)$.

$$V_z(t) = V_{mz} + v_z(t)$$

A range of mean and associated cyclic wind speeds can be extracted from an anemogram and divided into one- to four-hour groups over which the cyclic component of the wind speed is approximately equal. By describing cyclic wind speeds associated with an average value of the mean component of the wind speed over a particular period of time, a number of pairs of mean and associated cyclic speeds can be obtained. In addition to the applied, mean and cyclic wind speeds shown on Table A-2, their probability of occurrence is necessary to generate a scatter diagram. If sufficient data are not available, the number of occurrences can be extrapolated based on similar data. Table A-2 is given only to illustrate the wind make-up and the uncertainties associated with wind data.

Applied Wind Speed Vz(t) ft/s (m/s)	Mean Wind Speed Vmz ft/s (m/s)	Cyclic Wind Speed vz(t) ft/s (m/s)	Probability of Occurrence %
4.26 (13)	29.5 (9)	13.1 (4)	16.7
78.7 (24)	62.3 (19)	16.4 (5)	45.8
101.7 (31)	78.7 (24)	23.0 (7)	12.5
134.5 (41)	101.7 (31)	32.8 (10)	16.7
154.0 (50)	124.6 (38)	39.4 (12)	4.2
180.4 (55)	131.2 (40)	49.2 (15)	4.2

Table A-2 Applied, Mean and Cyclic Wind Speed Distribution for an Extreme Gust Environment

A.9.3 Gust Spectra

The power spectral density function provides information on the energy content of fluctuating wind flow at each frequency component. A study of 90 strong winds over terrains of different roughness in the United States, Canada, Great Britain, and Australia at heights ranging from 25 feet (8m) to 500 feet (150m) allowed Davenport (Reference A.12) to propose a power density spectrum of along-wind gust (the longitudinal component of gust velocity).

A modified version of the Davenport spectrum, due to Harris (Reference ??), is given by:

$$\frac{nS(n)}{k V_m^2} = \frac{4f}{(2 + f^2)^{5/6}}$$

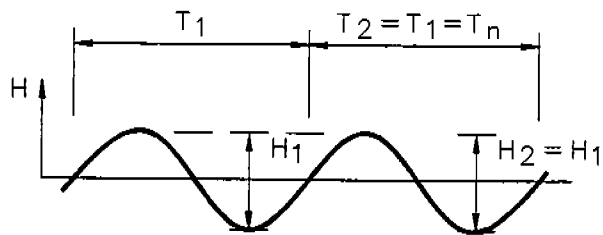
where:

n	=	fluctuating frequency ²
S(n)	=	power density [(m/sec)/Hz]
k	=	surface roughness drag factor corresponding to the mean velocity at 30 ft (10m) (i.e. 0.0015)
V	=	mean hourly wind speed at 30 ft (10m) m
f	=	non-dimensional frequency (nL/V) m
L	=	length scale of turbulence (1200 to 1800m, typical)

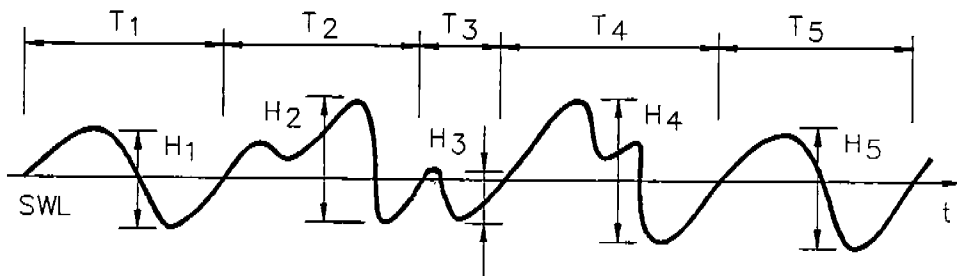
The Harris spectra may be used to develop the wind spectra for each one of the mean wind speeds associated with the scatter diagram.

A.10 REFERENCES

- A.1 Mechanics of Wave Forces on Offshore Structures, Sarpkaya, T. and Isaacson, M., Van Nostrand Reinhold Company, 1981.
- A.2 Bretschneider, C.L., "Wave Variability and Wave Spectra for Wind-Generated Gravity Waves," Beach Erosion Board, Corps of Engineers, Technical Memo No. 118, 1959, pp. 146- 180.
- A.3 Report of Committee 1, "Environmental Conditions," Proceedings Second International Ship Structures Congress, Delft, Netherlands, July 1964, Vol. 1, pp. 1:5-1:13.
- A.4 Pierson, W.J. and Moskowitz, L., "A Proposed Spectral Form for Fully Developed Wind Seas Based on the Similarity Theory of S.A. Kitaigorodsky," Journal of Geophysical Research, Vol. 69, No. 24, Dec 1964.
- A.5 Rye, H., Byrd, R., and Torum, A., "Sharply Peaked Wave Energy Spectra in the North Sea," Offshore Technology Conference, 1974, No. OTC 2107, pp. 739-744.
- A.6 Scott, J.R., "A Sea Spectrum for Model Tests and Long-Term Ship Prediction," Journal of Ship Research, Vol. 9, No. 3, Dec. 1965, pp. 145-152.
- A.7 Darbyshire, J., "The One-Dimensional Wave Spectrum in the Atlantic Ocean and in Coastal Waters," Proceedings of Conference on Ocean Wave Spectra, 1961, pp. 27-39.
- A.8 Wiegel, R.L., "Design of Offshore Structures Using Wave Spectra," Proceedings Oceanology International, Brighton, England, 1975, pp. 233-243.



REGULAR WAVES



IRREGULAR WAVES

Figure A-1 Regular and Irregular Waves

APPENDIX B

REVIEW OF LINEAR SYSTEM RESPONSE TO RANDOM EXCITATION

CONTENTS

- B. REVIEW OF LINEAR SYSTEM RESPONSE TO RANDOM EXCITATION
 - B.1 GENERAL
 - B.1.1 Introduction
 - B.1.2 Abstract
 - B.1.3 Purpose
 - B.2 RESPONSE TO RANDOM WAVES
 - B.2.1 Spectrum Analysis Procedure
 - B.2.2 Transfer Function
 - B.2.2.1 Equations of Motions
 - B.2.2.2 Response Amplitude Operator
 - B.2.3 Wave Spectra
 - B.2.3.1 Wave Slope Spectra
 - B.2.3.2 Wave Spectra for Moving Vessels
 - B.2.3.3 Short-Crested Seas
 - B.2.4 Force Spectrum
 - B.2.5 White Noise Spectrum
 - B.3 EXTREME RESPONSE
 - B.3.1 Maximum Wave Height Method
 - B.3.2 Wave Spectrum Method
 - B.4 OPERATIONAL RESPONSE
 - B.4.1 Special Family Method
 - B.4.2 Wave Spectrum Method

B. REVIEW OF LINEAR SYSTEM RESPONSE TO RANDOM EXCITATION

B.1 GENERAL

B.1.1 Introduction

Spectral analysis is used to determine the response of linear systems to random excitation. In the case of offshore structures, the random excitation comes from either irregular waves or winds. Typical offshore systems subjected to spectral analysis include ships, semisubmersibles, jack-ups, tension-leg platforms and bottom-supported fixed platforms. Responses of interest include motions, accelerations, and member internal forces, moments, and stresses.

Floating units are evaluated by spectral analysis for motions in random seas. The strength and structural fatigue integrity are often assessed with spectral analysis.

B.1.2 Abstract

A spectral analysis combines a set of regular wave response amplitude operators, RAOs, with a sea spectrum to produce a response spectrum. Characteristics of the response may be calculated from the response spectrum, and a random sea transfer function can be derived.

For certain spectral analyses, the sea spectrum must be modified to produce a wave slope spectrum or to adjust the sea spectrum for vessel speed. A spreading function can be applied to the sea spectrum to model a short-crested random sea.

A wave force spectrum can be created directly from force RAOs and the sea spectrum.

A regular wave transfer function is found as the solution to the equations of motion. The regular wave transfer function can be expressed in terms of RAO and a phase angle.

A white noise function may be used to represent a very broad banded input spectrum, if the response spectrum is narrow banded.

The extreme response can be calculated from a given extreme wave, or the extreme response may be statistically derived from a set of spectral analyses.

The sea spectra used in the computation of random sea response can be reduced in number by selecting a smaller family of representative spectra, or by creating a set of mean spectra.

B.1.3 Purpose

The purpose of this appendix is to provide a background of the spectral analysis method and to clarify the concept of a response spectrum and how its properties are derived.

B.2 RESPONSE TO RANDOM WAVES

The spectral analysis method is a means of taking the known response of an offshore structure to regular waves and determining the structure's response to a random sea. The input to the spectral analysis method is the response amplitude per unit wave amplitude (or equally, the response double amplitude per unit wave height) for a range of periods or frequencies of regular waves. These ratios of response amplitude to wave amplitude are known as "Response Amplitude Operators" or just "RAOs." The response of the offshore structure is first obtained for a set of unit amplitude, regular, sinusoidal waves. The regular wave response may be obtained either from model tests or from empirical or theoretical analyses.

A wave energy spectrum is selected to represent the random sea. Wave spectra are described in Appendix A. The wave spectrum represents the distribution of the random sea's energy among an infinite set of regular waves that when added together create the random character of

the sea. By assuming that the response is linear, the response of the offshore structure to a regular wave is equal to the RAO times the regular wave amplitude. By assuming that the response to one wave does not affect the response to another wave, the response of the offshore structure to a random sea is the sum of its responses to each of the constituent regular waves in the random sea. The response is therefore a collection of responses each with a different amplitude, frequency, and phase.

The energy of each constituent wave is proportional to the wave amplitude squared. The energy of the response to a constituent wave of the random sea is proportional to the response squared, or is proportional to the RAO squared times the wave amplitude squared. The response energy may also be represented by a spectrum from which characteristics of the response may be derived. From the response spectrum characteristics and the wave spectrum characteristics, a "transfer function" can be obtained which relates the response and wave characteristics.

B.2.1 Spectrum Analysis Procedure

The spectral analysis procedure involves four steps: 1) obtaining the response amplitude operators, 2) multiplying the wave spectrum ordinates by the RAOs squared to get the response spectrum, 3) calculating the response spectrum characteristics, and 4) using the response spectrum characteristics to compute the random sea response transfer function.

The RAOs are usually calculated for a discrete set of wave frequencies, and the discrete RAOs are then fit with a curve to produce a continuous function. The singular term "RAO" is used both to signify a single response amplitude to wave amplitude ratio and to signify the continuous function through all of the RAOs. Any response that is linearly related (proportional) to wave amplitude may be reduced to an RAO function. Typical responses are motions, accelerations, bending moments, shears, stresses, etc.

Multiplication of the wave spectrum ordinates by the RAO squared is simple. The two underlying assumptions are that the response varies linearly with wave amplitude and the assumption that the response to a wave of one frequency is independent of the response to waves of other frequencies.

Response spectrum characteristics are taken from the shape of the spectrum or are calculated from the area under the response spectrum and the area moments of the response spectrum. Typical characteristics are significant response amplitude, maximum response amplitude, mean period of the response, and peak period of the response spectrum.

The random sea transfer function is the ratio of a response spectrum characteristic to a wave spectrum characteristic. A random sea transfer function is usually presented as a function of the random sea characteristic period. A typical transfer function might be the ratio of maximum bending moment amplitude per unit significant wave height. The transfer function is useful for estimating the response to another wave spectrum with similar form but different amplitude.

B.2.2 Transfer Function

A transfer function converts input to output for linear systems. A transfer function is graphically represented in Figure B-1. A transfer function can relate motion response to the height of incident waves directly, or a transfer function can relate motion response to wave force, or a transfer function can relate member stresses to wave or wind force.

For typical applications to the design of offshore structures, the input energy forms are waves, current and wind. The desired output forms are static displacements, dynamic displacements, and member stresses.

B.2.2.1 Equation of Motions

By assuming that the motions are small enough that the inertial, damping and spring forces can be summed linearly, the equation of motion can be formulated.

$$M\ddot{X} + D\dot{X} + KX = F(x,t)$$

- where
- M is the mass matrix which includes the structure mass properties plus the hydrodynamic added mass effects,
 - D is the linearized damping matrix which includes the viscous damping, the wave damping, and the structural damping effects,
 - K is the stiffness matrix which includes the waterplane spring properties, the restoring properties of moorings or tendons, and the stiffness properties of the structure and any foundation,
 - X is the system displacement vector,
 - \dot{X} is the system velocity vector = (dx/dt),
 - \ddot{X} is the system acceleration vector, = (d²x/dt²), and
 - F is the force vector which may be calculated from empirical methods such as Morrison's equation or from diffraction theory methods.

The equations of motion can be solved with frequency domain or time domain techniques. The frequency domain solution involves the methods of harmonic analysis or the methods of Laplace and Fourier transforms. The time domain solution involves the numerical solution by a time step simulation of the motion.

B.2.2.2 Response Amplitude Operator

The solution of the equations of motion result in a transfer function. The motion transfer function has an in-phase component and an out-of-phase component. The transfer function is usually represented in complex form,

$$X(\omega) = A*[X_I(\omega) + i*X_O(\omega)]$$

or in angular form,

$$X(\omega) = A*[X_I*\cos(\omega t) + X_O*\sin(\omega t)]$$

where

X is the total response,

A is the wave height,

X_I is the in-phase component of the response for unit wave height, and

X_O is the out-of-phase component of the response for unit wave height.

From this equation, the response amplitude operator (amplitude per unit wave height), is found to be,

$$RAO = \text{SQRT}(X_I^2 + X_O^2),$$

and the phase of the harmonic response relative to the wave is,

$$\phi = \text{ATAN}(X_O/X_I).$$

The response can be written in terms of the RAO and phase as,

$$X(\omega) = A \cdot \text{RAO}(\omega) \cdot \cos(\omega t + \phi(\omega)).$$

When a spectral analysis is applied to the transfer function the wave amplitudes, A , become a function of wave frequency, ω , and the $X(\omega)$ is replaced by the differential slice of the response power density spectrum.

$$S_R(\omega) \cdot d\omega = [A(\omega) \cdot \text{RAO}(\omega)]^2$$

or

$$S_R(\omega) \cdot d\omega = A^2(\omega) \cdot \text{RAO}^2(\omega)$$

or

$$S_R(\omega) \cdot d\omega = S(\omega) \cdot d\omega \cdot \text{RAO}^2(\omega)$$

$$\text{Thus, } S_f(\omega) = S(\omega) \cdot \text{RAO}^2(\omega)$$

The response spectrum $S(\omega)$ is therefore just the sea spectrum times the RAO squared.

For multiple-degree-of-freedom systems, there is coupling between some of the motions, such as pitch and heave. For example, to obtain the motion or motion RAO for heave of a point distant from the center of pitch rotation, the pitch times rotation arm must be added to the structure heave. This addition must be added with proper consideration of the relative phase angles of the pitch and heave motions, and therefore, such addition must be performed at the regular wave analysis stage. The combined heave (w/pitch) RAO can then be used in a spectral analysis to obtain the heave spectrum and heave response characteristics at the point.

B.2.3 Wave Spectra

The wave spectrum used in the spectral analysis may be an idealized mathematical spectrum or a set of data points derived from the measurement of real waves. When a set of data points are used, a linear or higher order curve fit is employed to create a continuous function. Custom wave spectra for specific regions are often provided as one of the conventional idealized spectra with parameter values selected to match a set of measured wave data. For areas where there is little wave data, wave height characteristics are estimated from wind speed records from the general area.

B.2.3.1 Wave Slope Spectra

For certain responses, particularly the angular motions of pitch and roll, the RAO is often presented as response angle per unit wave slope angle. For these cases the wave spectrum in amplitude squared must be converted to a wave slope spectrum. The maximum slope of any constituent wave of the spectrum is assumed to be small enough that the wave slope angle in radians is approximately equal to the tangent of the wave slope. The water depth is assumed to be deep enough (at least one-half the longest wave length) that the wave length is approximately equal to:

$$(g/2\pi)*T^2 \text{ or } 2\pi g/\omega^2.$$

By using the Fourier series representation of the wave spectrum, selecting one constituent wave, and expressing the wave equation in spatial terms instead of temporal terms, the wave slope is derived as follows.

$$\eta = a*\cos(2\pi x/L) = a*\cos(x\omega^2/g)$$

$$d\eta/dx = -(a\omega^2/g)*\sin(x\omega^2/g)$$

$$[dn/dx]_{\max} = a\omega^2/g$$

Squaring the equation to get the slope squared,

$$[dn/dx]^2 = a^2*(\omega^4/g^2)$$

Therefore, the wave spectrum equation must be multiplied by (ω^4/g^2) to obtain the slope spectrum. The wave slope angle spectrum is the wave slope spectrum converted to degrees squared, i.e., multiplied by $(180/\pi)^2$.

B.2.3.2 Wave Spectra for Moving Vessels

For self-propelled vessels or structures under tow, the forward speed of the vessel or structure will have an effect upon the apparent frequency of the waves. The apparent frequency of the waves is usually referred to as the encounter frequency. For a vessel heading into the waves the encounter frequency is higher than the wave frequency seen by a stationary structure. For a vessel moving in the same direction as the waves, the encounter frequency is less than the wave frequency seen by a fixed structure, and if the vessel's speed is great enough it may be overrunning some of the shorter waves which will give the appearance that these shorter waves are coming from ahead instead of from behind.

The encounter frequency for a regular wave is given by the following relationship.

$$\omega_e = \omega + V\omega^2/g$$

where ω is the wave frequency in radians per second as seen from a stationary observer,

V is the velocity component parallel to and opposite in direction to the wave direction, and

g is the acceleration of gravity in units compatible with the velocity units.

The energy of, or area under the curve of the sea spectrum must remain constant.

$$\int S_e(\omega_e) * d\omega_e = \int S(\omega) * d\omega$$

Taking the derivative of the encounter frequency equation gives the following.

$$d\omega_e = [1 + 2V\omega/g] * d\omega$$

Substituting the derivative into the area integral gives the following.

$$\int S_e(\omega_e) * [1 + 2V\omega/g] * d\omega = \int S(\omega) * d\omega$$

Therefore, equating the integrands gives the relationship between the encounter spectrum and the stationary sea spectrum.

$$S_e(\omega_e) = S(\omega) / [1 + 2V\omega/g]$$

This equation is required to transform a stationary sea spectrum to an encounter spectrum for the purpose of integrating the responses.

$$m_0 = \int r_e^2 * S_e * d\omega_e$$

However, if only the response statistics are desired, and not the actual response spectrum, then the same substitutions as above can be made.

$$S_e = S / [1 + 2V\omega/g]$$

$$d\omega_e = [1 + 2V\omega /g] * d\omega$$

$$\int r_e^2 S_e d\omega_e = \int r_e^2 S d\omega$$

Therefore, the encounter frequency need only be used to select the response amplitude operator and the integration is still over the stationary frequency, ω .

$$\text{i.e., } r_e = r(\omega_e) = r(\omega + v\omega^2/g)$$

B.2.3.3 Short-Crested Seas

The usual mathematical representation of a sea spectrum is one-dimensional with the random waves traveling in a single direction with the crests and troughs of the waves extending to infinity on either side of the direction of wave travel. A one-dimensional irregular sea is also referred to as a long-crested irregular sea. In the real ocean the waves tend to be short-crested due to the interaction of waves from different directions.

A two-dimensional spectrum (short-crested sea) is created from a standard one-dimensional mathematical spectrum by multiplying the spectrum by a "spreading function." The most commonly used spreading function is the "cosine-squared" function.

$$f(\psi) = (2/\pi) \cos^2 \psi$$

where ψ is the angle away from the general wave heading,
 $(-\pi/2 < \psi < \pi/2)$

The cosine-squared spreading function spreads the sea spectrum over an angle +/- 90 degrees from the general wave heading.

To incorporate multi-directional or short-crested irregular seas into a spectral analysis, the RAOs for a range of wave headings must be obtained. A spectral analysis is performed for each heading using the one-dimensional sea spectrum. The results of the one-dimensional analyses are then multiplied by integration factors and summed.

The following is a sample of a set of heading angles and the integration factors for a cosine squared spreading function.

<u>ψ</u>	<u>Factor</u>
0°	0.2200
±20°	0.1945
±40°	0.1300
±60°	0.0567
±80°	0.0088

B.2.4 Force Spectrum

For simple single-degree-of-freedom systems, a force spectrum can be generated directly from the calculated or measured regular wave forces.

The force on the structure is calculated by empirical or theoretical methods, or is derived by analyzing measured strain records from tests on the structure or on a model of the structure. This force is the right hand side of the equation of motion as described in Section B.2.2.1.

The force itself has an in-phase and an out-of-phase component relative to the regular wave which generates the force. The force can be written in complex form,

$$F(\omega) = A*[F_I(\omega) + i*F_O(\omega)]$$

or in force RAO and phase form,

$$F(\omega) = A*RAO_f(\omega)*\cos(\omega t + \phi(\omega))$$

where $RAO_f = \text{SQRT}(F_I^2 + F_O^2)$, and

$$\phi = \text{ATAN}(F_O/F_I).$$

The force spectrum can be created by multiplying a selected wave spectrum times the force RAO squared.

$$S_f(\omega) = S(\omega) * RAO_f^2(\omega)$$

B.2.5 White Noise Spectrum

Most sea spectra have a well defined peak of energy and the energy trails off to near zero away from the peak. Other environmental inputs that are described by spectra, such as wind force, may not have a definite peak and may even appear constant over a wide range (broad band) of frequencies.

Often the response RAO is narrow banded, that is, the structure tends to respond at a narrow range of frequencies, centered about a resonant frequency. When the combination of a broad banded excitation spectrum and a narrow banded RAO exist, the spectral analysis can be greatly simplified.

A broad banded spectrum can be approximated by a "white noise spectrum" which has constant energy over the whole frequency range of the spectrum.

For a single degree of freedom system, the response can be defined in terms of a "dynamic amplification function" times an expected static displacement. The dynamic amplification function is as follows,

$$|H(\omega)| = 1/[(1-\omega/\omega_n)^2 + (2\xi\omega/\omega_n)^2]^{1/2}$$

where

ω is radial frequency,

ω_n is the undamped "natural frequency",

$$\omega_n = (k/m)^{1/2},$$

ξ is the damping ratio, the ratio of the actual damping to the critical damping. $\xi = c/(4km)^{1/2}$,

k is the spring constant,

m is the mass that is in motion, and

c is the actual damping.

The expected static displacement is simply force divided by the spring constant, or the expected static displacement spectrum is as follows,

$$S_{\delta}(\omega) = S_f(\omega)/k^2$$

From these equations, the response spectrum is found to be,

$$R(\omega) = (1/k^2) * |H(\omega)|^2 * S_f(\omega),$$

and the mean squared response is,

$$\overline{y^2(t)} = \int_0^{\infty} (1/k)^2 * |H(\omega)|^2 * S_f(\omega) * d\omega.$$

The $(1/k)^2$ is constant, and by approximating the force spectrum by a white noise spectrum with magnitude $S_f(\omega_n)$, the mean squared response is simplified to,

$$\overline{y^2(t)} = (S_f(\omega_n)/k^2) * \int_0^{\infty} |H(\omega)|^2 * d\omega.$$

For lightly damped systems, ($\xi \ll 1$), the integral may be evaluated to yield,

$$\overline{y^2(t)} = [\pi * \omega_n * S_f(\omega_n)] / (2 * \xi * k^2)$$

B.3 EXTREME RESPONSE

The extreme response of an offshore structure may be determined in two ways. An extreme environmental event may be selected, and the responses to the extreme event then calculated. A set of environmental spectra can be selected; the response spectra to each environmental spectra calculated; and the extreme responses derived by statistical analysis of the response spectra. The first method is often called a "deterministic" method, and the second method is referred to as a "probabilistic" method. In actual design practice the two methods are often intermixed or combined in order to confirm that the extreme response has been found.

B.3.1 Maximum Wave Height Method

In deterministic design, a set of extreme conditions is supplied by oceanographers or meteorologists. The extreme conditions are of course derived from statistical analyses of wave and weather records, but the design engineer is usually not involved in that stage of the calculations.

The given extreme conditions are applied to the offshore structure to determine the various responses. Unfortunately, the given extreme conditions may not always produce the extreme responses. For example, the prying and racking loads governing the design of many structural members of semisubmersibles are typically maximized in waves with lower heights and shorter lengths than the maximum height wave. Tendon loads on tension leg platforms (TLPs) are also often maximized in waves that are lower and shorter than the maximum wave.

Since the oceanographer or meteorologist who produced the set of extreme conditions does not have information about the characteristics of the offshore structure, he/she is unable to select an extreme or near extreme condition that will produce the greatest response. Conversely, the design engineer usually has little or no information about the wave and weather data that was used to derive

the set of extreme conditions, and thus, he/she is unable to create alternate conditions to check for greater response.

The design engineer may request a range of extreme conditions, such as: the maximum height wave with a period of 9 sec, the maximum height wave with a period of 10 sec, etc. The increased number of conditions increases the number of analyses required, but allows the design engineer to confirm which conditions produce the extreme responses.

The maximum wave height method is best used when the response is highly nonlinear and the spectral analysis method is therefore not appropriate.

B.3.2 Wave Spectrum Method

A full probabilistic analysis involves calculating responses to the entire suite of possible environmental conditions. Statistical analysis of these responses is then performed in order to predict a suitable extreme for each response. This requires far fewer assumptions on the part of those who supply environmental criteria, but a much more extensive set of environmental data.

With the wave spectrum method, a set of wave spectra are provided by oceanographers or meteorologists. The RAOs for the response of interest are squared and multiplied by the wave spectrum. A wave spectrum is assumed to represent a Gaussian random distribution. Since the response spectrum is created by a linear multiplication, the response spectrum also represents a Gaussian random distribution. The significant response, maximum response, etc. can be calculated using the equations for calculating the significant, maximum, etc. wave heights.

The equations for maximum wave height are summarized here in terms of response:

Significant response, (DA):

$$R_s = 4.00 \cdot (m_0)^{\frac{1}{2}}$$

Maximum response in 1000 cycles, (DA):

$$R_{1/1000} = 7.43 \cdot (m_0)^{\frac{1}{2}} = 1.86 \cdot R_s$$

Maximum response in t hours, (DA):

$$R_{\max} = 2 \cdot [2 \cdot m_0 \cdot \ln(3600 \cdot t / T_z)]^{\frac{1}{2}}$$

where m_0 is the area under the response spectrum,

T_z is the zero-up-crossing period of the response as found from the equation,

$$T_z = 2\pi \cdot (m_0 / m_2)^{\frac{1}{2}}, \text{ and}$$

m_2 is the second radial frequency moment of the response spectrum.

B.4 OPERATIONAL RESPONSE

In order to determine the normal day-to-day motions and stresses to assess motion related downtime and fatigue damage, the distribution of wave heights versus wave periods are considered. A wave scatter diagram condenses and summarizes wave height and wave period statistics. It is a two-parameter probability density function. Typically a wave scatter diagram is presented as a grid of boxes, with one axis of the grid being average zero-up-crossing periods and the other axis being significant wave heights. Within the boxes of the wave scatter diagram are numbers which represent the percentage of the sea records having the corresponding characteristics of H_s and T_z see Figure A-2.

A response scatter diagram could be generated by taking the wave spectrum for each sample used to create the wave scatter diagram and performing a spectral analysis for the response. The computed characteristics are then used to assign the percentage of occurrence to the appropriate box in the response scatter diagram. This entails considerable work and can be simplified by reducing the number of sea spectra considered, as described below.

B.4.1 Special Family Method

All of the original sea spectra used to define the wave scatter diagram must be available, in order to select a special family of sea spectra to represent the whole population.

The sea spectra are first grouped by wave height bands, such as 0 to 2 ft significant wave height, 2 ft to 4 ft H_s , etc. The average properties of the spectra within a group are computed. Within each group, which may contain thousands of sample sea spectra, a small set of sea spectra are selected to represent all of the spectra in the group. The small set will typically contain 4 to 10 spectra.

The spectra of a representative set are selected by a Monte Carlo (Shotgun) process which randomly picks, say 8, spectra from the group. The mean spectrum and the standard deviation of the spectral ordinates about the mean spectrum are computed for the 8 spectra. A weighted sum of differences in properties between the 8 spectra and the total population of the group represent the "goodness of fit" of that set of 8 spectra.

A second representative set of 8 spectra is then selected from the group, and the "goodness of fit" of the second set is computed. The better set (first or second) is retained and compared to a third sample of 8, etc. The process is repeated many times, say 1000, within each wave group.

From this process, the original number of sea spectra, which may have been thousands, is reduced to the number of wave height bands times the number of spectra in each representative set.

B.4.2 Wave Spectrum Method

A reduced set of sea spectra can be generated to represent the variation of H_s and T_z as given in a wave scatter diagram.

If the original sea spectra are not available, a set of sea spectra can be created directly from the wave scatter diagram. In this case the shape of the spectrum must be assumed. For various areas of the world's oceans, preferred mathematical spectrum equations exist. For the North Sea, the mean JONSWAP spectrum is preferred. For open ocean, the Bretschneider (ISSC) spectrum is preferred. For the Gulf of Mexico, the Scott spectrum has been recommended.

Using the H_s and T_z for each populated box in the wave scatter diagram, and the selected sea spectrum equation, a set of wave spectra are defined. With this method the number of sea spectra is reduced to the number of populated boxes in the wave scatter diagram, but no more than the number of wave height bands times the number of wave period band.

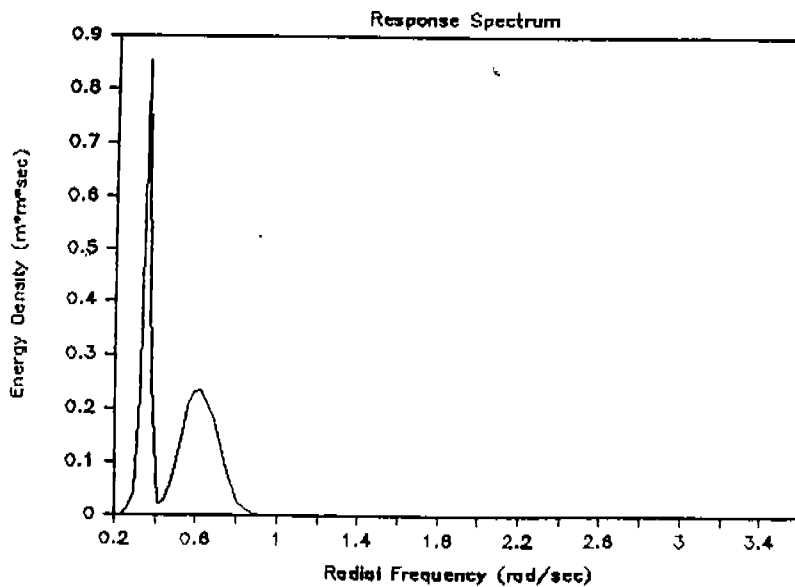
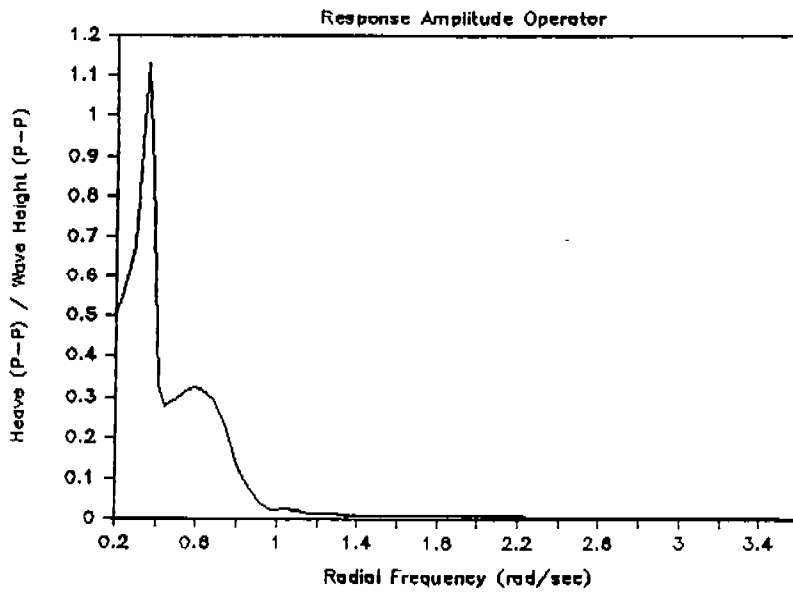
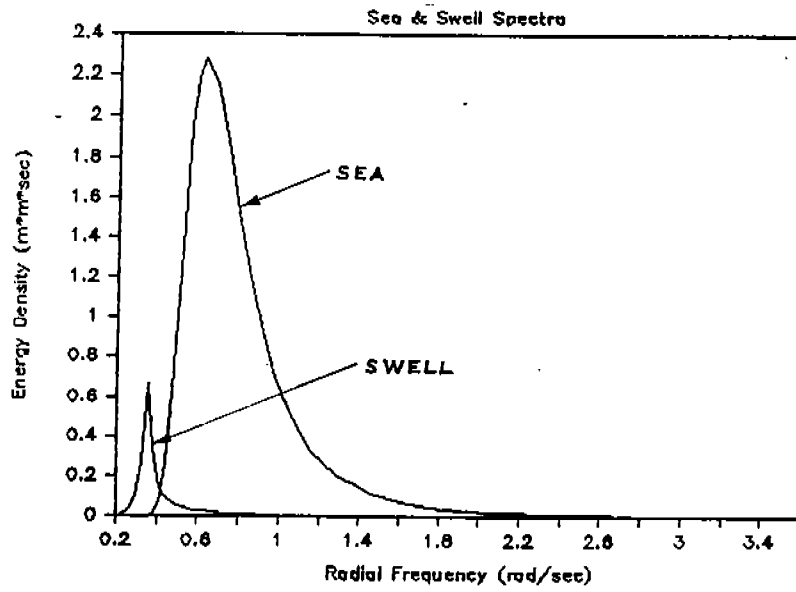


Figure B-1 Sea Spectra, Response Amplitude Operator (RAO) and Response Spectrum

60

APPENDIX C

STRESS CONCENTRATION FACTORS

CONTENTS

- C. STRESS CONCENTRATION FACTORS
 - C.1 OVERVIEW
 - C.1.1 Objectives and Scope
 - C.1.2 Current Technology
 - C.2 STRESS CONCENTRATION FACTOR EQUATIONS
 - C.2.1 Kuang with Marshall Reduction
 - C.2.2 Smedley-Wordsworth
 - C.3 PARAMETRIC STUDY RESULTS
 - C.3.1 Figures
 - C.3.2 Tables
 - C.4 FINITE ELEMENT ANALYSES RESULTS
 - C.4.1 Column-Girder Connection
 - C.5 REFERENCES

C. STRESS CONCENTRATION FACTORS

C.1 OVERVIEW

C.1.1 Objectives and Scope

A comprehensive document on stress Concentration factors (SCF) would include assessment of test results, detailed review of empirical equations, evaluation of finite element studies, and presentation of parametric studies showing the sensitivities of parameters affecting SCFs.

The objective of this appendix is limited. Following a brief discussion of empirical equations, parametric study results are presented to assist the engineer in avoiding undesirable joint details. The sensitivity and interaction of variables shown in tables and figures also allow quick assessment of steps necessary to improve other geometries.

Empirical formulations are applicable to a limited range of simple joint geometries. A complex joint often requires carrying out of a finite element analyses (FEA) to determine the SCFs. The results of a FEA is also presented to illustrate the applicable SCFs for a given geometry.

C1.2 Current Technology

The SCF values can be computed through the use of a number of alternative equations. These equations have been mostly based on analytical (finite element) and small-scale experimental (acrylic model test) work. The tests carried out on joints that reflect those in-service (i.e. both in size and fabrication methods) are few and limited to several simple joint configurations. Thus, the equations available should be reviewed carefully to ascertain their range of validity and overall reliability prior to their use in design. Considering the simple joint configurations of T, Y, DT, K and X, the equations available for use in design are:

- o Kuang (Reference C.1)
- o Wordsworth (References C.2, C.3)
- o Gibstein (References C.4, C.5)
- o Efthymiou (Reference C.6)
- o Marshall (Reference C.7)
- o UEG (Reference C.8)

There are significant differences in the validity ranges of these equations. The SCFs computed based on different equations also often vary considerably. The Kuang equations are applicable to T, Y, and K joints for various load types. Wordsworth and Woodsworth/Smedley equations are applicable to all simple joints. Gibstein equations are applicable to T joints while the Efthymiou equations cover T/Y joints and simple/overlapping K/YT joints. The equations proposed by Marshall are applicable to simple joints, based on those equations by Kellogg (Reference C.9), and were incorporated into API RP 2A.

Substantial work has been carried out to validate the applicability of various SCF equations. Although some of the work carried out by major oil companies are unpublished, such work still influence on-going analytical and experimental research. Delft von D.R.V. et al. (Reference C.10) indicate that the UEG equations offer a good combination of accuracy and conservatism while the Efthymiou (i.e., Shell-SIPM) equations show a good comparison with experimental data.

Ma and Tebbet (Reference C.11) report that there is no consensus on whether a design SCF should represent a mean, lower bound or some other level of confidence. Tebbett and Lalani's (Reference C.12) work on reliability aspects of SCF equations indicate that SCF equations underpredicting the SCF values in less than 16% of the cases can be considered reliable. Thus, when presenting the findings of 45 elastic tests carried out on 15 tubular joints representing typical construction, Ma and Tebbet report that Wordsworth, UEG and Efthymiou equations meet this criteria and offer the best reliability.

Ma and Tebbett also state that while both UEG and Wordsworth equations overpredict X joint SCFs, none of the equations overpredict the K joint SCFs. The comparative data indicate that the SCFs computed using Kuang and Gibstein equations for T/Y joints subjected to axial loading under predict the measured data in more than 16% of the cases. (See Figure C.1-1).

Tolloczko and Lalani (Reference C.13) have reviewed all available new test data and conclude that reliability trends described earlier for simple joints remain valid and also state that Efthymiou equations accurately predict the SCFs for overlapping joints.

C.2 STRESS CONCENTRATION FACTOR EQUATIONS

C.2.1 Kuang with Marshall Reduction

The Kuang stress Concentration factor equations for simple unstiffened joints are shown on the following page. The brace stress Concentration factor equations include Marshall reduction factor, Q^r . The validity ranges for the Kuang stress Concentration factor equations are:

<u>Term</u>	<u>Validity Range</u>
d/D	0.13 - 1.0
T/D	0.015 - 0.06
t/T	0.20 - 0.80
g/D	0.04 - 1.0
D/L	0.05 - 0.3
θ	25 - 90

where, D = chord diameter
T = chord thickness
d = brace diameter
t = brace thickness
g = gap between adjacent braces
L = chord length
 θ = angle between brace and chord

C.2.2 Smedley-Wordsworth

The Smedley-Wordsworth stress Concentration factor equations for simple unstiffened joints are shown on the following pages. The notes for the equations shown on the following pages include the Shell d/D limitation of 0.95. This interpretation is open to a project-by-project review.

The validity ranges for the Smedley-Wordsworth equations are:

<u>Term</u>	<u>Validity Range</u>
d/D	0.13 - 1.0
$D/2T$	12.0 - 32.0
t/T	0.25 - 1.0
g/D	0.05 - 1.0
$2L/D$	8.0 - 40
	30 - 90

where,

- D = chord diameter
- T = chord thickness
- d = brace diameter
- t = brace thickness
- g = gap between adjacent braces
- L = chord length
- = angle between brace and chord

C.3 PARAMETRIC STUDY RESULTS

C.3.1 Figures

The Kuang and Smedley-Wordsworth chord stress Concentration factors for T joints are shown in Section C.3.1(a) and C.3.1(b), respectively. The Kuang and Smedley-Wordsworth chord stress Concentration factors for K joints are shown in Section C.3.1(c) and C.3.1(d), respectively. The Smedley-Wordsworth chord stress Concentration factors for X joints are shown in Section C.3.1(e). Since the chord side of the weld stress Concentration factor is generally higher than the brace side of the weld stress Concentration factor, only the chord side of the weld stress Concentration factors are shown.

C.3.1(a) Kuang Chord SCF's for T-Joints

The Kuang chord SCF's for T-joints are shown on the following pages. The following parameters are assumed for the Kuang figures:

- 1) $\gamma = D/2T = 12.0$
- 2) $\theta = \quad = 30.0$ degrees
- 3) $\alpha = D/L = 0.0571$

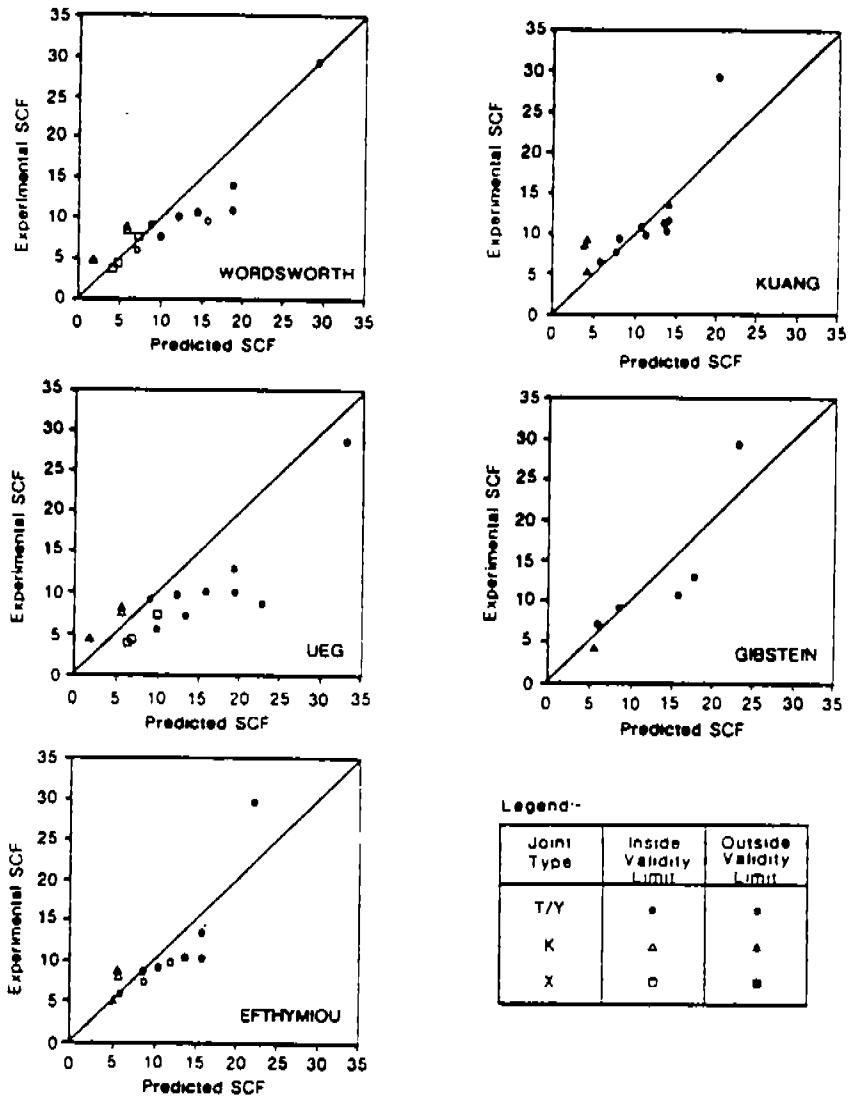


Fig. 6—Results of comparison—axial loading.

Side of Weld of Interest	Stub Type	Axial SCF	Inplane Bending SCF	Out of Plane Bending SCF
Chord	T and Y	$\frac{(1.177)(\frac{d}{b})^{1.333} (\sin \theta)^{1.694}}{(\frac{d}{b})^{.808} (\frac{d}{b})^{.057} \exp \left[(1.2)(\frac{d}{b})^2 \right]}$	$\frac{(1.463)(\frac{d}{b})^{.86} (\sin \theta)^{.57}}{(\frac{d}{b})^{.6} (\frac{d}{b})^{.04}}$	$\frac{(1.507)(\frac{d}{b})^{.889} (\frac{d}{b})^{.787} (\sin \theta)^{1.567}}{(\frac{d}{b})^{1.014}}$ for $\frac{d}{b} < .55$ $\frac{(1.229)(\frac{d}{b})^{.889} (\sin \theta)^{1.567}}{(\frac{d}{b})^{1.014} (\frac{d}{b})^{.619}}$ for $\frac{d}{b} > .55$
Chord	K1	$\frac{(1.949)(\frac{d}{b})^{1.104} (\frac{d}{b})^{.067} (\sin \theta)^{1.521}}{(\frac{d}{b})^{.666} (\frac{d}{b})^{.059}}$	$\frac{(1.400)(\frac{d}{b})^{.94} (\frac{d}{b})^{.06} (\sin \theta)^{.9}}{(\frac{d}{b})^{.38}}$	As for Chord Side T and Y
Chord	K2 and K3	$\frac{(1.26)(\frac{d}{b})^{1.068} (\frac{d}{b})^{.12} (\sin \theta)}{(\frac{d}{b})^{.54}}$	As for Chord Side K1	As for Chord Side T and Y
Brace	T and Y	$1.0 + (Q_R) \left[\frac{(2.784)(\frac{d}{b})^{1.94}}{(\frac{d}{b})^{.55} (\frac{d}{b})^{.12} \exp \left[(1.35)(\frac{d}{b})^2 \right]} - 1.0 \right]$	$1.0 + (Q_R) \left[\frac{(1.109)(\frac{d}{b})^{.38} (\sin \theta)^{.21}}{(\frac{d}{b})^{.23} (\frac{d}{b})^{.38}} - 1.0 \right]$	$1.0 + (Q_R) \left[\frac{(-.843)(\frac{d}{b})^{.543} (\frac{d}{b})^{.801} (\sin \theta)^{2.033}}{(\frac{d}{b})^{.852}} - 1.0 \right]$ For $\frac{d}{b} < .55$ $1.0 + (Q_R) \left[\frac{(-.441)(\frac{d}{b})^{.543} (\sin \theta)^{2.033}}{(\frac{d}{b})^{.852} (\frac{d}{b})^{.781}} - 1.0 \right]$ For $\frac{d}{b} > .55$
Brace	K1	$1.0 + (Q_R) \left[\frac{(1.825)(\frac{d}{b})^{.56} (\frac{d}{b})^{.058} \exp(1.448 \sin \theta)}{(\frac{d}{b})^{.157} (\frac{d}{b})^{.441}} - 1.0 \right]$	$1.0 + (Q_R) \left[\frac{(12.827)(\frac{d}{b})^{.35} (\sin \theta)^{.5}}{(\frac{d}{b})^{.35}} - 1.0 \right]$	As for Brace Side T and Y
Brace	K2	$1.0 + (Q_R) \left[\frac{(5.65)(\frac{d}{b})^{.68} (\frac{d}{b})^{.92} (\frac{d}{b})^{.126} (\sin \theta)^{.5}}{(\frac{d}{b})^{.1} (\frac{d}{b})^{.36}} - 1.0 \right]$ For $\theta < 45$ $1.0 + (Q_R) \left[\frac{(12.88)(\frac{d}{b})^{.68} (\frac{d}{b})^{.92} (\frac{d}{b})^{.126} (\sin \theta)^{2.88}}{(\frac{d}{b})^{.1} (\frac{d}{b})^{.36}} - 1.0 \right]$ For $\theta > 45$	As for Brace Side K1	As for Brace Side T and Y
Brace	K3	$1.0 + (Q_R) \left[\frac{(4.49)(\frac{d}{b})^{.672} (\frac{d}{b})^{.92} (\frac{d}{b})^{.159} (\sin \theta)^{2.267}}{(\frac{d}{b})^{.123} (\frac{d}{b})^{.396}} - 1.0 \right]$	As for Brace Side K1	As for Brace Side T and Y

NOTES: $Q_R = \exp - (.5T + t11.5at)^2$ $Q_R > 0.7$

Chord Side

Brace Side

K-Joints

$$\begin{aligned} \text{SCF}_{cx} &= 0.949 \gamma^{-0.666} \beta^{-0.059} \tau^{1.104} \eta^{0.067} \sin 1.521 \theta & \text{SCF}_{bx} &= 0.825 \gamma^{-0.157} \beta^{-0.441} \tau^{0.560} \eta^{0.058} e^{1.448} \sin \theta \\ \text{SCF}_{cy} &= 1.400 \gamma^{-0.38} \beta^{0.06} \tau^{0.94} \sin 0.9 \theta & \text{SCF}_{by} &= 2.827 \beta^{-0.35} \tau^{0.35} \sin 0.5 \theta \end{aligned}$$

T-Joints

$$\begin{aligned} \text{SCF}_{cx} &= 1.177 \gamma^{-0.808} e^{-1.2\beta^3} \tau^{1.333} \alpha^{-0.057} \sin 1.694 \theta & \text{SCF}_{bx} &= 2.784 \gamma^{-0.55} e^{-1.35\beta^3} \tau \alpha^{-0.12} \sin 1.94 \theta \\ \text{SCF}_{cy} &= 0.463 \gamma^{-0.6} \beta^{-0.04} \tau^{0.86} \sin 0.57 \theta & \text{SCF}_{by} &= 1.109 \gamma^{-0.23} \beta^{-0.38} \tau^{0.38} \sin 0.21 \theta \\ \text{SCF}_{cz} &= 0.507 \gamma^{-1.014} \tau^{0.889} \beta^{0.787} \sin 1.557 \theta & \text{SCF}_{bz} &= 0.843 \gamma^{-0.852} \tau^{0.543} \beta^{0.801} \sin 2.033 \theta \\ & \text{for } 0.3 \leq \beta \leq 0.55 & & \text{for } 0.3 \leq \beta \leq 0.55 \\ \text{SCF}_{cz} &= 0.229 \gamma^{-1.014} \tau^{0.889} \beta^{-0.619} \sin 1.557 \theta & \text{SCF}_{bz} &= 0.441 \gamma^{-0.852} \tau^{0.543} \beta^{-0.281} \sin 2.033 \theta \\ & \text{for } 0.55 < \beta \leq 0.75 & & \text{for } 0.55 < \beta \leq 0.75 \end{aligned}$$

TK-Joints

$$\begin{aligned} \text{SCF}_{cx} &= 1.26 \gamma^{-0.54} \beta^{0.12} \tau^{1.068} \sin \theta & \text{SCF}_{bx} &= 5.65 \gamma^{-0.1} \beta^{-0.36} \tau^{0.68} \omega^{0.126} \sin 0.5 \theta \\ & & & \text{for } 0^\circ < \theta \leq 45^\circ \\ \text{SCF}_{bx} & & \text{SCF}_{bx} &= 12.88 \gamma^{-0.1} \beta^{-0.36} \tau^{0.68} \omega^{0.126} \sin 2.88 \theta \\ & & & \text{for } 45^\circ < \theta < 90^\circ \\ \text{SCF}_{bx(\text{central})} & & &= 4.4918 \gamma^{-0.123} \beta^{-0.396} \tau^{0.672} \omega^{0.159} \sin 2.267 \theta \end{aligned}$$

Where

- γ = chord thickness/chord diameter
- θ = angle between brace and chord
- τ = brace thickness/chord thickness
- α = chord diameter/chord length between supports
- η = separation distance between braces/chord diameter
- ω = separation distance between braces for TK joints/chord diameter
- β = brace diameter/chord diameter

Chord SideBrace SideK-Joints

$$SCF_{cx} = 1.8 (\tau \sin \theta \sqrt{\gamma})$$

$$SCF_{cy} = 1.2 (\tau \sin \theta \sqrt{\gamma})$$

$$SCF_{cz} = 2.7 (\tau \sin \theta \sqrt{\gamma})$$

$$SCF_{bx} = 1.0 + 0.6 Q_r [1.0 + \sqrt{\frac{T}{\beta}} \cdot SCF_{cx}] \geq 1.8$$

$$SCF_{by} = 1.0 + 0.6 Q_r [1.0 + \sqrt{\frac{T}{\beta}} \cdot SCF_{cy}] \geq 1.8$$

$$SCF_{bz} = 1.0 + 0.6 Q_r [1.0 + \sqrt{\frac{T}{\beta}} \cdot SCF_{cz}] \geq 1.8$$

Y-Branch Joints

$$SCF_{Kuang} = 2.06 \gamma^{0.808} e^{-1.2\beta^3} (\sin \theta)^{1.694} \tau^{1.333}$$

$$SCF_{AWS} = 14 \tau \sin \theta \quad \text{for } \gamma \leq 25$$

$$= 1.5 \tau \sin \theta \gamma^{0.7} \quad \text{for } \gamma > 25$$

$$SCF_{cxmod} = SCF_{cx} + \tau \cos \theta$$

$$SCF_{Tc} = SCF_{Kuang} < SCF_{AWS}$$

$$\geq SCF_{cxmod}$$

$$SCF_y = \text{same as for K}$$

$$SCF_z = \text{same as for K}$$

$$SCF_{Tb} = 1.0 + 0.6 Q_r [1.0 + \sqrt{\frac{T}{\beta}} \cdot SCF_{Tc}] \geq 1.8$$

$$\geq SCF_{bx}$$

$$SCF_y = \text{same as for K}$$

$$SCF_z = \text{same as for K}$$

Unreinforced Cross Joints

$$SCF_x = 1.333 (SCF_{Tc})_{y\text{-branch}} + \frac{t_c}{T}$$

$$SCF_y = 1.333 (SCF_{cy})$$

$$SCF_z = 1.333 (SCF_{cz})$$

$$SCF_{bx} = 1.0 + 0.6 Q_r [1.0 + \sqrt{\frac{T}{\beta}} \cdot SCF_x] \geq 1.8$$

$$SCF_{by} = 1.0 + 0.6 Q_r [1.0 + \sqrt{\frac{T}{\beta}} \cdot SCF_y] \geq 1.8$$

$$SCF_{bz} = 1.0 + 0.6 Q_r [1.0 + \sqrt{\frac{T}{\beta}} \cdot SCF_z] \geq 1.8$$

Where

θ = angle between brace and chord

D = can diameter

T = can thickness

t_c = nominal chord thickness

d = brace diameter

t = stub thickness

τ = t/T

γ = $(D-T)/2T$

β = d/D

Q_r = $\exp [-(0.5 T + t)\sqrt{0.5 dt}]$

Chord Side

$$SCF_{cx} = 1.7\gamma\tau\beta(2.42 - 2.28\beta^{2.2})\sin^{\beta^2}(15 - 14.4\beta)\theta$$

$$SCF_{cy} = 0.75\gamma^{0.6}\tau^{0.8}(1.6\beta^{1/4} - 0.7\beta^2)\sin(1.5 - 1.6\beta)\theta$$

$$SCF_{cz} = \gamma\tau\beta(1.56 - 1.46\beta^5)\sin^{\beta^2}(15 - 14.4\beta)\theta$$

Brace Side

$$SCF_{bx} = 1 + 0.63 SCF_{cx}$$

$$SCF_{by} = 1 + 0.63 SCF_{cy}$$

$$SCF_{bz} = 1 + 0.63 SCF_{cz}$$

Where

- β = Brace Diameter/Chord Diameter
- γ = Chord Radius/Chord Thickness
- τ = Brace Thickness/Chord Thickness
- θ = Acute Angle Between Brace and Chord

Smedley Formulas Used for Computing Stress Concentration Factors
for Unreinforced Cross Joints

(3) Table 2 only

(1) If $\beta \geq 0.95$ for out-of-plane bending then use $\beta = 0.95$.

(2) The equations indicated for K and KT joints apply only to loading on all braces in the same direction for out-of-plane bending.

(4) Table 3 only

(1) For K joints in out-of-plane bending replace the constant 0.9 by the term $1 - (0.1)^{1+4\zeta}$ when $\zeta \geq 0$.

(2) For KT joints in out-of-plane bending replace the constant 0.8 by the term $(1 - 0.1)^{1+4\zeta}$ when $\zeta \geq 0$.

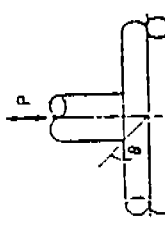
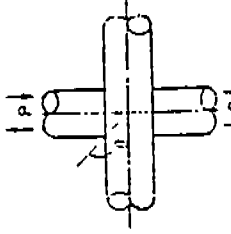
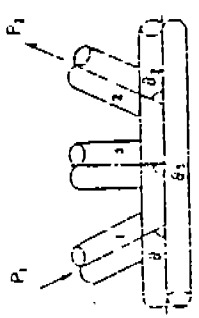
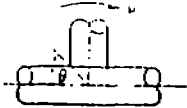
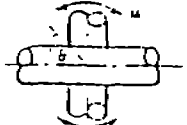
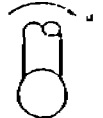
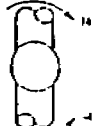
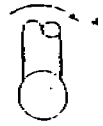
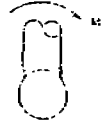
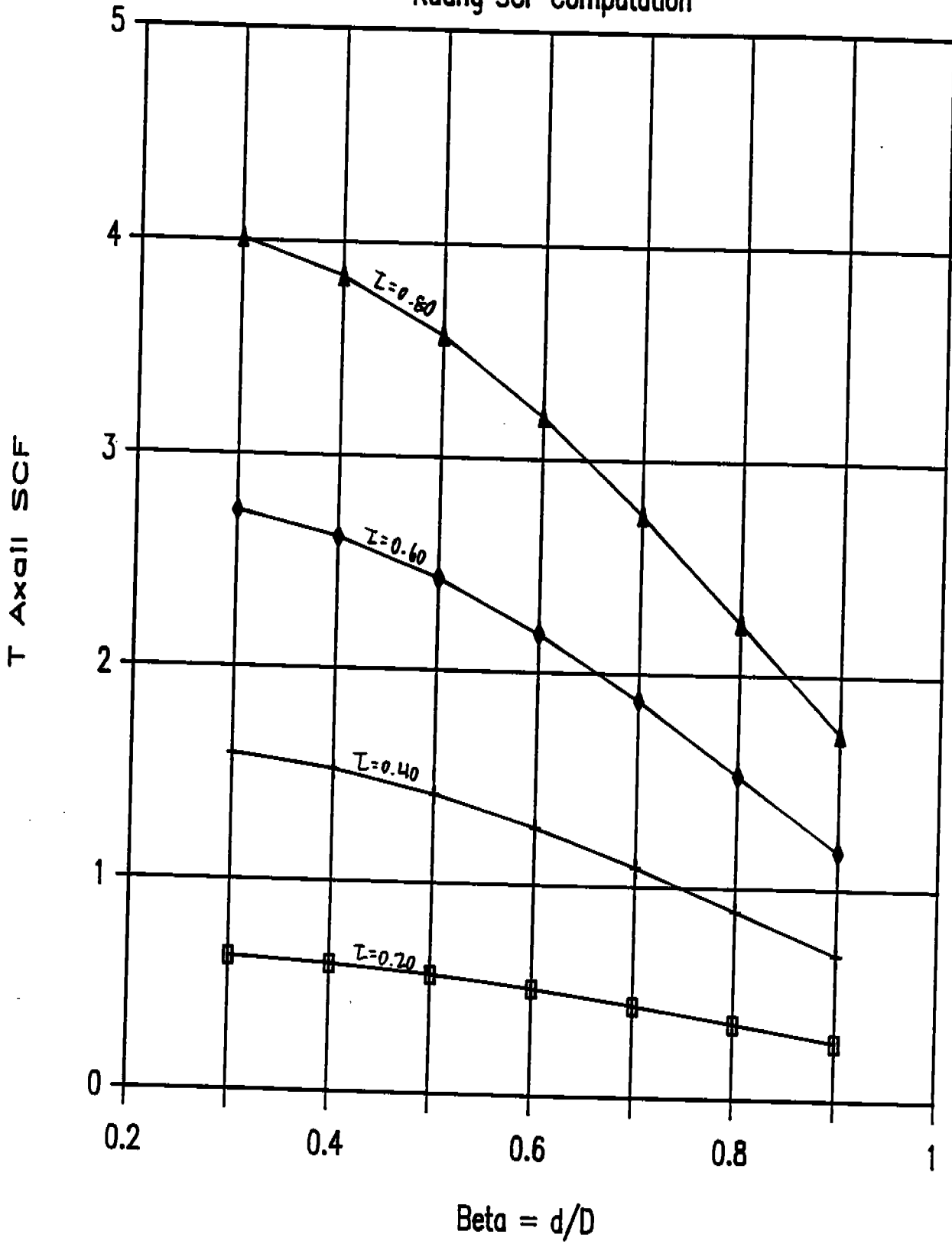
JOINT TYPE AND LOADING	CHORD, SADDLE SCF	CHORD, CROWN SCF
<p>Axial T, T Joints</p> 	$\gamma r \theta (6.70 - 6.42\beta^{0.5}) \sin(1.7 + 0.7\beta^3) \theta$	$\left[0.7 + 1.37\gamma^{0.5} r(1-\beta) \right] \left[2 \sin^{0.5}\theta - \sin^3\theta \right] +$ $\left[\frac{\gamma(2\gamma\beta - r)(\alpha/2 - \beta/\sin\theta) \sin\theta}{2\gamma - 3} \right] \times$ $\left[1.05 + \frac{30r^{1.5}(1.2-\beta)}{\gamma} (\cos^4\theta + 0.15) \right]$
<p>DT, X Joints</p> 	$1.7\gamma r \beta (2.42 - 2.29\beta^{2.2}) \sin(\beta^2(15 - 14.4\beta)) \theta$	<p>No information available on SCF</p>
<p>K, KF Joints</p> 	$\left[\gamma r \beta (6.70 - 6.42\beta^{0.5}) \right] \times$ $\left[\left(\sin(\gamma + 0.7\beta^3) \right)_{d_1} \right] -$ $\left(\left(0.012\gamma \right) (2\gamma/3 + 0.4) \right) \left(\frac{\sin\theta}{\sin\theta_2} \right)^{1.8} \sin(1.7 + 0.7\beta^3) \theta_2$	$1.1\gamma^{0.65} r \left(\frac{\sin\theta_1}{\sin^{0.5}\theta_1} \right) (2r)^{0.05/\beta} (1.5\beta^{0.25} - \beta^2)$

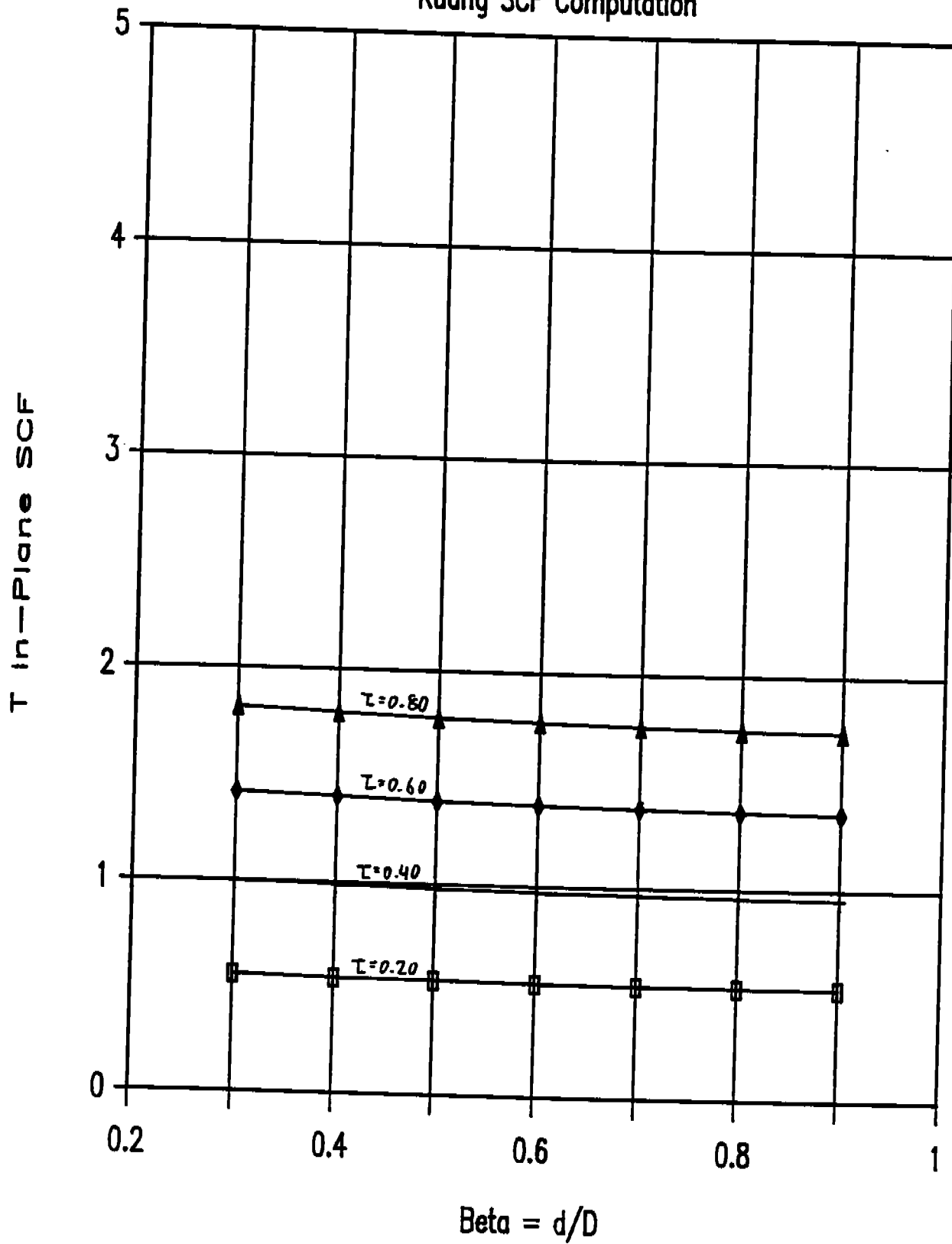
Table 1. Parametric Equations for SCF's of Unstiffened, Non-overlapped Tubular Joints - Axial Loading in Brace

JOINT TYPE AND LOADING	CHORD, SADDLE SCF	CHORD, CROWN SCF
In-Plane Bending T, Y Joints 	SCF = 0	$0.75\gamma^{0.6, 0.8} (1.6\beta^{0.25} + 0.7\beta^2) \sin^{(1.5 - 1.6\beta)}\theta$
DT, X Joints 		
K, KT Joints 		
Out-of-Plane Bending T, Y Joints 	$\gamma\tau\beta(1.6 - 1.15\beta^5) \sin^{(1.35 + \beta^2)}\theta$	SCF = 0
DT, X Joints 	$\gamma\tau\beta(1.56 - 1.46\beta^5) \sin^{(\beta^2(15 - 14.4\beta))}\theta$	
K Joints 	$\left[\gamma\tau\beta(1.6 - 1.15\beta^5) \right] \times$ $\left[\left(\sin^{(1.35 + \beta^2)}\theta_1 \right) + \left(\sin^{(1.35 + \beta^2)}\theta_2 \right) \right] \times$ $\left((0.016\beta\gamma)^{(1 + 0.45)} \right) (\theta_1, \theta_2)^{0.3} \left[1 - 0.1(1 + \tau) \right]$	
KT Joints 	$\left[\gamma\tau\beta(1.6 - 1.15\beta^5) \right] \times$ $\left[\left(\sin^{(1.35 + \beta^2)}\theta_1 \right) + \left(\sin^{(1.35 + \beta^2)}\theta_2 \right) \right] \times$ $\left((0.016\beta\gamma)^{(1 + 0.45)} \right) 2(\theta_1, \theta_2)^{0.3} \left[1 - 0.1(1 + \tau) \right]^2$	
Table 2. Parametric Equations for SCFs of Unsufficed, Non-Overlapped Tubular Joints - Moment Loading in Brace		

Kuang SCF Computation

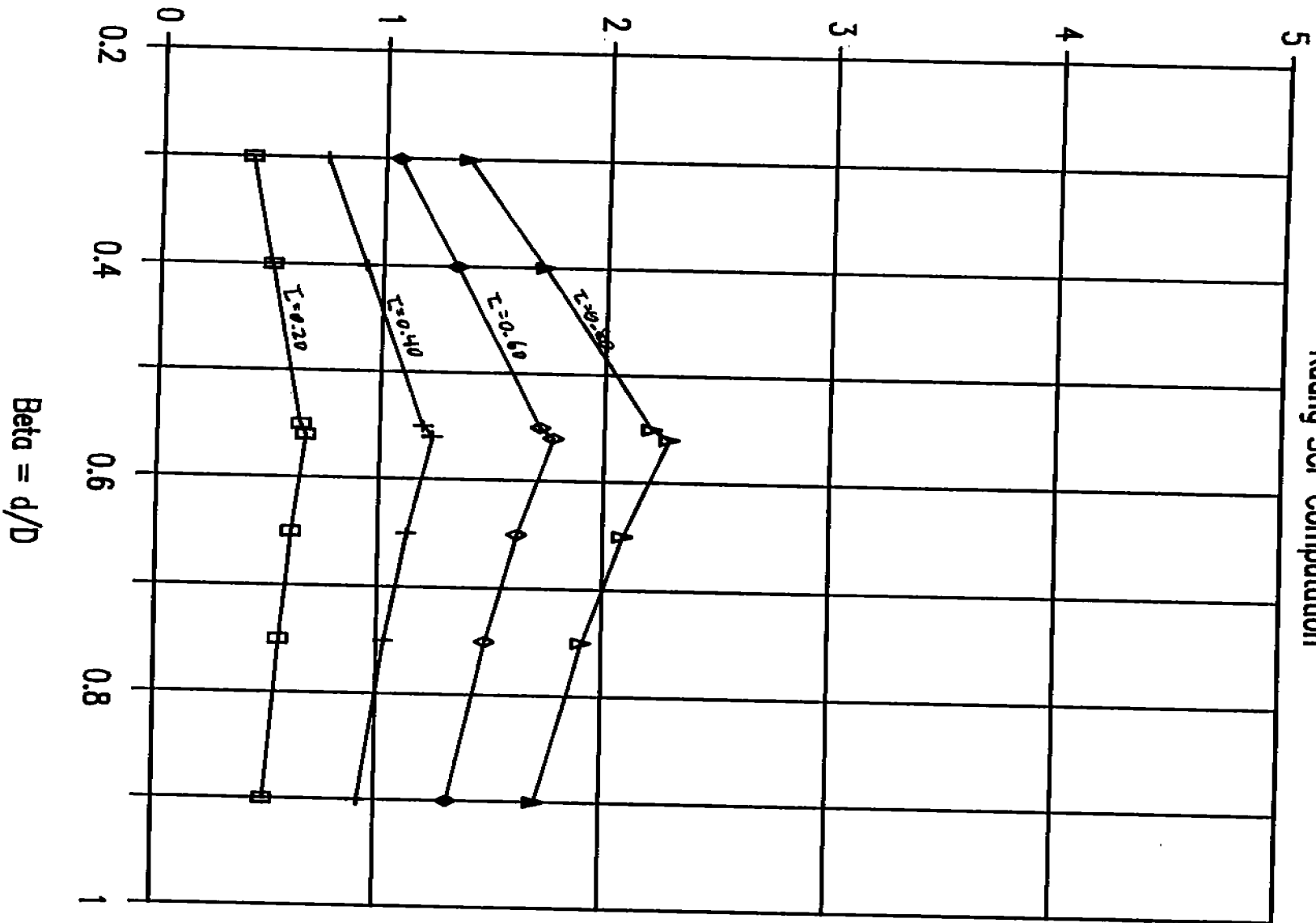


Kuang SCF Computation



T Out-Plane SCF

Kuang SCF Computation



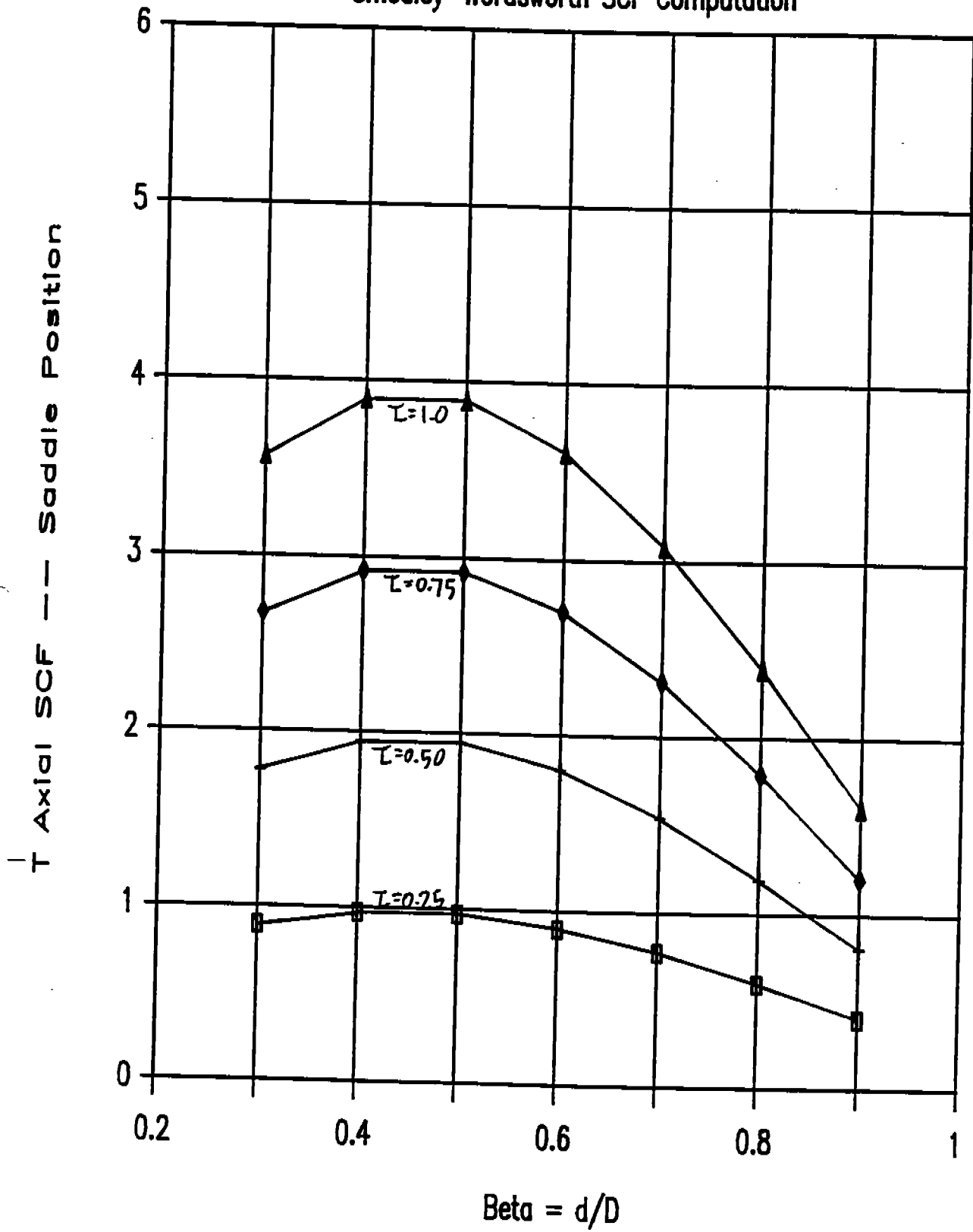
C.3.1(b) Smedley-Wordsworth Chord SCF's for T-Joints

The Smedley-Wordsworth chord SCF's for T-joints are shown on the following pages. The following parameters are assumed for the Smedley-Wordsworth figures:

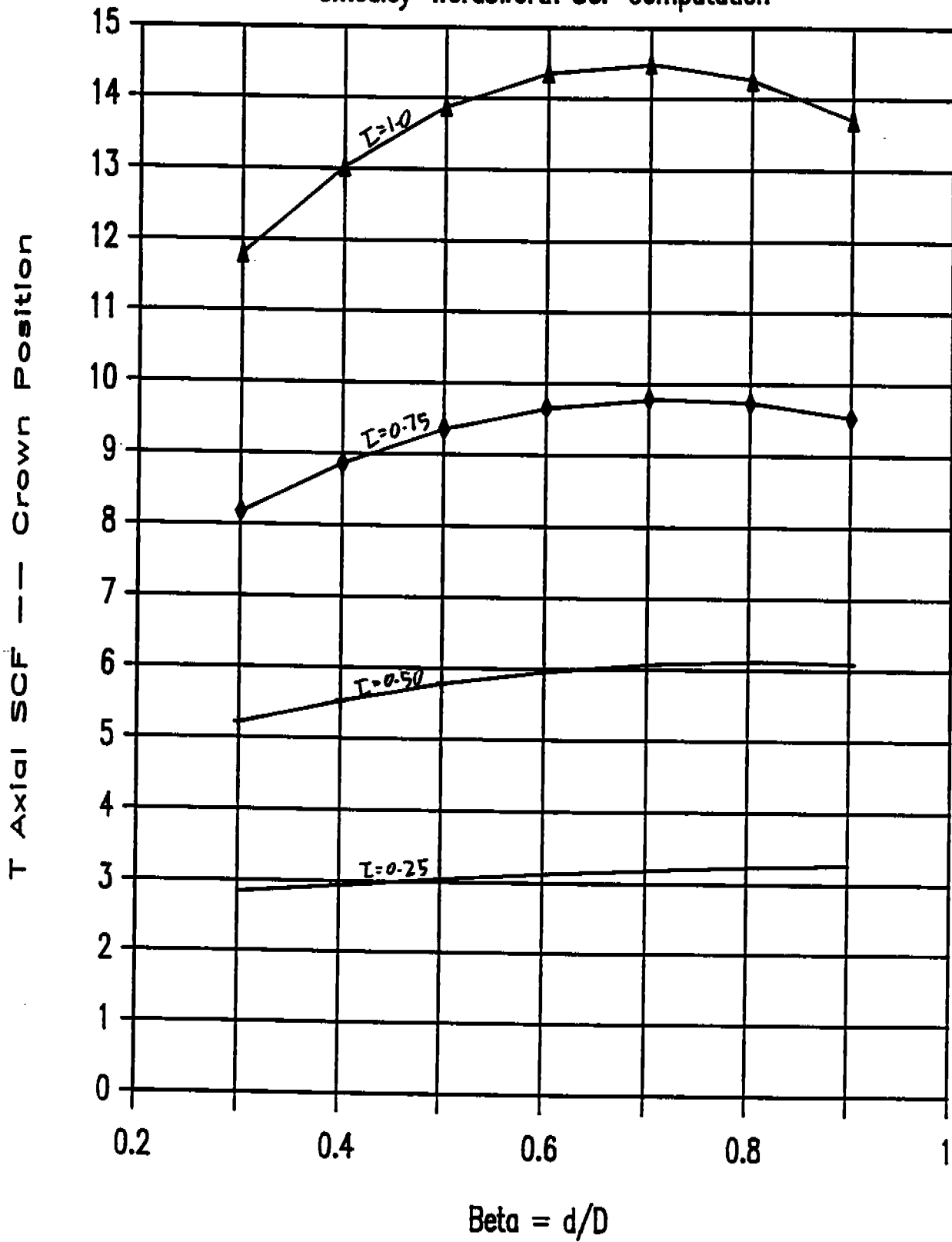
- 1) $\gamma = D/2T = 12.0$
- 2) $\theta = \quad = 30.0$ degrees
- 3) $\alpha = 2L/D = 35.0$

The Shell d/D limitations have not been imposed for the SCF calculation.

Smedley-Wordsworth SCF Computation

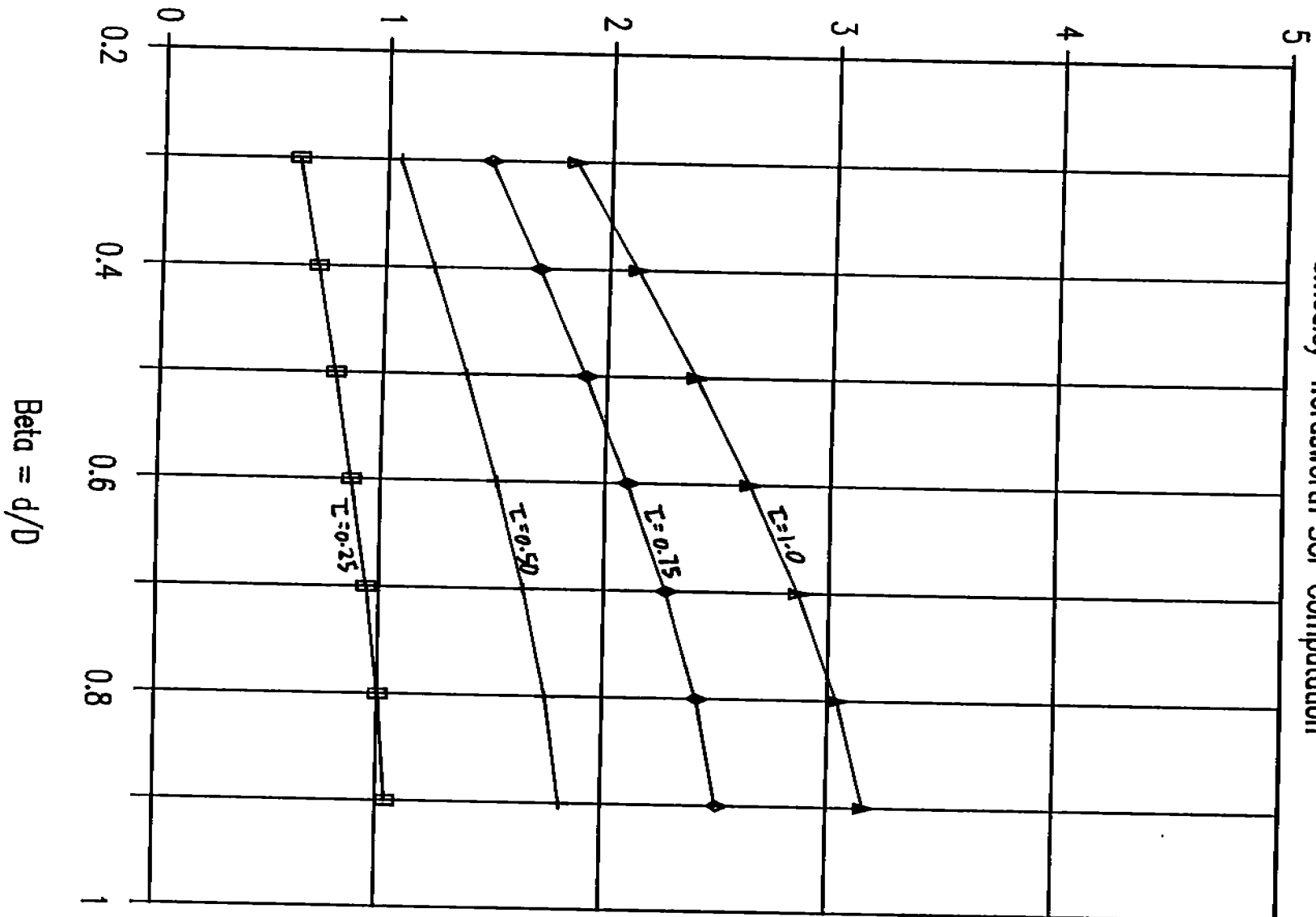


Smedley-Wordsworth SCF Computation



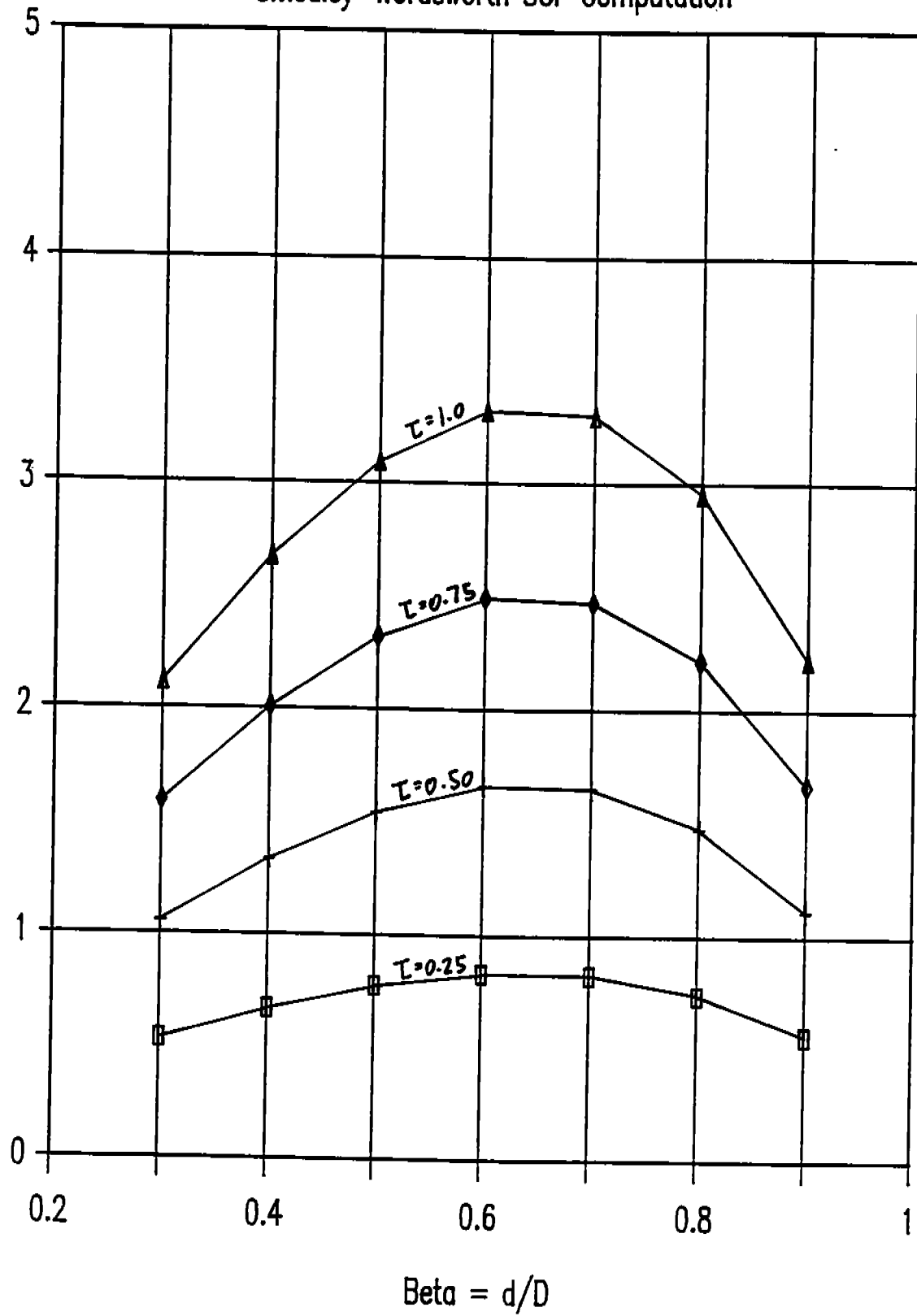
T In-Plane SCF Crown Position

Smedley-Wordsworth SCF Computation



Smedley-Wordsworth SCF Computation

T Out-Plane SCF --- Saddle Position

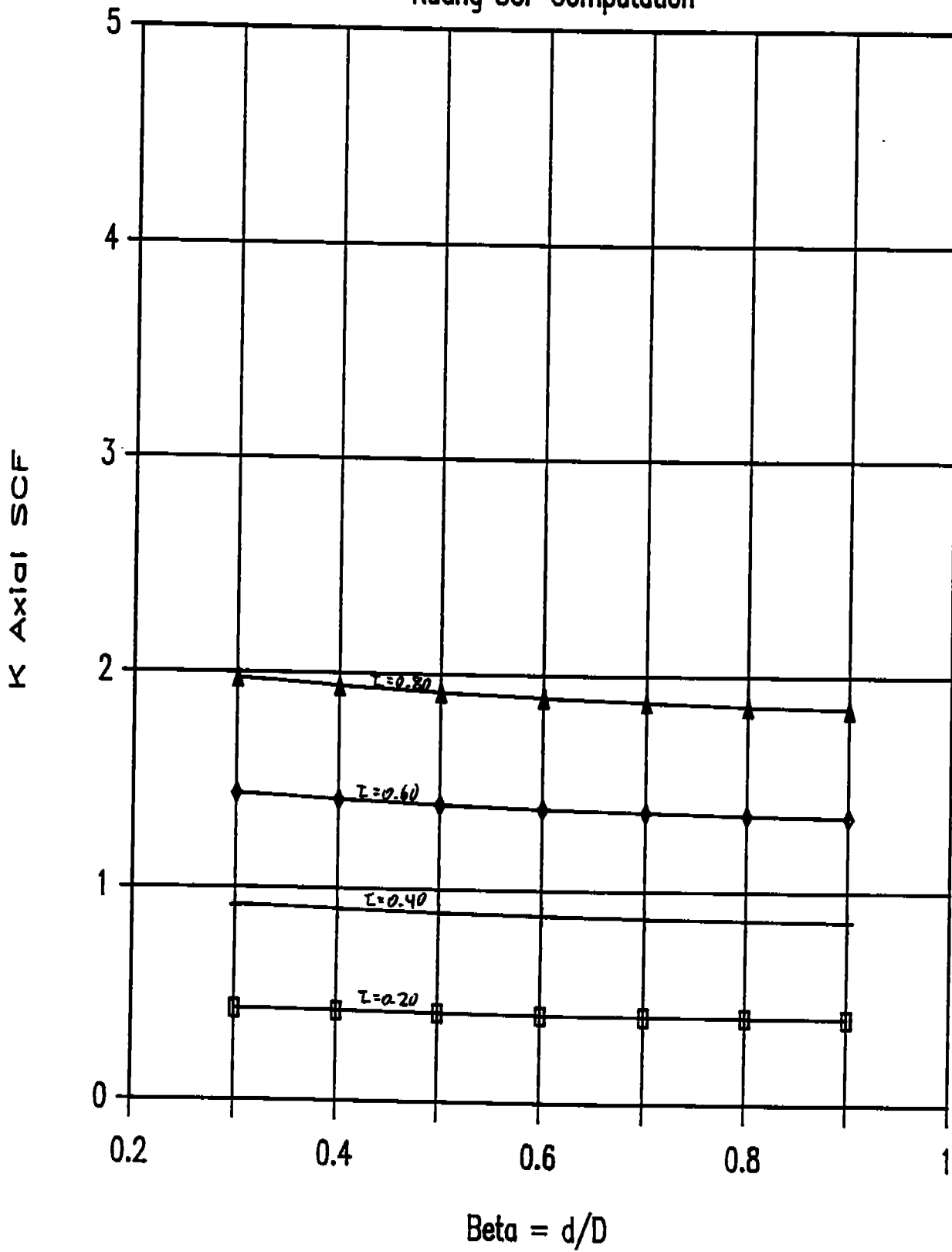


C.3.1(c) Kuang Chord SCF's for T-Joints

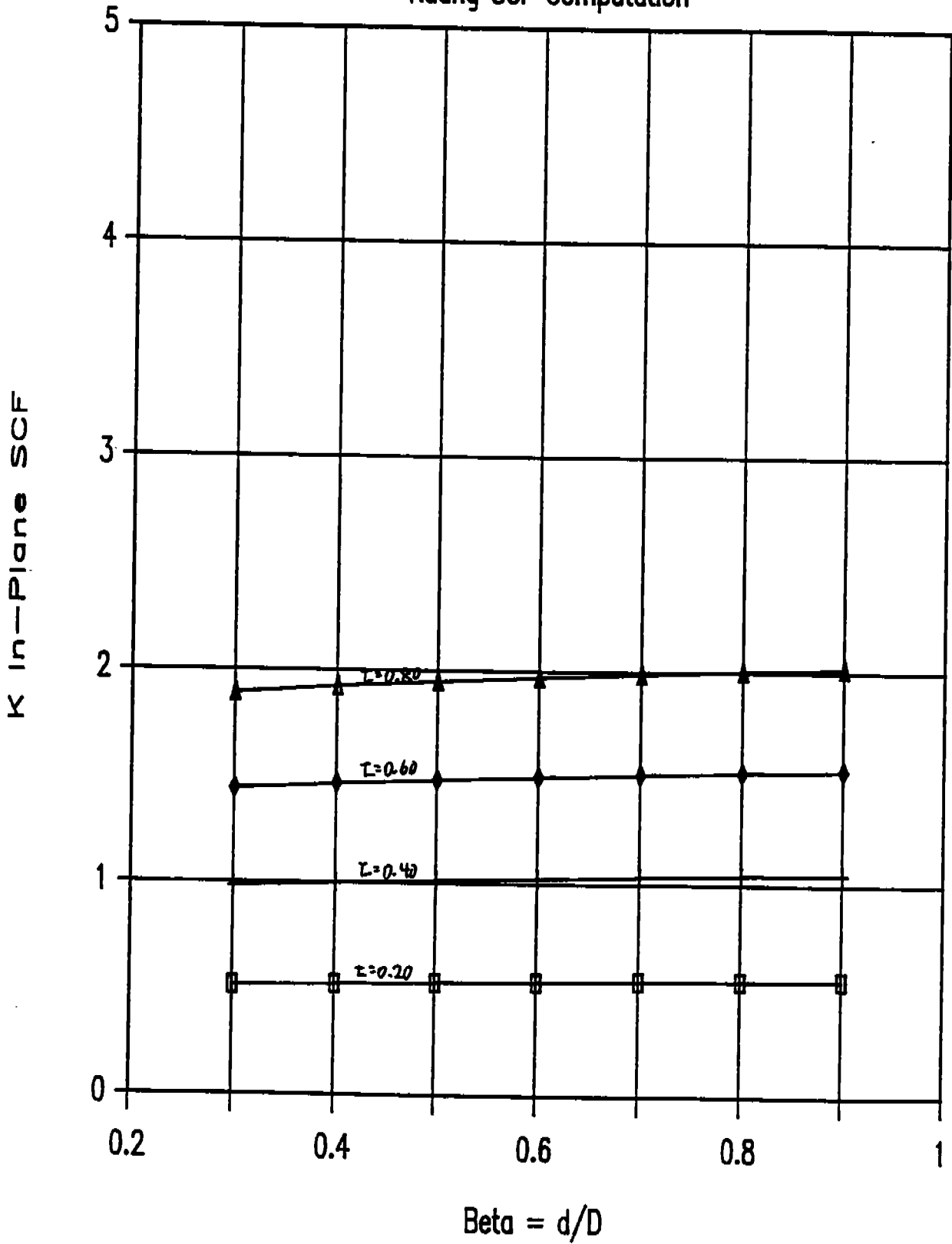
The Kuang chord SCF's for K-joints are shown on the following pages. The following parameters are assumed for the Kuang figures:

- 1) $\gamma = D/2T = 12.0$
- 2) $\theta = \quad = 30.0$ degrees
- 3) $\alpha = D/L = 0.0571$

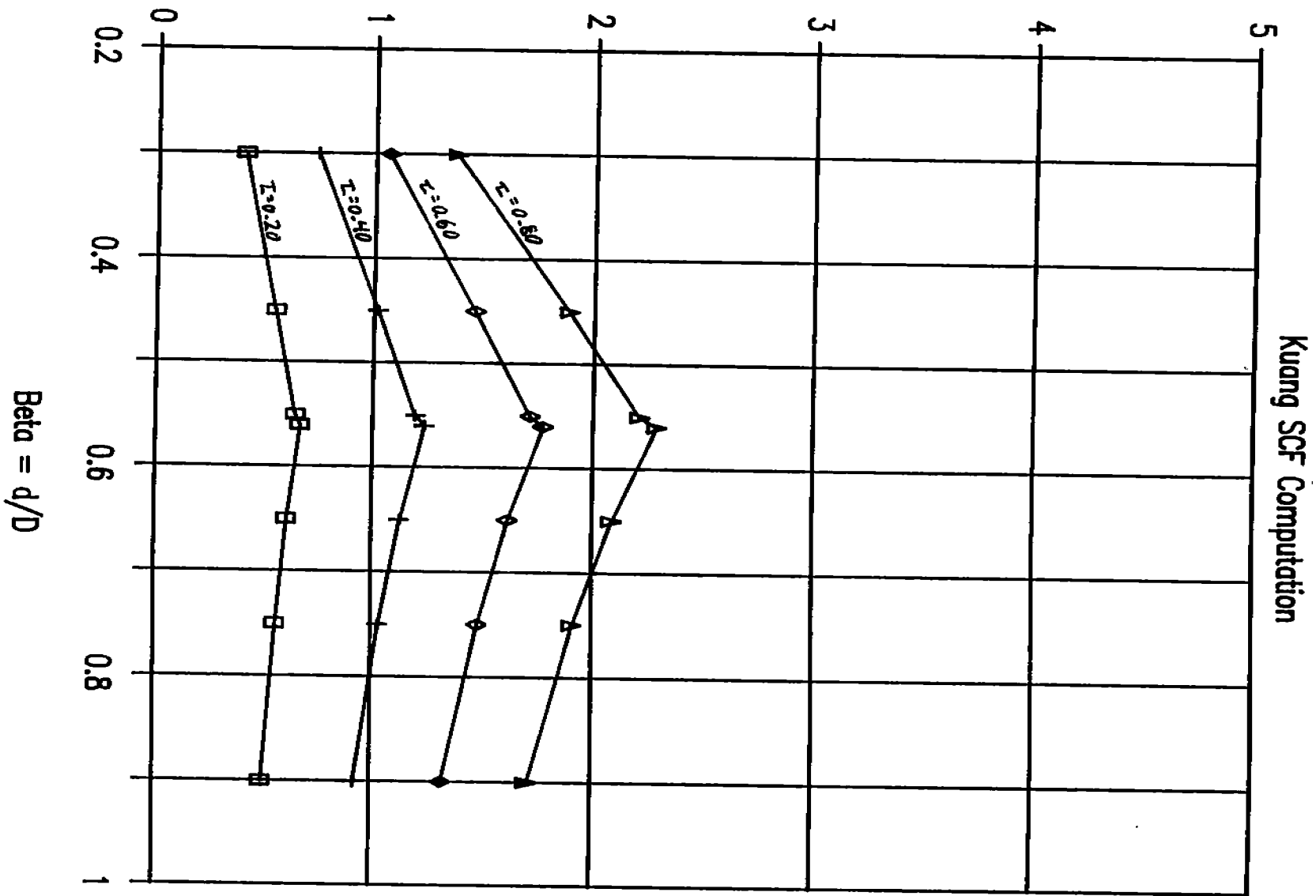
Kuang SCF Computation



Kuang SCF Computation



K Out-Plane SCF



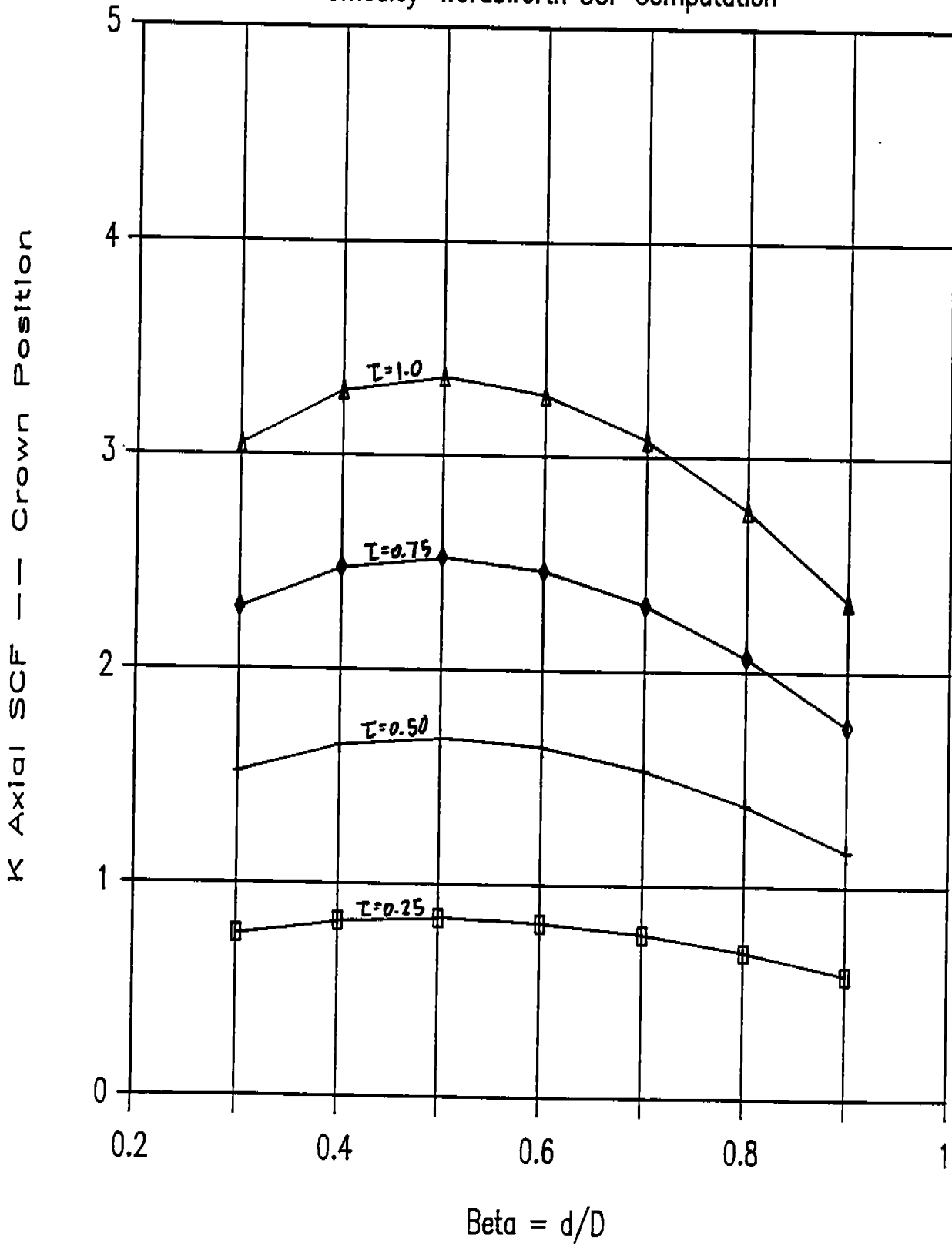
C.3.1(d) Smedley-Wordsworth Chord SCF's for K-Joints

The Smedley-Wordsworth chord SCF's for K-joints are shown on the following pages. The following parameters are assumed for the Smedley-Wordsworth figures:

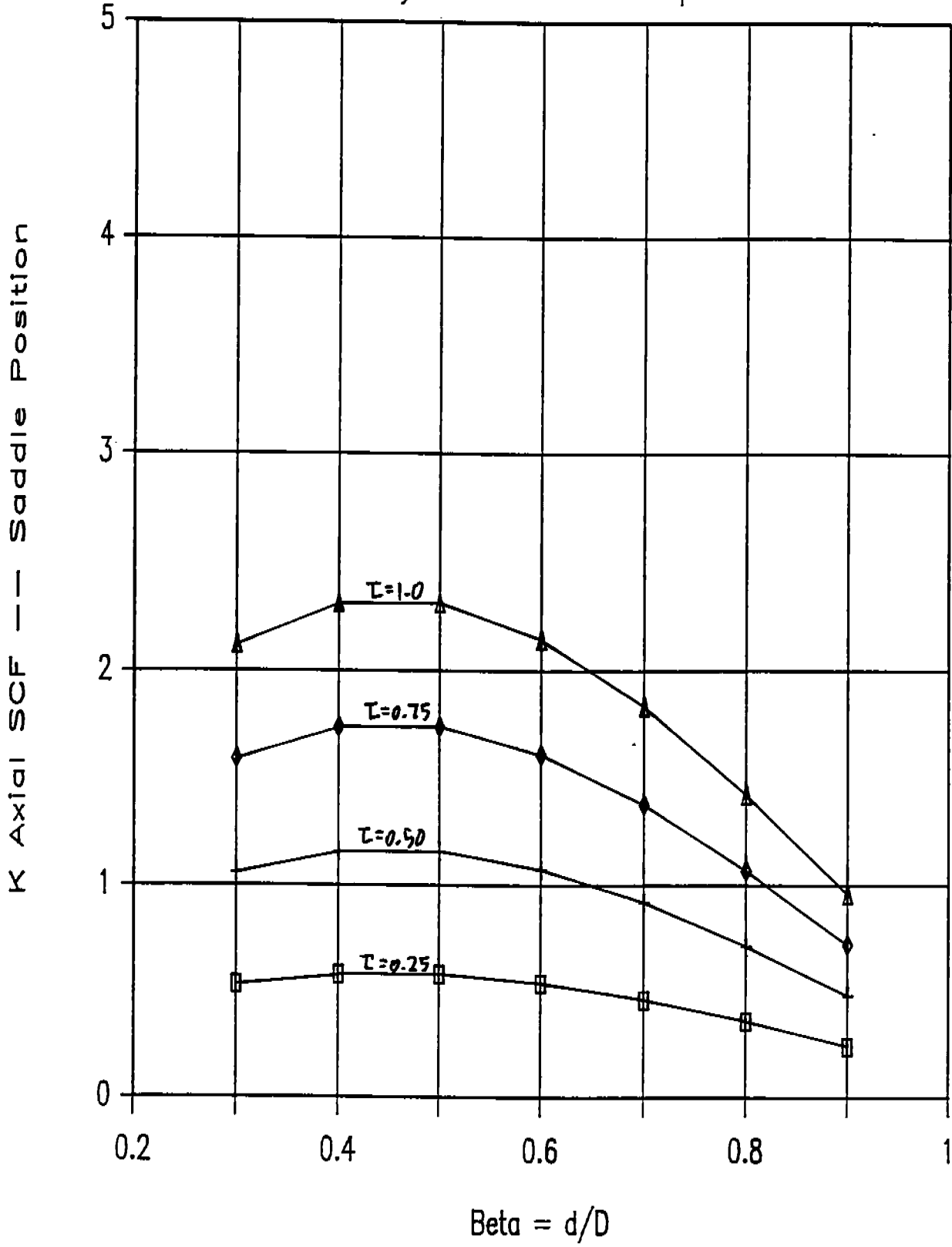
- 1) $\gamma = D/2T = 12.0$
- 2) $\theta = \theta_2 = 30.0$ degrees
- 3) $\alpha = 2L/D = 35.0$

The Shell d/D limitations have not been imposed for the SCF calculation.

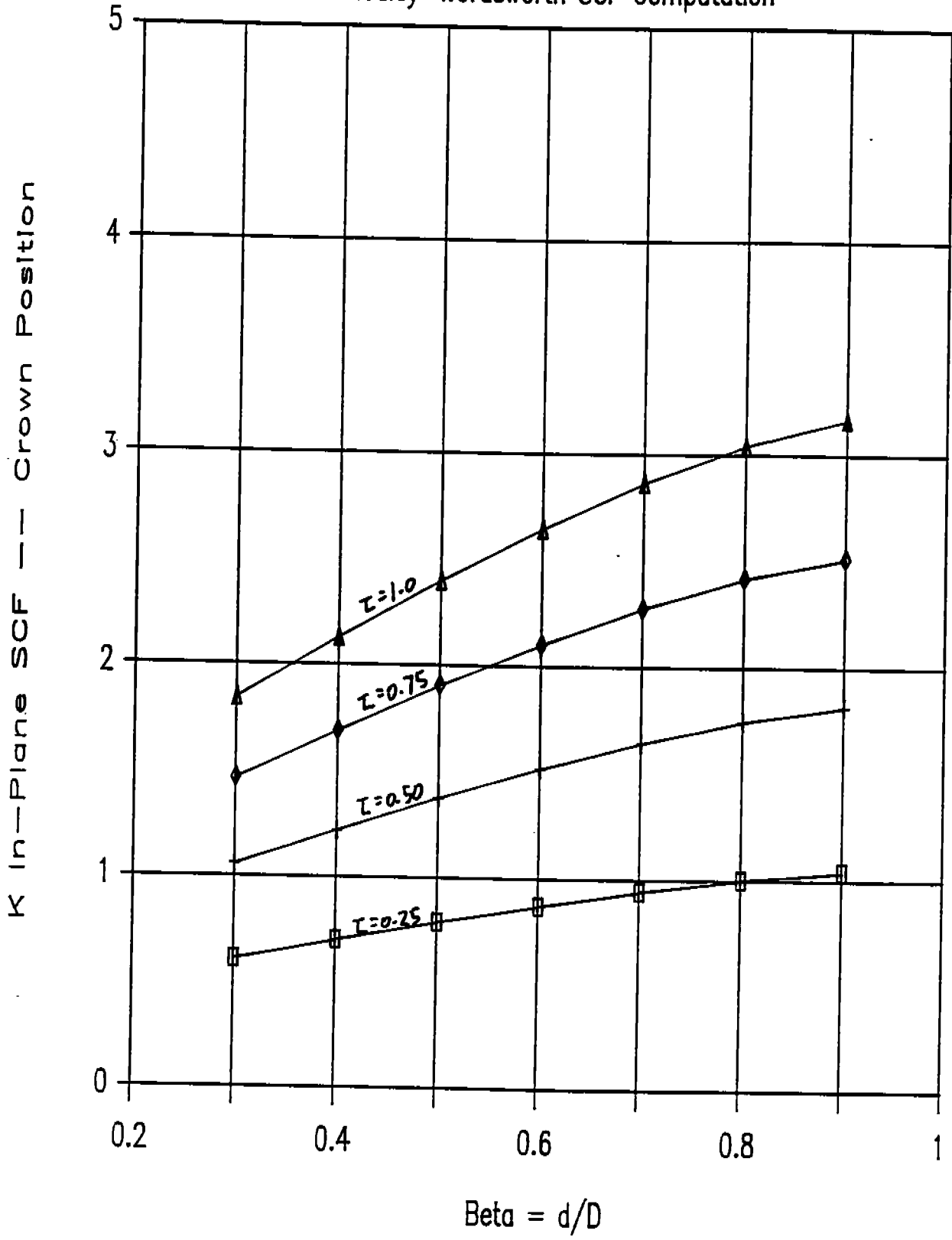
Smedley-Wordsworth SCF Computation



Smedley-Wordsworth SCF Computation

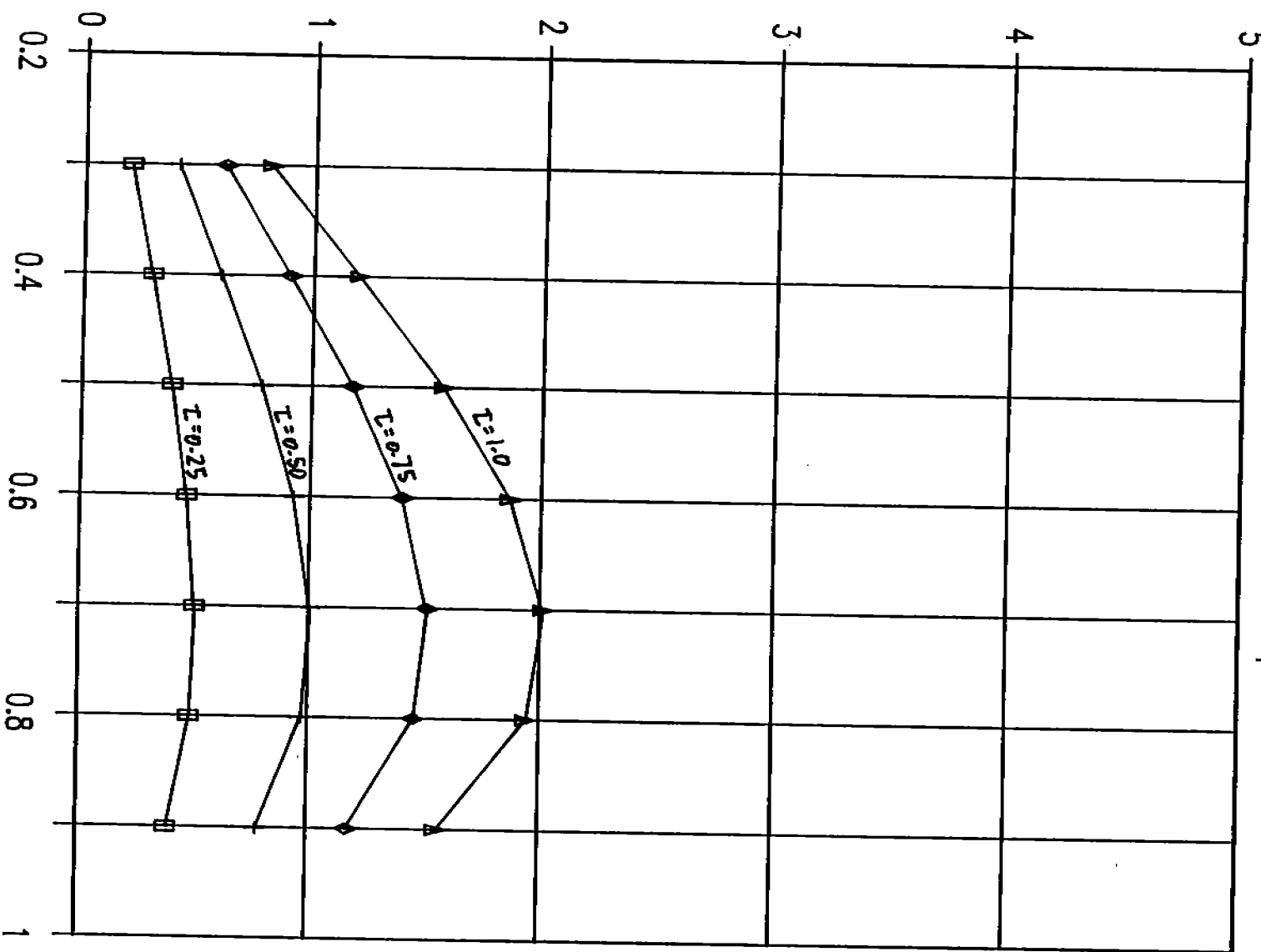


Smedley-Wordsworth SCF Computation



K Out-Plane SCF — Saddle Position

Smedley-Wordsworth SCF Computation



Beta = d/D

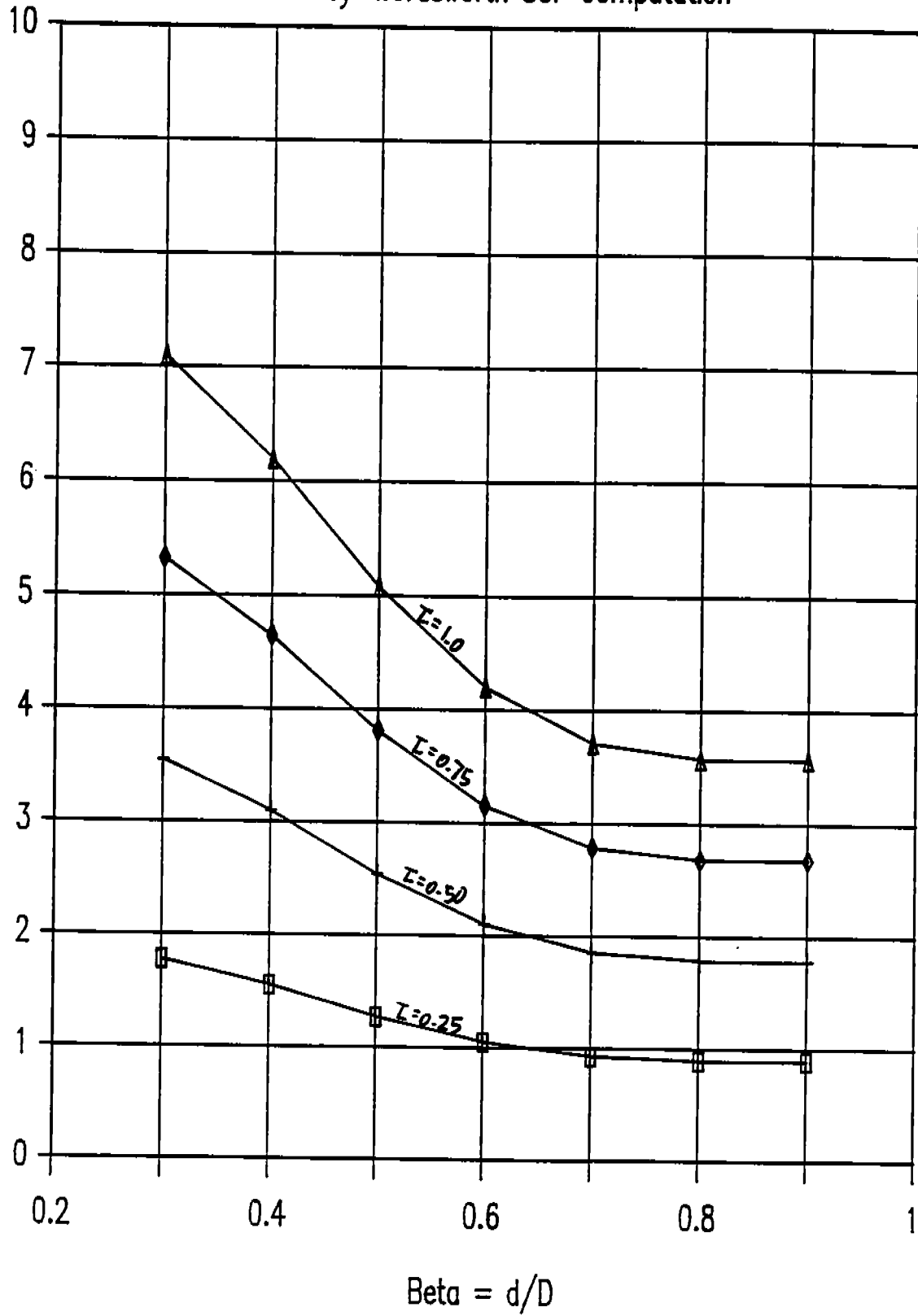
C.3.1(e) Smedley-Wordsworth Chord SCF's for X-Joints

The Smedley-Wordsworth chord SCF's for X-joints are shown on the following pages. The following parameters are assumed for the Smedley-Wordsworth figures:

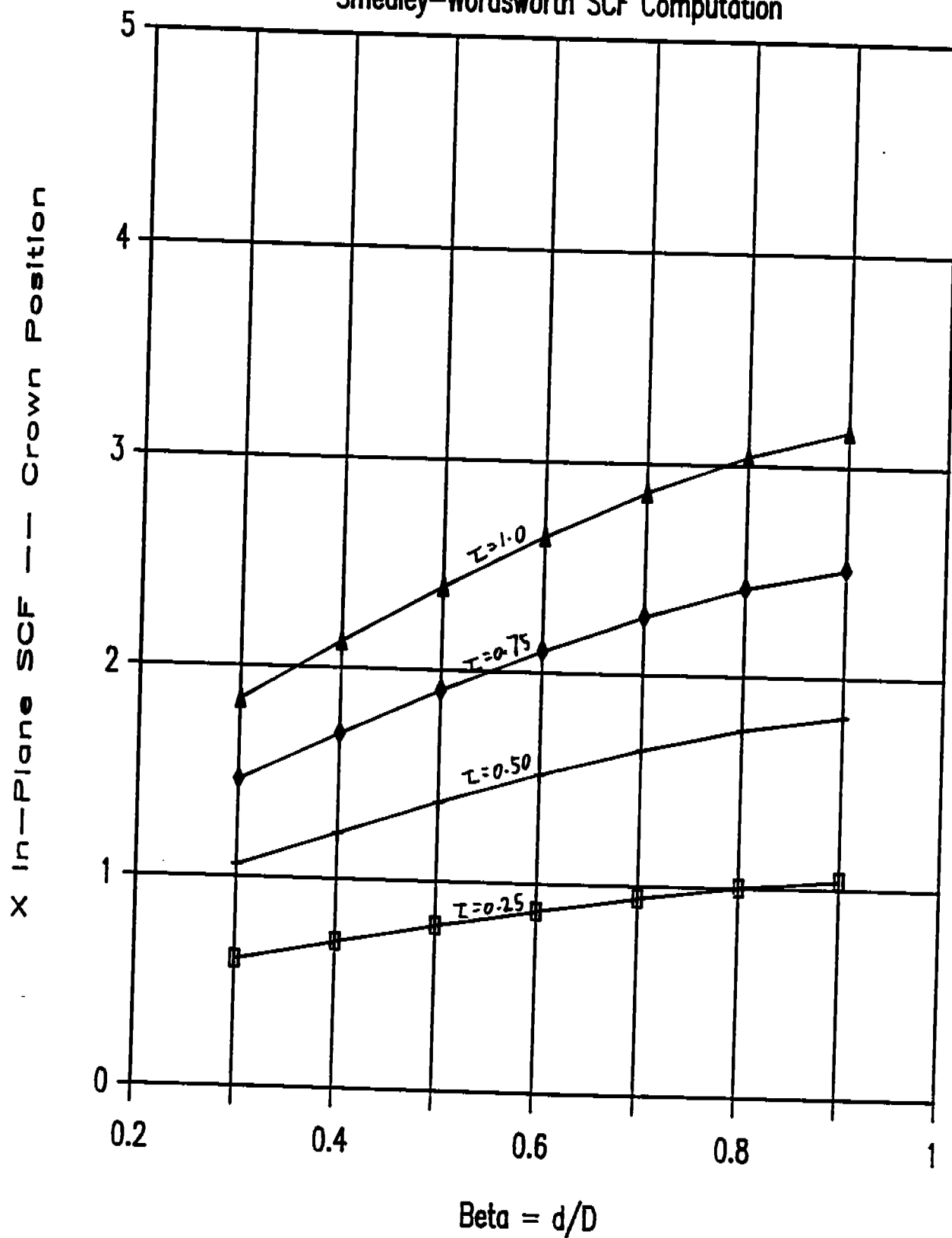
- 1) $\gamma = D/2T = 12.0$
- 2) $\theta = \quad = 30.0$ degrees
- 3) $\alpha = D/L = 35.0$

The Shell d/D limitations have not been imposed for the SCF calculation.

Smedley-Wordsworth SCF Computation

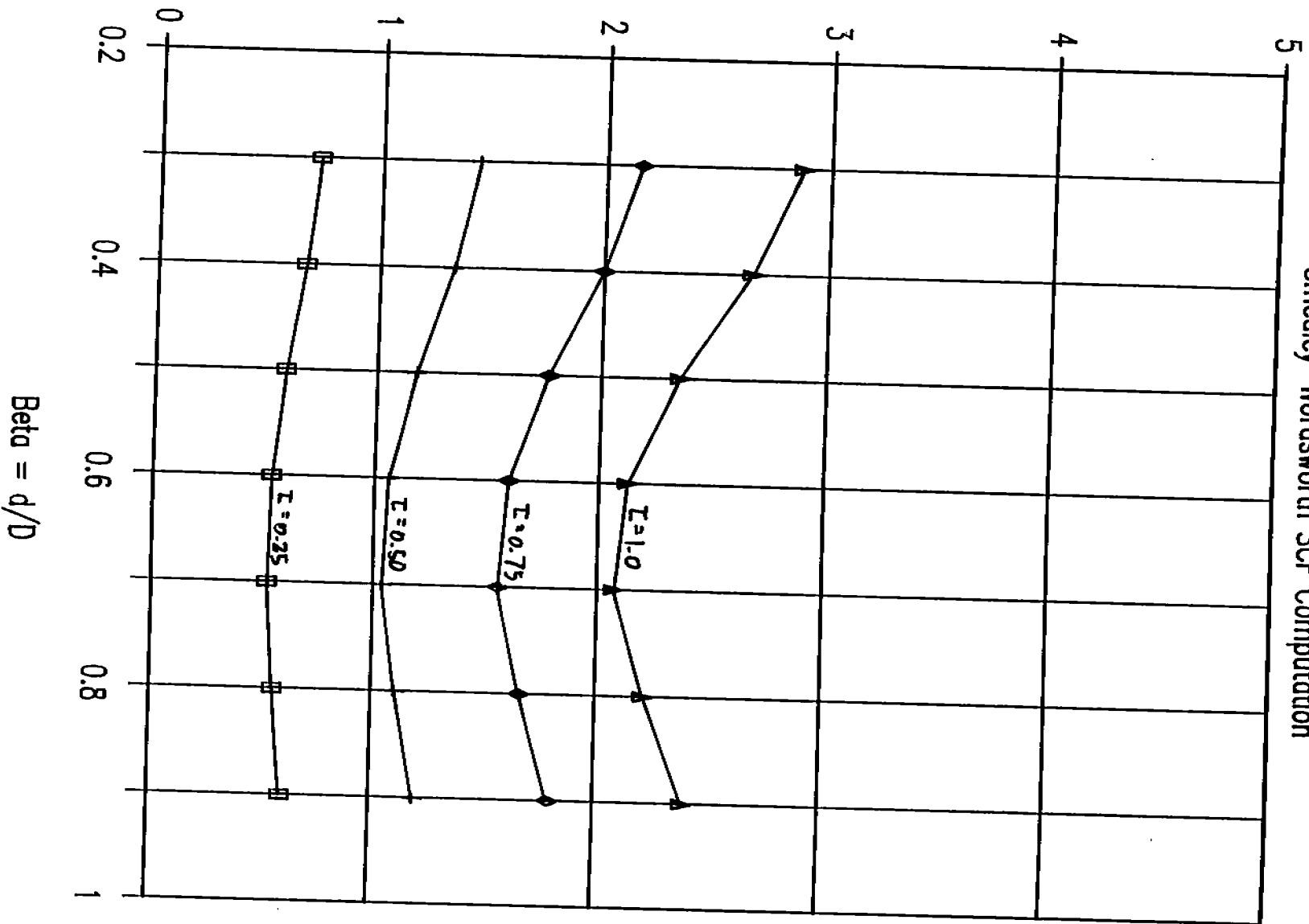


Smedley-Wordsworth SCF Computation



X Out-Plane SCF — Saddle Position

Smedley-Wordsworth SCF Computation



C.3.2 Tables

The Kuang and Smedley-Wordsworth chord stress Concentration factors for T joints are shown in Section C.3.2(a) and C.3.2(b), respectively. Since the chord side of the weld stress Concentration factor is generally higher than the brace side of the weld stress Concentration factor, only the chord side of the weld stress Concentration factors are shown.

C.3.2(a) Kuang Chord SCF's for T-Joints

The Kuang chord SCF's for T-joints are shown on the following pages. The following parameters are assumed for the Kuang figures:

$$1) \quad \alpha = D/L = 0.0571$$

Kuang SCF Computation

T-joint Axial SCF
Chord Side of Weld

Theta =	Tau = t/T	Gamma = 12.0				Gamma = 15.0				Gamma = 20.0				Gamma = 25.0			
		Beta =d/D				Beta =d/D				Beta =d/D				Beta =d/D			
		0.3	0.5	0.7	0.9	0.3	0.5	0.7	0.9	0.3	0.5	0.7	0.9	0.3	0.5	0.7	0.9
	0.20	0.632	0.562	0.432	0.272	0.757	0.673	0.518	0.326	0.955	0.849	0.654	0.411	1.144	1.017	0.783	0.492
30.0 deg 0.524 rad	0.40	1.593	1.416	1.090	0.686	1.908	1.696	1.306	0.821	2.407	2.140	1.648	1.037	2.883	2.563	1.973	1.241
	0.60	2.736	2.432	1.872	1.178	3.276	2.913	2.242	1.411	4.134	3.675	2.829	1.780	4.950	4.401	3.388	2.132
	0.80	4.014	3.569	2.747	1.729	4.808	4.274	3.290	2.070	6.066	5.393	4.151	2.612	7.264	6.458	4.972	3.128
	0.20	1.137	1.011	0.778	0.490	1.362	1.211	0.932	0.586	1.719	1.528	1.176	0.740	2.058	1.830	1.409	0.886
45.0 deg 0.785 rad	0.40	2.866	2.548	1.961	1.234	3.432	3.052	2.349	1.478	4.331	3.850	2.964	1.865	5.187	4.611	3.550	2.233
	0.60	4.921	4.375	3.368	2.119	5.893	5.239	4.033	2.538	7.436	6.611	5.089	3.202	8.905	7.917	6.094	3.835
	0.80	7.221	6.420	4.942	3.110	8.648	7.688	5.919	3.724	10.91	9.700	7.467	4.699	13.06	11.61	8.943	5.627
	0.20	1.604	1.426	1.097	0.690	1.921	1.707	1.314	0.827	2.423	2.154	1.658	1.043	2.902	2.580	1.986	1.250
60.0 deg 1.047 rad	0.40	4.041	3.592	2.765	1.740	4.839	4.302	3.312	2.084	6.106	5.428	4.179	2.629	7.312	6.501	5.004	3.149
	0.60	6.938	6.168	4.748	2.988	8.308	7.387	5.686	3.578	10.48	9.320	7.174	4.514	12.55	11.16	8.592	5.406
	0.80	10.18	9.051	6.967	4.384	12.19	10.83	8.344	5.250	15.38	13.67	10.52	6.625	18.42	16.37	12.60	7.933
	0.20	2.046	1.819	1.400	0.881	2.451	2.179	1.677	1.055	3.092	2.749	2.116	1.331	3.703	3.292	2.534	1.595
90.0 deg 1.571 rad	0.40	5.156	4.584	3.528	2.220	6.175	5.489	4.226	2.659	7.790	6.926	5.332	3.355	9.330	8.295	6.385	4.018
	0.60	8.852	7.870	6.058	3.812	10.60	9.425	7.255	4.565	13.37	11.89	9.154	5.760	16.01	14.24	10.96	6.898
	0.80	12.98	11.54	8.890	5.594	15.55	13.83	10.64	6.699	19.62	17.44	13.43	8.452	23.50	20.89	16.08	10.12

Kuang SCF Computation

T-joint In-Plane SCF
Chord Side of Weld

		Gamma = 12.0				Gamma = 15.0				Gamma = 20.0				Gamma = 25.0			
Theta =	Tau = t/T	Beta =d/D															
		0.3	0.5	0.7	0.9	0.3	0.5	0.7	0.9	0.3	0.5	0.7	0.9	0.3	0.5	0.7	0.9
	0.20	10.551	0.540	0.533	0.528	10.631	0.618	0.610	0.603	10.749	0.734	0.724	0.717	10.857	0.840	0.828	0.820
30.0 deg	0.40	11.001	0.981	0.968	0.958	11.145	1.122	1.107	1.096	11.361	1.333	1.315	1.302	11.556	1.524	1.504	1.489
0.524 rad	0.60	11.419	1.391	1.372	1.358	11.623	1.590	1.569	1.553	11.929	1.890	1.864	1.846	12.205	2.160	2.131	2.110
	0.80	11.818	1.781	1.757	1.740	12.078	2.036	2.009	1.989	12.470	2.420	2.388	2.364	12.824	2.767	2.730	2.703
	0.20	10.672	0.658	0.650	0.643	10.768	0.753	0.743	0.735	10.913	0.895	0.883	0.874	11.044	1.023	1.009	0.999
45.0 deg	0.40	11.220	1.195	1.179	1.168	11.395	1.367	1.349	1.335	11.658	1.624	1.603	1.587	11.896	1.857	1.832	1.814
0.785 rad	0.60	11.729	1.694	1.672	1.655	11.977	1.937	1.911	1.892	12.350	2.302	2.272	2.249	12.687	2.632	2.597	2.571
	0.80	12.215	2.170	2.141	2.120	12.532	2.481	2.448	2.424	13.010	2.949	2.909	2.880	13.441	3.371	3.326	3.293
	0.20	10.754	0.739	0.729	0.722	10.863	0.845	0.834	0.825	11.025	1.004	0.991	0.981	11.172	1.148	1.133	1.122
60.0 deg	0.40	11.370	1.342	1.324	1.311	11.566	1.534	1.514	1.499	11.861	1.823	1.799	1.781	12.128	2.065	2.057	2.036
1.047 rad	0.60	11.941	1.902	1.877	1.858	12.220	2.175	2.146	2.124	12.638	2.585	2.550	2.524	13.016	2.955	2.915	2.886
	0.80	12.486	2.436	2.404	2.380	12.843	2.785	2.748	2.721	13.378	3.310	3.266	3.233	13.863	3.784	3.734	3.696
	0.20	10.819	0.802	0.792	0.784	10.936	0.917	0.905	0.896	11.113	1.090	1.076	1.065	11.272	1.247	1.230	1.218
90.0 deg	0.40	11.487	1.457	1.437	1.423	11.700	1.665	1.643	1.627	12.020	1.979	1.953	1.933	12.310	2.263	2.233	2.210
1.571 rad	0.60	12.107	2.065	2.037	2.017	12.409	2.361	2.329	2.306	12.863	2.805	2.768	2.740	13.274	3.207	3.164	3.133
	0.80	12.699	2.644	2.609	2.583	13.086	3.023	2.983	2.953	13.667	3.593	3.545	3.509	14.193	4.108	4.053	4.012

	Sigma = 12.0					Sigma = 15.0					Sigma = 20.0					Sigma = 25.0				
Theta =	Beta =/D					Beta =/D					Beta =/D					Beta =/D				
Tau =	0.3	0.55	0.56	0.75	0.3	0.55	0.56	0.75	0.3	0.55	0.56	0.75	0.3	0.55	0.56	0.75				
30.0 deg	0.198	0.158	0.668	0.557	10.502	0.809	0.639	0.699	10.672	1.084	1.122	0.936	10.843	1.359	1.407	1.174				
0.524 rad	0.40	10.182	0.293	1.238	1.033	10.930	1.499	1.552	1.295	11.246	2.007	2.078	1.734	11.562	2.517	2.606	2.174			
0.60	10.260	0.420	1.775	1.481	11.334	2.150	2.226	1.838	11.786	2.878	2.980	2.487	12.240	3.609	3.737	3.118				
0.80	10.337	0.543	2.282	1.913	11.723	2.777	2.875	2.399	12.307	3.717	3.848	3.212	12.893	4.662	4.826	4.027				
45.0 deg	0.168	0.271	1.146	0.957	10.862	1.389	1.438	1.200	11.154	1.839	1.925	1.606	11.447	2.331	2.413	2.014				
0.765 rad	0.40	10.312	0.503	2.123	1.772	11.596	2.572	2.663	2.222	12.137	3.443	3.565	2.975	12.680	4.318	4.470	3.730			
0.60	10.447	0.721	3.045	2.541	12.289	3.688	3.818	3.187	13.064	4.938	5.112	4.266	13.843	6.192	6.410	5.349				
0.80	10.578	0.931	3.933	3.282	12.956	4.763	4.931	4.115	13.939	6.377	6.602	5.510	14.963	7.996	8.278	6.999				
60.0 deg	0.231	0.372	1.572	1.312	11.182	1.904	1.971	1.645	11.582	2.549	2.639	2.282	11.984	3.197	3.309	2.762				
1.047 rad	0.40	10.428	0.689	2.912	2.430	12.189	3.527	3.631	3.047	12.930	4.722	4.888	4.079	13.674	5.921	6.129	5.115			
0.60	10.613	0.989	4.175	3.485	13.139	5.038	5.236	4.370	14.202	6.771	7.009	5.850	15.269	8.490	8.789	7.335				
0.80	10.792	1.277	5.392	4.500	14.054	6.532	6.762	5.643	15.427	9.744	9.982	7.935	16.805	10.96	11.35	9.473				
90.0 deg	0.289	0.465	1.967	1.641	11.478	2.382	2.466	2.038	11.979	3.189	3.302	2.755	12.482	3.999	4.140	3.455				
1.571 rad	0.40	10.535	0.862	3.643	3.040	12.738	4.412	4.568	3.812	13.666	5.907	6.115	5.103	14.597	7.407	7.668	6.399			
0.60	10.767	1.237	5.224	4.339	13.927	6.327	6.530	5.467	15.257	8.471	8.789	7.318	16.592	10.62	10.99	9.177				
0.80	10.991	1.597	6.746	5.630	15.071	8.171	8.439	7.060	16.789	10.93	11.32	9.451	18.513	13.71	14.20	11.85				

C.3.2(b) Smedley-Wordsworth Chord SCF's for T-Joints

The Smedley-Wordsworth chord SCF's for T-joints are shown on the following pages. The following parameters are assumed for the Smedley-Wordsworth figures:

$$1) \quad \alpha = 2L/D = 35.0$$

The Shell d/D limitations have not been imposed for the SCF calculation.

Wordsworth-Seedley SCF Computation

T-joint Axial SCF Crown Position

		Gamma = 12.0				Gamma = 15.0				Gamma = 20.0				Gamma = 25.0			
Theta =	Tau =	Beta =d/D															
	t/T	0.3	0.5	0.7	0.9	0.3	0.5	0.7	0.9	0.3	0.5	0.7	0.9	0.3	0.5	0.7	0.9
	0.25	12.847	3.058	3.203	3.283	12.928	3.081	3.177	3.218	13.069	3.148	3.180	3.166	13.207	3.228	3.206	3.145
30.0 deg	0.50	15.223	5.799	6.084	6.094	15.296	5.719	5.907	5.871	15.492	5.734	5.793	5.678	15.716	5.823	5.775	5.583
0.524 rad	0.75	18.185	9.361	9.793	9.527	18.140	9.012	9.291	9.015	18.276	8.808	8.891	8.552	18.516	8.807	8.730	8.308
	1.00	111.80	13.88	14.49	13.71	111.53	13.08	13.46	12.75	111.48	12.46	12.57	11.87	111.66	12.26	12.15	11.38
	0.25	13.194	3.607	3.961	4.258	13.278	3.627	3.925	4.175	13.425	3.694	3.920	4.105	13.567	3.774	3.942	4.074
45.0 deg	0.50	15.771	6.724	7.433	7.909	15.875	6.670	7.267	7.672	16.106	6.714	7.165	7.466	16.354	6.821	7.157	7.364
0.785 rad	0.75	18.785	10.47	11.54	12.03	18.829	10.21	11.11	11.54	19.059	10.11	10.78	11.10	19.359	10.16	10.67	10.87
	1.00	112.29	14.96	16.43	16.75	112.19	14.36	15.58	15.88	112.33	13.96	14.87	15.09	112.62	13.88	14.55	14.66
	0.25	13.218	3.814	4.364	4.868	13.294	3.827	4.320	4.772	13.428	3.884	4.304	4.690	13.557	3.954	4.318	4.651
60.0 deg	0.50	15.749	7.026	8.128	9.058	15.869	7.001	7.986	8.830	16.104	7.063	7.905	8.631	16.345	7.175	7.903	8.531
1.047 rad	0.75	18.523	10.60	12.27	13.52	18.643	10.47	11.95	13.10	18.933	10.46	11.72	12.73	19.256	10.57	11.66	12.54
	1.00	111.57	14.63	16.88	18.33	111.65	14.30	16.29	17.65	111.94	14.14	15.83	17.03	112.32	14.19	15.65	16.71
	0.25	13.084	3.868	4.609	5.308	13.138	3.862	4.547	5.196	13.240	3.892	4.511	5.097	13.343	3.941	4.509	5.046
90.0 deg	0.50	15.569	7.205	8.690	10.02	15.658	7.158	8.530	9.778	15.842	7.184	8.422	9.558	16.035	7.262	8.397	9.443
1.571 rad	0.75	18.220	10.81	13.05	14.93	18.315	10.67	12.73	14.51	18.550	10.64	12.50	14.13	18.814	10.71	12.41	13.93
	1.00	111.06	14.76	17.76	20.10	111.14	14.45	17.22	19.45	111.39	14.30	16.78	18.86	111.70	14.33	16.60	18.54

Wordsworth-Smedley SCF Computation

T-joint Axial SCF Saddle Position

Theta =	Tau = t/T	Gamma = 12.0				Gamma = 15.0				Gamma = 20.0				Gamma = 25.0			
		Beta =d/D				Beta =d/D				Beta =d/D				Beta =d/D			
		0.3	0.5	0.7	0.9	0.3	0.5	0.7	0.9	0.3	0.5	0.7	0.9	0.3	0.5	0.7	0.9
	0.25	10.892	0.973	0.770	0.402	11.115	1.216	0.963	0.502	11.487	1.622	1.284	0.670	11.858	2.028	1.606	0.838
30.0 deg 0.524 rad	0.50	11.784	1.946	1.541	0.804	12.230	2.433	1.927	1.005	12.974	3.244	2.569	1.340	13.717	4.056	3.212	1.676
	0.75	12.676	2.920	2.312	1.206	13.346	3.650	2.890	1.508	14.461	4.867	3.854	2.011	15.576	6.084	4.818	2.514
	1.00	13.569	3.893	3.083	1.609	14.461	4.867	3.854	2.011	15.948	6.489	5.139	2.681	17.435	8.112	6.424	3.352
	0.25	11.618	1.808	1.510	0.865	12.023	2.260	1.887	1.081	12.698	3.014	2.516	1.442	13.372	3.768	3.146	1.602
45.0 deg 0.785 rad	0.50	13.237	3.617	3.020	1.730	14.047	4.521	3.775	2.163	15.396	6.028	5.033	2.884	16.745	7.536	6.292	3.605
	0.75	14.856	5.426	4.530	2.596	16.070	6.782	5.662	3.245	18.094	9.043	7.550	4.326	19.11	11.30	9.438	5.408
	1.00	16.475	7.234	6.040	3.461	18.094	9.043	7.550	4.326	19.79	12.05	10.06	5.768	21.49	15.07	12.58	7.211
	0.25	12.293	2.598	2.237	1.354	12.867	3.248	2.797	1.693	13.823	4.331	3.729	2.257	14.778	5.413	4.662	2.821
60.0 deg 1.047 rad	0.50	14.587	5.197	4.475	2.709	15.734	6.496	5.594	3.386	17.646	8.662	7.459	4.515	19.557	10.82	9.324	5.643
	0.75	16.881	7.795	6.713	4.063	18.601	9.744	8.391	5.079	19.46	12.99	11.18	6.772	21.433	16.24	13.98	8.465
	1.00	19.175	10.39	8.951	5.418	19.46	12.99	11.18	6.772	21.29	17.32	14.91	9.030	23.11	21.65	18.64	11.28
	0.25	12.937	3.360	2.958	1.861	13.671	4.200	3.697	2.326	14.895	5.600	4.930	3.102	16.119	7.001	6.162	3.878
90.0 deg 1.571 rad	0.50	15.874	6.721	5.916	3.723	17.343	8.401	7.395	4.653	19.790	11.20	9.860	6.205	22.23	14.00	12.32	7.756
	0.75	18.811	10.08	8.874	5.584	19.101	12.60	11.09	6.980	21.68	16.80	14.79	9.307	24.35	21.00	18.48	11.63
	1.00	21.74	13.44	11.83	7.446	21.68	16.80	14.79	9.307	24.58	22.40	19.72	12.41	26.47	28.00	24.65	15.51

Wordsworth-Saedley SCF Computation

T-joint In-Plane SCF Crown Position

Theta =	Tau = t/T	Gamma = 12.0				Gamma = 15.0				Gamma = 20.0				Gamma = 25.0			
		Beta =d/D				Beta =d/D				Beta =d/D				Beta =d/D			
		0.3	0.5	0.7	0.9	0.3	0.5	0.7	0.9	0.3	0.5	0.7	0.9	0.3	0.5	0.7	0.9
	0.25	0.607	0.791	0.946	1.044	0.694	0.905	1.081	1.194	0.825	1.075	1.285	1.419	0.943	1.229	1.469	1.623
30.0 deg 0.524 rad	0.50	1.057	1.378	1.647	1.819	1.209	1.575	1.883	2.080	1.437	1.872	2.238	2.471	1.642	2.141	2.558	2.826
	0.75	1.462	1.906	2.278	2.516	1.672	2.179	2.604	2.877	1.987	2.590	3.095	3.419	2.272	2.961	3.539	3.908
	1.00	1.841	2.399	2.868	3.167	2.105	2.743	3.278	3.621	2.501	3.260	3.896	4.303	2.860	3.727	4.455	4.920
	0.25	0.865	1.009	1.079	1.066	0.989	1.153	1.233	1.219	1.175	1.370	1.466	1.449	1.343	1.567	1.676	1.657
45.0 deg 0.785 rad	0.50	1.506	1.756	1.879	1.857	1.721	2.008	2.148	2.123	2.046	2.386	2.553	2.523	2.339	2.728	2.918	2.885
	0.75	2.083	2.429	2.599	2.569	2.381	2.778	2.971	2.937	2.830	3.301	3.531	3.490	3.235	3.774	4.037	3.991
	1.00	2.622	3.058	3.271	3.234	2.998	3.497	3.740	3.697	3.562	4.155	4.445	4.394	4.073	4.751	5.082	5.023
	0.25	1.063	1.162	1.165	1.080	1.216	1.329	1.332	1.234	1.445	1.579	1.583	1.467	1.652	1.806	1.810	1.677
60.0 deg 1.047 rad	0.50	1.852	2.024	2.029	1.880	2.117	2.314	2.320	2.149	2.516	2.750	2.757	2.554	2.876	3.144	3.152	2.920
	0.75	2.561	2.800	2.807	2.600	2.928	3.201	3.209	2.973	3.480	3.804	3.814	3.533	3.979	4.350	4.360	4.039
	1.00	3.224	3.525	3.533	3.273	3.686	4.030	4.040	3.742	4.381	4.789	4.801	4.448	5.009	5.475	5.489	5.085
	0.25	1.231	1.286	1.231	1.089	1.408	1.470	1.407	1.245	1.673	1.747	1.672	1.480	1.913	1.997	1.912	1.692
90.0 deg 1.571 rad	0.50	2.144	2.239	2.143	1.896	2.452	2.559	2.450	2.168	2.914	3.042	2.912	2.576	3.331	3.478	3.329	2.946
	0.75	2.966	3.097	2.965	2.623	3.391	3.540	3.389	2.999	4.030	4.207	4.028	3.564	4.608	4.810	4.605	4.074
	1.00	3.734	3.898	3.732	3.302	4.269	4.457	4.267	3.775	5.073	5.296	5.070	4.486	5.800	6.055	5.797	5.129

Wordsworth-Saedley SCF Computation

T-joint Out-of-Plane SCF Saddle Position

Theta =	Tau = t/T	Gamma = 12.0				Gamma = 15.0				Gamma = 20.0				Gamma = 25.0			
		Beta =d/D				Beta =d/D				Beta =d/D				Beta =d/D			
		0.3	0.5	0.7	0.9	0.3	0.5	0.7	0.9	0.3	0.5	0.7	0.9	0.3	0.5	0.7	0.9
	0.25	10.529	0.773	0.825	0.556	10.662	0.967	1.031	0.695	10.883	1.289	1.375	0.927	11.103	1.612	1.719	1.159
30.0 deg 0.524 rad	0.50	11.059	1.547	1.650	1.112	11.324	1.934	2.062	1.390	11.766	2.579	2.750	1.854	12.207	3.224	3.438	2.318
	0.75	11.589	2.321	2.475	1.669	11.986	2.902	3.094	2.086	12.649	3.869	4.125	2.781	13.311	4.837	5.157	3.477
	1.00	12.119	3.095	3.300	2.225	12.649	3.869	4.125	2.781	13.532	5.159	5.500	3.709	14.415	6.449	6.876	4.636
	0.25	10.872	1.347	1.561	1.176	11.090	1.684	1.951	1.470	11.454	2.245	2.602	1.960	11.818	2.807	3.252	2.450
45.0 deg 0.785 rad	0.50	11.745	2.694	3.122	2.352	12.181	3.368	3.903	2.940	12.908	4.491	5.204	3.920	13.636	5.614	6.505	4.900
	0.75	12.618	4.042	4.683	3.528	13.272	5.053	5.854	4.410	14.363	6.737	7.806	5.880	15.454	8.421	9.757	7.351
	1.00	13.490	5.389	6.245	4.704	14.363	6.737	7.806	5.880	15.817	8.983	10.40	7.841	17.272	11.22	13.01	9.801
	0.25	11.168	1.863	2.267	1.822	11.460	2.329	2.833	2.278	11.947	3.106	3.778	3.037	12.434	3.882	4.723	3.796
60.0 deg 1.047 rad	0.50	12.337	3.727	4.534	3.644	12.921	4.659	5.667	4.556	13.895	6.212	7.557	6.074	14.868	7.765	9.446	7.593
	0.75	13.505	5.591	6.801	5.467	14.382	6.989	8.501	6.834	15.842	9.318	11.33	9.112	17.303	11.64	14.16	11.39
	1.00	14.674	7.455	9.068	7.289	15.842	9.318	11.33	9.112	17.790	12.42	15.11	12.14	19.737	15.53	18.89	15.18
	0.25	11.437	2.346	2.954	2.486	11.796	2.932	3.692	3.108	12.395	3.910	4.923	4.144	12.994	4.887	6.154	5.180
90.0 deg 1.571 rad	0.50	12.874	4.692	5.908	4.973	13.593	5.865	7.385	6.216	14.791	7.820	9.847	8.288	15.989	9.775	12.30	10.36
	0.75	14.312	7.038	8.862	7.459	15.390	8.797	11.07	9.324	17.187	11.73	14.77	12.43	18.984	14.66	18.46	15.54
	1.00	15.749	9.384	11.81	9.946	17.187	11.73	14.77	12.43	19.583	15.64	19.69	16.57	111.97	19.55	24.61	20.72

Kuang SCF Computation

K-joint Axial SCF
Chord Side of Weld

Theta =	Tau = t/T	Gamma = 12.0				Gamma = 15.0				Gamma = 20.0				Gamma = 25.0			
		Beta =d/D				Beta =d/D				Beta =d/D				Beta =d/D			
		0.3	0.5	0.7	0.9	0.3	0.5	0.7	0.9	0.3	0.5	0.7	0.9	0.3	0.5	0.7	0.9
	0.20	10.427	0.414	0.406	0.400	10.495	0.481	0.471	0.464	10.600	0.582	0.571	0.562	10.696	0.676	0.662	0.653
30.0 deg 0.524 rad	0.40	10.918	0.891	0.873	0.860	11.065	1.034	1.013	0.998	11.290	1.252	1.227	1.209	11.497	1.453	1.424	1.403
	0.60	11.437	1.394	1.367	1.347	11.667	1.618	1.586	1.562	12.019	1.959	1.921	1.892	12.343	2.273	2.229	2.196
	0.80	11.974	1.915	1.878	1.850	12.290	2.222	2.179	2.147	12.774	2.692	2.639	2.600	13.219	3.123	3.062	3.017
	0.20	10.724	0.702	0.688	0.678	10.840	0.815	0.799	0.787	11.017	0.987	0.967	0.953	11.180	1.145	1.122	1.106
45.0 deg 0.785 rad	0.40	11.556	1.510	1.480	1.458	11.805	1.751	1.717	1.692	12.186	2.121	2.080	2.049	12.537	2.461	2.413	2.378
	0.60	12.434	2.362	2.316	2.282	12.825	2.741	2.687	2.647	13.421	3.320	3.254	3.206	13.969	3.852	3.776	3.720
	0.80	13.345	3.245	3.182	3.135	13.881	3.765	3.691	3.637	14.700	4.561	4.471	4.405	15.453	5.291	5.187	5.111
	0.20	10.985	0.956	0.937	0.923	11.143	1.109	1.087	1.071	11.384	1.343	1.317	1.297	11.606	1.559	1.528	1.505
60.0 deg 1.047 rad	0.40	12.118	2.055	2.015	1.985	12.457	2.384	2.337	2.303	12.976	2.888	2.831	2.789	13.453	3.351	3.285	3.236
	0.60	13.314	3.215	3.152	3.106	13.845	3.731	3.657	3.604	14.657	4.519	4.430	4.365	15.403	5.243	5.140	5.064
	0.80	14.553	4.418	4.331	4.267	15.282	5.126	5.025	4.951	16.398	6.208	6.086	5.996	17.423	7.203	7.061	6.957
	0.20	11.226	1.190	1.166	1.149	11.423	1.380	1.353	1.333	11.723	1.672	1.639	1.615	11.999	1.940	1.902	1.874
90.0 deg 1.571 rad	0.40	12.636	2.558	2.507	2.470	13.058	2.968	2.909	2.866	13.704	3.594	3.524	3.472	14.298	4.170	4.088	4.028
	0.60	14.124	4.002	3.923	3.866	14.785	4.643	4.552	4.485	15.796	5.624	5.513	5.432	16.725	6.525	6.397	6.303
	0.80	15.666	5.498	5.390	5.311	16.574	6.379	6.254	6.162	17.963	7.726	7.575	7.463	19.239	8.965	8.788	8.659

Kuang SCF Computation

K-joint In-Plane SCF
Chord Side of Weld

		Gamma = 12.0				Gamma = 15.0				Gamma = 20.0				Gamma = 25.0			
Theta =	Tau = t/T	Beta =d/D															
		0.3	0.5	0.7	0.9	0.3	0.5	0.7	0.9	0.3	0.5	0.7	0.9	0.3	0.5	0.7	0.9
	0.20	10.514	0.530	0.541	0.549	10.559	0.577	0.589	0.598	10.624	0.644	0.657	0.667	10.679	0.700	0.715	0.726
30.0 deg: 0.524 rad:	0.40	10.986	1.017	1.038	1.054	11.074	1.107	1.130	1.147	11.198	1.235	1.260	1.279	11.304	1.344	1.372	1.393
	0.60	11.444	1.489	1.520	1.543	11.572	1.621	1.654	1.679	11.754	1.808	1.845	1.873	11.909	1.968	2.008	2.039
	0.80	11.893	1.952	1.992	2.022	12.060	2.124	2.168	2.201	12.298	2.370	2.418	2.455	12.502	2.580	2.632	2.672
	0.20	10.702	0.724	0.739	0.750	10.764	0.788	0.804	0.816	10.853	0.879	0.897	0.911	10.928	0.957	0.977	0.991
45.0 deg: 0.785 rad:	0.40	11.348	1.390	1.418	1.439	11.467	1.513	1.543	1.567	11.636	1.687	1.722	1.748	11.781	1.837	1.874	1.903
	0.60	11.973	2.034	2.076	2.107	12.148	2.214	2.260	2.294	12.396	2.470	2.521	2.559	12.608	2.689	2.744	2.786
	0.80	12.586	2.666	2.721	2.762	12.815	2.902	2.961	3.006	13.140	3.238	3.304	3.354	13.418	3.524	3.596	3.651
	0.20	10.843	0.869	0.887	0.900	10.917	0.946	0.965	0.980	11.023	1.055	1.077	1.093	11.114	1.149	1.172	1.190
60.0 deg: 1.047 rad:	0.40	11.617	1.668	1.702	1.728	11.761	1.815	1.852	1.881	11.964	2.025	2.066	2.098	12.138	2.204	2.249	2.284
	0.60	12.368	2.442	2.492	2.529	12.578	2.658	2.712	2.753	12.875	2.965	3.025	3.071	13.130	3.227	3.293	3.343
	0.80	13.103	3.200	3.265	3.315	13.378	3.483	3.554	3.608	13.768	3.886	3.965	4.025	14.102	4.230	4.316	4.382
	0.20	10.959	0.989	1.009	1.025	11.044	1.077	1.099	1.115	11.165	1.201	1.226	1.244	11.268	1.308	1.334	1.355
90.0 deg: 1.571 rad:	0.40	11.841	1.898	1.937	1.966	12.004	2.066	2.108	2.141	12.236	2.305	2.352	2.388	12.433	2.509	2.560	2.599
	0.60	12.695	2.779	2.836	2.879	12.934	3.025	3.087	3.134	13.273	3.375	3.444	3.496	13.563	3.673	3.748	3.805
	0.80	13.532	3.642	3.717	3.773	13.845	3.965	4.046	4.107	14.289	4.423	4.513	4.582	14.669	4.814	4.913	4.987

Kuang SCF Computation

K-joint Out-of-Plane SCF
Chord Side of Weld

		Gamma = 12.0				Gamma = 15.0				Gamma = 20.0				Gamma = 25.0			
Theta =	Tau =	Beta =d/D															
	t/T	0.3	0.55	0.56	0.75	0.3	0.55	0.56	0.75	0.3	0.55	0.56	0.75	0.3	0.55	0.56	0.75
	0.20	0.400	0.645	0.668	0.557	0.502	0.809	0.838	0.699	0.672	1.084	1.122	0.936	0.843	1.359	1.407	1.174
30.0 deg	0.40	0.742	1.196	1.238	1.033	0.930	1.499	1.552	1.295	1.1246	2.007	2.078	1.734	1.562	2.517	2.606	2.174
0.524 rad	0.60	1.064	1.715	1.775	1.481	1.334	2.150	2.226	1.858	1.786	2.878	2.980	2.487	2.240	3.609	3.737	3.118
	0.80	1.374	2.214	2.292	1.913	1.723	2.777	2.875	2.399	2.307	3.717	3.848	3.212	2.893	4.662	4.826	4.027
	0.20	0.687	1.107	1.146	0.957	0.862	1.389	1.438	1.200	1.154	1.859	1.925	1.606	1.447	2.331	2.413	2.014
45.0 deg	0.40	1.273	2.051	2.123	1.772	1.596	2.572	2.663	2.222	2.137	3.443	3.565	2.975	2.680	4.318	4.470	3.730
0.785 rad	0.60	1.825	2.941	3.045	2.541	2.289	3.688	3.818	3.187	3.064	4.938	5.112	4.266	3.843	6.192	6.410	5.349
	0.80	2.357	3.799	3.933	3.282	2.956	4.763	4.931	4.115	3.958	6.377	6.602	5.510	4.963	7.996	8.278	6.909
	0.20	0.942	1.519	1.572	1.312	1.182	1.904	1.971	1.645	1.582	2.549	2.639	2.202	1.984	3.197	3.309	2.762
60.0 deg	0.40	1.745	2.813	2.912	2.430	2.189	3.527	3.651	3.047	2.930	4.722	4.888	4.079	3.674	5.921	6.129	5.115
1.047 rad	0.60	2.503	4.033	4.175	3.485	3.139	5.058	5.236	4.370	4.202	6.771	7.009	5.850	5.269	8.490	8.789	7.335
	0.80	3.233	5.209	5.392	4.500	4.054	6.532	6.762	5.643	5.427	8.744	9.052	7.555	6.805	10.96	11.35	9.473
	0.20	1.179	1.900	1.967	1.641	1.478	2.382	2.466	2.058	1.979	3.189	3.302	2.755	2.482	3.999	4.140	3.455
90.0 deg	0.40	2.184	3.519	3.643	3.040	2.738	4.412	4.568	3.812	3.666	5.907	6.115	5.103	4.597	7.407	7.668	6.399
1.571 rad	0.60	3.131	5.046	5.224	4.359	3.927	6.327	6.550	5.467	5.257	8.471	8.769	7.318	6.592	10.62	10.99	9.177
	0.80	4.044	6.517	6.746	5.630	5.071	8.171	8.459	7.060	6.789	10.93	11.32	9.451	8.513	13.71	14.20	11.85

Wordsworth-Saedley SCF Computation

K-joint Axial SCF Crown Position

		Gamma = 12.0				Gamma = 15.0				Gamma = 20.0				Gamma = 25.0			
Theta =	Tau = t/T	Beta =d/D															
		0.3	0.5	0.7	0.9	0.3	0.5	0.7	0.9	0.3	0.5	0.7	0.9	0.3	0.5	0.7	0.9
	0.25	10.762	0.841	0.768	0.582	10.881	0.973	0.888	0.673	11.063	1.173	1.071	0.811	11.229	1.356	1.238	0.938
30.0 deg	0.50	11.525	1.683	1.537	1.164	11.763	1.946	1.777	1.346	12.126	2.347	2.143	1.622	12.458	2.713	2.477	1.876
0.524 rad																	
30.0 deg	0.75	12.288	2.525	2.306	1.746	12.645	2.920	2.666	2.019	13.189	3.520	3.214	2.434	13.687	4.070	3.716	2.814
0.524 rad																	
	1.00	13.051	3.367	3.075	2.328	13.527	3.893	3.555	2.692	14.253	4.694	4.286	3.245	14.916	5.426	4.955	3.752
	0.25	10.907	1.001	0.914	0.692	11.048	1.157	1.057	0.800	11.264	1.395	1.274	0.964	11.461	1.613	1.473	1.115
45.0 deg	0.50	11.814	2.002	1.828	1.384	12.097	2.315	2.114	1.600	12.528	2.791	2.548	1.929	12.923	3.226	2.946	2.231
0.785 rad																	
45.0 deg	0.75	12.721	3.003	2.742	2.076	13.146	3.472	3.171	2.401	13.793	4.186	3.823	2.894	14.385	4.840	4.419	3.346
0.785 rad																	
	1.00	13.628	4.005	3.657	2.769	14.195	4.630	4.228	3.201	15.057	5.582	5.097	3.859	15.847	6.453	5.893	4.462
	0.25	11.321	1.458	1.331	1.008	11.527	1.685	1.539	1.165	11.841	2.032	1.856	1.405	12.129	2.349	2.145	1.624
60.0 deg	0.50	12.642	2.916	2.663	2.016	13.055	3.371	3.079	2.331	13.683	4.065	3.712	2.810	14.258	4.699	4.291	3.249
1.047 rad																	
30.0 deg	0.75	13.963	4.374	3.995	3.024	14.582	5.057	4.618	3.497	15.524	6.097	5.568	4.216	16.387	7.049	6.437	4.874
0.524 rad																	
	1.00	15.285	5.833	5.326	4.033	16.110	6.743	6.158	4.662	17.366	8.130	7.424	5.621	18.516	9.399	8.533	6.499
	0.25	11.282	1.415	1.293	0.979	11.483	1.637	1.494	1.131	11.788	1.973	1.802	1.364	12.067	2.281	2.083	1.577
90.0 deg	0.50	12.565	2.831	2.586	1.958	12.766	3.274	2.989	2.263	13.576	3.947	3.604	2.729	14.134	4.563	4.167	3.155
1.571 rad																	
45.0 deg	0.75	13.848	4.247	3.879	2.937	14.449	4.911	4.484	3.395	15.364	5.920	5.406	4.093	16.201	6.845	6.250	4.732
0.785 rad																	
	1.00	15.131	5.663	5.172	3.916	15.932	6.548	5.979	4.527	17.152	7.894	7.209	5.458	18.269	9.126	8.334	6.310

Wordsworth-Saedley SCF Computation

K-joint Axial SCF Saddle Position

		Gamma = 12.0				Gamma = 15.0				Gamma = 20.0				Gamma = 25.0			
Theta =	Tau = t/T	Beta =d/D															
		0.3	0.5	0.7	0.9	0.3	0.5	0.7	0.9	0.3	0.5	0.7	0.9	0.3	0.5	0.7	0.9
	0.25	0.531	0.579	0.458	0.239	0.614	0.670	0.530	0.276	0.723	0.788	0.624	0.325	0.799	0.871	0.690	0.360
30.0 deg	0.50	1.062	1.158	0.917	0.478	1.228	1.340	1.061	0.553	1.446	1.577	1.249	0.651	1.598	1.743	1.380	0.720
0.524 rad																	
30.0 deg	0.75	1.593	1.738	1.376	0.718	1.842	2.010	1.592	0.830	2.169	2.366	1.874	0.977	2.397	2.615	2.071	1.080
0.524 rad																	
	1.00	2.124	2.317	1.835	0.957	2.457	2.680	2.122	1.107	2.892	3.155	2.498	1.303	3.196	3.487	2.761	1.440
	0.25	0.963	1.076	0.898	0.515	1.114	1.245	1.039	0.595	1.311	1.465	1.223	0.701	1.449	1.619	1.352	0.774
45.0 deg	0.50	1.927	2.153	1.797	1.030	2.229	2.490	2.079	1.191	2.623	2.931	2.447	1.402	2.899	3.239	2.704	1.549
0.785 rad																	
45.0 deg	0.75	2.890	3.229	2.696	1.545	3.343	3.735	3.118	1.787	3.935	4.397	3.671	2.103	4.349	4.859	4.056	2.324
0.785 rad																	
	1.00	3.854	4.306	3.595	2.060	4.458	4.980	4.158	2.383	5.247	5.863	4.895	2.805	5.799	6.478	5.409	3.099
	0.25	1.323	1.539	1.399	0.916	1.520	1.779	1.633	1.086	1.769	2.090	1.955	1.331	1.930	2.305	2.200	1.537
60.0 deg	0.50	2.646	3.078	2.798	1.833	3.041	3.558	3.267	2.172	3.538	4.181	3.910	2.663	3.860	4.611	4.401	3.075
1.047 rad																	
30.0 deg	0.75	3.969	4.618	4.197	2.750	4.561	5.337	4.901	3.258	5.308	6.271	5.866	3.995	5.790	6.917	6.692	4.613
0.524 rad																	
	1.00	5.292	6.157	5.596	3.667	6.082	7.116	6.534	4.344	7.077	8.362	7.821	5.327	7.720	9.223	8.803	6.150
	0.25	1.714	1.994	1.817	1.207	1.975	2.305	2.115	1.420	2.308	2.710	2.517	1.719	2.530	2.992	2.615	1.960
90.0 deg	0.50	3.428	3.988	3.634	2.415	3.950	4.610	4.230	2.840	4.617	5.421	5.034	3.439	5.061	5.984	5.651	3.920
1.571 rad																	
45.0 deg	0.75	5.143	5.982	5.452	3.623	5.925	6.916	6.346	4.260	6.925	8.132	7.551	5.159	7.592	8.976	8.446	5.880
0.785 rad																	
	1.00	6.857	7.977	7.269	4.831	7.900	9.221	8.461	5.680	9.234	10.84	10.06	6.879	10.12	11.96	11.26	7.840

Wordsworth-Saedley SCF Computation

K-joint In-Plane SCF Crown Position

		Gamma = 12.0				Gamma = 15.0				Gamma = 20.0				Gamma = 25.0			
Theta =	Tau =	Beta =d/D															
	t/T	0.3	0.5	0.7	0.9	0.3	0.5	0.7	0.9	0.3	0.5	0.7	0.9	0.3	0.5	0.7	0.9
	0.25	10.607	0.791	0.946	1.044	10.694	0.905	1.081	1.194	10.825	1.075	1.265	1.419	10.943	1.227	1.469	1.623
30.0 deg	0.50	11.057	1.378	1.647	1.819	11.209	1.575	1.883	2.080	11.437	1.872	2.238	2.471	11.642	2.141	2.558	2.826
0.524 rad	0.75	11.462	1.906	2.278	2.516	11.672	2.179	2.604	2.877	11.987	2.590	3.095	3.419	12.272	2.961	3.539	3.908
	1.00	11.841	2.399	2.868	3.157	12.105	2.743	3.278	3.621	12.501	3.260	3.896	4.303	12.860	3.727	4.455	4.920
	0.25	10.865	1.009	1.079	1.066	10.989	1.153	1.233	1.219	11.175	1.370	1.466	1.449	11.343	1.567	1.676	1.657
45.0 deg	0.50	11.506	1.756	1.879	1.857	11.721	2.008	2.148	2.123	12.046	2.386	2.553	2.523	12.339	2.728	2.918	2.885
0.785 rad	0.75	12.083	2.429	2.599	2.569	12.381	2.778	2.971	2.937	12.830	3.301	3.531	3.490	13.235	3.774	4.037	3.991
	1.00	12.622	3.058	3.271	3.234	12.998	3.497	3.740	3.697	13.562	4.155	4.445	4.394	14.073	4.751	5.082	5.023
	0.25	11.063	1.162	1.165	1.080	11.216	1.329	1.332	1.234	11.445	1.579	1.583	1.467	11.652	1.806	1.810	1.677
60.0 deg	0.50	11.852	2.024	2.029	1.980	12.117	2.314	2.320	2.149	12.516	2.750	2.757	2.554	12.876	3.144	3.152	2.920
1.047 rad	0.75	12.561	2.800	2.807	2.600	12.928	3.201	3.209	2.973	13.480	3.604	3.614	3.533	13.979	4.350	4.360	4.039
	1.00	13.224	3.525	3.533	3.273	13.686	4.030	4.040	3.742	14.361	4.789	4.801	4.448	15.009	5.475	5.489	5.085
	0.25	11.231	1.286	1.231	1.089	11.408	1.470	1.407	1.245	11.673	1.747	1.672	1.480	11.913	1.997	1.912	1.692
90.0 deg	0.50	12.144	2.239	2.143	1.896	12.452	2.559	2.450	2.168	12.914	3.042	2.912	2.576	13.331	3.478	3.329	2.946
1.571 rad	0.75	12.966	3.097	2.965	2.623	13.391	3.540	3.389	2.999	14.030	4.207	4.028	3.564	14.608	4.810	4.605	4.074
	1.00	13.734	3.898	3.732	3.302	14.269	4.457	4.267	3.775	15.073	5.296	5.070	4.486	15.800	6.055	5.797	5.129

Wardsworth-Smedley SCF Computation

K-Joint Out-of-Plane SCF Saddle Position

		Gamma = 12.0				Gamma = 15.0				Gamma = 20.0				Gamma = 25.0				
Theta =		Tau =		Beta =d/D		Beta =d/D		Beta =d/D		Beta =d/D		Beta =d/D		Beta =d/D		Beta =d/D		
		t/T		0.3 0.5 0.7 0.9		0.3 0.5 0.7 0.9		0.3 0.5 0.7 0.9		0.3 0.5 0.7 0.9		0.3 0.5 0.7 0.9		0.3 0.5 0.7 0.9		0.3 0.5 0.7 0.9		
30.0 deg:		0.50	0.406	0.786	1.009	0.781	10.574	1.111	1.426	1.104	10.897	1.736	2.227	1.724	11.268	2.453	3.147	2.457
0.524 rad:		0.50	0.406	0.786	1.009	0.781	10.574	1.111	1.426	1.104	10.897	1.736	2.227	1.724	11.268	2.453	3.147	2.457
30.0 deg:		0.75	10.609	1.179	1.513	1.171	10.861	1.667	2.139	1.656	11.746	2.604	3.341	2.386	11.902	3.660	4.721	3.655
0.524 rad:		0.75	10.609	1.179	1.513	1.171	10.861	1.667	2.139	1.656	11.746	2.604	3.341	2.386	11.902	3.660	4.721	3.655
1.00		10.813	1.573	2.018	1.562	11.149	2.223	2.652	2.208	11.794	3.472	4.454	3.448	12.535	4.907	6.295	4.874	
45.0 deg:		0.25	10.334	0.684	0.954	0.825	10.473	0.967	1.349	1.167	10.739	1.511	2.107	1.822	11.044	2.135	2.977	2.576
0.785 rad:		0.25	10.334	0.684	0.954	0.825	10.473	0.967	1.349	1.167	10.739	1.511	2.107	1.822	11.044	2.135	2.977	2.576
45.0 deg:		0.50	10.669	1.339	1.909	1.651	10.946	1.935	2.698	2.334	11.478	3.022	4.214	3.645	12.089	4.271	5.955	5.152
0.785 rad:		0.50	10.669	1.339	1.909	1.651	10.946	1.935	2.698	2.334	11.478	3.022	4.214	3.645	12.089	4.271	5.955	5.152
45.0 deg:		0.75	11.004	2.054	2.863	2.477	11.419	2.902	4.047	3.501	12.217	4.534	6.321	5.468	13.133	6.407	8.933	7.728
0.785 rad:		0.75	11.004	2.054	2.863	2.477	11.419	2.902	4.047	3.501	12.217	4.534	6.321	5.468	13.133	6.407	8.933	7.728
1.00		11.339	2.738	3.818	3.303	11.892	3.870	5.396	4.668	12.956	6.045	8.428	7.291	14.178	8.543	11.91	10.30	
60.0 deg:		0.25	12.606	5.361	7.563	6.680	13.683	7.576	10.68	9.441	15.753	11.83	16.69	14.74	18.130	16.72	23.59	20.83
1.047 rad:		0.25	12.606	5.361	7.563	6.680	13.683	7.576	10.68	9.441	15.753	11.83	16.69	14.74	18.130	16.72	23.59	20.83
60.0 deg:		0.50	15.213	10.72	15.12	13.36	17.367	15.15	21.37	18.88	111.50	23.66	33.38	29.49	16.26	33.44	47.18	41.67
1.047 rad:		0.50	15.213	10.72	15.12	13.36	17.367	15.15	21.37	18.88	111.50	23.66	33.38	29.49	16.26	33.44	47.18	41.67
70.0 deg:		0.75	17.819	16.08	22.68	20.04	111.05	22.73	32.06	28.32	117.26	35.50	50.08	44.23	124.39	50.17	70.77	62.51
0.524 rad:		0.75	17.819	16.08	22.68	20.04	111.05	22.73	32.06	28.32	117.26	35.50	50.08	44.23	124.39	50.17	70.77	62.51
1.00		10.42	21.44	30.25	26.72	14.73	30.30	42.75	37.76	123.01	47.33	66.77	58.98	132.52	66.89	94.37	83.35	
90.0 deg:		0.25	13.545	7.507	11.04	10.28	15.010	10.60	15.60	14.53	17.826	16.57	24.37	22.70	111.06	23.41	34.45	32.08
1.571 rad:		0.25	13.545	7.507	11.04	10.28	15.010	10.60	15.60	14.53	17.826	16.57	24.37	22.70	111.06	23.41	34.45	32.08
90.0 deg:		0.50	17.091	15.01	22.08	20.57	10.02	21.21	31.21	29.07	115.65	33.14	48.75	45.41	122.12	46.83	68.90	64.17
1.571 rad:		0.50	17.091	15.01	22.08	20.57	10.02	21.21	31.21	29.07	115.65	33.14	48.75	45.41	122.12	46.83	68.90	64.17
45.0 deg:		0.75	10.63	22.52	33.13	30.85	15.03	31.92	46.82	43.61	123.47	49.71	73.13	68.11	133.18	70.23	103.3	96.26
0.785 rad:		0.75	10.63	22.52	33.13	30.85	15.03	31.92	46.82	43.61	123.47	49.71	73.13	68.11	133.18	70.23	103.3	96.26
1.00		14.18	30.03	44.17	41.14	20.04	42.43	62.42	59.14	131.30	66.28	97.50	90.82	144.24	93.67	137.8	128.3	

Wordsworth-Baedley SCF Computation

X-joint Axial SCF Saddle Position

		Gamma = 12.0				Gamma = 15.0				Gamma = 20.0				Gamma = 25.0			
Theta =	Tau = t/T	Beta =d/D															
		0.3	0.5	0.7	0.9	0.3	0.5	0.7	0.9	0.3	0.5	0.7	0.9	0.3	0.5	0.7	0.9
	0.25	11.775	1.269	0.926	0.893	12.218	1.587	1.157	1.116	12.958	2.116	1.543	1.488	13.697	2.645	1.929	1.860
30.0 deg 0.524 rad	0.50	13.550	2.539	1.852	1.786	14.437	3.174	2.315	2.232	15.916	4.232	3.087	2.977	17.395	5.290	3.859	3.721
	0.75	15.325	3.808	2.778	2.679	16.656	4.761	3.473	3.349	18.875	6.348	4.631	4.465	111.09	7.935	5.789	5.582
	1.00	17.100	5.078	3.705	3.572	18.875	6.348	4.631	4.465	111.83	8.464	6.175	5.954	114.79	10.58	7.718	7.443
	0.25	12.476	2.495	2.135	1.583	13.095	3.119	2.669	1.979	14.127	4.159	3.539	2.639	15.159	5.199	4.449	3.299
45.0 deg 0.785 rad	0.50	14.953	4.991	4.271	3.167	16.191	6.239	5.339	3.959	18.255	8.319	7.119	5.278	110.31	10.39	8.899	6.598
	0.75	17.430	7.487	6.407	4.750	19.287	9.358	8.009	5.938	112.38	12.47	10.67	7.918	115.47	15.59	13.34	9.897
	1.00	19.906	9.982	8.543	6.334	112.38	12.47	10.67	7.918	116.51	16.63	14.23	10.55	120.63	20.79	17.79	13.19
	0.25	13.009	3.705	3.482	2.213	13.761	4.632	4.352	2.767	15.015	6.176	5.803	3.689	16.269	7.720	7.254	4.612
60.0 deg 1.047 rad	0.50	16.019	7.411	6.964	4.427	17.523	9.264	8.705	5.534	110.03	12.35	11.60	7.379	112.53	15.44	14.50	9.224
	0.75	19.028	11.11	10.44	6.641	111.28	13.89	13.05	8.301	115.04	18.52	17.41	11.06	118.80	23.16	21.76	13.83
	1.00	112.03	14.82	13.92	8.855	115.04	18.52	17.41	11.06	120.06	24.70	23.21	14.75	125.07	30.58	29.01	18.44

Wordsworth-Swedley SCF Computation

X-joint In-Plane SCF Crown Position

Theta =	Tau = t/T	Gamma = 12.0				Gamma = 15.0				Gamma = 20.0				Gamma = 25.0			
		Beta =d/D				Beta =d/D				Beta =d/D				Beta =d/D			
		0.3	0.5	0.7	0.9	0.3	0.5	0.7	0.9	0.3	0.5	0.7	0.9	0.3	0.5	0.7	0.9
	0.25	0.607	0.791	0.946	1.044	0.694	0.905	1.061	1.194	0.825	1.075	1.265	1.419	0.943	1.229	1.469	1.623
30.0 deg 0.524 rad	0.50	1.057	1.378	1.647	1.819	1.209	1.575	1.983	2.060	1.437	1.972	2.238	2.471	1.642	2.141	2.558	2.826
	0.75	1.462	1.906	2.278	2.516	1.672	2.179	2.604	2.877	1.987	2.590	3.095	3.419	2.272	2.961	3.539	3.908
	1.00	1.941	2.399	2.868	3.167	2.105	2.743	3.278	3.621	2.501	3.260	3.896	4.303	2.860	3.727	4.455	4.920
	0.25	0.865	1.009	1.079	1.066	0.969	1.153	1.233	1.219	1.175	1.370	1.466	1.449	1.343	1.567	1.676	1.657
45.0 deg 0.785 rad	0.50	1.506	1.756	1.879	1.857	1.721	2.008	2.148	2.123	2.046	2.386	2.553	2.523	2.339	2.728	2.918	2.885
	0.75	2.083	2.429	2.599	2.569	2.381	2.778	2.971	2.937	2.830	3.301	3.531	3.490	3.235	3.774	4.037	3.991
	1.00	2.622	3.058	3.271	3.234	2.998	3.497	3.740	3.697	3.562	4.155	4.445	4.394	4.073	4.751	5.082	5.023
	0.25	1.063	1.162	1.165	1.080	1.216	1.329	1.332	1.234	1.445	1.579	1.583	1.467	1.652	1.806	1.810	1.677
60.0 deg 1.047 rad	0.50	1.852	2.024	2.029	1.980	2.117	2.314	2.320	2.149	2.516	2.750	2.757	2.554	2.876	3.144	3.152	2.920
	0.75	2.561	2.800	2.807	2.600	2.928	3.201	3.209	2.973	3.480	3.804	3.814	3.533	3.979	4.350	4.360	4.039
	1.00	3.224	3.525	3.533	3.273	3.686	4.030	4.040	3.742	4.381	4.789	4.801	4.448	5.009	5.475	5.489	5.085

Wordsworth-Saedley SCF Computation

X-joint Out-of-Plane SCF Saddle Position

		Gamma = 12.0				Gamma = 15.0				Gamma = 20.0				Gamma = 25.0			
Theta =	Tau = t/T	Beta =d/D															
		0.3	0.5	0.7	0.9	0.3	0.5	0.7	0.9	0.3	0.5	0.7	0.9	0.3	0.5	0.7	0.9
	0.25	10.719	0.587	0.519	0.599	10.899	0.734	0.648	0.749	11.199	0.979	0.865	0.999	11.498	1.224	1.081	1.248
30.0 deg	0.50	11.438	1.175	1.038	1.198	11.798	1.469	1.297	1.498	12.398	1.959	1.730	1.998	12.997	2.449	2.163	2.497
0.524 rad	0.75	12.158	1.763	1.557	1.798	12.698	2.204	1.946	2.247	13.597	2.939	2.595	2.997	14.496	3.674	3.244	3.746
	1.00	12.877	2.351	2.076	2.297	13.597	2.939	2.595	2.997	14.796	3.919	3.461	3.996	15.995	4.699	4.326	4.995
	0.25	11.003	1.155	1.197	1.062	11.254	1.444	1.496	1.328	11.673	1.926	1.995	1.771	12.091	2.407	2.494	2.214
45.0 deg	0.50	12.007	2.311	2.394	2.125	12.509	2.889	2.992	2.656	13.346	3.852	3.990	3.542	14.183	4.815	4.988	4.428
0.785 rad	0.75	13.011	3.466	3.591	3.188	13.764	4.333	4.489	3.985	15.019	5.778	5.985	5.313	16.274	7.222	7.482	6.642
	1.00	14.015	4.622	4.788	4.251	15.019	5.778	5.985	5.313	16.692	7.704	7.981	7.085	18.366	9.630	9.976	8.856
	0.25	11.219	1.715	1.951	1.485	11.524	2.144	2.439	1.857	12.033	2.859	3.252	2.476	12.541	3.574	4.066	3.095
60.0 deg	0.50	12.439	3.431	3.903	2.971	13.049	4.289	4.879	3.714	14.066	5.719	6.505	4.952	15.083	7.149	8.132	6.190
1.047 rad	0.75	13.659	5.147	5.855	4.457	14.574	6.434	7.318	5.571	16.099	8.579	9.758	7.428	17.624	10.72	12.19	9.285
	1.00	14.879	6.863	7.806	5.942	16.099	8.579	9.758	7.428	18.132	11.43	13.01	9.904	10.16	14.29	16.26	12.38

C.4 FINITE ELEMENT ANALYSES RESULTS

Finite element analyses were performed on the connections between the column tops and upper hull girders and between the corner columns and tubular bracing of the column-stabilized, twin-hulled semisubmersible. The overall geometry and locations of the two connections are indicated in Figures C.4-1 and C.4-2. Longitudinal and transverse girders (8.2 m deep) coincide with the column faces. The columns are 10.6 by 10.6 m in cross section.

Some dimensions of interest are:

Overall length	96.0 m
Overall width	65.0 m

Lower Hulls (two)

Length	96.0 m
Width	16.5 m
Depth	8.0 m

Stability Columns (six)

Size (square w/ rounded columns)	10.6x10.6 m
Transverse spacing (center-to-center)	54.0 m
Longitudinal spacing	33.0 m

Upper Hull

Length	77.0 m
Width	65.0 m
Depth	8.2 m

C.4.1 Column-Girder Connection

The location of the connection is shown in Figure C.4-1. The joint dimensions are given in Figure C.4-3. The loading analyzed was a combined axial, shear and moment load. The SCF is defined as:

MAXIMUM PRINCIPAL STRESS

$$\text{SCF} = \frac{\text{MAXIMUM PRINCIPAL STRESS}}{\text{NOMINAL STRESS IN GIRDER (P/A + M/S)}}$$

The moment M is due to a combination of moment and shear load.

The maximum SCF was found in the gusset plate connecting the transverse girder and column top, at the edge of the gusset plate in the weld between the gusset web and flange. It was equal to 1.66. The SCF in the longitudinal girder at the windlass cutouts reached a value of 1.87. Figure C.4-4 shows the equivalent stress variation over the entire connection. The maximum stress, as already noted, occurs in the crotch region. Figure C.4-5 shows an equivalent stress contour plot of the windlass holes. Table C.4-1 summarizes the SCFs.

MEMBER	LOCATION	DIRECTION TO WELD	SCF
Center Column Transverse	Middle of Gusset	Parallel	1.66
Girder-Column Connection	Gusset-Girder Connection	Perpendicular	1.37
2.3x2.3x1.1 m Gusset	Gusset-Column Connection	Perpendicular	1.10
	Girder Flange	Parallel	1.05
Longitudinal Girder-Column Connection	Middle of Gusset	Parallel	1.52
	Gusset-Girder Connection	Perpendicular	1.14
1.1x1.1x.55 m	Gusset-Column Connection	Perpendicular	1.05
	Girder Flange	Parallel	1.01
Exterior Longitudinal Girder	Bottom Right Corner of Exterior Hole	Parallel	1.87
@ Windlass Holes	Upper Left Corner of Interior Hole	Parallel	1.73

Table C.4-1 Summary of SCFs for a Column - Girder Connection

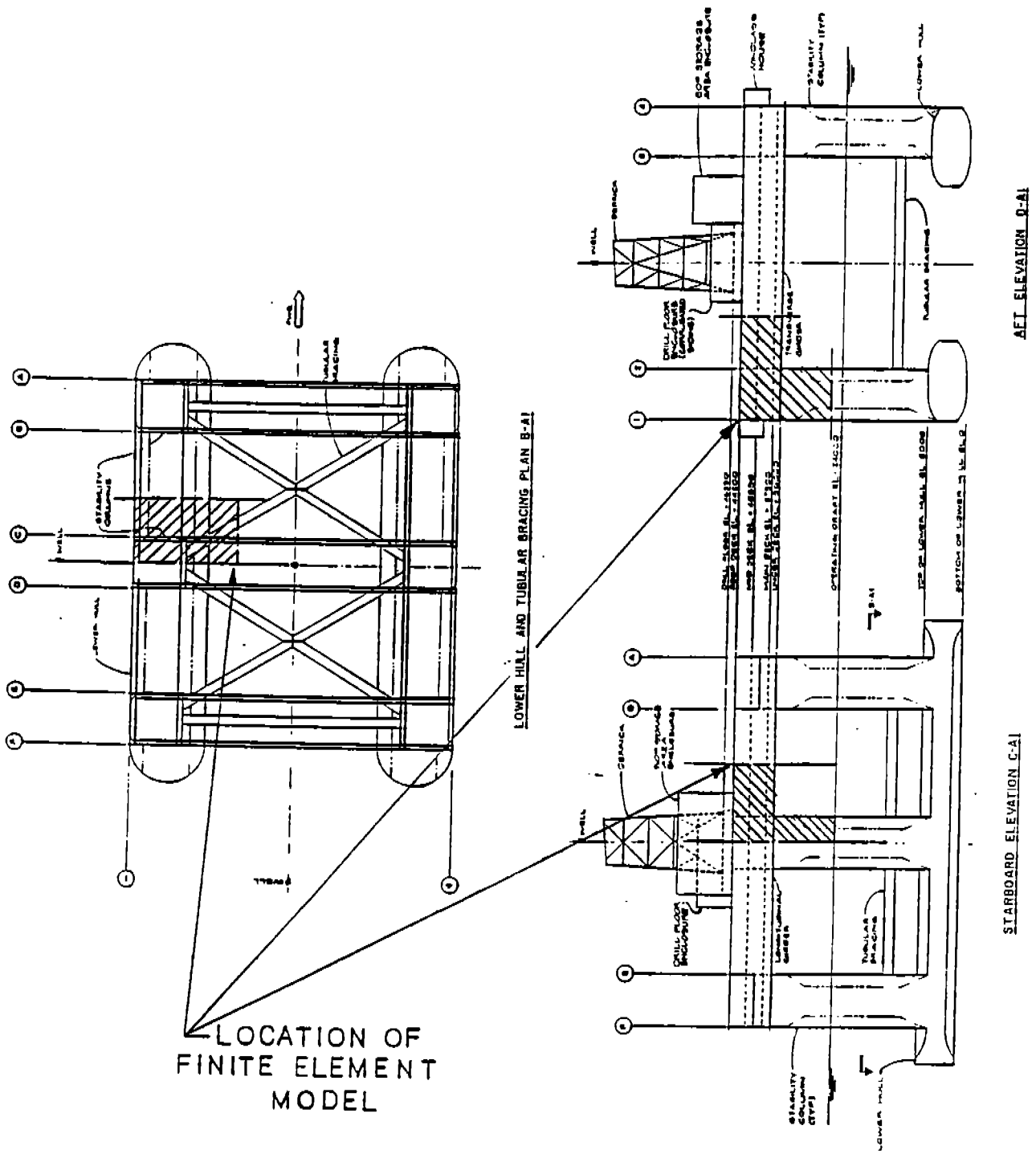
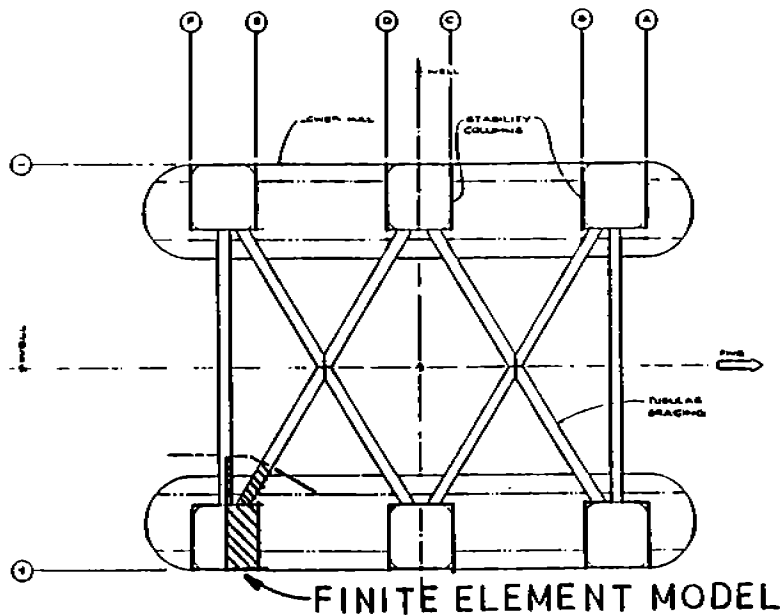
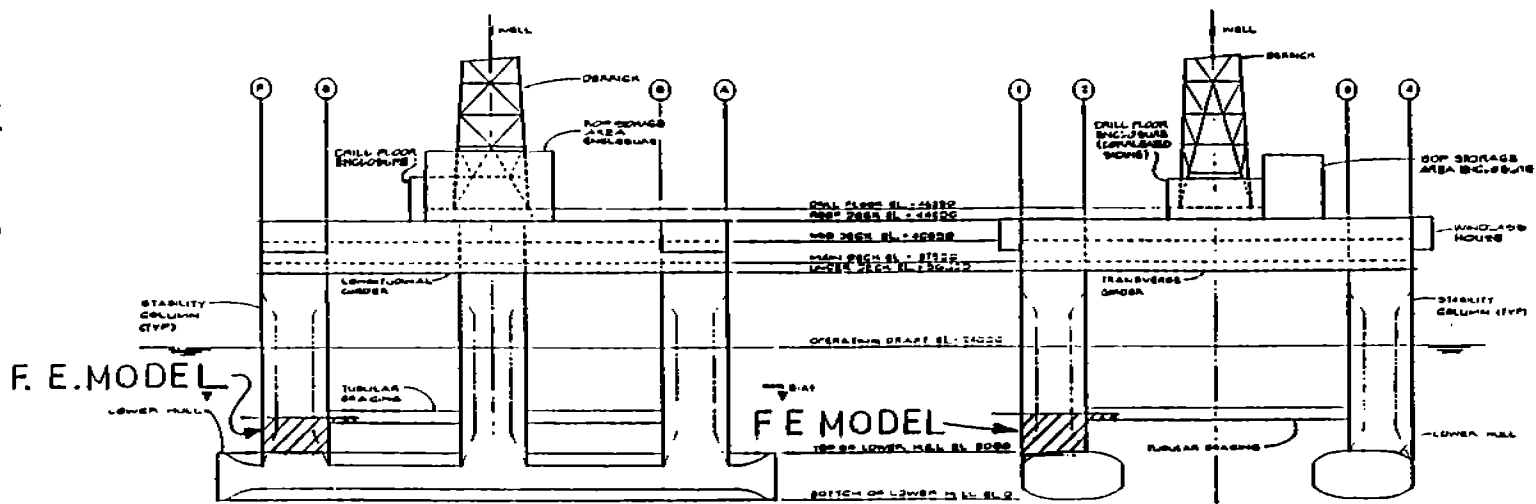


Figure C.4-1 Overall Geometry of Vessel and Location of Column-to-Girder Connection

Figure C.4-2 Overall Geometry of Vessel and Location of Corner Column Tubular Connection



LOWER HULL AND TUBULAR BRACING PLAN B-A1



STARBOARD ELEVATION C-A1

AFT ELEVATION D-A1

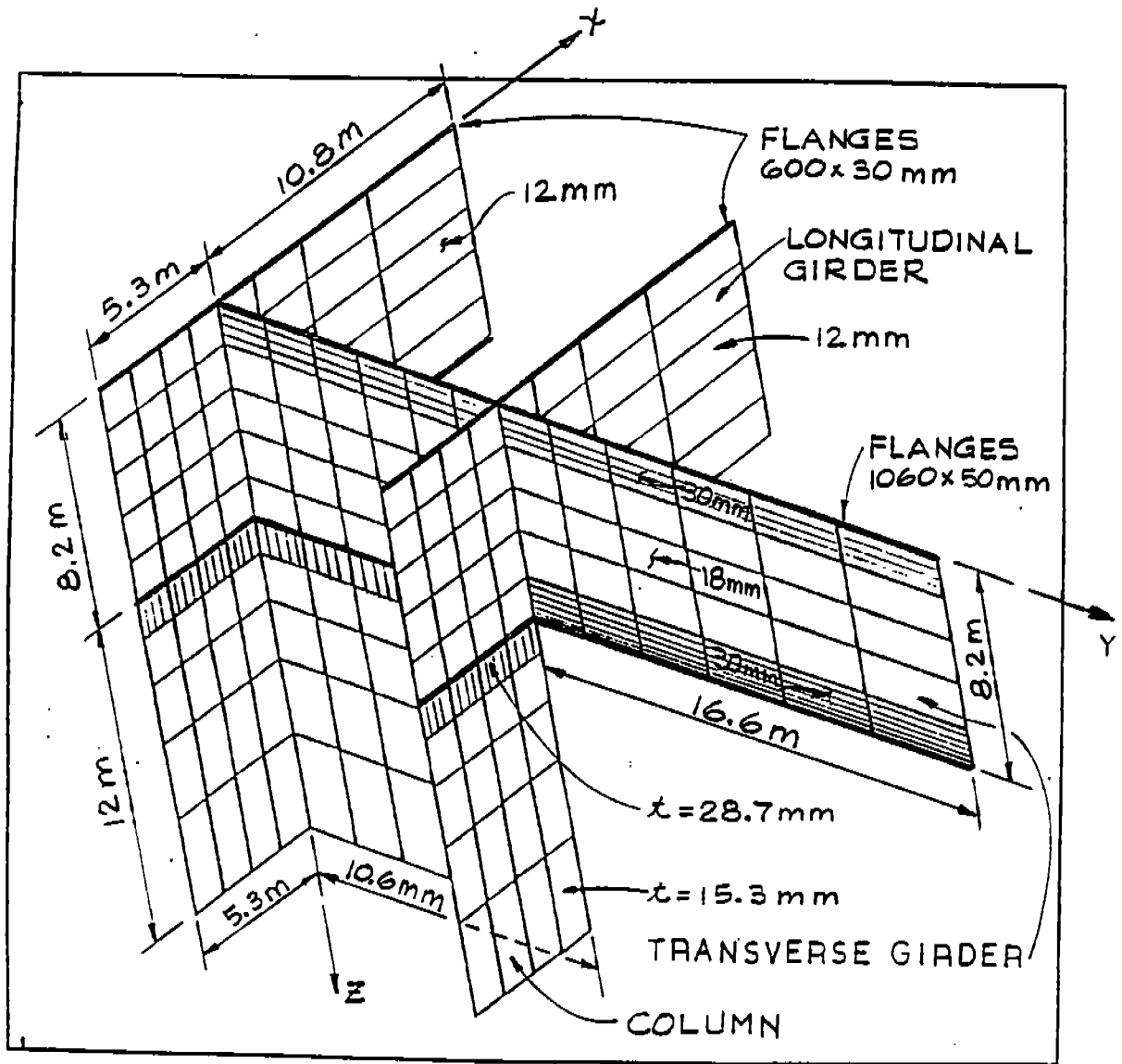


Figure C.4-3 Finite Element Model and Dimensions of Column-to-Girder Connection

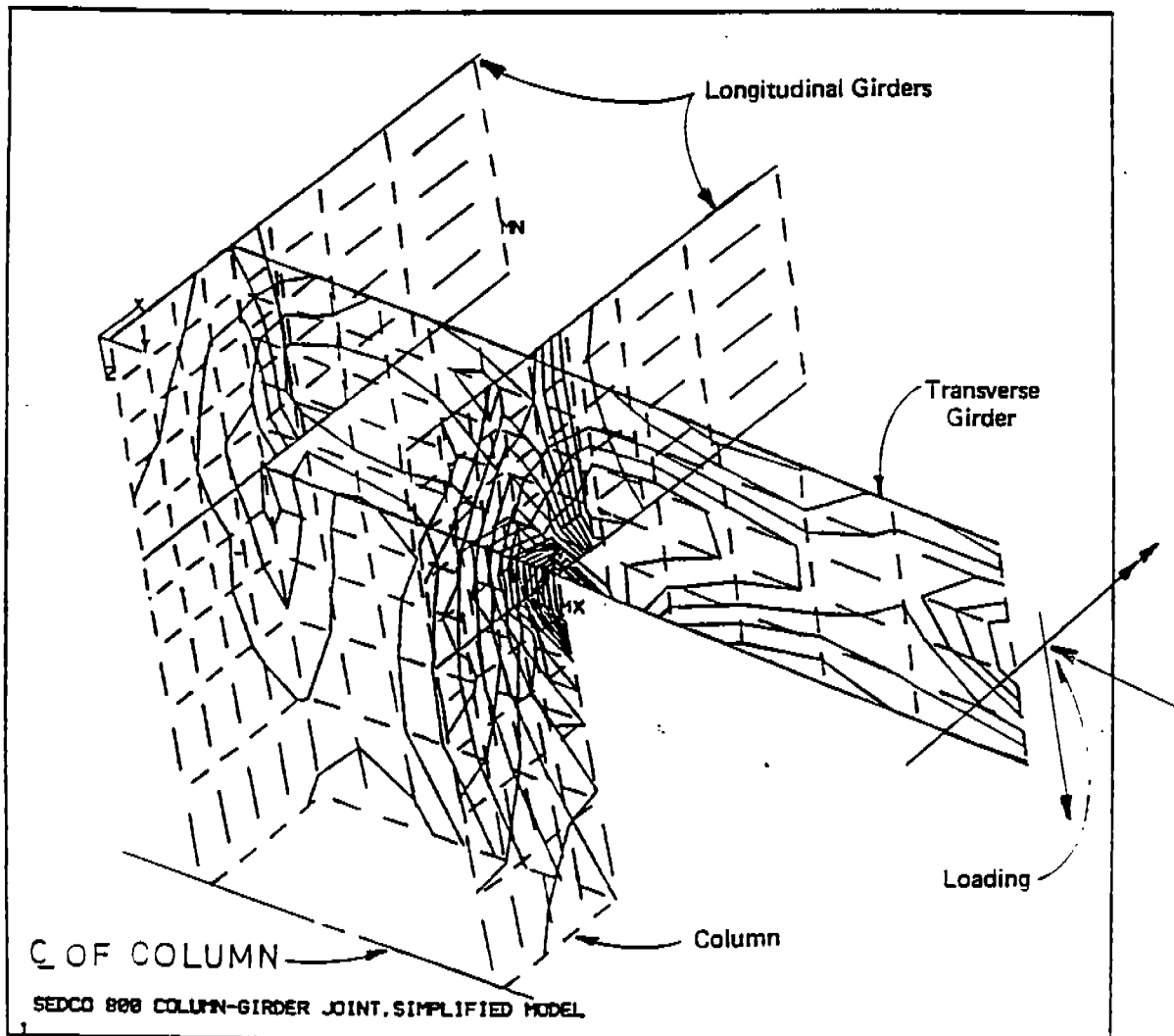


Figure C.4-4 Equivalent Stress Contour Plot for the Column-to-Girder Connection

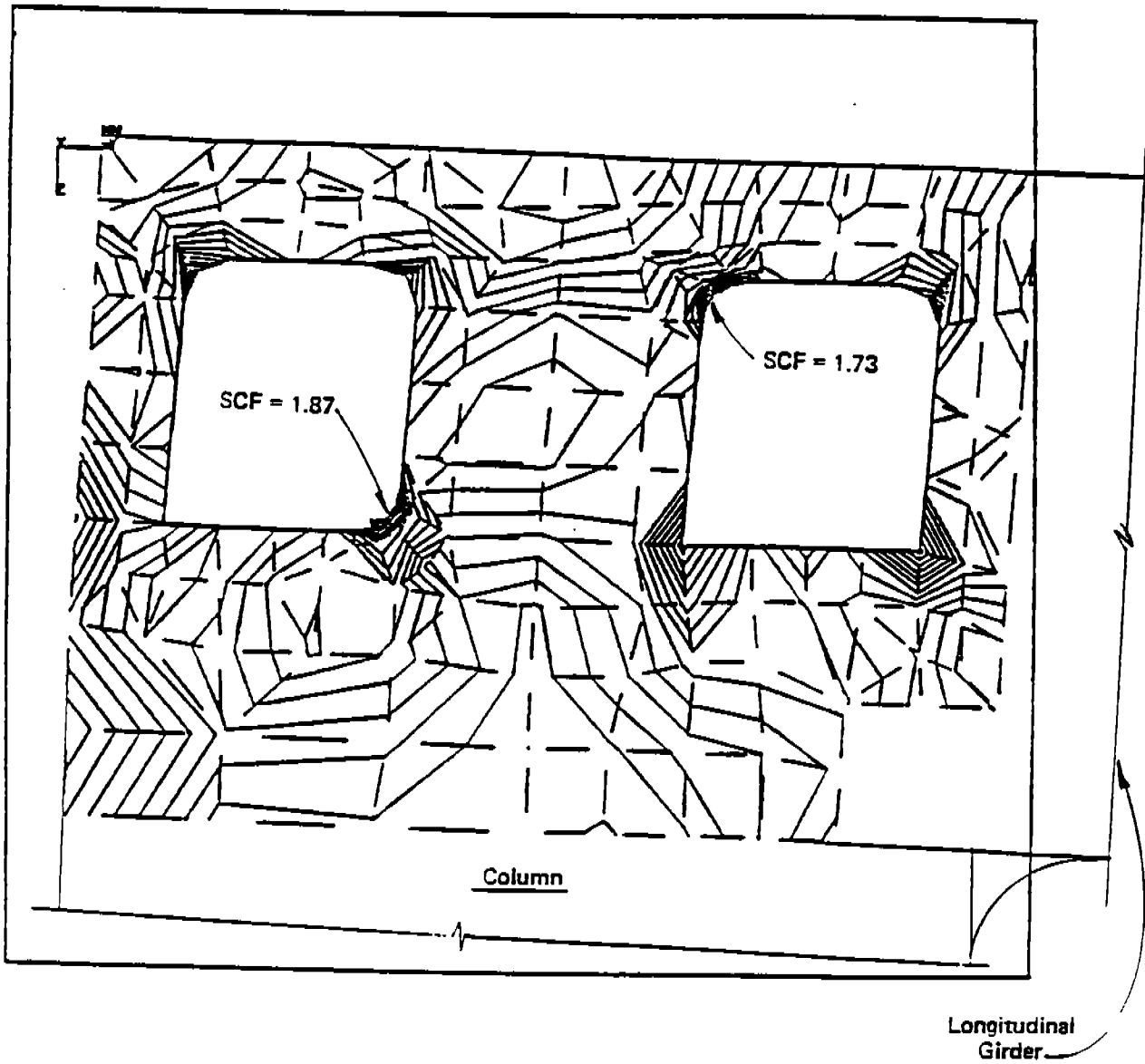


Figure C.4-5 Equivalent Stress Contour Plot of Windlass Holes

C.5 REFERENCES

- C.1 Kuang, J.G. et al., "Stress Concentrations in Tubular Joints," Proceedings of Offshore Technology Conference, OTC Paper No. 2205, Houston, TX. 1975 (Revisions introduced in SPE Journal, pp. 287-299, August 1977).
- C.2 Wordsworth, A.C., "Stress Concentration Factors at K and KT Tubular Joints," Fatigue in Offshore Structural Steels, Institution of Civil Engineers, London, February 1981.
- C.3 Wordsworth, A.C., "Aspects of Stress Concentration Factors at Tubular Joints," TS8, Proceedings of the 3rd International Offshore Conference on Steel in Marine Structures, (SIMS 87), Delft, The Netherlands, June 1987.
- C.4 Gibstein, M.B., "Parametric Stress Analyses of T Joints," Paper No. 26, European Offshore Steels Research Seminar, Cambridge, November 1978.
- C.5 Gibstein, M.B., "Stress Concentration in Tubular K Joints with Diameter Ratio Equal to One," TS10, International Offshore Conference on Steel in Marine Structures (SIMS 87), Delft, The Netherlands, 1985.
- C.6 Efthymiou, M., et al. "Stress Concentrations in T/Y and Gap/Overlap K Joints," The 4th International Conference on Behavior of Offshore Structures (BOSS 1985), Amsterdam, The Netherlands, 1985.
- C.7 Marshall, P.W. and Luyties, W.H., "Allowable Stresses for Fatigue Design," International Conference on Behavior of Offshore Structures (BOSS 1982), Cambridge, Massachusetts, August 1982.

- C.8 Underwater Engineering Group, "Design of Tubular Joints for Offshore Structures," UEG Publication, UR33, 1985.
- C.9 Kellogg, M.W., "Design of Piping Systems", Second Edition, Wiley, 1956.
- C.10 Delft, van D.R.V. et al. "The Results of the European Fatigue Tests on Welded Tubular Joints Compared with SCF Formulas and Design Lives," Paper No. TS 24, Proceedings of the 3rd International Conference on Steel in Marine Structures (SIMS 87), Delft, The Netherlands, June 1987.
- C.11 Ma, S.Y., Tebbett, I.E., "Estimations of Stress Concentration Factors for Fatigue Design of Welded Tubular Connections," Proceedings of the 20th Annual Offshore Technology Conference, OTC Paper No. 5666, Houston, TX., May 1988.
- C.12 Tebbett, I.E., and Lalani, M., "A New Approach to Stress Concentration Factors for Tubular Joint Design," Proceedings of 16th Annual Offshore Technology Conference, ITC Paper No. 4825, Houston, TX, May 1984.
- C.13 Tolloczko, J.A., and Lalani, M., "The Implications of New Data on the Fatigue Life Assessment of Tubular Joints," Proceedings of the 20th Annual Offshore Technology Conference, OTC Paper No. 5662, Houston, TX, May 1988.

(THIS PAGE INTENTIONALLY LEFT BLANK)

APPENDIX D

VORTEX SHEDDING AVOIDANCE AND FATIGUE DAMAGE COMPUTATION

CONTENTS

NOMENCLATURE

D. VORTEX SHEDDING

D.1 INTRODUCTION

D.2 VORTEX SHEDDING PARAMETERS

D.3 SUSCEPTIBILITY TO VORTEX SHEDDING

- D.3.1 In-Line Vortex Shedding
- D.3.2 Cross-Flow Vortex Shedding
- D.3.3 Critical Flow Velocities

D.4 AMPLITUDES OF VIBRATION

- D.4.1 In-Line Vortex Shedding Amplitudes
- D.4.2 Cross-Flow Vortex Shedding Amplitudes

D.5 STRESSES DUE TO VORTEX SHEDDING

D.6 FATIGUE LIFE EVALUATION

D.7 EXAMPLE PROBLEMS

- D.7.1 Avoidance of Wind-Induced Cross-Flow Vortex Shedding
- D.7.2 Analysis for Wind-Induced Cross-Flow Vortex Shedding

D.8 METHODS OF MINIMIZING VORTEX SHEDDING OSCILLATIONS

- D.8.1 Control of Structural Design
- D.8.2 Mass and Damping
- D.8.3 Devices and Spoilers

D.9 REFERENCES

NOMENCLATURE

C_D	=	Coefficient of drag
CL_j	=	Design lift coefficient
CL_0	=	Base lift coefficient
D	=	Fatigue damage
D_{tot}	=	Total fatigue damage
D_1	=	Fatigue damage due to vortex shedding
D_2	=	Fatigue damage due to storm
E	=	Modulus of elasticity
H	=	Submerged length of member
I	=	Member moment of inertia
I	=	Turbulence parameter
I_0	=	Turbulence parameter
K	=	Constant representing member fixity
K_S	=	Stability parameter
L	=	Span between member supports
N	=	Number of cycles to failure at hot spot stress range
Re	=	Reynolds number
S	=	Hot spot stress range
S	=	Member section modulus
SCF	=	Stress concentration factor
S_t	=	Strouhal number
S_1	=	Corresponding hot spot stress range
T	=	Wave period
T_e	=	Time for which V_{min} is exceeded
V	=	Flow velocity normal to member axis
V_m	=	Maximum orbital velocity due to wave motion
V_{max}	=	Maximum water particle velocity
V_{min}	=	Minimum V_r , required for motion
V_r	=	Reduced velocity
Y	=	Member midspan deflection
Y_m	=	Maximum member midspan deflection
Y_R	=	Refined maximum member midspan deflection

a	=	Maximum modal amplitude
a_n	=	Natural frequency coefficient
b	=	Pit depth
d	=	Member diameter
f_v	=	Member vortex shedding frequency
f_{ar}	=	Turbulence parameter
f_b	=	Member bending stress
f_{bmax}	=	Member maximum bending stress
f_H	=	Member maximum hot spot stress
f_n	=	Member natural frequency
f_s	=	Member vortex shedding frequency
m	=	Mass of member per unit length excluding marine growth
\bar{m}	=	Effective mass per unit length
m_i	=	Mass of member per unit length including marine growth
m_j	=	Generalized mass per unit length for mode j
n	=	Mode of vibration
n_e	=	Member end condition coefficient
n_o	=	Total number of occurrences per year
n_s	=	Actual number of cycles at hot spot stress range
n_w	=	Number of oscillations during one wave cycle
t	=	Nominal caisson thickness
V	=	Applied velocity
v_{cr}	=	Critical wind velocity
v_r	=	Reduced velocity
w	=	Load per unit length
w_o	=	Weight per unit length of member
w_1	=	Weight per unit length of supported items
$y(x)$	=	Fundamental mode shape
$y'(x)$	=	Equivalent fundamental mode shape
δ	=	Logarithmic decrement of damping
ϵ	=	Damping ratio
ν	=	Kinematic viscosity
η_N	=	Ratio of midspan deflection to member diameter (Y/d)
ρ	=	Mass density of fluid

X

(THIS PAGE INTENTIONALLY LEFT BLANK)

D. VORTEX SHEDDING

D.1. INTRODUCTION

When a fluid flows about a stationary cylinder, the flow separates, vortices are shed, and a periodic wake is formed. Each time a vortex is shed from the cylinder, the local pressure distribution is altered, and the cylinder experiences a time-varying force at the frequency of vortex shedding.

In steady flows, vortices are shed alternately from either side of the cylinder producing an oscillating lift force transverse to the flow direction at a frequency equal to that at which pairs of vortices are shed. In the flow direction, in addition to the steady drag force, there is a small fluctuating drag force associated with the shedding of individual vortices at a frequency twice that of the lift force.

As the flow velocity increases, the vortex shedding frequency increases. Thus, provided the flow velocity is high enough, a condition will be reached where the vortex shedding frequency coincides with the natural frequency of the flexible element.

In general, marine members and appurtenant pipework are of a diameter and length that preclude the occurrence of in-line vibrations induced by vortex shedding. However, all susceptible members must be analyzed to ensure that the stresses due to in-line vibrations and possible synchronized oscillations are small and do not result in a fatigue failure.

Response to vortex shedding cannot be predicted using conventional dynamic analysis techniques since the problem is non-linear. The motion of the structure affects the strength of the shedding which, in turn affects the motion of the structure. This feedback mechanism causes the response to be either significantly large or negligibly small. Once excited, there is also a tendency for the vortex

shedding frequency to synchronize with the natural frequency of the structure. This results in sustained resonant vibration even if the flow velocity moves away from the critical velocity.

Oscillations can be predominantly in-line with the flow direction or transverse to it. In-line motion occurs at lower flow velocities than transverse or cross-flow motion, but the latter is invariably more severe and can lead to catastrophic failure due to a small number of cycles of oscillation.

Response to vortex shedding is further complicated as the excitational force is not necessarily uniform along the length of the members and the actual amplitude of oscillation depends to a large extent on the degree of structural damping.

D.2. VORTEX SHEDDING PARAMETERS

A number of parameters are common to this phenomenon:

Reduced velocity (V_r)

$$V_r = V/f_n d$$

where:

$$\begin{aligned} V &= \text{flow velocity normal to the member axis} \\ f_n &= \text{fundamental frequency of the member (Hz)} \\ d &= \text{diameter of the member} \end{aligned}$$

Reynolds number (R_e)

$$R_e = Vd/\nu$$

where:

$$\nu = \text{kinematic viscosity of the fluid}$$

The Strouhal number (S_t) is a function of the Reynolds number for circular members. The Reynolds number for typical cylindrical members under storm current ranges from 3.5×10^5 to 1.0×10^6 . The Strouhal number is reasonably approximated as 0.21 for this range of Reynolds numbers.

Vortex Shedding Frequency (f_v)

$$f_v = \frac{S_t V}{d} = \text{vortex shedding frequency of the member}$$

If the vortex shedding frequency of the member coincides with the natural frequency of the member, resonance will occur.

Stability parameter (K_s)

where:

$$K_s = 2 \bar{m} \delta / \rho d^2$$
$$\delta = 2 \pi \varepsilon = \text{logarithmic decrement}$$
$$\varepsilon = \text{damping ratio}$$
$$\rho = \text{mass density of the fluid}$$
$$\bar{m} = \text{effective mass per unit length}$$
$$= \frac{\int_0^L (m) [y(x)]^2 dx}{\int_0^L [y'(x)]^2 dx}$$
$$L = \text{span between member supports}$$
$$m = \text{mass of member per unit length}$$
$$y(x),$$
$$\& y'(x) = \text{fundamental mode shapes as a function of the ordinate } x \text{ measured from the lower support along the longitudinal axis of the member}$$

As given in References D.1 and D.2, the effective mass is used to equate the real structure with an equivalent structure for which

deflection and stability parameters are known. The deflected form of this equivalent structure is a cantilever, while typical structure members and appurtenances deflect as a simply supported beam. Hence, the equivalent structure has a mode shape given by:

$$y'(x) = a - a \cos\left(\frac{\pi x}{2L}\right)$$

while the real structure has a mode shape given by:

$$y(x) = a \sin\left(\frac{\pi x}{L}\right)$$

Substituting into the effective mass formulation, we obtain:

$$m = \frac{\int_0^L [m] \left[a \sin \frac{\pi x}{L} \right]^2 dx}{\int_0^L \left[a - a \cos \frac{\pi x}{2L} \right]^2 dx}$$

where:

$$a = \text{maximum modal amplitude}$$

Integration of the above equation leads to the relationship:

$$\bar{m} = 2.205 m \text{ for simple supported span}$$

$$\bar{m} = 1.654 m \text{ for fixed supports}$$

$$\bar{m} = m \text{ for cantilever span}$$

Damping Ratio

Welded marine structures exhibit very low values of structural damping. Vibratory energy is typically dissipated by material and aerodynamic (radiation) damping. Individual members subjected to large vibratory motions dissipate energy through the connections to the main structure largely as dispersive bending and compression

waves. When only isolated members undergo large vibration response, energy dispersion exceeds reflected energy and represents a major source of damping.

Structural members may be grouped into two classes, depending on the fixity of their supports. Tubular braces welded on to regions of high rigidity, such as structure columns or legs, are defined as Class 1 members. Tubular braces welded on to regions of low rigidity, such as other braces, are defined as Class 2 members. The damping ratio applicable for structural members are:

Structural Member - Class 1	Damping ratio	$\epsilon = 0.0035$
Structural Member - Class 2	Damping ratio	$\epsilon = 0.0015$

Although the recommended damping ratios are for vibrations in air, they may be conservatively used for vibrations in water.

Non-structural continuous members, such as tubulars supported by multiple guides, have both structural and hydrodynamic damping. The hydrodynamic damping occurs due to sympathetic vibration of spans adjacent to the span being evaluated for shedding. Recent work by Vandiver and Chung (Reference D.3) supports the effectiveness of hydrodynamic damping mechanism. The lower bound structural damping ratio for continuous tubulars supported by loose guides is given as 0.009 by Blevins (Reference D.4). The applicable damping ratios are assumed to be:

Non-Structural Members - Continuous Spans

Damping ratio	$\epsilon = 0.009$ in air
Damping ratio	$\epsilon = 0.02$ in water

Natural Frequency

The fundamental natural frequency (in Hz) for uniform beams may be calculated from:

$$f_n = \frac{a_n}{2\pi} (EI/m_j L^4)^{1/2}$$

where:

I = the moment of inertia of the beam

a_n = 3.52 for a beam with fix-free ends (cantilever)
 = 9.87 for a beam with pin-pin ends
 = 15.4 for a beam with fix-pin ends
 = 22.4 for a beam with fix-fix ends

L = length

n = mode of vibration

m_j = mass per unit length

The amount of member fixity assumed in the analysis has a large effect on vortex shedding results, because of its impact on member stiffness, natural period, amplitude of displacement, and member stress. Hence, careful consideration should be given to member end conditions. Members framing into relatively stiff members can usually be assumed to be fixed. Other members, such as caissons and risers, may act as pinned members if supports are detailed to allow member rotation.

For members with non-uniform spans, complex support arrangements or non-uniform mass distribution, the natural frequency should be determined from either a dynamic analysis or from Tables provided in References D.5 and D.6. Reid (Reference D.7) provides a discussion and a model to predict the response of variable geometry cylinders subjected to a varying flow velocities.

The natural frequency of a member is a function of the member's stiffness and mass. For the purposes of vortex shedding analysis and design, the member's stiffness properties are computed from the

member's nominal diameter and thickness. The member mass per unit length m is taken to include the mass of the member steel including sacrificial corrosion allowance, anodes, and contained fluid. For the submerged portion of the member, the added mass of the surrounding water is also included. This added mass is the mass of water that would be displaced by a closed cylinder with a diameter equal to the nominal member outside diameter plus two times the appropriate marine growth thickness.

Because of insufficient knowledge of the effect of marine growth on vortex shedding, the member diameter "d" in vortex-shedding parameters V_r , R_e , K_s , and the member effective mass \bar{m} in parameter K_s do not include any allowance for the presence of marine growth.

D.3. SUSCEPTIBILITY TO VORTEX SHEDDING

The vortex shedding phenomena may occur either in water or in air. The susceptibility discussed and the design guidelines presented are applicable for steady current and wind. Wave induced vortex shedding has not been investigated in depth. Since the water particle velocities in waves continually change both in magnitude and direction (i.e. restricting resonant oscillation build-up), it may be reasonable to investigate current-induced vortex shedding and overlook wave actions.

To determine susceptibility of a member to wind- or current-induced vortex shedding vibrations, the reduced velocity (V_r) is computed first. For submerged members, the stability parameter (K_s) is also calculated. Vortex shedding susceptibility defined here is based upon the method given in Reference D.8, with a modified lower bound for current-induced shedding to reflect present thinking on this subject (Reference D.9).

D.3.1 In-Line Vortex Shedding

In-line vibrations in wind and current environments may occur when:

Current Environment

$$1.2 \leq V_r < 3.5$$
$$\text{and } K_S \leq 1.8$$

Wind Environment

$$1.7 < V_r < 3.2$$

The value of V_r may be more accurately defined for low K_S values from Figure D-1, which gives the reduced velocity necessary for the onset of in-line motion as a function of combined mass and damping parameter (i.e. stability parameter). Corresponding amplitude of motion as a function of K_S is given on Figure D-2. As illustrated on this Figure, in-line motion is completely suppressed for K_S values greater than 1.8.

Typical marine structure members (i.e. braces and caissons on a platform) generally have values of K_S greater than 1.8 in air but less than 1.8 in water. Hence, in-line vibrations with significant amplitudes are often likely in steady current but unlikely in wind.

D.3.2 Cross-Flow Vortex Shedding

The reduced velocity necessary for the onset of cross-flow vibrations in either air or in water is shown on Figure D-3 as a function of Reynold's number, R_e , cross flow vibrations in water and in air may occur when:

Current Environment

$$3.9 \leq V_r \leq 9$$
$$\text{and } K_S \leq 16$$

Wind Environment

$$4.7 < V_r < 8$$

The cross-flow vibrations of members in steady current will invariably be of large amplitude, causing failures after small number

of cycles. Thus, the reduced velocity necessary for the onset of cross-flow vibrations in steady current should be avoided.

D.3.3 Critical Flow Velocities

The criteria for determining the critical flow velocities for the onset of VIV can be expressed in terms of the reduced velocity (Section D.2):

$$V_{cr} = (V_r)_{cr} (f_n \cdot d)$$

where:

$$\begin{aligned} (V_r)_{cr} &= 1.2 \text{ for in-line oscillations in water} \\ &= 1.7 \text{ for in-line oscillations in air} \\ &= 3.9 \text{ for cross-flow oscillations in water} \\ &= 4.7 \text{ for cross-flow oscillations in air} \end{aligned}$$

D.4. AMPLITUDES OF VIBRATION

Amplitudes of vibrations can be determined by several methods. A DnV proposed procedure (Reference D.8) is simple to apply and allows determination of member natural frequencies, critical velocities and maximum amplitudes of vortex-shedding induced oscillations. The procedure yields consistent results, comparable to the results obtained by other methods, except for oscillation amplitudes. The DnV calculation of oscillation amplitudes is based on a dynamic load factor of a resonant, damped, single-degree-of-freedom system. This approach is not valid unless the nonlinear relationship between the response and damping ratio is known and accounted for. Consequently, in-line and cross-flow vortex shedding amplitudes are assessed separately.

D.4.1 In-Line Vortex Shedding Amplitudes

The reduced velocity and the amplitude of vibrations shown on Figures D-1 and D-2, respectively, as functions of stability parameter are based on experimental data. The experimental data obtained are for the cantilever mode of deflection for in-line and cross-flow vibrations.

Sarpkaya (Reference D.10) carried out tests on both oscillatory flow and uniform flow and observed smaller amplitudes of vibration for the oscillatory flow than for the uniform flow. It is also suggested by King (Reference D.1) that the maximum amplitude for an oscillatory flow is likely to occur at a V_r value in excess of 1.5 (as opposed to 1.0 assumed by DnV) and that an oscillation build-up of about 15 cycles is required before "lock-in" maximum-amplitude vibration occurs. In light of this evidence, the amplitude of vibrations shown in Figure D-2 is based on Hallam et al (Reference D.2) rather than the DnV (Reference D.8).

Since typical marine structure members have stability parameters (K_s) in excess of 1.8, in-line vibrations of these members in air are unlikely.

D.4.2 Cross-flow Vortex Shedding Amplitudes

The amplitude of the induced vibrations that accompanies cross-flow vibration are generally large and creates very high stresses. Therefore, it is desirable to preclude cross-flow induced vibrations. Figure D-4 illustrates a curve defining the amplitude of response for cross-flow vibrations due to current flow and based on a cantilever mode of deflection.

Cross-flow oscillations in air may not be always avoidable, requiring the members to have sufficient resistance. The DnV procedure (Reference D.8) to determine the oscillation amplitudes is derived from a simplified approach applicable to vortex shedding due to

steady current, by substituting the mass density of air for the mass density of water. Hence, the oscillation amplitude is not linked with the velocity that causes vortex-induced motion. The resulting predicted amplitudes are substantially higher than amplitudes predicted based on an ESDU (Reference D.11) procedure that accounts for interaction between vortices shed and the forces induced.

The iterative ESDU procedure to determine the amplitudes can be simplified by approximating selected variables. The peak amplitude is represented in Equation 9 of the ESDU report by:

$$\frac{Y}{d} = \eta_N = \frac{0.00633}{\epsilon} \rho \frac{d^2}{m_j} \frac{1}{S_t^2} \quad CL_j = \frac{0.0795 CL_j}{K_s S_t^2}$$

Using this formulation, a corresponding equation can be established for a structure, while making assumptions about the individual parameters. Following step 3 of the procedure, the parameters may be set as:

m_j = generalized mass/unit length for mode j
 = 2.205 m for pinned structure,
 = 1.654 m for fixed structure

K_s = stability parameter = $\frac{2m_j \delta}{\rho d^2}$

ρ = mass density of air = 1.024 kg/m³

δ = decrement of damping = $2\pi\epsilon$

ϵ = damping parameter = 0.002 for wind

S_t = Strouhal Number = 0.2

$$\begin{aligned}
CL_0 &= \text{base lift coefficient} &= 0.29 \text{ high Reynolds number} \\
& &= 0.42 \text{ low Reynolds number} \\
CL_j &= \text{design lift coefficient} &= CL_0 \times f_{ar} \times I_0 \times \frac{I}{I_0} \times 1.2 \\
f_{ar} &= \text{turbulence parameter} &= 1.0 \\
\frac{I}{I_0} &= \text{turbulence parameter} &= 1.0 \\
I_0 &= \text{turbulence parameter} &= 0.45
\end{aligned}$$

Evaluating the equation based on the high Reynolds number ($Re > 500,000$) leads to:

$$\eta_N = 0.0795 (0.29)(1.0)(0.45)(1.0)(1.2)/[K_s(0.2)^2]$$

$$\eta_N = \frac{0.3114}{K_s} \quad (\text{high Reynolds number, } Re > 500,000)$$

or

$$\eta_N = \frac{0.4510}{K_s} \quad (\text{low Reynolds number, } Re < 500,000)$$

The amplitude can also be determined iteratively by utilizing the ESDU recommended turbulence parameter and following steps 1 through 5.

Step 1: Determine correlation length factor, I_0 . Depending on the end fixity, I_0 is:

$$\begin{aligned}
I_0 &= 0.66 && \text{for fixed and free (cantilever)} \\
&= 0.63 && \text{for pin and pin (simple beam)} \\
&= 0.58 && \text{for fixed and pin} \\
&= 0.52 && \text{for fixed and fixed}
\end{aligned}$$

Step 2: Assume $I/I_0 = 1.0$ and calculate the amplitude.

Step 3: Obtain a new value of I/I_0 based on initial amplitude.

Step 4: Recompute the amplitude based on the new value of I/I_0 .

Step 5: Repeat Steps 3 and 4 until convergence.

D.5. STRESSES DUE TO VORTEX SHEDDING

Once the amplitude of vibration has been calculated, stresses can be computed according to the support conditions. For a simply supported beam with a uniform load w , the midspan deflection Y , and the midspan bending stress f_b are given as follows:

$$\frac{Y}{d} = \frac{5}{384} \cdot \frac{w L^4}{EI} \cdot \frac{1}{d}$$

$$w = \frac{384}{5} \cdot \frac{EIY}{L^4}$$

$$M_{\max} = \frac{w L^2}{8} = \frac{384}{40} \frac{EIY}{L^2}$$

$$f_{b\max} = \frac{M}{I} \cdot \frac{d}{2} = 4.8 \frac{EDY}{L^2} \quad \text{at midspan}$$

$$\text{Expressing } f_{b\max} = K \cdot \frac{EDY}{L^2}$$

The K value varies with support conditions and location as shown on Table D-1.

<u>Fixity</u>		<u>Mid-Span</u>	<u>Ends</u>
Fix	Fix	8.0	16.0
Fix	Pin	6.5	11.6
Pin	Pin	4.8	0
Fix	Free	N.A.	2.0

Table D-1 K Values Based on Fixity and Location

The vortex shedding bending stress is combined with the member axial and bending stresses due to global deformation of the marine structure.

D.6. FATIGUE LIFE EVALUATION

The fatigue life evaluation can be carried out in a conservative two-step process. First, the fatigue damage due to the vortex-induced oscillations is calculated as D_1 . Second, a deterministic fatigue analysis is performed by computer analysis. Hot spot stress range vs wave height (or wind velocity) for the loading directions considered is determined from the computer analysis. The critical direction is determined and a plot is made. From the plot of hot spot stress range vs wave height (or wind velocity), the stress ranges for the fatigue waves are determined. The maximum vortex-induced stress ranges for the fatigue environment are added to the deterministic fatigue stress ranges. Then, the standard deterministic fatigue analysis is performed using the increased stress range. The fatigue damage calculated in this second step is D_2 . Therefore the total fatigue damage is equal to the sum of D_1 and D_2 , or $D_{tot} = D_1 + D_2$. The fatigue life in years is therefore calculated as $1/D_{tot}$.

A typical fatigue life evaluation procedure is given below:

Step 1:

- a. Calculate the natural frequency f_n (H_z) of the member.
- b. Calculate the stability parameter of the member.

$$K_s = \frac{2\bar{m}\delta}{\rho d^2}$$

- c. Determine the minimum V_r required for vibrations based on K_s in Figure D-1.
- d. Calculate V_{min} , the minimum velocity at which current- or wind-

vortex shedding will occur, i.e., $V_{\min} = V_{r(\text{req'd})} \times f_n \times d$.

- e. Check the applied velocity profile to see if V_{\max} is greater than V_{\min} . If V_{\max} is less than V_{\min} , then no vortex oscillations can occur.
- f. For V_{\max} greater than V_{\min} , vortex oscillations can occur. The displacement amplitude is based on stability parameter K_S , and is determined from Figure D-2 for in-line vibration. A conservative approach is used to determine Y/d vs K_S . For $K_S < 0.6$ the first instability region curve is used. For $K_S > 0.6$ the second instability region curve is used. This conservatively represents an envelope of maximum values of Y/d vs K_S from Figure D-2. Displacement amplitude is normalized to Y/d .
- g. Given (Y/d) , calculate the bending stress, f_b .
- h. Multiply bending stress f_b by an SCF of 1.5 to produce hot spot stress f_H . A larger SCF will be used where necessary.
- i. From the maximum hot spot stress, the hot spot stress range is calculated as $2f_H$.
- j. Allowable number of cycles to failure (N) should be calculated using an applicable S-N curve (based on weld type and environment).
- k. Assume conditions conducive to resonant vortex shedding occur for a total time of T (seconds) per annum (based on current or wind data relevant to applicable loading condition).
- l. Hence, in time T , number of cycles $n = f_n T$ and the cumulative damage $D_1 = n/N = f_n T/N$ in one year.

Step 2:

- a. Depending on marine structure in service conditions (i.e. structure in water or in air) run an applicable loading analysis. Assuming a marine environment, run a storm wave deterministic fatigue analysis and obtain the results of hot spot stress range vs wave height for the wave directions considered and as many hot spots as are needed.
- b. Determine the critical hot spot and wave direction and draw the hot spot stress range vs wave height graph.
- c. Determine the hot spot stress range for each of the fatigue waves.
- d. For the larger fatigue waves in which vortex-induced oscillations occur, add the increase in stress range due to vortex-induced oscillations to the stress range from the deterministic fatigue analysis.
- e. Calculate the fatigue damage D_2 over a 1 yr period for the full range of wave heights:

$$D_2 = \sum_1^H \left(\frac{\sigma}{N} \right)$$

- f. Calculate the total fatigue damage:

$$D_{\text{tot}} = D_1 + D_2$$

- g. Calculate the fatigue life in years as:

$$\text{Life} = \frac{1}{D_{\text{tot}}}$$

- h. The fatigue life may be modified to include the effects of corrosion pitting in caissons. Corrosion pitting produces an SCF at the location of the pit. The SCF is calculated as:

$$SCF = \frac{1}{(1 - \frac{b}{t})} + \frac{3 (\frac{b}{t})}{(1 - \frac{b}{t})^2}$$

where:

b = pit depth
t = nominal caisson thickness

The new life including corrosion damage is calculated as:

$$\text{New Life} = \frac{\text{Old Life}}{(SCF)^3}$$

This estimate of fatigue damage can, if necessary, be refined by consideration of the number of wave occurrences for different directions and evaluation of the damage at a number of points around the circumference of the member.

D.7. EXAMPLE PROBLEMS

D.7.1 Avoidance of Wind-Induced Cross-Flow Vortex Shedding

It can be shown that for a steel beam of circular cross section, the following relationship holds:

where:

$$V_{cr} = \frac{c \cdot V_r n_e^2}{(L/d)^2} \left[\frac{w_0}{w_0 + w_1} \right]^{1/2}$$

V_{cr} = critical wind velocity of the tubular necessary for the onset of cross-flow wind-induced vortex shedding

- c = constant (See NOTE, next page)
 V_r = reduced velocity
 n_e = member end efficiency
 = 1.5 fixed ends
 = 1.0 pinned ends
 w_0 = weight per unit length of tubular
 w_1 = weight per unit length of supported item (e.g.,
 anodes)
 L = beam length
 d = tubular mean diameter

For $V_r = 4.7$, $n_e = 1.5$ (fixed condition), and $w_1 = 0$, this reduces to:

$$\begin{aligned}
 V_{cr} &= 97240/(L/d)^2 \text{ ft/sec} \\
 &= 29610/(L/d)^2 \text{ m/sec}
 \end{aligned}$$

Hence, if maximum expected wind speed is 65.6 ft/s (20 m/s), then setting all brace L/d ratios at 38 or less precludes wind-induced cross-flow vortex shedding, and no further analyses or precautions are required.

However, maximum wind speeds may be so high that the above approach may be uneconomical. In this case, either precautionary measures must be taken or additional analyses considering strength and fatigue must be undertaken.

NOTE:

The relationship given is based on:

$$V_{cr} = V_r f_n d = V_r \left(\frac{a_n}{2\pi} \left[\frac{EI}{M_i L^4} \right]^{\frac{1}{2}} \right) d$$

substituting

$$a_n = (n_e \pi)^2$$

$$m_i = (w_0 + w_1)/g$$

$$I = \pi d^3 t / 8$$

$$E = 4176 \times 10^6 \text{ lbs/ft}^2 \quad (200,000 \text{ MN/m}^2)$$

$$g = 32.2 \text{ ft/sec}^2 \quad (9.806 \text{ m/sec}^2)$$

$$w_0 = \gamma_s \pi d t$$

$$\gamma_s = \text{weight density of steel, } 490 \text{ lbs/ft}^3 \quad (0.077 \text{ MN/m}^3)$$

$$V_{cr} = V_r \left(\frac{n_e^2 \pi^2}{2\pi} \right) \left[\frac{E (\pi d^3 t / 8) g}{(w_0 + w_1) L^4} \right]^{\frac{1}{2}} \cdot d$$

$$V_{cr} = V_r \left(\frac{n_e^2 \pi}{2} \right) \left[\frac{E (w_0 / \gamma_s) d^2 g}{8 (w_0 + w_1) L^4} \right]^{\frac{1}{2}} \cdot d$$

Substituting for E, γ_s , and g

$$V_{cr} = V_r \cdot \frac{C n_e^2}{(L/d)^2} \left[\frac{w_0}{w_0 + w_1} \right]^{\frac{1}{2}}$$

where

$$\begin{aligned} \text{constant } C &= 9195 && \text{for } V_{cr} \text{ as ft/sec} \\ &= 2800 && \text{for } V_{cr} \text{ as m/sec} \end{aligned}$$

D.7.2 Analysis for Wind-Induced Cross-flow Vortex Shedding

Using procedures discussed in Section D.4 a flare structure bracing members are analyzed for crossflow oscillations produced by vortex shedding. The analysis is performed using a Lotus spreadsheet. The general procedure is as follows:

- (a) Member and environmental parameters are input.
- (b) Critical velocity, peak amplitudes of oscillation and corresponding stress amplitudes are computed.
- (c) The time (in hours) of crossflow oscillation required to cause fatigue failure is computed.

Analysis Description

The following is a detailed description of the spread sheet input and calculation.

(a) Spread Sheet Terminology

Columns are labeled alphabetically while rows are labeled numerically. A "cell" is identified by referring to a specific row and column.

(b) General Parameters

The following are parameters common to all members analyzed as given at the top of the spread sheet.

CELL C5: DAMPING RATIO = ϵ

CELL C6: AIR MASS DENSITY = ρ

CELL C7: KINEMATIC VISCOSITY = ν

CELL C8: STRESS CONCENTRATION FACTOR = SCF

CELL C9: MODULUS OF ELASTICITY = E

CELL K5: RATIO OF GENERALIZED MASS TO EFFECTIVE MASS = $(\frac{m_j}{m_e})$

CELL K6: FIXITY PARAMETER IN FORMULA FOR CRITICAL VELOCITY = n_e

CELL K7: FIXITY PARAMETER IN FORMULA FOR STRESS AMPLITUDE = C

CELL K8: FIXITY PARAMETER IN FORMULA FOR MEMBER FREQUENCY = a_n

(c) Specific Member Analysis

The following describes the content of each column in analyzing a specific member. Entries and formulas for vortex shedding analysis of member group H1 on line 16 are also provided. Formula coding is described in the LOTUS 1-2-3 Users Manual.

COLUMN A: ENTER THE MEMBER GROUP IDENTIFIER

COLUMN B: ENTER THE EFFECTIVE SPAN OF THE MEMBER = L (m)

COLUMN C: ENTER THE OUTSIDE DIAMETER OF THE TUBULAR = d (mm)

COLUMN D: ENTER THE TOTAL OUTSIDE DIAMETER = D (mm) INCLUDING AS APPLICABLE, MARINE GROWTH, FIRE PROTECTION, ETC.

COLUMN E: ENTER THE TUBULAR WALL THICKNESS = t (mm)

COLUMN F: ENTER ADDED MASS (kg/m), IF APPLICABLE

COLUMN G: THE MOMENT OF INERTIA OF THE TUBULAR = I (cm⁴) IS COMPUTED.

$$I = \frac{\pi}{4} \left[\left(\frac{d}{2}\right)^4 - \left(\frac{d}{2} - t\right)^4 \right] \quad (\text{cm}^4)$$

COLUMN H: THE TOTAL EFFECTIVE MASS IS COMPUTED

$$m_e = \pi \left[\left(\frac{d}{2}\right)^2 - \left(\frac{d}{2} - t\right)^2 \right] (0.785) + m_a \quad (\text{kg/m})$$

COLUMN I: THE CRITICAL VELOCITY FOR CROSSFLOW OSCILLATION IS COMPUTED.

$$V_{cr} = \frac{13160 n_e^2}{(L/D)^2} \quad (\text{m/s})$$

COLUMN J: ENTER THE THRESHOLD WIND VELOCITY = V_{thr}

COLUMN K: THE STABILITY PARAMETER IS COMPUTED

$$K_s = \frac{2m_e (2\pi E)}{PD^2}$$

COLUMN L: THE REYNOLDS NUMBER IS COMPUTED

$$R_e = \frac{V_{cr}}{D_v}$$

Before performing calculation in the following columns, the critical velocity is compared with the threshold velocity. If the critical velocity is larger, crossflow oscillations will not occur and the computations are suppressed. An "N.A." is then inserted in each column.

If the critical velocity is less than the threshold value, the following computations are performed.

COLUMN M: THE AMPLITUDE OF VIBRATION IS COMPUTED

$$\gamma = \frac{\alpha D}{\left(\frac{m_j}{m_e}\right) K_s} \quad \begin{array}{l} \text{Where } \alpha = 0.04925 \text{ for } Re > 500,000 \\ \text{and } \alpha = 0.07178 \text{ for } Re < 500,000 \end{array}$$

COLUMN N: THE STRESS AMPLITUDE IS COMPUTED

$$f_b = \frac{CEdY}{L^2} \quad (\text{MPa})$$

where C depends on beam end fixity (see Section D.4)

COLUMN O: THE HOT SPOT STRESS RANGE IS COMPUTED

$$S = 2 (\text{SCF}) f_b \quad (\text{MPa})$$

COLUMN P: THE NUMBER OF CYCLES TO FAILURE UNDER THE HOT SPOT STRESS RANGE IS COMPUTED.

$$N = 10^{(14.57 - 4.1 \log_{10} S)} \quad (\text{cycles})$$

COLUMN Q: THE MEMBER NATURAL FREQUENCY IS COMPUTED

$$f_n = \frac{a_n}{2\pi} \left(\frac{EI}{m_e L^4} \right)^{\frac{1}{2}} \quad (\text{Hz})$$

where a_n depends on beam end fixity (see Section D.2)

COLUMN R: THE TIME IN HOURS TO FATIGUE FAILURE UNDER N CYCLES OF STRESS RANGE S IS COMPUTED

$$T = \frac{N}{f_n}$$

D.8. METHODS OF MINIMIZING VORTEX SHEDDING OSCILLATIONS

D.8.1 Control of Structural Design

The properties of the structure can be chosen to ensure that critical velocity values in steady flow do not produce detrimental oscillations.

Experiments have shown that for a constant mass parameter ($m/\rho d^2 = 2.0$), the critical velocity depends mainly on the submerged length/diameter (L/d) ratio of the member.

Thus, either high natural frequency or large diameter is required to avoid VIV's in quickly flowing fluid. A higher frequency will be obtained by using larger diameter tubes, so a double benefit occurs. An alternative method of increasing the frequency is to brace the structure with guy wires.

D.8.2 Mass and Damping

Increasing the mass parameter, $m/\rho d^2$, and/or the damping parameter reduces the amplitude of oscillations; if the increase is large enough, the motion is suppressed completely. While high mass and damping are the factors that prevent most existing structures from vibrating, no suitable design criteria are presently available for these factors, and their effects have not been studied in detail.

Increasing the mass of a structure to reduce oscillatory effects may not be entirely beneficial. The increase may produce a reduction in the natural frequency (and hence the flow speeds at which oscillation will tend to occur). It is thus possible that the addition of mass may reduce the critical speed to within the actual speed range. However, if increased mass is chosen as a method of limiting the amplitude of oscillation, this mass should be under stress during the motion. If so, the mass will also contribute to the structural damping. An unstressed mass will not be so effective.

If the structure is almost at the critical value of the combined mass/damping parameter for the suppression of motion, then a small additional amount of damping may be sufficient.

D.8.3 Devices and Spoilers

Devices that modify flow and reduce excitation can be fitted to tubular structures. These devices (see Figure D-5) work well for isolated members but are less effective for an array of piles or cylinders. Unfortunately, there is no relevant information describing how the governing stability criteria are modified. The most widely used devices are described below.

Guy Wires

Appropriately placed guy wires may be used to increase member stiffness and preclude wind-induced oscillations. Guy wires should be of sufficient number and direction to adequately brace the tubular member; otherwise, oscillations may not be eliminated completely and additional oscillations of the guys themselves may occur.

Strakes or Spoilers

Strakes and spoilers consist of a number (usually three) of fins wound as a helix around the tubular. These have proven effective in preventing wind-induced cross-flow oscillations of structures, and there is no reason to doubt their ability to suppress in-line motion, provided that the optimum stroke design is used. This comprises a three-star helix, having a pitch equal to five times the member diameter. Typically each helix protrudes one-tenth of the member diameter from the cylinder surface. To prevent in-line motion, strakes need only be applied over approximately in the middle one-third of the length of the tubular with the greatest amplitude. Elimination of the much more violent cross-flow motion requires a longer strake, perhaps covering the complete length of tube. The main disadvantage of strakes, apart from construction difficulties and problems associated with erosion or marine growth, is that they increase the time-averaged drag force produced by the flow. The drag coefficient of the straked part of the tube is independent of the Reynold's number and has a value of $C_D = 1.3$ based on the tubular diameter.

Shrouds

Shrouds consist of an outer shell, separated from the tubular by a gap of about 0.10 diameter, with many small rectangular holes. The limited data available indicates that shrouds may not always be effective. The advantage of shrouds over strakes is that their drag penalty is not as great; for all Reynold's numbers, $C_D = 0.9$ based on the inner tubular diameter. Like strakes, shrouds can eliminate the in-line motion of the two low-speed peaks without covering the complete length of the tubular. However, any design that requires shrouds (or strakes) to prevent cross-flow motion should be considered with great caution. Their effectiveness can be minimized by marine growth.

Offset Dorsal Fins

This is the simplest device for the prevention of oscillations. It is probably the only device that can be relied upon to continue to work in the marine environment over a long period of time without being affected adversely by marine growth. It has some drag penalty, but this is not likely to be significant for most designs.

The offset dorsal fin is limited to tubular structures that are subject to in-line motion due to flow from one direction only (or one direction and its reversal, as in tidal flow).

This patented device comprises a small fin running down the length of the tubular. Along with the small drag increase there is a steady side force. This may be eliminated in the case of the total force on multi-tubular design by placing the fin alternately on opposite sides of the tubulars.

D.9 REFERENCES

- D.1 King, R., "A Review of Vortex Shedding Research and Its Application," Ocean Engineering, Vol. 4, pp. 141-171, 1977.
- D.2 Hallam, M.G., Heaf, N.J., Wootton, L.R., Dynamics of Marine Structures, CIRIA, 1977.
- D.3 Vandiver, J.K., and Chung, T.Y., "Hydrodynamic Damping in Flexible Cylinders in Sheared Flow," Proceedings of Offshore Technology Conference, OTC Paper 5524, Houston, 1988.
- D.4 Blevins, R.D., Flow Induced Vibrations, Van Nostrand Reinhold, 1977.
- D.5 Blevins, R.D., Formulas for Natural Frequency and Mode Shape, Van Nostrand Reinhold, 1979.
- D.6 Gorman, D.I., Free Vibration Analyses of Beams and Shafts, Wiley-Interscience, 1975.
- D.7 Reid, D.L., "A Model for the Prediction of Inline Vortex Induced Vibrations of Cylindrical Elements in a Non-Uniform Steady Flow," Journal of Ocean Engineering, August 1989.
- D.8 Det Norske Veritas, "Rules for Submarine Pipeline Systems," Oslo, Norway, 1981.
- D.9 Griffin, O.M. and Ramberg, S.E., "Some Recent studies of Vortex Shedding with Application to Marine Tubulars, and Risers," Proceedings of the First Offshore Mechanics and Arctic Engineering/Deep Sea Systems Symposium, March 7 - 10, 1982, pp. 33 - 63.
- D.10 Sarpkaya, T., Hydroelastic Response of Cylinders in

Harmonic Flow, Royal Institute of Naval Architects, 1979.

- D.11 Engineering Sciences Data Unit, Across Flow Response Due to Vortex Shedding, Publication No. 78006, London, England, October, 1978.

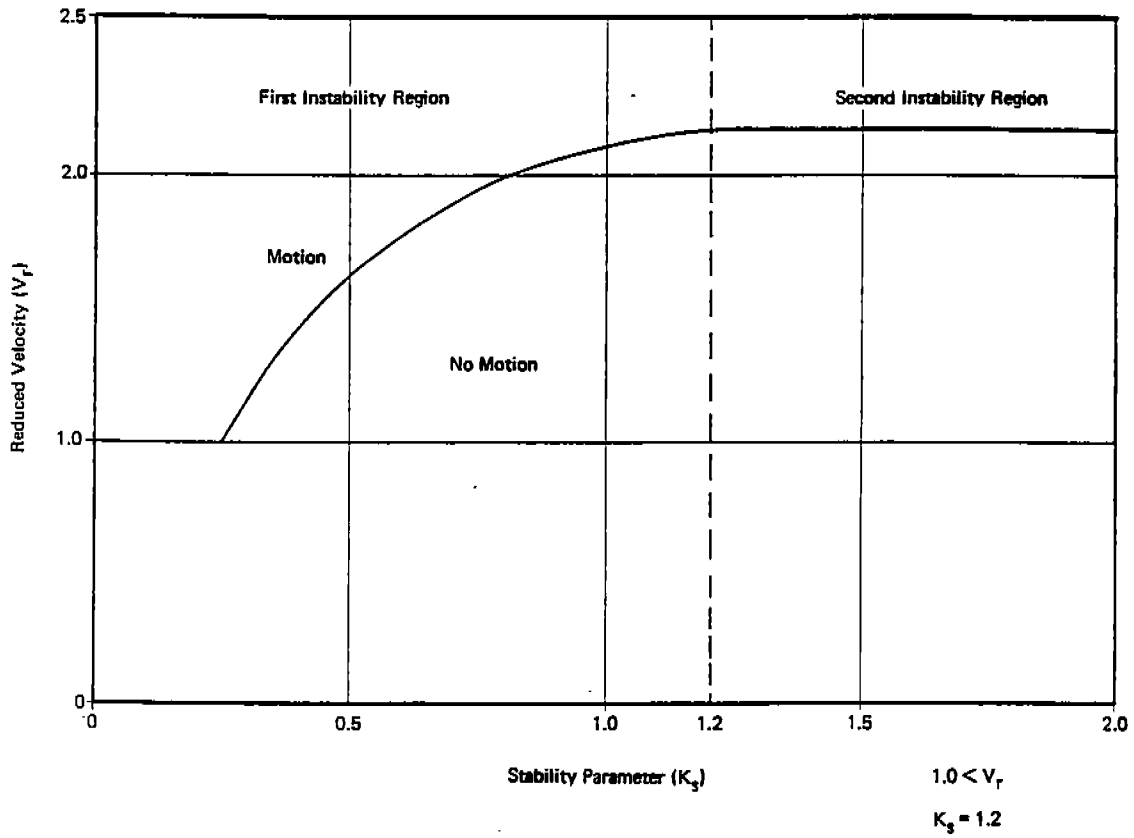


Figure D-1 Oscillatory Instability Relationship

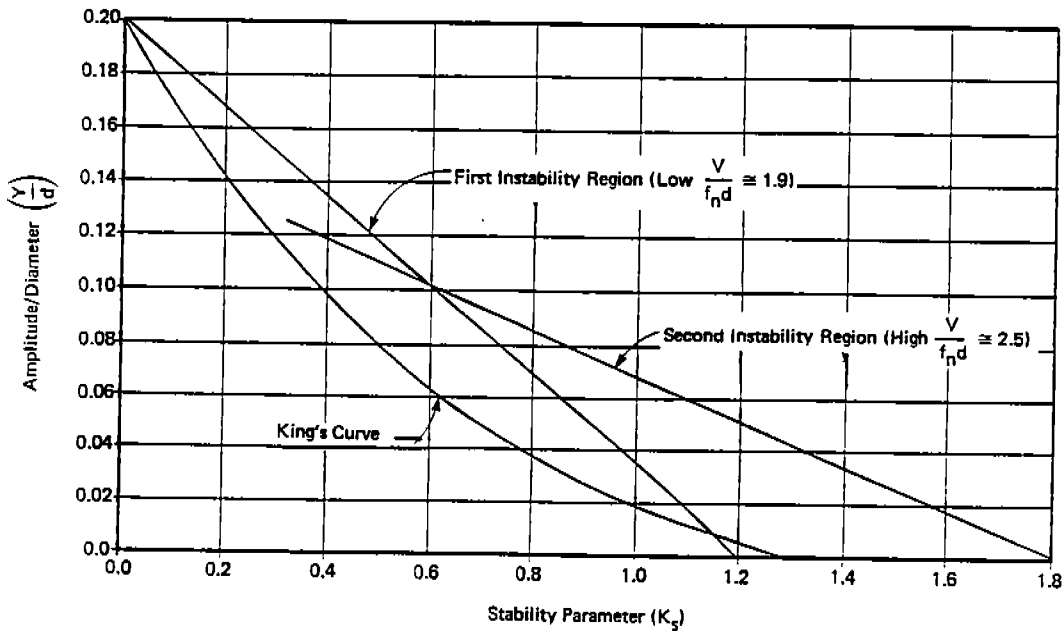


Figure D-2 Amplitude of Response for In-Line Vibrations

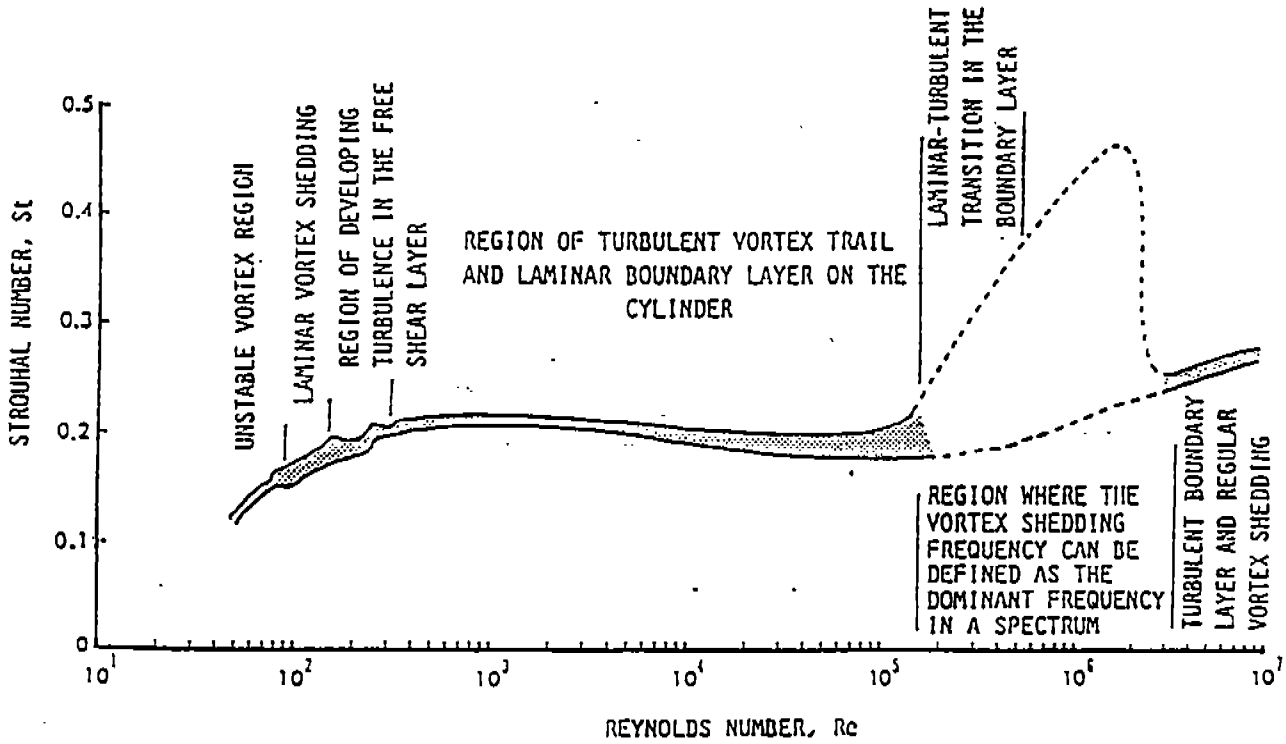


Figure D-3 The Strouhal versus Reynold's Numbers for Cylinders

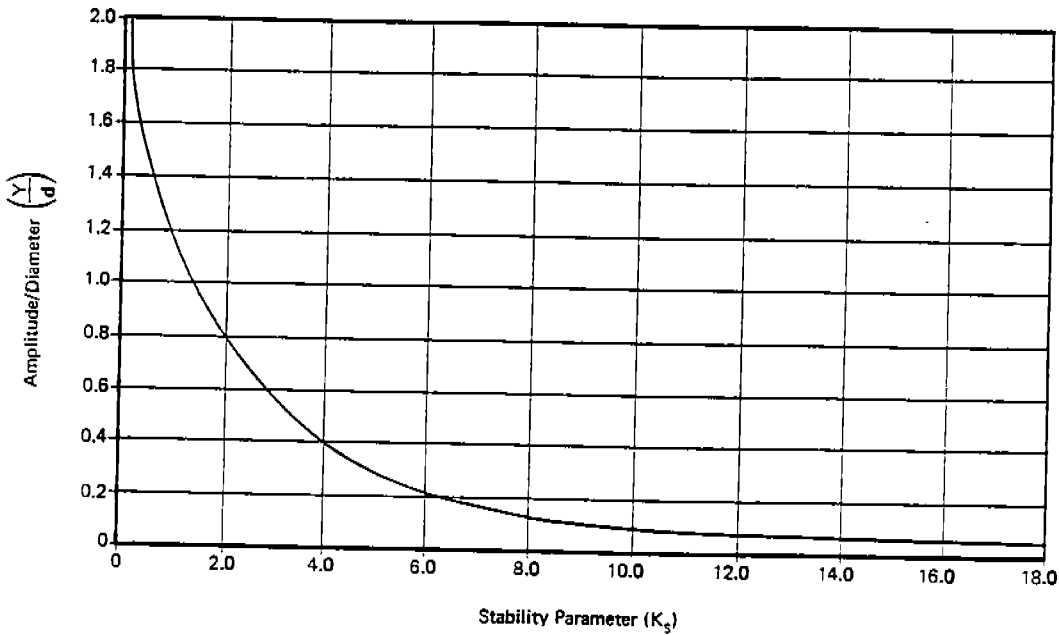
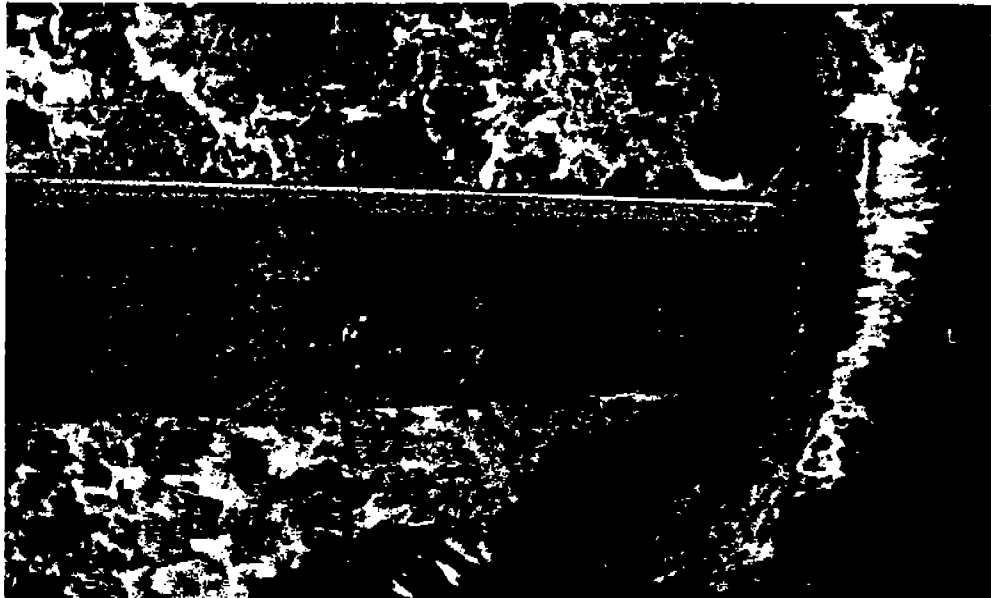
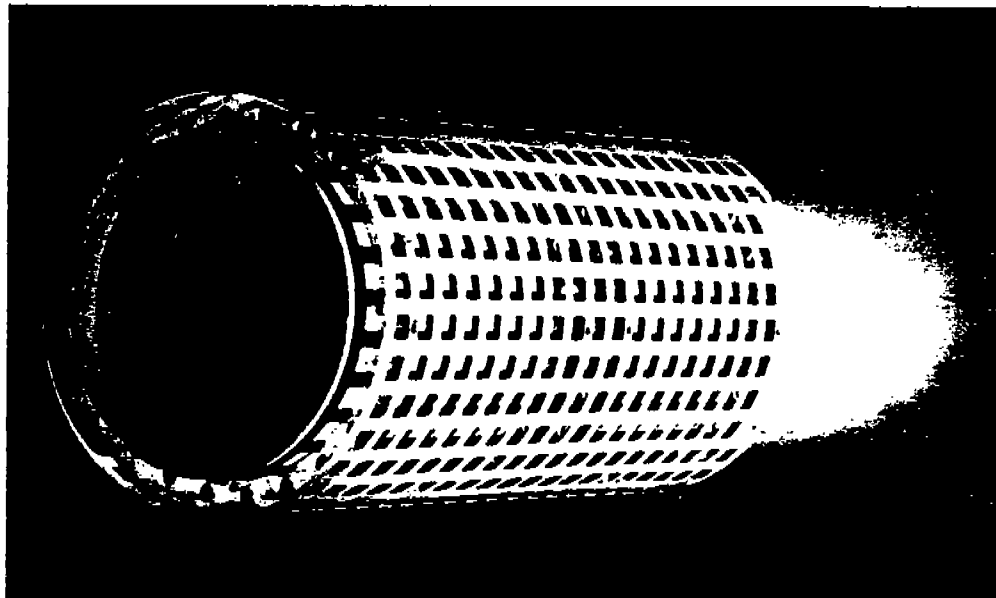


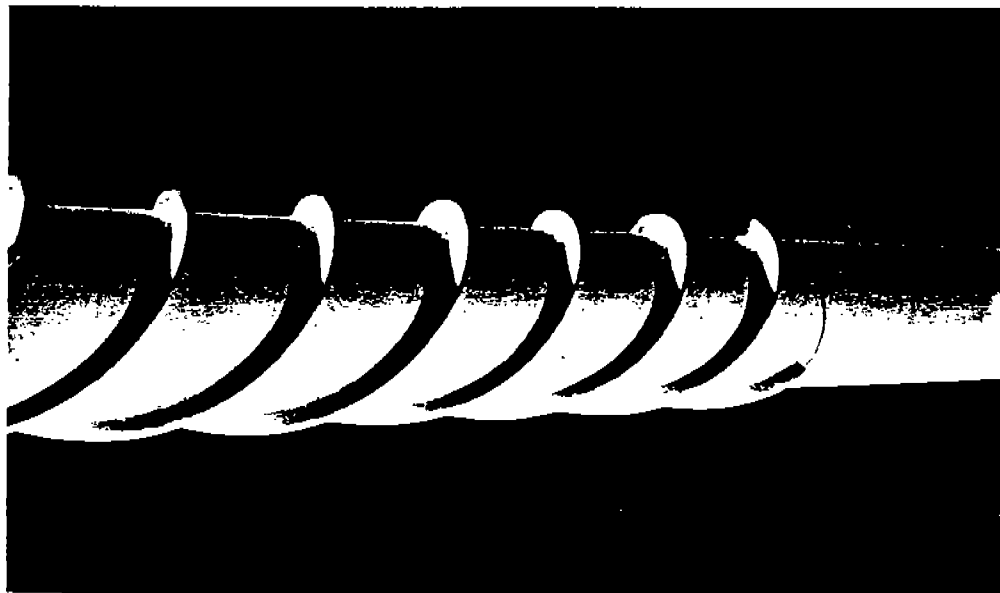
Figure D-4 Amplitude of Response for Cross-Flow Vibrations



Offset Dorsal Fin



Shrouds



Strakes

Figure D-5 Typical Devices and Spoilers

(THIS PAGE INTENTIONALLY LEFT BLANK)

~~151~~

COMMITTEE ON MARINE STRUCTURES

Commission on Engineering and Technical Systems

National Academy of Sciences – National Research Council

The COMMITTEE ON MARINE STRUCTURES has technical cognizance over the interagency Structure Committee's research program.

Peter M. Palermo Chairman, Alexandria, VA

Mark Y. Berman, Amoco Production Company, Tulsa, OK

Subrata K. Chakrabarti, Chicago Bridge and Iron, Plainfield, IL

Rolf D. Glasfeld, General Dynamics Corporation, Groton, CT

William H. Hartt, Florida Atlantic University, Boca Raton, FL

Alexander B. Stavovy, National Research Council, Washington, DC

Stephen E. Sharpe, Ship Structure Committee, Washington, DC

LOADS WORK GROUP

Subrata K. Chakrabarti Chairman, Chicago Bridge and Iron Company, Plainfield, IL

Howard M. Bunch, University of Michigan, Ann Arbor, MI

Peter A. Gale, John J. McMullen Associates, Arlington, VA

Hsien Yun Jan, Martech Incorporated, Neshanic Station, NJ

Naresh Maniar, M. Rosenblatt & Son, Incorporated, New York, NY

Solomon C. S. Yim, Oregon State University, Corvallis, OR

MATERIALS WORK GROUP

William H. Hartt Chairman, Florida Atlantic University, Boca Raton, FL

Santiago Ibarra, Jr., Amoco Corporation, Naperville, IL

John Landes, University of Tennessee, Knoxville, TN

Barbara A. Shaw, Pennsylvania State University, University Park, PA

James M. Sawhill, Jr., Newport News Shipbuilding, Newport News, VA

Bruce R. Somers, Lehigh University, Bethlehem, PA

Jerry G. Williams, Conoco, Inc., Ponca City, OK

C-3 80117/659

SHIP STRUCTURE COMMITTEE PUBLICATIONS

- SSC-351 An Introduction to Structural Reliability Theory by Alaa E. Mansour 1990
- SSC-352 Marine Structural Steel Toughness Data Bank by J. G. Kaufman and M. Prager 1990
- SSC-353 Analysis of Wave Characteristics in Extreme Seas by William H. Buckley 1989
- SSC-354 Structural Redundancy for Discrete and Continuous Systems by P. K. Das and J. F. Garside 1990
- SSC-355 Relation of Inspection Findings to Fatigue Reliability by M. Shinozuka 1989
- SSC-356 Fatigue Performance Under Multiaxial Load by Karl A. Stambaugh, Paul R. Van Mater, Jr., and William H. Munse 1990
- SSC-357 Carbon Equivalence and Weldability of Microalloyed Steels by C. D. Lundin, T. P. S. Gill, C. Y. P. Qiao, Y. Wang, and K. K. Kang 1990
- SSC-358 Structural Behavior After Fatigue by Brian N. Leis 1987
- SSC-359 Hydrodynamic Hull Damping (Phase I) by V. Ankudinov 1987
- SSC-360 Use of Fiber Reinforced Plastic in Marine Structures by Eric Greene 1990
- SSC-361 Hull Strapping of Ships by Nedret S. Basar and Roderick B. Hulla 1990
- SSC-362 Shipboard Wave Height Sensor by R. Atwater 1990
- SSC-363 Uncertainties in Stress Analysis on Marine Structures by E. Nikolaidis and P. Kaplan 1991
- SSC-364 Inelastic Deformation of Plate Panels by Eric Jennings, Kim Grubbs, Charles Zanis, and Louis Raymond 1991
- SSC-365 Marine Structural Integrity Programs (MSIP) by Robert G. Bea 1992
- SSC-366 Threshold Corrosion Fatigue of Welded Shipbuilding Steels by G. H. Reynolds and J. A. Todd 1992
- None Ship Structure Committee Publications - A Special Bibliography

C-4 80117/659

10

SSC-367 Fatigue Technology Assessment and Avoidance Strategies - Appendices
Ship Structure Committee 1993

sp. 20117
CS9